



HAL
open science

Etudes de synthèse électrochimiques et de fluorescence de nouveaux dérivés de la 1,2,4,5-tétrazines en tant que sondes moléculaires pour des anions et des composés riches en électrons et étude de synthèses électrochimiques de sels de ferrocène à base de pyridinium.

Yong-Hua Gong

► **To cite this version:**

Yong-Hua Gong. Etudes de synthèse électrochimiques et de fluorescence de nouveaux dérivés de la 1,2,4,5-tétrazines en tant que sondes moléculaires pour des anions et des composés riches en électrons et étude de synthèses électrochimiques de sels de ferrocène à base de pyridinium.. Autre. École normale supérieure de Cachan - ENS Cachan, 2007. Français. NNT : . tel-00160587

HAL Id: tel-00160587

<https://theses.hal.science/tel-00160587>

Submitted on 6 Jul 2007

HAL is a multi-disciplinary open access archive for the deposit and dissemination of scientific research documents, whether they are published or not. The documents may come from teaching and research institutions in France or abroad, or from public or private research centers.

L'archive ouverte pluridisciplinaire **HAL**, est destinée au dépôt et à la diffusion de documents scientifiques de niveau recherche, publiés ou non, émanant des établissements d'enseignement et de recherche français ou étrangers, des laboratoires publics ou privés.



N° ENSC-2007n°41

**THESE DE DOCTORAT
DE L'ECOLE NORMALE SUPERIEURE DE CACHAN**

Présentée par

Monsieur Yong-Hua GONG

pour obtenir le grade de

DOCTEUR DE L'ECOLE NORMALE SUPERIEURE DE CACHAN

Domaine :

SCIENCES PHYSIQUES et CHIMIQUES

Sujet de la thèse :

Synthesis, electrochemical and fluorescence studies of 1,2,4,5-tetrazine derivatives: towards molecular sensors for anions and electron-rich compounds and synthesis and electrochemical study of ferrocene-containing pyridinium salts.

Thèse présentée et soutenue à Cachan le 12 juin 2007 devant le jury composé de :

Gérard JAOUEN	Professeur-ENSCP	Président
Jean-Claude MOUTET	Professeur Université Grenoble I	Rapporteur
Damien PRIM	Professeur Université de Versailles	Rapporteur
Pierre AUDEBERT	Professeur-ENS Cachan	Examineur
Jie TANG	Professeur-ECNU Shanghai	Examineur
Gilles CLAVIER	Chargé de recherche CNRS	Examineur
Rachel MEALLET-RENAULT	Professeur Agrégée-ENS Cachan	Examinatrice

Laboratoire de Photophysique et Photochimie Supramoléculaires et Macromoléculaires
(ENS CACHAN/CNRS/UMR 8531)

61 av President Wilson, F-94230 CACHAN, France

Table of contents

Acronyms	5
-----------------------	---

Abstract	7
-----------------------	---

Part I: Synthesis, electrochemical and fluorescence studies of 1,2,4,5-tetrazine derivatives: towards molecular sensors for anions and electron-rich compounds

Chapter 1 Introduction of 1,2,4,5-tetrazine chemistry and applications .. 15

1.1 Introduction of 1,2,4,5-tetrazines	15
1.2 Synthesis of tetrazines	16
1.2.1 Pinner synthesis	17
1.2.2 Ring closure of <i>S</i> -methylisothiocarbonohydrazide salt with ortho-formate/ortho-acetates or iminium chlorides	19
1.2.3 Aromatic Nucleophilic Substitution (S_NAr reaction)	20
1.3 Reactivity of tetrazines	23
1.3.1 Aromatic nucleophilic substitution (S_NAr reaction)	23
1.3.2 Azaphilic addition with carbanions	25
1.3.3 Cross-coupling reactions with terminal alkynes	27
1.3.4 Inverse electron-demand Diels-Alder reaction	27
1.4 Research development and applications of tetrazines	33
1.4.1 Tetrazines as molecular models for theoretical studies	33
1.4.2 Tetrazine derivatives for NLO	36
1.4.3 Tetrazines in coordination chemistry	36
1.4.4 Tetrazines as energetic materials	38
1.4.5 Tetrazines as pharmaceuticals	39
1.4.6 Tetrazine derivatives for anticorrosion applications	40
References	41

Chapter 2 Development of anion and electron-rich compound sensors 45

2.1 Supramolecular chemistry and receptors	45
2.2 Optical (colorimetric, fluorescent) sensors and electrochemical sensors	45
2.2.1 Fluorescent molecular sensors	46
2.2.2 Electrochemical sensors	48
2.3 Anion sensors	50
2.3.1 Roles of anions	50
2.3.2 Difficulties in anion recognition and sensing	50
2.3.3 Developments in research for anion sensors	52
2.4 Sensors for electron-rich compounds	58
2.4.1 General Strategy used for detecting neutral analytes: π - π stacking	58
2.4.2 Redox-switched binding	60
2.4.3 Rare examples of sensors for electron-rich compounds	60

References	62
Chapter 3 Tetrazine derivatives for sensor applications	65
3.1 Interaction of tetrazines with anions/electron-rich compounds—anion- π interaction/ π - π interaction	65
3.2 Development of tetrazines in sensor applications: previous work in Audebert's group	66
3.3 Molecular designing of sensors	71
References	76
Chapter 4 Synthesis: results and discussion	79
4.1 Preparation of 3,6-dichloro-1,2,4,5-tetrazine	79
4.2 Attempts to synthesize novel tweezer molecular sensors	81
4.2.1 <i>S_NAr</i> reaction of tetrazines	81
4.2.2 <i>Tweezers with flexible chains</i>	82
4.2.3 <i>Tweezers with rigid frameworks</i>	83
4.3 Synthesis of tripod molecular sensors	87
4.3.1 <i>Using triethanolamine</i>	87
4.3.2 <i>Using 2-(bromomethyl)-2-(hydroxymethyl)propane-1,3-diol as triol</i> ..	88
4.4 Synthesis of cyclophane molecular sensors	89
4.4.1 <i>The first cyclophane-tetrazine</i>	89
4.4.2 <i>Attempt to synthesize cyclophane-tetrazine 92</i>	93
4.4.3 <i>Reconsideration of cyclophane-tetrazine 90</i>	96
4.5 Synthesis of calycular molecular sensors: new multichromophoric cyclodextrin functionalized by fluorescent tetrazines	97
4.5.1 <i>Attachment of tetrazines onto cyclodextrins via S_NAr reactions</i>	97
4.5.2 <i>Attempt to attach tetrazines via "click chemistry"</i>	99
References	101
Chapter 5 UV/Visible absorption, fluorescence and electrochemical studies	
5.1 Introduction of fluorescence quenching: Stern-Volmer equation and Rehm-Weller equation	103
5.2 Spectroscopic and electrochemical study of tripod-tetrazine (86)	106
5.2.1 <i>Absorption and fluorescence studies</i>	106
5.2.2 <i>Fluorescence quenching of tripod-tetrazine</i>	107
5.2.3 <i>Preliminary electrochemical studies of tripod-tetrazine</i>	110
5.3 Spectroscopic and electrochemical studies of the first cyclophane (93)	112
5.3.1 <i>Spectroscopic study</i>	112
5.3.2 <i>Electrochemistry study</i>	113
5.3.3 <i>Sensitivity of the electrochemical response to added organic compounds</i>	114
5.4 Discussion of fluorescence of new cyclophane-tetrazine (90), tetrazine 118 and 128	116
5.4.1 <i>Trimer-tetrazine 118</i>	116
5.4.2 <i>Cyclophane-tetrazine 90</i>	119
5.4.3 <i>Tetrazine 128</i>	121
5.4.4 <i>Molecular modeling and fluorescence properties</i>	122

5.5 Fluorescence and electrochemical study of β -CD-tetrazine	126
5.5.1 Absorption and fluorescence studies	126
5.5.2 Fluorescence quenching of β -CD-tetrazine	127
5.5.3 Electrochemical study of β -CD-tetrazine	129
5.6 α -CD-tetrazine (95)	131
5.6.1 Absorption and fluorescence studies of 95	131
5.6.2 Fluorescence quenching	131
5.6.3 Electrochemical study	133
References	135
General conclusion and perspectives	137
Chapter 6 Experimental Section	139
Part II : Synthesis and electrochemical study of ferrocene-containing pyridinium salts	
Chapter 1 Introduction	183
1.1 Introduction of ferrocene	183
1.2 Basic electrochemical behavior	183
1.3 Development in research of molecules containing multiple ferrocenes	184
1.3.1 Molecules containing two ferrocene units	184
1.3.2 Molecules containing multiple ferrocene units	187
1.3.3 Dendrimers containing ferrocenes	193
References	197
Chapter 2 Molecular design of ferrocene-containing pyridinium salts ..	201
2.1 Previous work in Tang's group	201
2.2 Molecular design	202
References	204
Chapter 3 Results and discussion	205
3.1 Synthesis of dibranched and tribranched pyridiniums	205
3.1.1 Improvement of synthesis of <i>trans</i> -5-(2-ferrocenyl-vinyl)-2-carbaldehyde-thiophene	205
3.1.2 Influence of base for Wittig olefination	206
3.1.3 Isomerization of <i>Z</i> -isomers to <i>E</i> -isomers with I_2	207
3.1.4 Condensation of aromatic aldehyde with multimethyl-pyridiniums ..	208
3.2 Electrochemical results and discussion	213
3.2.1 Preliminary electrochemical study of 45i and 46i	213
3.2.2 Preliminary electrochemical study of 45h	213
3.2.3 Preliminary electrochemical study of 46h	214
3.2.4 Preliminary electrochemical study of 45j	215
3.2.5 Preliminary electrochemical study of 46j	217
References	219

General conclusion and perspectives	221
Chapter 4 Experimental section	223
List of publications	233
Acknowledgement	235

Acronyms

BTH: bithiophene

CD: cyclodextrin ($\alpha=6$, $\beta=7$)

CV: cyclic voltammogram

DA: Diels-Alder

DBU: 1,8-diazabicyclo[5,4,0]undec-7-ene

DHP: 3,4-dihydro-2H-pyran

DM: dichloromethane

DMAP: 4-dimethylamino-pyridine

DMF: dimethylformamide

EA: ethyl acetate

Fc: ferrocene

HOMO: highest occupied molecular orbital

LUMO: lowest unoccupied molecular orbital

mCPBA: m-chloro-peroxybenzoic acid (3-chloro-peroxybenzoic acid)

NLO: nonlinear optical

NMP: *N*-methyl pyrrole

PE: petroleum ether

TBDMS: *tert*-butyldimethylsilyl

THF: tetrahydrofuran

THP: tetrahydro-2H-pyran

Tz: 1,2,4,5-tetrazine (or *s*-tetrazine)

TPA: triphenylamine

TTF: tetrathiafulvalenen

Abstract

This thesis consists of two parts. The first one deals with the synthesis and electrochemical and fluorescence studies of new 1,2,4,5-tetrazine derivatives as molecular sensors for anions and electron-rich compounds, and the second one with the synthesis and preliminary electrochemical studies of ferrocene-containing pyridinium salts.

In part I, a short overview of 1,2,4,5-tetrazine chemistry (*s*-tetrazine) is presented. *s*-Tetrazines have already found applications in many fields, but their ability to bind anions or electron-rich compounds through anion- π interaction or π - π stacking has not been noticed until very recently. In this context, a series of novel molecular sensors containing tetrazine moieties as both binding units and sensing units are designed, including tweezer-tetrazines, tripod-tetrazines, cyclophane-tetrazines, and calycular tetrazines. Among them, a tripod-tetrazine (**86**), two cyclophane-tetrazines (**90**, **93**) and two calycular tetrazines (**94**, **95**) have been successfully synthesized based on S_NAr reactions of 3,6-dichlorotetrazine (**23**). Fluorescence studies show that the fluorescence of **86**, **90**, **94** and **95** can be efficiently quenched by electron-rich compounds such as triphenylamine (TPA), tris(4-bromophenyl)amine, pyrrole, tetrathiafulvalene (TTF) and 1,3,5-trimethoxybenzene. Electrochemical studies also indicate the interactions between the tetrazine sensors and these electron-rich compounds. The fluorescence quenching mechanisms are investigated in some cases, and calculations on molecular orbitals are carried out to investigate the relationship between molecular structures and fluorescence properties.

In part II, the synthesis of a dibranched ferrocene-containing pyridinium salt (**45j**) and two tri-branched ones (**46h**, **46j**) through the condensations of 1,2,6-trimethyl pyridinium or 1,2,4,6-tetramethyl pyridinium with aromatic aldehydes is presented. A new synthetic route is also developed for the two important intermediates, *trans*-5-(2-ferrocenyl-vinyl)-2-carbaldehyde-thiophene (**47**), and ferrocenylethenyl-bithiophenyl aldehyde (**48**). Preliminary electrochemical studies show that bithiophene units influence greatly the redox behaviors of the molecules.

Résumé

Cette thèse se compose de deux parties. La première traite de la synthèse et des études électrochimiques et de fluorescence de nouveaux dérivés de la 1,2,4,5-tétrazine en tant que sondes moléculaires pour des anions et des composés riches en électrons. La seconde traite de la synthèse et des études électrochimiques préliminaires de sels de ferrocène à base de pyridinium.

Dans la partie I, une vue d'ensemble de la chimie des 1,2,4,5-tétrazine (*s*-tétrazines) est présentée. Les *s*-tétrazines ont déjà trouvé des applications dans beaucoup de domaines, mais leur capacité à se lier avec des anions ou des composés riches en électrons par interactions anion- π ou empilement π - π n'a été démontrée que très récemment. Dans ce contexte, une série de nouvelles sondes moléculaires contenant des noyaux tétrazine servant d'unités liantes et de détection a été conçue, comprenant des pinces-tétrazines, des trépied-tétrazines, des cyclophane-tétrazines, et des calices-tétrazines. Parmi eux, un trépied-tétrazine (**86**), deux cyclophane-tétrazines (**90**, **93**) et deux calices-tétrazines (**94**, **95**) ont été synthétisés avec succès en se basant sur des réactions de type S_NAr avec la 3,6-dichloro-*s*-tétrazine (**23**). Les études photophysiques prouvent que la fluorescence de **86**, **90**, **94** et **95** peut être efficacement éteinte par les composés riches en électrons tels que la triphénylamine (TPA), la tris (4-bromophényl) amine, le pyrrole, le tétrathiafulvalène (TTF) et le 1,3,5-triméthoxybenzène. Les études électrochimiques indiquent également la présence d'interactions entre les sondes de tétrazine et ces composés électron-donneurs. Les mécanismes d'extinction de fluorescence sont étudiés dans certains cas, et des calculs d'orbitales moléculaires sont présentés pour expliquer le rapport entre les structures et les propriétés moléculaires de fluorescence.

Dans la partie II, la synthèse d'un sel de pyridinium à deux branches contenant des ferrocènes (**45j**) et de deux analogues à trois branches (**46h**, **46j**) obtenus par condensations du 1,2,6-triméthylpyridinium ou 1,2,4,6-tétraméthylpyridinium avec des aldéhydes aromatiques est présentée. Une nouvelle voie de synthèse est également développée pour les deux intermédiaires importantes, le trans-5- (2-ferrocényl-vinyl) - 2-carbaldéhydethiophène (**47**), et l'aldéhyde du ferrocényléthényl-bithiophényle (**48**). Les études électrochimiques préliminaires prouvent que les sous-unités bithiophène influencent considérablement le comportement redox des molécules.

摘要

本论文分为两部分：第一部分为“1, 2, 4, 5-四嗪的合成, 电化学以及荧光性质研究”；第二部分为“含二茂铁的吡啶盐类化合物的合成与电化学性质研究”。

第一部分中, 首先在第一章简要介绍了 1, 2, 4, 5-四嗪化学, 包括其一般合成方法, 反应性以及在不同领域的应用。第二章介绍了超分子化学的一般概念, 包括非共价键相互作用, 荧光分子探针以及电化学分子探针等。鉴于阴离子在生物体系和环境体系中的重要作用, 关于阴离子探针分子的研究进展也做了简要介绍。富电子化合物的检测在环境监测和污染控制方面具有重要意义, 但对于该类探针分子的研究却相对很少。作为缺电子的杂环, 四嗪经由阴离子- π 相互作用络合阴离子的能力已经由理论计算予以证实。Audebert 小组的工作又表明, 部分四嗪化合物具有良好的电化学可逆性以及荧光特性, 并且其荧光信号可随富电子化合物的加入而发生响应。在此基础上我们设计了一系列探针分子, 包括镊子型、三足型、环番以及杯状构造的分子, 其中的四嗪既作为络合单元同时又作为信号单元。其中, 一个三足型四嗪 (86), 两个含四嗪的环番 (90, 93) 和两个杯状构造的四嗪 (94, 95) 被成功合成。荧光性质研究表明, 化合物 86, 90, 94 和 95 的荧光能够有效地被加入的富电子化合物如三苯胺, 三-4-溴苯胺, 吡咯, 四硫富瓦烯以及 1, 3, 5-三甲氧基苯等淬灭。电化学研究也表明这些探针分子与富电子化合物之间存在相互作用。对某些荧光淬灭实验中的淬灭机理也进行了研究; 对于部分分子的轨道能级进行了计算, 用于解释荧光性质与分子结构的关系。

第二部分介绍了一个双臂的二茂铁吡啶盐 (45j) 和两个三臂的二茂铁吡啶盐 (46h, 46j) 的合成。目标化合物经过 1, 2, 6-三甲基吡啶盐或 1, 2, 4, 6-四甲基吡啶盐与相应的芳香醛缩合得到; 同时建立了一条新的合成路线合成了两个重要的中间体芳香醛, 反式-二茂铁乙烯基噻吩甲醛 (47) 和反式-二茂铁乙烯基联噻吩甲醛 (48)。初步的电化学研究表明联噻吩共轭桥对于分子的电化学行为具有极大影响。

Part I

**Synthesis, electrochemical and
fluorescence studies of 1,2,4,5-tetrazine
derivatives: towards molecular sensors for
anions and electron-rich compounds**

Chapter 1 Introduction of 1,2,4,5-tetrazine chemistry and applications

1.1 Introduction of 1,2,4,5-tetrazines

1,2,4,5-tetrazines (or *s*-tetrazines) are aromatic heterocycles with four nitrogen atoms centered on the ring¹ (Figure 1):

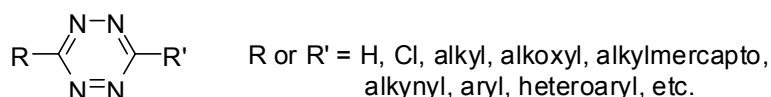


Figure 1. 1,2,4,5-tetrazines.

The two substituents located on the two sides of the ring can be identical (symmetrical tetrazines) or different (unsymmetrical tetrazines); the substituents include alkyl, alkynyl, aryl, heteroaryl, alkoxy, alkylmercapto- and other heteroatoms. If *s*-tetrazine is considered as a benzene derivative with four CH groups replaced by nitrogen atoms, the symmetry is lowered from D_{6h} to D_{2h} . The most distinct character of tetrazines is their high electron affinity, which can be deduced from the replacement of four CH group by four more electronegative nitrogen atoms on the prototypical aromatic ring. In fact they are the electron poorest C-N heterocycles², and consequently are reduced at high to very high potentials (-0.8 ~ -0.4V vs Ag^+/Ag). The other remarkable character of tetrazines is their low-lying π^* orbital (Figure 2)³, resulting in an $n\text{-}\pi^*$ transition in the visible range⁴⁻⁷.

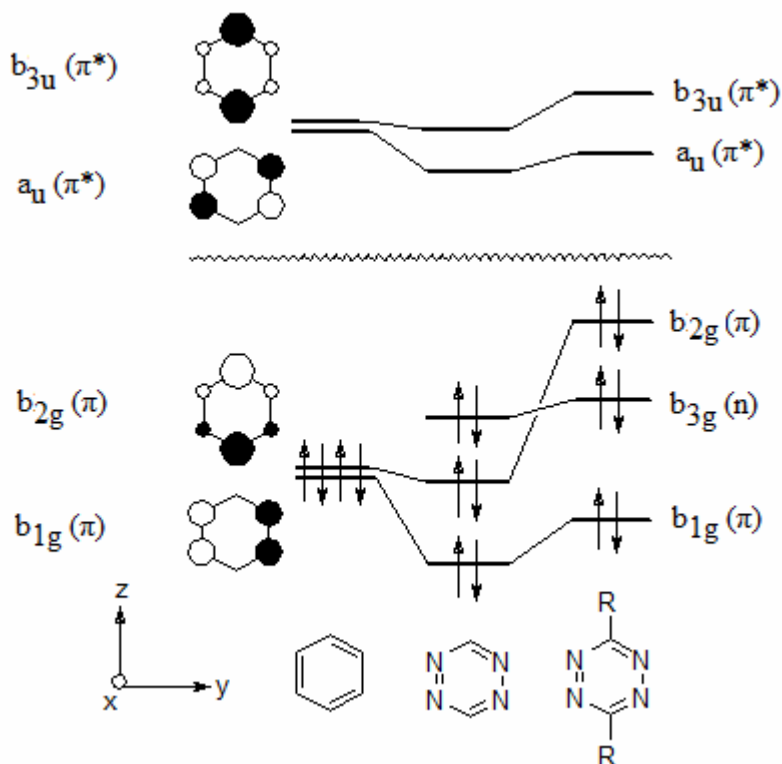
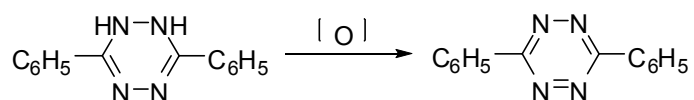


Figure 2. Qualitative diagram illustrating the energy shifts of the frontier orbitals of benzene and *s*-tetrazine as a result of 1,2,4,5-tetraaza replacement and 3,6-disubstitution by electron donating groups R (Adapted from ref. 3).

1,2,4,5-Tetrazine compounds were firstly synthesized more than 100 years ago⁸ and have gained much attention from chemists during the last decades. Several synthetic methods have been developed and a lot of applications have been found in various fields such as organic synthesis⁹, crop protection^{10,11}, pyrotechnics (high-nitrogen content energetic materials)¹²⁻¹⁴, etc. Very recently, research for new compounds gathering optical and electrochemical properties became increasingly active because these compounds have a huge potential especially in sensor applications¹⁵⁻¹⁸. The group of Professor Audebert and others dedicated much attention to the tetrazine family for such applications given their outstanding photophysical and electron accepting properties, the details of which are presented in Chapter 3.2.

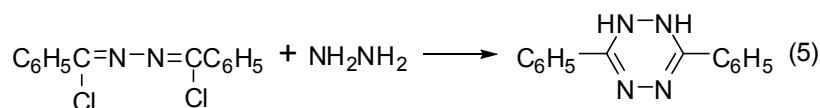
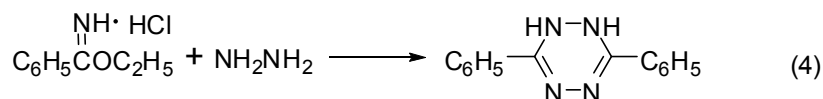
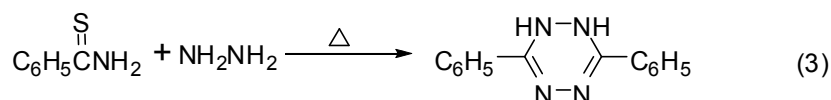
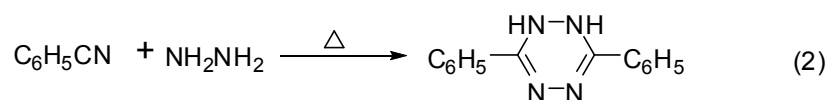
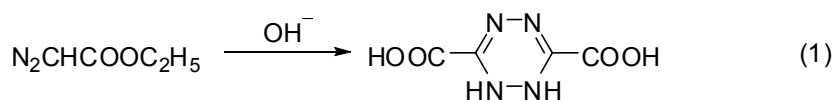
1.2 Synthesis of *s*-tetrazines

The main preparative method for *s*-tetrazines is oxidation of dihydro-*s*-tetrazines, by mild oxidizing agents such as amyl nitrite, bromine, air, ferric chloride, hydrogen peroxide or chromic oxide, for example¹⁹ (Scheme 1):



Scheme 1. oxidation of diphenyldihydro-*s*-tetrazine.

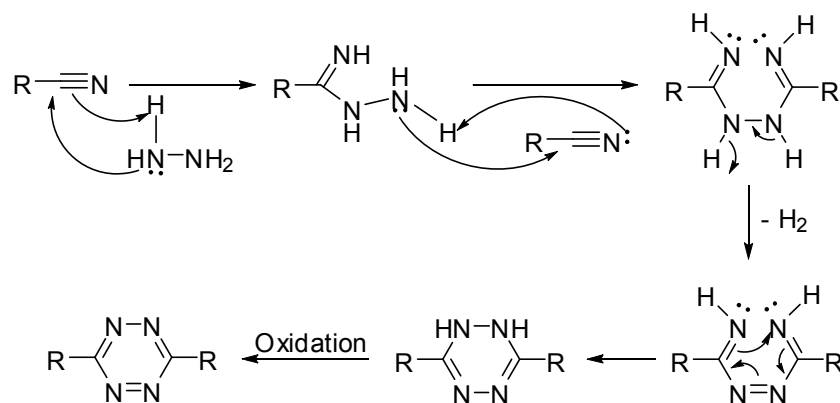
There are several methods for preparing dihydro-*s*-tetrazines (Scheme 2). A number of modifications of the standard Pinner synthesis have been used as well as a number of special procedures. Most of the procedures presented have been shown as applying only to aromatic compounds, except for (2) and (4), which can be used to prepare 3, 6- dialkyl-1,2-dihydro-*s*-tetrazines.



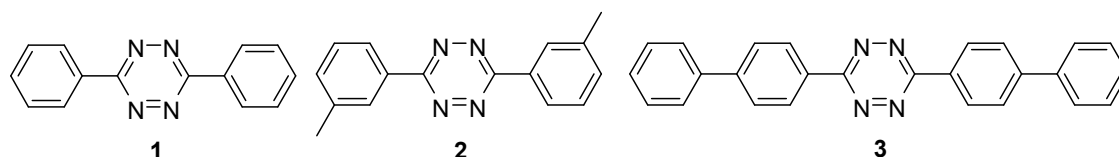
Scheme 2. Preparation of dihydro-*s*-tetrazines.

1.2.1 Pinner synthesis

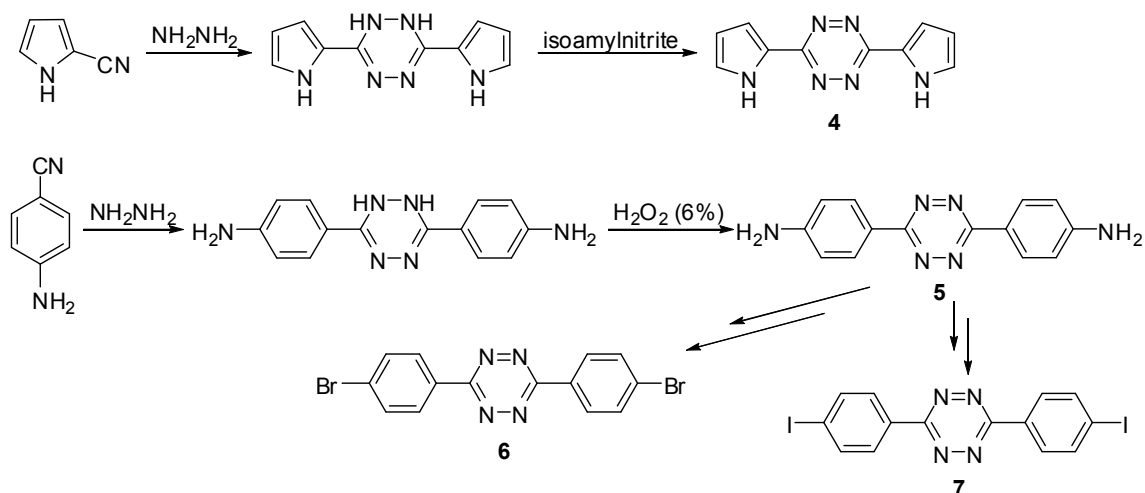
Diaryl-*s*-tetrazines are often obtained via a variation of the original Pinner synthesis⁸, in which the imido ester of an aromatic nitrile is reacted with hydrazine in an aqueous solution of either ammonium hydroxide or potassium hydroxide. Under these conditions the dihydro-*s*-tetrazine is formed, which is then oxidized by oxidants like H₂O₂, isoamyl nitrite or FeCl₃ to give the desired tetrazine (Scheme 3).



Wiley and co-workers²⁰ have improved the syntheses by carrying out the reaction under anhydrous conditions in a mixture of methanol and triethylamine. Some 3,6-diaryl-1,2,4,5-tetrazines (**1**, **2**) and 3,6-di-*p*-biphenyl-1,2,4,5-tetrazine (**3**) were obtained in moderate yields (Figure 3).



Using the same protocol, Sołoducho and his colleagues have recently synthesized a series of novel linear oligoheterocycles based on substituted tetrazines, for example, bis(pyrrolyl)tetrazines (**4**) and bis(phenyl)tetrazines (**5**, **6**, **7**), from the reactions of the respective aromatic nitriles with hydrazine (Scheme 4). Quantum chemical calculations were performed to assess the usefulness of the synthesized compounds for electropolymerization, and the results have indicated qualitative differences between bis-pyrrole tetrazine and bis-phenyl tetrazines regarding the electronic density rearrangement due to the loss of one electron.



Scheme 4. Bis-aryl-tetrazines synthesized by Soloducho *et al.*

At the same time but independently, Audebert and colleagues^{21, 22} have synthesized some new original tetrazines (**8**, **9**) substituted by heterocyclic rings using a related protocol and submitted them to electropolymerization (Figure 4):

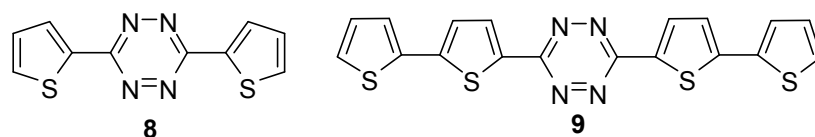
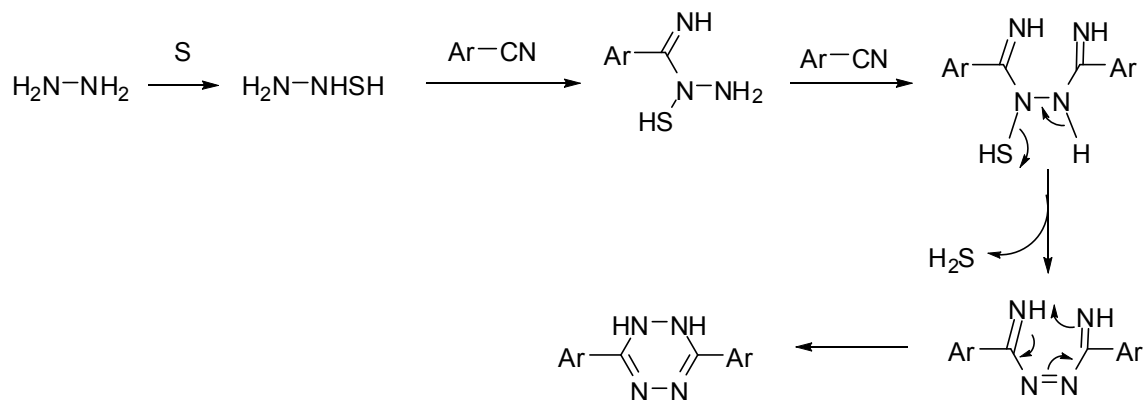


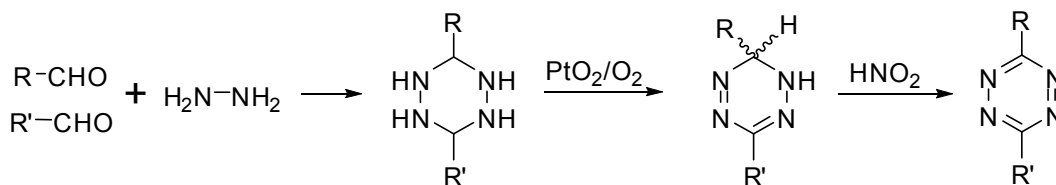
Figure 4. Tetrazines synthesized by Audebert's group.

Although it has already been shown in the past that hydrazine reacts with aromatic nitriles preferably in the presence of sulfur²³, leading to the formation of dihydro-1,2,4,5-tetrazines, the reactions require highly concentrated conditions as well as a neat excess of hydrazine in many cases, and no mechanism was suggested. On the basis of observations made during the course for the reaction (the colour change of solution from colorless to light orange after the sulfur is added, and the vigorous H₂S gas emission taking place through out the reaction), Audebert *et al.* have proposed that the active nucleophile was the fast addition product of hydrazine to sulfur, namely H₂N-NH-SH, with the mechanism shown below (Scheme 5):



Scheme 5. Mechanism of formation of aromatic tetrazines proposed by Audebert *et al.*

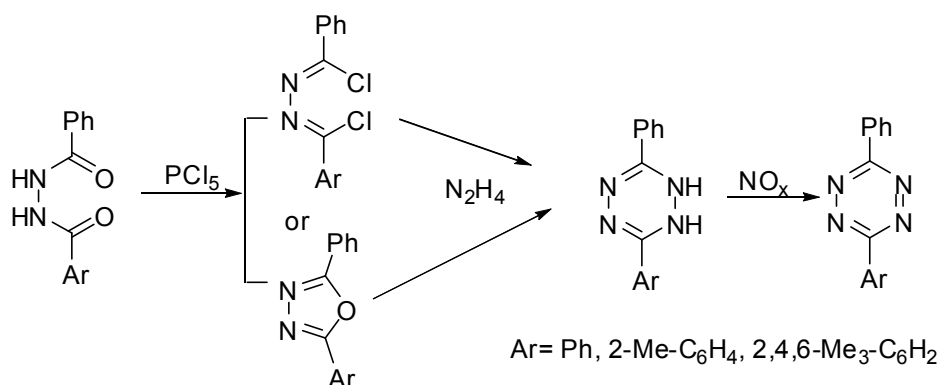
3,6-Dialkyl-hexahydro-1,2,4,5-tetrazines, also can be obtained through the reaction of alkyl aldehydes with hydrazine, which are then oxidized stepwise to give the 3,6-dialkyl-1,2,4,5-tetrazines^{24, 25} (Scheme 6). *s*-Tetrazines with branched substituents and mixed alkyl-*s*-tetrazines can be prepared by this procedure, however, in low yields.



R=R'=Me, Et, n-Pr, i-Pr, t-Bu, n-C₁₁H₁₃
 or R=Me, R'=Et
 R=Me, R'=i-Pr
 R=Me, R'=t-Bu
 R=Et, R'=i-Pr

Scheme 6. Preparation of 3,6-dialkyl-1,2,4,5-tetrazines.

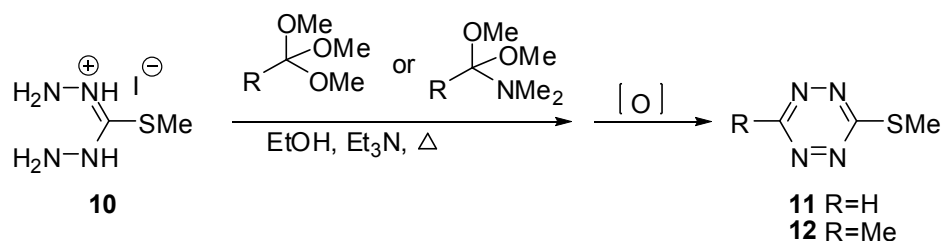
Another alternative method was developed by Stollé about 100 years ago^{26, 27}. Activation of the hydrazides with phosphorus pentachloride in refluxing tetrachloromethane affords the hydrazidedioyl dichloride or the 1,3,4-oxadiazole. Both react smoothly with hydrazine hydrate to yield dihydrotetrazines, which are oxidized by nitrous gases to the tetrazines (Scheme 7).



Scheme 7. Stollé's method for preparation of diaryl-1,2,4,5-tetrazines.

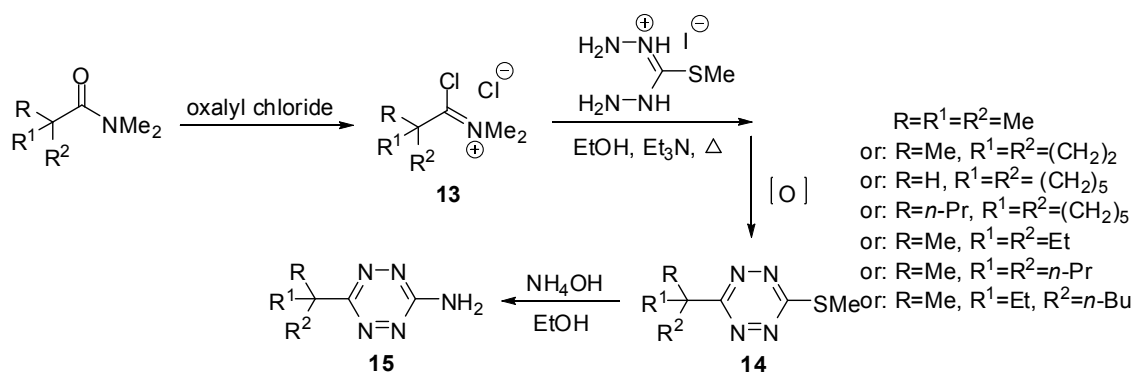
1.2.2 Ring closure of *S*-methylisothiocarbonohydrazide salt with orthoformate/ortho-acetates or iminium chlorides

Fields and his colleagues²⁸ have developed a two-step, one pot procedure for preparing unsymmetrically substituted 6-alkyl (or H)-3-(methylthio)-1,2,4,5-tetrazines (**11**, **12**). Reactions of *S*-methylisothiocarbonohydrazide salt (**10**) with trimethyl orthoformate, triethyl orthoacetate or dimethylformamide dimethyl acetal, and subsequent *in-situ* oxidation by either bubbling air through the reaction vessel or by adding H₂O₂, Br₂, or NaNO₂/CF₃COOH afforded a modest yield of tetrazines (Scheme 8).



Scheme 8. Fields' procedure for the preparation of tetrazines.

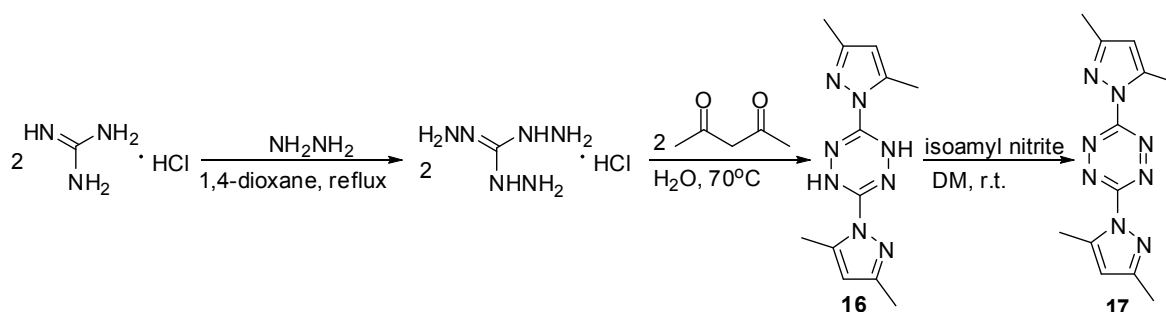
More highly-substituted substrates such as pivalate orthoesters and amide acetals were difficult to prepare and reacted poorly with **10**, giving invariably low yields of 6-tert-butyl-3-(methylthio)tetrazine (**14**). However, utilization of the more reactive iminium chloride **13** (Vilsmeier-type salt, formed by action of oxalyl chloride on N,N'-dimethylpivalamide) followed by *in situ* oxidation and amination with NH_4OH gave moderate yields of desired products (Scheme 9). This method supplements existing methodologies in being able to access tetrazines bearing tertiary alkyl groups and is amenable to scale-up. These compounds are also readily converted to 6-alkyl-3-aminotetrazines, broadening the applications of the method.



Scheme 9. Fields' procedure for the preparation of more hindered substituted tetrazines.

1.2.3 Aromatic Nucleophilic Substitution (S_NAr reaction)

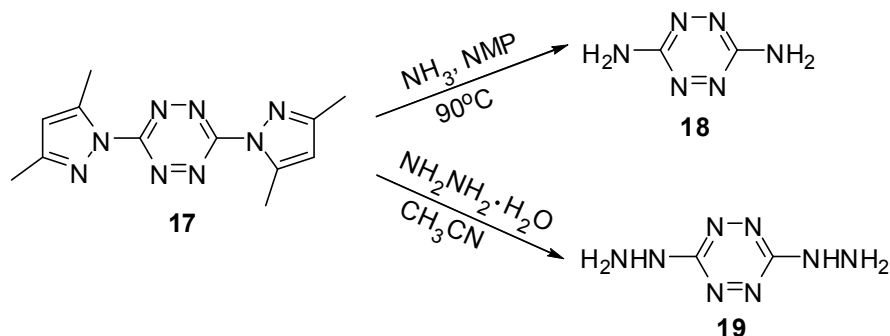
The elegant work of Hiskey's group²⁹⁻³² opened an access to the preparation of a large amount of symmetric and unsymmetric tetrazines. The basic starting compound, bis(dimethylpyrazolyl)-*s*-tetrazine (**17**), can be obtained efficiently from very cheap and accessible starting materials: guanidine, hydrazine, and 2,4-pentanedione (Scheme 10).



Scheme 10. Preparation of bis(dimethylpyrazolyl)-*s*-tetrazine.

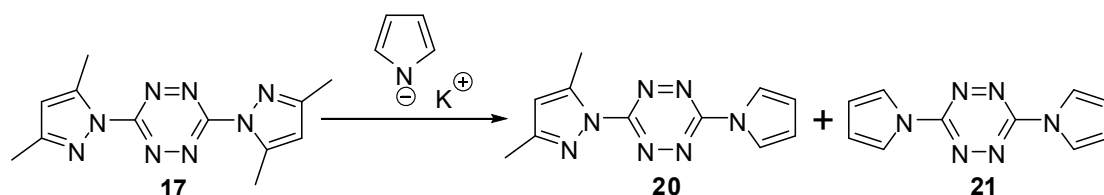
It should, however, be pointed out that the reaction involved had been discovered before²³, while **17** itself had been prepared for the first time even earlier, although in low yield³³.

The pyrazolyl groups in **17** act as soft leaving groups, allowing a large range of heterocyclic substituents to be introduced on the tetrazine ring, provided that the basic character of the entering nucleophile is not too strong and its hardness of medium strength. This has been done in particular with hydrazine and ammonia^{29, 30} (Scheme 11).



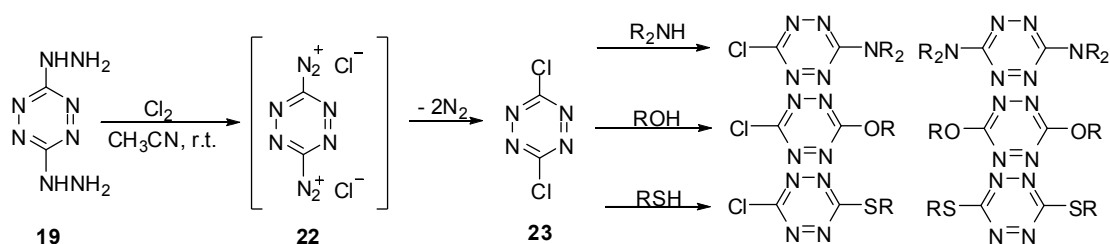
Scheme 11. Substitution of bis(pyrazolyl)-s-tetrazine with hydrazine and ammonia.

Audebert and colleagues²¹ have also used the S_NAr reaction of tetrazines with N-pyrrolyl anion to prepare mono- and bis- pyrrolyl tetrazines (**20** and **21**) to investigate their electrochemical and spectroscopic properties, as well as their electrochemical polymerization (Scheme 12):



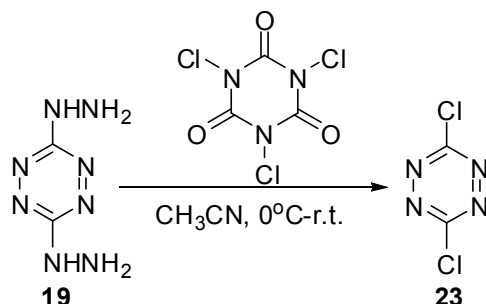
Scheme 12. Substitution of bis(pyrazolyl)-s-tetrazine with pyrrolyl anion.

Thereafter, Hiskey *et al.* have found a more general method that is to convert bis(hydrazino)-s-tetrazine (**19**) to dichloro-s-tetrazine (**23**) with chlorine gas, which, due to its stronger electron affinity, is more readily to undergo S_NAr reaction with a large variety of nucleophiles such as NH_3 , morpholine, pyrrolidine, hydrazine, alcohols, mercaptans, carbanions, etc, thus opening an access to various symmetric and unsymmetric tetrazines (Scheme 13).



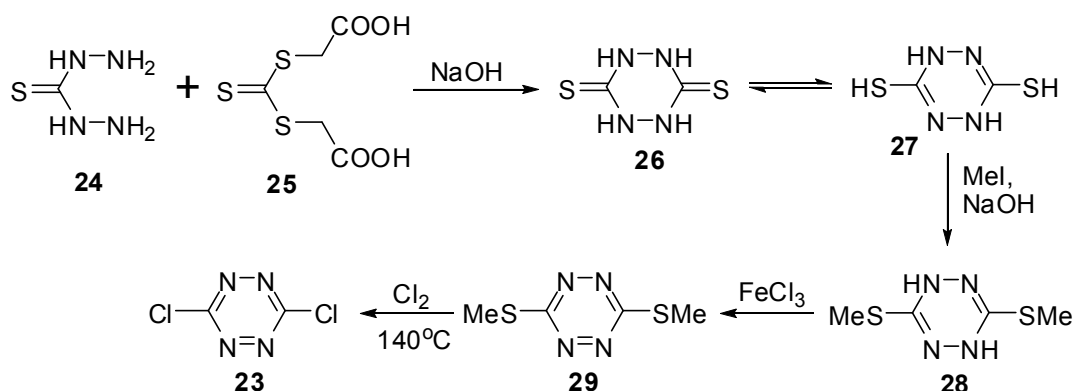
Scheme 13. Preparation of dichloro-s-tetrazine and its S_NAr reactions with nucleophiles.

Very recently, Helm and colleagues³⁴ have reported a new method for chlorination of bis(hydrazino)tetrazine. Using a solid chlorination agent, trichloroisocyanuric acid, the bis(hydrazino)-*s*-tetrazine is converted smoothly to dichloro-*s*-tetrazine, thus the use of more dangerous, less controllable gaseous chlorine is avoided (Scheme 14).

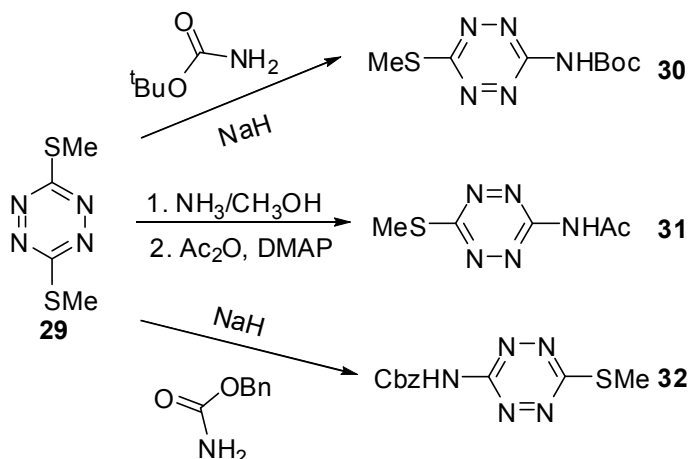


Scheme 14. Chlorination of bis(hydrazino)-*s*-tetrazine using trichloroisocyanuric acid.

3,6-Dimethylthio-*s*-tetrazine (**29**), historically obtained before dichloro-*s*-tetrazine because it is readily available from the reaction of thiocarbohydrazide **24** with dicarboxymethyl-trithiocarbonate **25** (Scheme 15)³⁵⁻³⁷, was also and today is still an often-used starting compound for the preparation of unsymmetrically disubstituted tetrazines via S_NAr reaction³⁸ (Scheme 16). In fact dichloro-*s*-tetrazine was firstly prepared from the chlorination of dimethylthio-*s*-tetrazine with chlorine gas at high temperature, although in poor yield³⁹.



Scheme 15. Preparation of dimethylthio-*s*-tetrazine and dichloro-*s*-tetrazine.



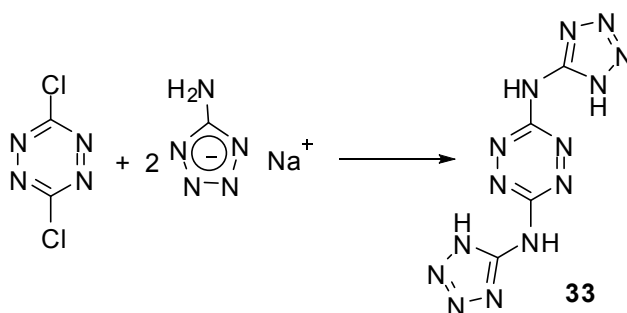
Scheme 16. Substitution of dimethylthio-*s*-tetrazine.

1.3 Reactivity of tetrazines

1.3.1 Aromatic nucleophilic substitution (S_NAr reaction)

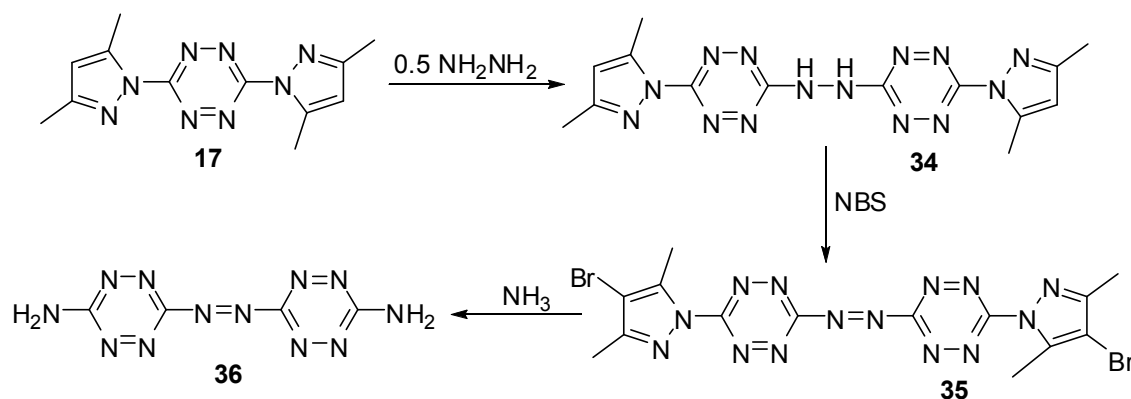
Due to their electron affinity on the aromatic core, tetrazines bearing appropriate leaving groups readily undergo aromatic nucleophilic substitution in the presence of nucleophiles. This is especially true for 3,6-dichloro-1,2,4,5-tetrazine, because chlorine acts as a good leaving group and at the same time, a strong $-I$ (electron-withdrawing inductive effect) group that enhances the electron deficiency of the tetrazine ring, thus facilitating the nucleophilic attack on the ring.

Hiskey and colleagues³⁰ have synthesized 3,6-bis(1H-1,2,3,4-tetrazol-5-ylamino)-1,2,4,5-tetrazine (**33**), an energetic molecular material, by substitution of dichloro-*s*-tetrazine with the sodium salt of 5-amino-tetrazole (Scheme 17):



Scheme 17. Substitution of dichloro-*s*-tetrazine with tetrazole anion.

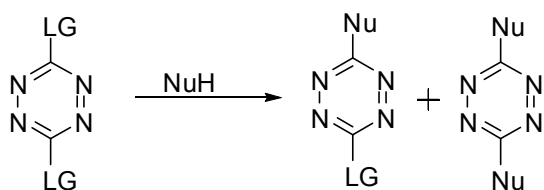
Bis-substituted pyrazolyl-*s*-tetrazine (**17**) also undergo substitution reactions with nucleophiles like hydrazine or ammonia, as already mentioned above (Chapter 1.2.3). This has been used by Hiskey's group to prepare a new high-nitrogen energetic material: 3,3'-azobis(6-amino-1,2,4,5-tetrazine)³¹ (**36**, Scheme 18):



Scheme 18. Substitution of tetrazines with hydrazine and ammonia.

Kotschy's group⁴⁰ has explored the selectivity of nucleophilic substitutions on various tetrazines. They established that 3,6-dichloro-*s*-tetrazine (**23**), 3,6-bis(3,5-dimethylpyrazol-1-yl)-*s*-tetrazine (**17**) and 3,6-bis(4-bromo-3,5-dimethylpyrazol-1-yl)-*s*-tetrazine (**37**) undergo nucleophilic substitution with a variety of nucleophiles to give mono- and/or disubstituted products depending on the nature of the leaving group and the nucleophile used (Scheme 19). When dichloro-*s*-tetrazine was reacted

with a series of nucleophiles, the chlorine atoms were both good leaving groups, while the electron donating substituents led to a marked decrease of reactivity, which in turn allowed for only mono-substitution (in the cases of NH₃, KOH, N₂H₄, morpholine, BuNH₂, Et₂NH and pyrrolidine). When MeOH, a stronger nucleophile, was used, the yield of the monosubstituted product decreased to ~50%, and a nearly equal amount of the disubstituted one was isolated. With ⁱBuSH, an even stronger nucleophile, most tetrazines were disubstituted even when the mercaptan was present in less than one equivalent per chlorine atom, indicating a strong tendency for disubstitution of dichloro-*s*-tetrazine with mercaptans. The other tetrazines, **17** and **37**, showed the same tendency albeit less markedly, reflecting the lower ability of pyrrazolyl rings to act as good leaving group (Table 1).



LG: chloro; 3,5-dimethylpyrazol-1-yl; 4-bromo-3,5-dimethylpyrazol-1-yl

Nu: NH₃, MeOH, ⁱBuSH, KOH, N₂H₄, morpholine, BuNH₂, Et₂NH, pyrrolidine

Scheme 19. Substitution of tetrazines by various nucleophiles.

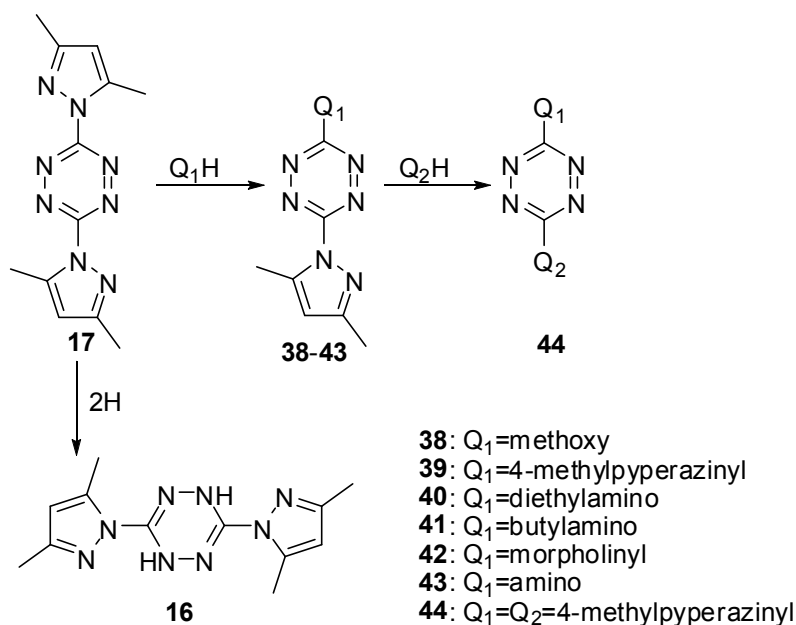
Table 1. Results observed for the substitution of tetrazines by various nucleophiles (yield %).

LG	NuH	monosubstitution	disubstitution
Chloro (23)	NH ₃	78%	
	MeOH	52%	39%
	ⁱ -BuSH	5%	76%
	morpholine	83%	
	BuNH ₂	65%	
	Et ₂ NH	89%	
	pyrrolidine	68%	
3,5-dimethylpyrazol-1-yl (17)	NH ₃	96%	
	MeOH	80%	3%
	ⁱ -BuSH	66%	12%
	KOH	78%	
	N ₂ H ₄	85%	
	morpholine	77%	
	BuNH ₂	91%	
	Et ₂ NH	46%	
	pyrrolidine	74%	
4-bromo-3,5-dimethylpyrazol-1-yl (37)	NH ₃	72%	
	MeOH	63%	8%
	ⁱ -BuSH	23%	43%
	KOH	81%	
	morpholine	83%	

When a high-energy positron (e⁺), the antiparticle of an electron (e⁻), enters a condensed medium, it will thermalize in a few picoseconds by losing its kinetic

energy via ionization of the molecules of the medium^{41,42}. After thermalization, the positron annihilates with an electron into γ quanta either via a free annihilation process or from a bound state, which is known as a positronium (Ps) atom. Ps is the simplest hydrogen-like exotic atom which can be considered as the lightest, “0 mass number isotope” of hydrogen, where the heavy proton has been exchanged by the much lighter positron. Due to the different spin combinations of a positron and an electron, there are two possible Ps states, the para-positronium (p-Ps) with antiparallel (singlet) spin state and the ortho-positronium (o-Ps) with parallel (triplet) spin state. The intrinsic lifetimes of p-Ps and o-Ps are 0.125 and 140 ns, respectively. According to the basic idea of the spur model of positronium formation, a thermalized positron can form a Ps atom with an electron which is freed by the positron itself in its ionization track or spur. Through its different decay modes Ps can be used as an efficient microprobe of various physical or chemical properties of matter.

Lévy and co-workers have measured the chemical reaction rate constants of the nucleophilic ortho-positronium (o-Ps) atom with a series of tetrazine derivatives (**16**, **17**, **38-44**, Scheme 20) by positron annihilation lifetime spectroscopy⁴³. The pronounced reactivity of tetrazines toward o-Ps stems from the electrondeficient tetrazine core: when the aromaticity of the tetrazine core is destroyed by reduction to 1,2- or 1,4-dihydro-*s*-tetrazines, the reactivity decreases dramatically by nearly 200-fold. The introduction of electron-donating substituents onto the tetrazine ring decreases the reactivity of the molecule toward o-Ps. The measured reaction rate constants of o-Ps also result in a good linear correlation with the calculated LUMO energies of the tetrazines. The reactivity of tetrazines toward o-Ps correlated well also with their reactivity toward classical nucleophiles.



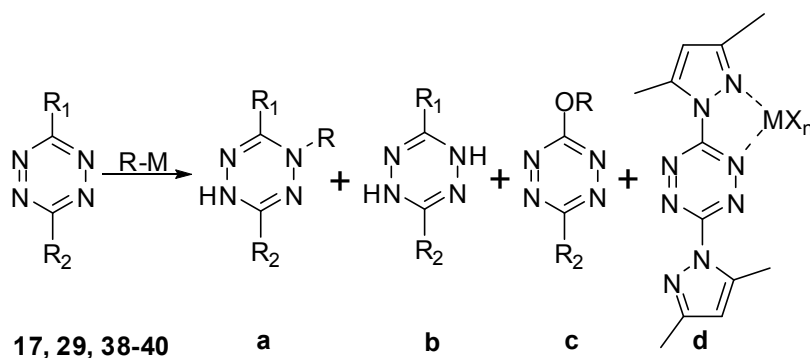
Scheme 20. Tetrazines used in annihilation with o-Ps.

1.3.2 Azaphilic addition with carbanions

When reactive carbon nucleophiles such as organolithium or Grignard reagents are used in an attempt to substitute 3,6-bis(methylthio)-*s*-tetrazine, the organic groups only add onto a ring nitrogen atom, giving “azaphilic addition”

transformation⁴⁴, which is quite unprecedented for other heterocycles, but had been reported previously for 3,6-diphenyl tetrazine, too⁴⁵⁻⁴⁸.

Kotschy's group⁴⁹ has reacted a series of organometallic reagents with different tetrazines (Scheme 21). They observed that more polar organometallic reagents, especially lithium, magnesium and zinc derivatives showed a marked affinity towards the nitrogen atom of the tetrazine core, a behaviour fairly unusual in heterocyclic chemistry. Some reduction or oxidative rearrangement of the azaphilic adducts to alkoxy/aryloxy tetrazines were also observed in certain cases (Table 2).



17: R₁=R₂=3,5-dimethyl-pyrazol-1-yl

29: R₁=R₂=methylthio

45: R₁=R₂=3-pyridyl

46: R₁=3,5-dimethyl-pyrazol-1-yl, R₂=morpholino

47: R₁=morpholino, R₂=chloro

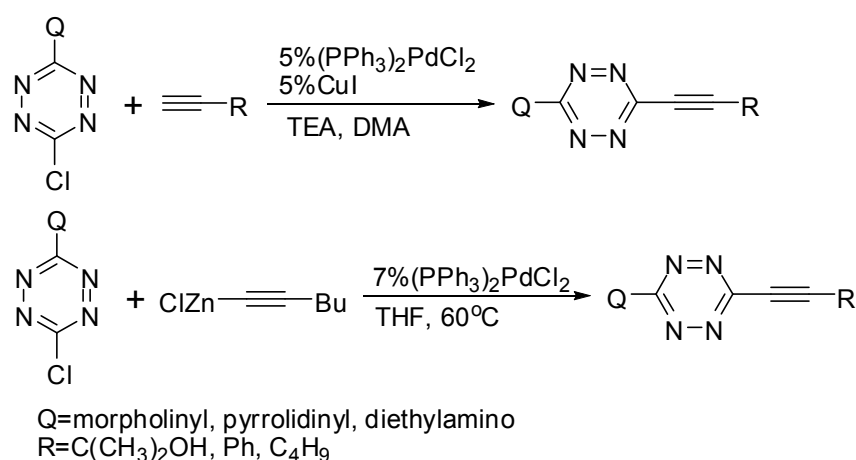
Scheme 21. Azaphilic addition reactions of tetrazines with carbanions.

Table 2. Results of azaphilic addition reactions of tetrazines with carbanions (yield %).

No.	Substrate	R-M	a (%)	b (%)	c (%)	d (%)
1	17	BuLi	70	5		
2	17	PhLi	62			
3	17	PhMgCl	85			
4	17	BuCuLiI	60			40
5	17	BuZnBr	85			15
6	17	PhZnBr	90			
7	17	PhZnBr	45			35
8	17	(C ₃ H ₅) ₃ In ₂ Br ₃	60			
9	17	(C ₃ H ₅) ₃ In ₂ Br ₃	50	50		
10	45	BuLi	13	32		
11	45	BuMgI	96			
12	45	PhLi	35	25		
13	45	PhMgCl	58			
14	46	BuLi	13		80	
15	46	BuMgI	43		56	
16	46	PhLi	85			
17	46	PhMgCl	90			
18	29	BuLi	90			
19	29	PhLi	80			
20	29	PhMgCl	94			
21	47	PhMgCl	dec.			

1.3.3 Cross-coupling reactions with terminal alkynes

There remains some difficulty in the preparation of nonsymmetrically substituted tetrazines, since the frequently utilized nucleophilic substitution reactions have been mostly limited to amines and alcohols, which decrease the electron affinity of the tetrazines after monosubstitution because of the electron donating nature of these substituents. Kotschy's group⁵⁰ has successfully accomplished the cross-coupling reactions of a series of substituted chlorotetrazines with different terminal alkynes under Sonogashira or Negishi coupling conditions to furnish alkynyl-*s*-tetrazines in good to moderate yield (Scheme 22). The electron-donating properties of the substituent on the tetrazine core were found to have a significant influence on the success of the reaction. These results constitute the first cross-coupling reactions on tetrazines.



Scheme 22. Cross-coupling reactions of tetrazines with terminal alkynes.

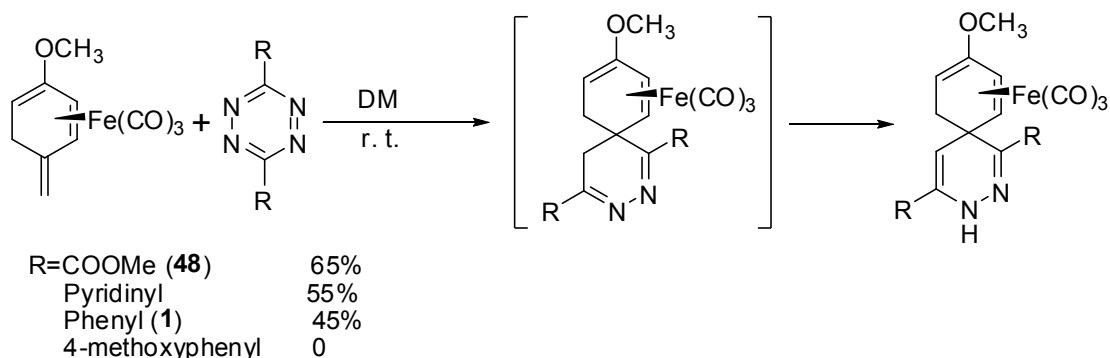
1.3.4 Inverse electron-demand Diels-Alder reaction

1,2,4,5-Tetrazines, as electron deficient dienes, are largely involved in inverse electron demand Diels-Alder reactions, which are adopted as convenient methods for the preparation of various substituted pyridazines or the construction of fused heterocycles, or as key steps in total synthesis of complex natural products. Since the initial report of symmetrical perfluoroalkyl 1,2,4,5-tetrazines participating in [4+2] cycloaddition reactions with olefins, which constituted the first demonstration of the viability of the inverse electron demand Diels-Alder reaction⁵¹, extensive investigations have defined the scope and potential of 1,2,4,5-tetrazine participating in [4+2] cycloaddition processes. A wide range of dienophiles and heterodienophiles are capable of participating in Diels-Alder reactions with electron-deficient 1,2,4,5-tetrazines, including electron-rich, neutral, and electrondeficient olefins, acetylenes, dienes, enol ethers and acetates, enamines, ynamines, ketene acetals, enolates, benzyne, selected aromatics, imidates, amidines, thioimidates, imines, aziridines and cyanamides.

There have already been several reviews^{52, 53} and book chapters^{54, 55} concerning the inverse electron demand Diels-Alder reactions of 1,2,4,5-tetrazines till

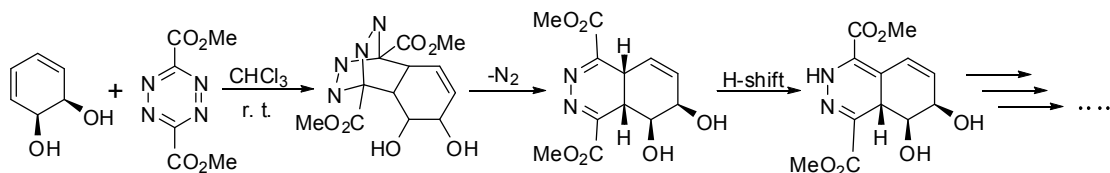
1996. During recent years, the Diels-Alder cycloaddition reaction of tetrazines has continued to be the subject of extensive studies, and a lot of molecules containing heterocycles, including natural products are synthesized through this type of reaction.

For example, Chi Wi Ong⁵⁶ and co-workers have used highly electron deficient 1,2,4,5-tetrazines to react with tricarbonyl[(1-4-η)-2-methoxy-5-methylene-cyclohexa-1,3-diene]iron to construct spiro skeletons (Scheme 23). They found that the (4+2) cycloaddition reactions took place exclusively with highly electron deficient tetrazines to form spiro[5.5]undecane system in good yield, while due to its more electron-rich nature, the bis(4-methoxyphenyl)-1,2,4,5-tetrazine did not react.



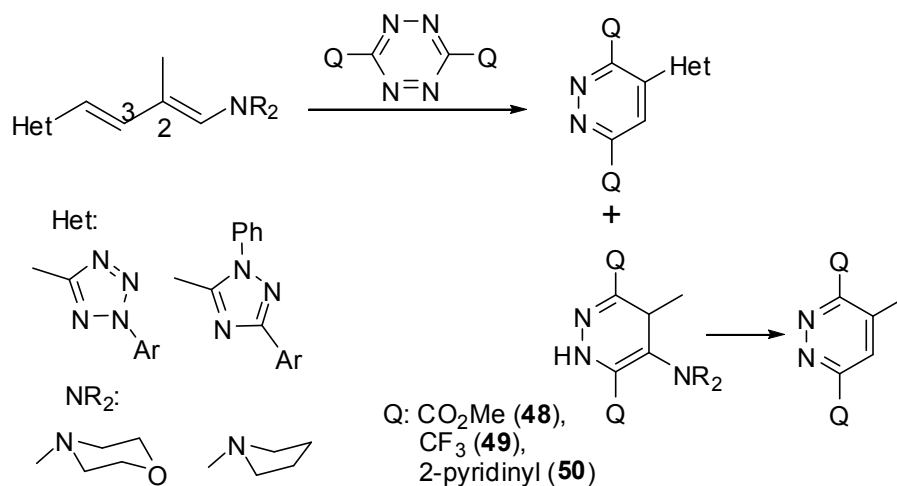
Scheme 23. Tetrazines for construction of spiro skeletons.

Balci and co-workers⁵⁷ also used inverse-Diels-Alder reaction of electron deficient tetrazine **48** with benzene cis-diol to produce dihydrodiol containing the 1,4-dihydropyridazine ring, a carcinogenic compound which is useful in biological study (Scheme 24).



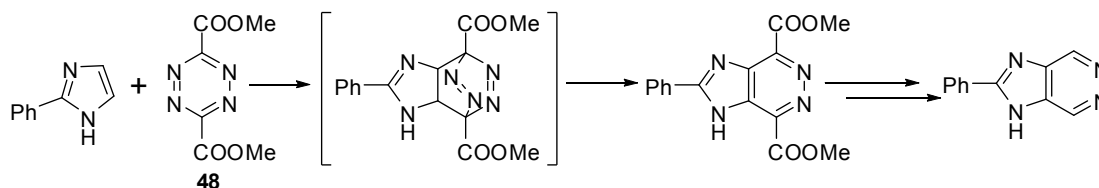
Scheme 24. Reaction of tetrazine with benzene cis-diol.

Kotschy and co-workers⁵⁸ found that appropriately substituted azolydienamines are readily to undergo double “inverse electron-demand” Diels-Alder reactions with tetrazine derivatives, yielding azolypyridazines and dihydropyridazines as products, which implies that any of the double bonds of dienamine can react with a molecule of tetrazine and at some stage, fission of the C(2)-C(3) bond also took place. The highly electron-deficient bis(methylcarboxylate)-*s*-tetrazines (**48**), bis(trifluoromethyl)-*s*-tetrazine (**49**) and bis(2-pyridyl)-*s*-tetrazine (**50**) were used as dienes (Scheme 25).



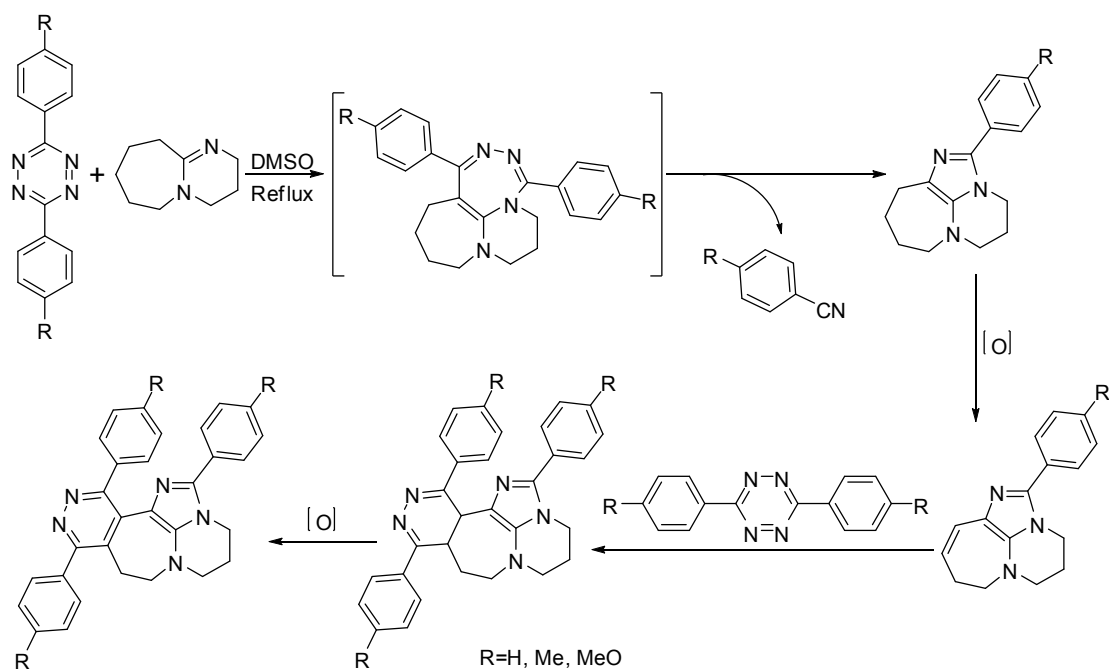
Scheme 25. Reaction of tetrazine with azolydienamines.

Snyder and colleagues⁵⁹ have used 2-substituted imidazoles as dienophiles in inverse electron demand Diels-Alder reactions with **48** to produce imidazo[4,5,d]pyridazines in excellent yields (Scheme 26), while the cycloadditions of imidazoles with 3-hydro-6-methylthio-*s*-tetrazine (**11**) or 3,6-bis(methylthio)-*s*-tetrazine (**29**) are unproductive.



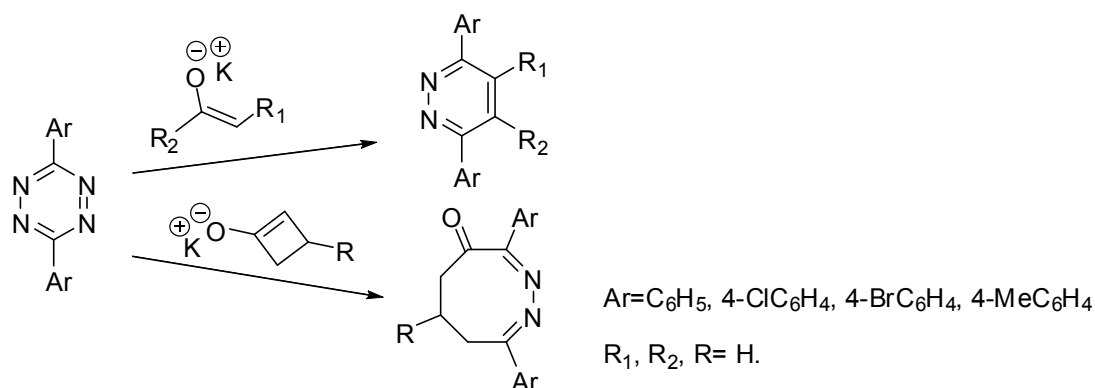
Scheme 26. Tetrazines used for synthesis of imidazo[4,5,d]pyridazines.

Given high enough temperature, bis-aryl-1,2,4,5-tetrazines can react with DBU to give a fused heterocyclic ring system (Scheme 27)⁶⁰. In this process, DBU acts as both reactant and reducing agent while the tetrazine acts as both reactant and oxidizing agent. It is noteworthy that this novel reaction involves the sequential addition of amidines, enamines, and dienamines (originally present or generated from DBU) to the tetrazine moiety. It also demonstrates the ability of 1,2,4,5-tetrazines to perform oxidation.



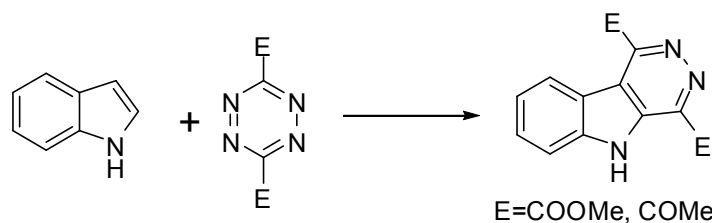
Scheme 27. Reactions of tetrazines with DBU.

Kurth's group has investigated reactions of 1,2,4,5-tetrazines with acyclic and cyclic enolate nucleophiles⁶¹. When the carbon nucleophile is derived from cyclobutanone, condensation is followed by nitrogen extrusion and ring expansion to give a conformationally restricted 8-member ring (Scheme 28).



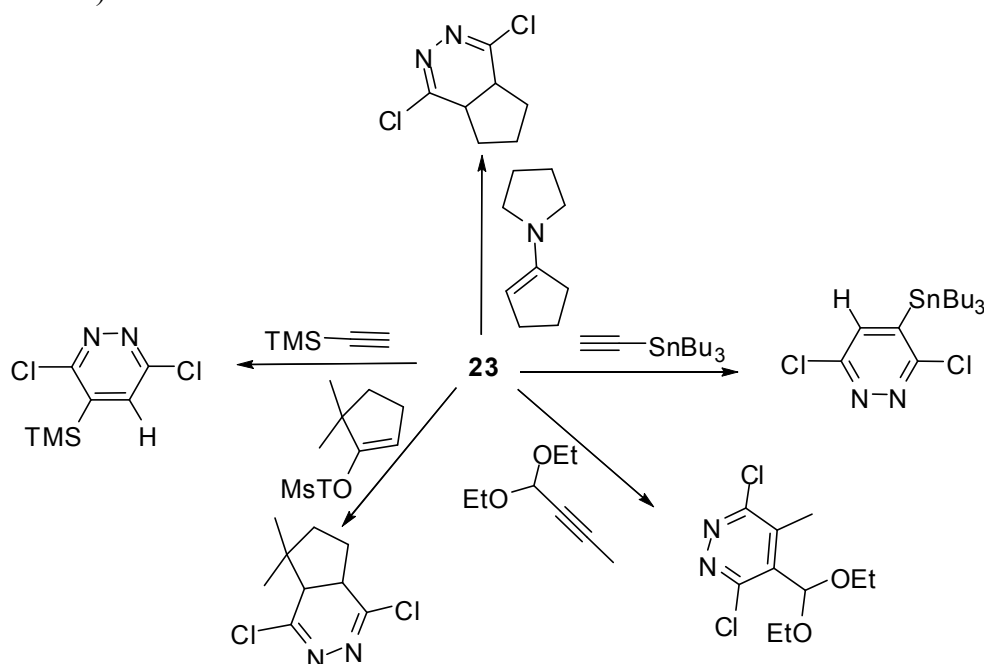
Scheme 28. Reactions of 1,2,4,5-tetrazines with acyclic and cyclic enolate nucleophiles.

Snyder and colleagues⁶² have found that indoles react readily with 3,6-dimethylcarboxylate-1,2,4,5-tetrazine (**48**) through inverse electron demand Diels-Alder reaction (Scheme 29). 3,6-bis-acetyl-*s*-tetrazine also reacts with indoles to obtain pyridazino[4,5,*b*]indoles, although in lower yields.



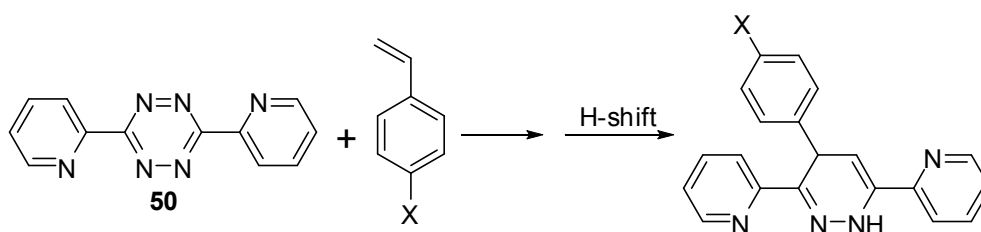
Scheme 29. Inverse electron demand Diels-Alder reactions of tetrazines with indoles.

3,6-Dichloro-*s*-tetrazine, due to its more electrodefficient character than bis-methylthio-*s*-tetrazine, undergoes D-A reaction with a variety of alkenes and alkynes, in toluene or dichloromethane to provide pyridazines. Stannyl and silyl alkynes, enol ethers and enamines all react readily to afford substituted pyridazines in good yield (Scheme 30)⁶³.



Scheme 30. Inverse electron demand Diels-Alder reactions of dichloro-*s*-tetrazine with alkenes and alkynes.

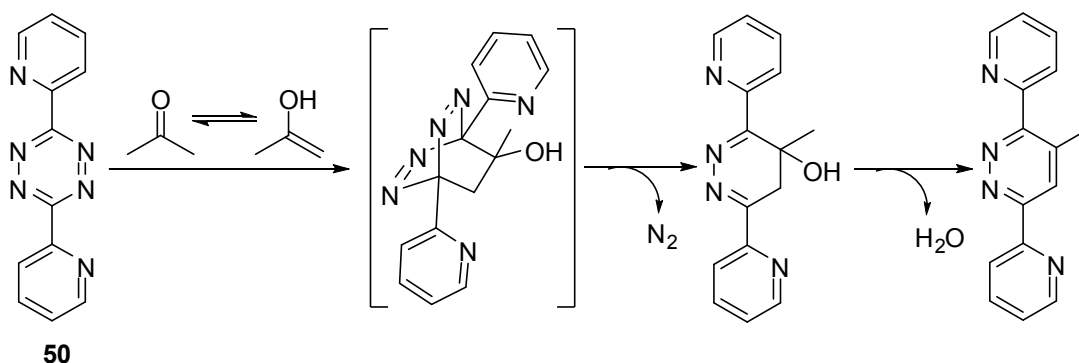
The di(2-pyridyl)-1,2,4,5-tetrazine (**50**) reacts readily with substituted styrenes in aqueous media and in organic solvents (Scheme 31)⁶⁴. The reaction is solvent sensitive:



X=MeO, Me, H, Cl, NO₂

Scheme 31. Reactions of di(2-pyridyl)-1,2,4,5-tetrazine with substituted styrenes.

Tetrazine **50** also reacts with alkynes, and the reaction can be accelerated under super heated microwave conditions. Moreover, ketones and aldehydes can also be applied as dienophiles in the reaction with **50** (Scheme 32)⁶⁵. The reactions proceed via the cycloaddition of enol tautomers with tetrazines and the subsequent extrusion of N₂ followed by loss of a water molecule.

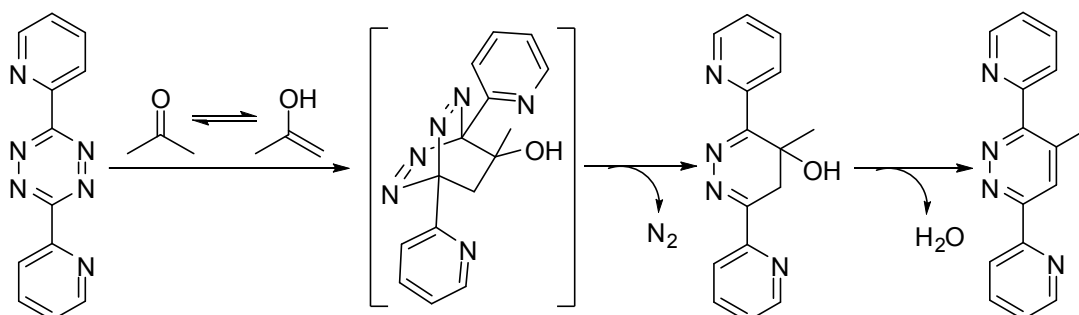


50

Scheme 32. Reaction of 3,6-di(pyridin-2-yl)-1,2,4,5-tetrazine with acetone.

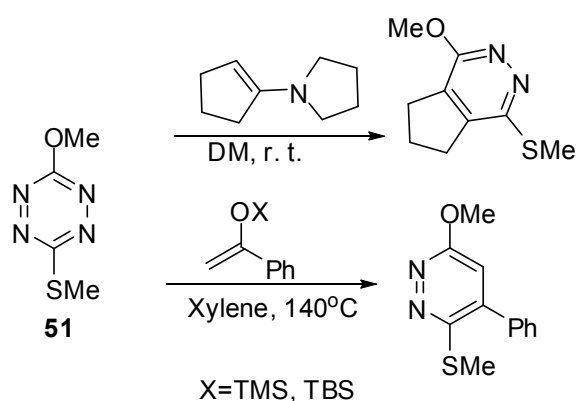
The reaction of di-methylthio-*s*-tetrazine with methanol in the presence of catalytic NaOMe affords the unsymmetric 3-methoxy-6-methylthio-*s*-tetrazine (**51**), which reacts readily with various electron-rich and neutral dienophiles (Scheme 33)⁶⁶. The reaction pathway is similar to the one described in Scheme

32



50

Scheme 32. Reaction of 3,6-di(pyridin-2-yl)-1,2,4,5-tetrazine with acetone, with a final loss of HX instead of H₂O.



Scheme 33. Reactions of unsymmetric tetrazine with electron-rich and neutral dienophiles.

Boger and colleagues⁶⁷ have disclosed the order of reactivity of a series of tetrazines in inverse electron demand D-A reactions with electron-rich dienophiles (Figure 5):

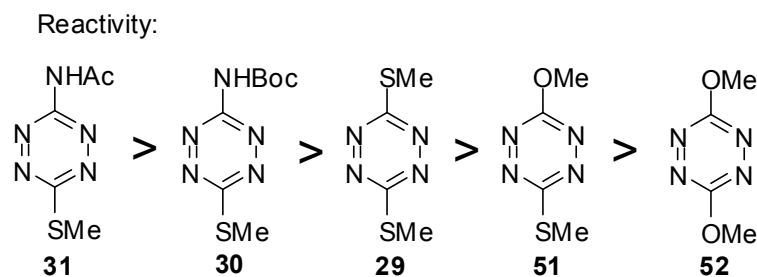
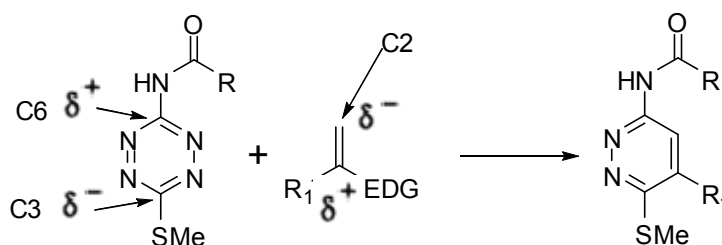


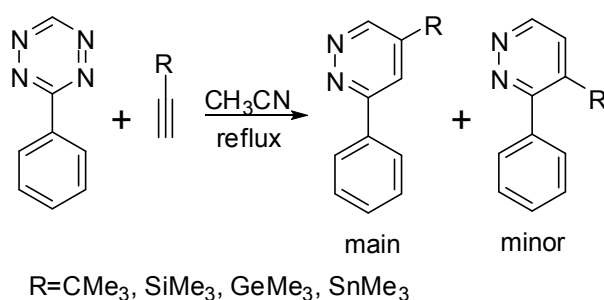
Figure 5. The order of reactivity of a series of tetrazines in inverse electron demand D-A reactions with electron-rich dienophiles.

They also found that the cycloaddition regioselectivity is consistent with the polarization of the diene and the ability of the methylthio group to stabilize a partial negative charge at C-3, and the N-acylamino group to stabilize a partial positive charge at C-6 (Scheme 34):



Scheme 34. The cycloaddition regioselectivity of 3-acylamino-6-methylthio-tetrazine in inverse electron demand D-A reactions.

The cycloaddition of 3-aryl-1,2,4,5-tetrazines with various monosubstituted alkynes occurs with high regioselectivity to yield corresponding 3,5-disubstituted pyridazines in high yield⁶⁸. The production of minors 3,4-disubstituted pyridazines is neglectable (Scheme 35).



Scheme 35. The cycloaddition of 3-aryl-1,2,4,5-tetrazines with monosubstituted alkynes.

1.4 Research development and applications of tetrazines

1.4.1 Tetrazines as molecular models for theoretical studies

1.4.1.1 Research about their electronic states

s-Tetrazines, due to their special structural features (symmetric substitution of C by N, low-lying π^* orbital, etc.), are subjects of numerous theoretical investigations. For example, *s*-tetrazine ($\text{C}_2\text{N}_4\text{H}_2$), with eight atoms and an aromatic ring, can truly represent polyatomic systems, yet small enough to allow a detailed

vibronic analysis of excited-state spectra. In fact *s*-tetrazine features a rich set of vibrational motions, including ring breathing, puckering, bending, and stretching vibrations, which can be selectively observed by tunable laser beams.

It is particularly interesting to investigate tetrazine derivatives, since they represent the special, rare case of a “three-dimensional” organic chromophore with well separated and relatively strong transitions in three perpendicular directions, determined by molecular symmetry. Much effort has already been devoted to characterize their ground and excited electronic states.

Early in 1959, the vibrational structures of the visible absorption spectrum of *s*-tetrazine, dideutero-*s*-tetrazine, and dimethyl-*s*-tetrazine have been measured in the vapour at low temperature by Mason⁶⁹. For the vapour of *s*-tetrazine the strongest band is the 0-0, which shifts towards the red end of the spectrum in the dideutero-derivative. The observed upper-state progressions are short, indicating that the electronic transition, whilst of low oscillator strength, is allowed by symmetry, and that there is little change in the size of the molecule in excitation, although the molecular zero-point energy increases. The particular vibrations active in the electronic transition suggest that *s*-tetrazine assumes a more regular hexagonal shape on excitation.

Barone and colleagues⁷⁰ have also applied Time-dependent density functional theory (TDDFT) to calculate vertical excitation energies of *s*-tetrazine both in the gas-phase and in aqueous solution. The model density functional (PBE0) is obtained by combining the Perdew-Burke-Erzenrhof (PBE) generalized gradient functional with a predetermined amount of exact exchange, while the polarizable continuum model (PCM) is used to mime solvent effects on electronic transitions. The results in the gas phase show that the PBE0 functional provides accurate excitations both to valence and to low-lying Rydberg states. At the same time, the experimental solvent shifts in aqueous solution are well reproduced when the solute and the first solvation shell are embedded by a continuum solvent. These results show the potentialities of the combined TDDFT/PCM approach for the study of UV spectra of aromatic compounds.

Weber and colleagues⁷¹ have calculated the electron diffraction patterns of *s*-tetrazine in specific electronic and vibrational states for isotropic samples, for molecules that are aligned in high-intensity laser fields, and for orientationally clamped molecules. They found that both the electronic and the vibrational excitations lead to changes in the diffraction patterns of isotropic samples in the range of $\pm 1\%$.

Thulstrup and colleagues³ have studied six symmetrically disubstituted derivatives of *s*-tetrazine by linear dichroism spectroscopy in the UV-visible region, magnetic circular dichroism spectroscopy, and theoretical calculations of structure and spectra (Figure 6). The electronic absorption spectra show three major, characteristic transitions: an out-of-plane polarized $n\text{-}\pi^*$ transition at lowest energy, an in-plane, short axis polarized $\pi\text{-}\pi^*$ transition at higher energy and a third, long axis polarized transition at higher energy. The calculated and observed transition moments and energies for these transitions are in good agreement.

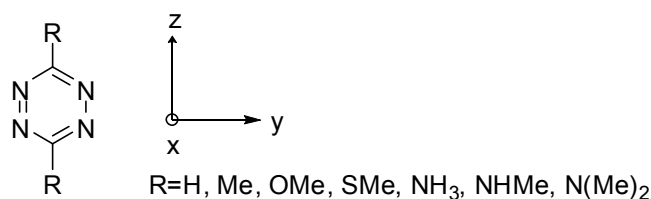


Figure 6. Tetrazines studied by Thulstrup's group.

Thulstrup and colleagues⁷ have also investigated the electronic structures of 3,6-diphenyl-*s*-tetrazine (**1**), 3,6-bis(4-pyridyl)-*s*-tetrazine (**53**), 3,6-bis(3-pyridyl)-*s*-tetrazine (**45**), and 3,6-bis(2-pyridyl)-*s*-tetrazine (**50**), by linear dichroism (LD) UV-Vis absorption spectroscopy, magnetic circular dichroism (MCD) spectroscopy, and quantum chemical calculations (Figure 7). The LD spectra contain information on the transition moment directions of the observed electronic transitions, and lead to resolution of the otherwise hidden transitions in combination with the MCD spectra. The electronic transitions predicted by time dependent density functional theory using molecular geometries determined by X-ray crystallography are in excellent agreement with the observed transitions. The combined experimental and theoretical evidence lead to a consistent assignment of electronic states.

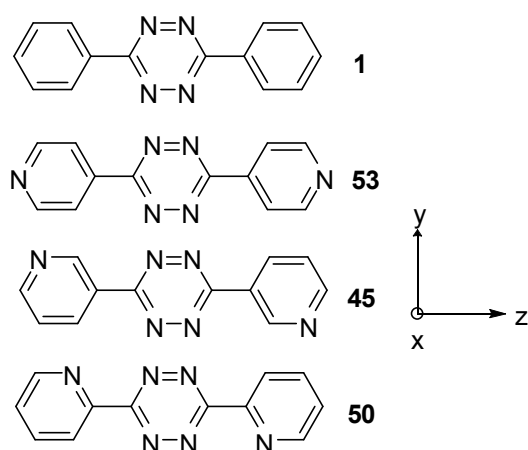


Figure 7. Tetrazines studied by Thulstrup's group.

1.4.1.2 Research on electron interactions: complexes with rare gas atoms

Apart from understanding their electronic ground and excited states, the *s*-tetrazine is also of considerable interest from the standpoint of understanding the interactions amongst non-bonding electrons and between bonding and non-bonding electrons. Levy's group⁷²⁻⁷⁵ has investigated detailedly the van der Waals complexes of *s*-tetrazines with the rare gases He, Ar and Kr. For example, they have formed the complexes of *s*-tetrazine with He and Ar in a supersonic free jet, and observed them by the technique of laser induced fluorescence⁷². The resolution of rotational structure in the $n-\pi^*$ electronic transition of the *s*-tetrazine chromophore allows the structure of these complexes to be measured. The complex between *s*-tetrazine and one argon atom is similar to that observed between *s*-tetrazine and He. The argon lies near the out-of-plane *A* rotational axis with a ground state separation of 3.44 Å, which decreases to 3.40 Å in the excited state. When the number of complexing atom is two or less, they are found to always bind directly above and below the tetrazine ring. Complexes containing three or more rare gas atoms have also been observed and their structures have been measured. In this case the out-of-plane preferential binding sites

are filled by the first two atoms and additional atoms must find new sites. As long as one or more argon atoms are present, additional rare gas atoms bind to an argon atom which is itself bound to the tetrazine ring at an out-of-plane site. The fluorescence excitation and dispersed fluorescence spectra of the complexes have been studied to determine the van der Waals bond stretch and bend frequencies⁷⁴. In the case of tetrazine-Xe, a vibrational progression spanning $\nu = 0$ to 8 in the bend vibrations was detected. The harmonic frequencies of the van der Waals bond stretch and bond bend vibrations are found to be very similar for the tetrazine-Xe, tetrazine-Kr and tetrazine-Ar clusters. Spectra of the symmetric trimer of xenon-tetrazine-xenon show progressions in the van der Waals bond stretch vibration up to $\nu'' = 5$. The frequencies of the stretch vibration on tetrazine-xenon and the symmetric stretch vibration in xenon-tetrazine-xenon support the validity of pairwise additivity of the van der Waals potentials. The excitation spectra also indicate the presence of other more complicated clusters of tetrazine with xenon.

1.4.2 Tetrazine derivatives for NLO

Tetrazine derivatives appear to be very promising targets with respect to the search for new optical and electroactive molecules as potential candidates for devices. Tetrazine is the most electrodeficient aromatic heterocycle of the C-N family², and their strong electron affinity is expected to enhance the charge transfer in related conjugated molecules leading to enhanced nonlinear optical (NLO) properties. Moreover, the reversible electrochemical reduction displayed by most tetrazines might also constitute a useful feature for the achievement of electroswitchable NLO devices.

Within this topic, Audebert's group⁷⁶ has prepared two donor-acceptor-donor tetrazines containing ferrocene moieties as donor units (Figure 8, **54a** and **54b**), one of them also containing a phenyl unit as a π -bridge (**54b**), and investigated their spectral and electrochemical properties. UV-vis spectroscopic and cyclic voltammetric studies show intramolecular charge transfer interaction in the solution, especially when there is no spacer in the molecule. The oxidation potential of ferrocene moieties indicates that the influence of the tetrazine ring on Fc is considerably greater in **54a** than in **54b** in the ground state due to the presence of the phenyl linkage between the ferrocene and tetrazine moieties, which increases the electron density on the Fc units. On the other hand, UV-vis studies show an increase of charge delocalization due to the phenyl linkage between the ferrocene and tetrazine moieties. Both tetrazines display reduction potentials in the same range, showing a much weaker influence of the Fc substituents on the tetrazines than the other way around. Although the voltammograms are not fully reversible for compound **54a**, both tetrazines constitute potential molecules for device applications. The third-order NLO properties of **54a** and **54b** were also investigated, and the results show that the ferrocenyl group does not play a highly positive role in the optimization of γ values. However, it evidences the possible role of metal-to-ligand charge transfer on third-order hyperpolarizability values, confirming the counteractive effect of the charge transfer process already reported for quadratic nonlinear responses.

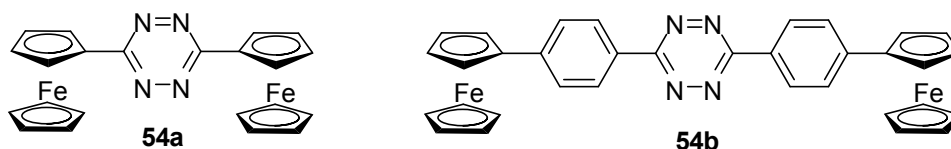


Figure 8. Third order NLO active tetrazine derivatives.

1.4.3 Tetrazines in coordination chemistry

With four π -accepting and σ -donating sp^2 N atoms in the electron-deficient aromatic ring, the 1,2,4,5-tetrazines exhibit a particular coordination chemistry, characterized by electron and charge transfer phenomena and by the ability of these heteroatom-rich ligands to bridge metal centers in various ways. A very low-lying π^* orbital localized at the four nitrogen atoms is responsible for intense low-energy charge transfer absorptions, electrical conductivity of coordination polymers, unusual stability of paramagnetic radical or mixed-valence intermediates and for often well-resolved EPR hyperfine structure in the radical complexes. The structural consequences of electron transfer as well as the capability for efficient and variable metal-metal bridging render the tetrazines valuable components of supramolecular materials.

The obvious interest of tetrazines in coordination chemistry is the presence of multiple metal binding sites. Discrete dinuclear complexes or linear coordination oligomers and polymers may result. The latter motif has been used abundantly in the construction of electrically conducting 1D materials.

Kaim has reviewed the established coordination variety of substituted tetrazine ligands and their unique electronic structure (Figure 9)⁴. The coordination chemistry of these 1,2,4,5-tetrazines with Cr, Mo, W, Mn, Fe, Ru, Os, Ag, Cu, Zn, Cd, Tc is thoroughly explored. The results show that as remarkable small bridging ligands which can convey efficient metal-metal interaction (as evident from stable mixed-valence intermediates and high electrical conductivity), the tetrazines continue to be promising components of functional supramolecular entities in further efforts towards “molecular electronics”.

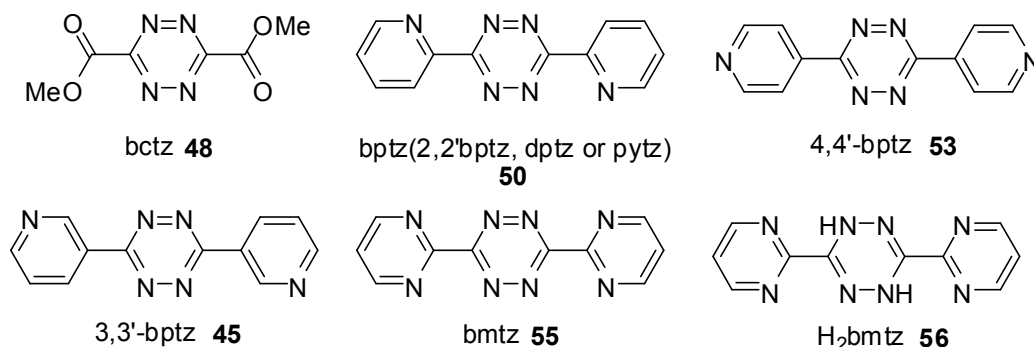


Figure 9. Tetrazines used in coordination chemistry.

More recently, an important example is given by Dunbar’s group⁷⁷, who used anion- π interactions as controlling elements in self-assembly reactions of Ag(I) complexes with π -acidic tetrazine rings. Reactions of **50** and 3,6-bis(2’-pyridyl)-1,2-pyridazine (Figure 10, **57**) with AgX salts ($X=PF_6^-$, AsF_6^- , SbF_6^- , and BF_4^-) afford

complexes of different structural motifs, depending on the π -acidity of the ligand central ring and the outer-sphere anion.

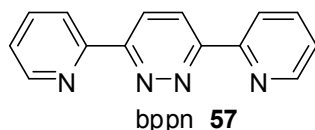


Figure 10. bppn, used for comparison with tetrazines in self-assembly reactions of Ag(I) complexes.

The reaction with **50** leads to the polymeric $\{[Ag(\mathbf{50})][PF_6]\}_\infty$ (Figure 11), the dinuclear compounds $[Ag_2(\mathbf{50})_2(CH_3CN)_2][PF_6]_2$ and $[Ag_2(\mathbf{50})_2(CH_3CN)_2][AsF_6]_2$, as well as the propeller-type species $[Ag_2(\mathbf{50})_3][AsF_6]_2$ and $[Ag_2(\mathbf{50})_3][SbF_6]_2$. As comparison, reaction of **57** with AgX produces the grid-type structures $[Ag_4(\mathbf{57})_4][X]_4$, regardless of the anion present. In complexes of **57**, π - π stacking interactions are maximized, whereas multiple and shorter (therefore stronger) anion- π interactions between the anions and the tetrazine rings are established in complexes of **50**. These differences reflect the more electron-deficient character of the tetrazine ring in **50** as compared to the pyridazine ring in **57**. Furthermore, the evidence obtained from the solid-state structures was corroborated by density functional theory calculations. In the electrostatic potential maps of the free ligands, a higher positive charge is present in **50** as compared to the central ring of **57**. Therefore it is concluded from these systems that anion- π interactions in complexes of **50** play an important role in the outcome of self-assembly reactions.

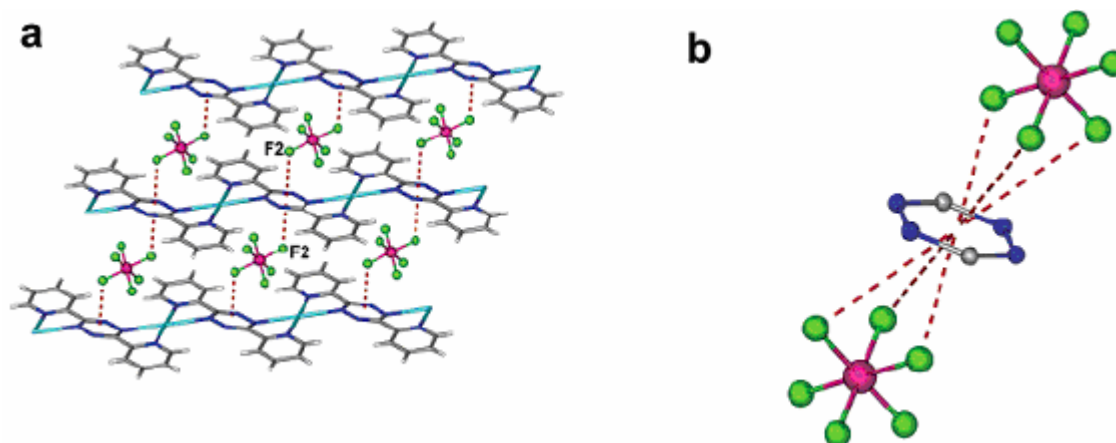


Figure 11. (a) Packing diagram of $\{[Ag(\mathbf{50})][PF_6]\}_\infty$ depicting the shortest contacts between the PF_6^- anions and the tetrazine ring centroids. (b) Tetrazine ring with two PF_6^- anions in $\{[Ag(\mathbf{50})][PF_6]\}_\infty$, displaying the three F atoms involved in each anion- π interaction.

1.4.4 Tetrazines as energetic materials

Tetrazines possess high positive heat of formation and crystal densities, which are important properties for energetic materials applications. Hiskey's group has contributed a lot in the research of tetrazines derivatives as high-nitrogen energetic materials. A lot of tetrazine derivatives have been synthesized and characterized in their laboratory (Figure 12)^{78, 79}.

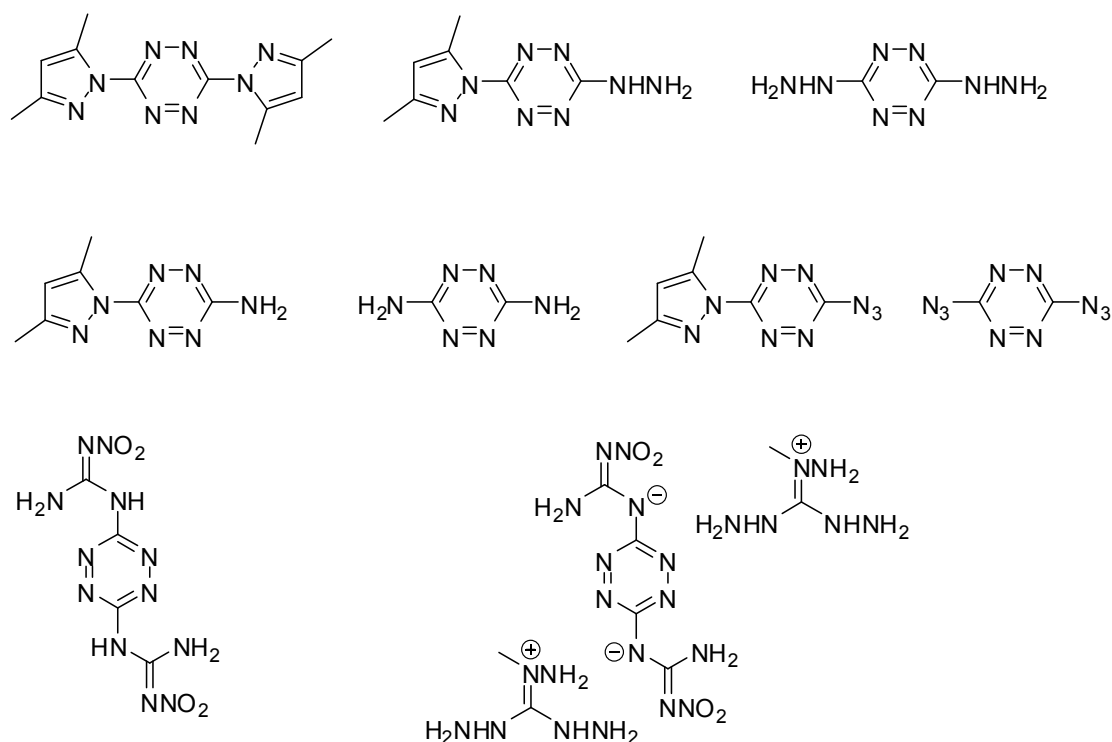


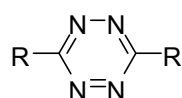
Figure 12. Tetrazines synthesized in Hiskey's group for energetic materials applications.

Talawar and co-workers⁸⁰ have also contributed a lot by the synthesis and theoretical performance computation of some 1,2,4,5-tetrazine high energetic materials (HEMs), some of which are similar to the tetrazines synthesized by Hiskey's group and display potential as energetic additives for high explosive/rocket propellant formulations.

1.4.5 Tetrazines as pharmaceuticals

There are several reviews^{81, 82} indicating that the use of compounds containing 1,2,4,5-tetrazine skeleton have been claimed for use as pharmaceuticals. For example, 3-amino-6-aryl-1,2,4,5-tetrazines have showed modest antimalarial activity in a preliminary research⁸³.

Wei-Xiao Hu and colleagues⁸⁴ have prepared a series of *s*-tetrazine derivatives and evaluated their antitumor activities *in vitro* (Figure 13). The results show that some compounds at 10^{-6} μ M have more than 50% inhibition rate to A-549 cancer cell growth, and some at 10^{-6} μ M have more than 50% inhibition rate to P-388 cancer cell growth.



R=Pyrazinyl, Ph, p-CH₃Ph, m-CIPh, p-CIPh, o-CIPh, PhCH₂, p-CIPhCH₂, p-CF₃Ph, etc.

Figure 13. Tetrazines with antitumor activities.

Another two tetrazine derivatives, **58** and **59** (Figure 14), show strong inhibition activity for P-388 and HL-60 growth, respectively.⁸⁵

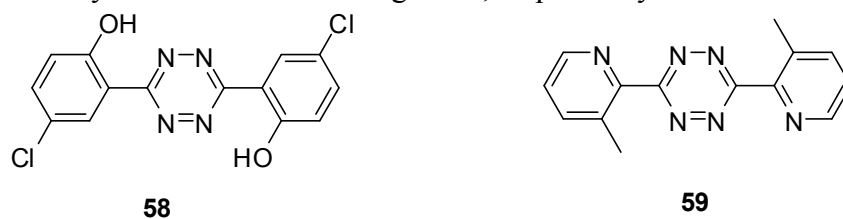
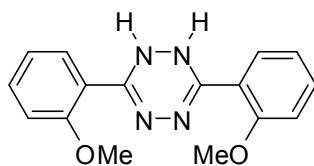


Figure 14. Tetrazines with strong inhibition activity for P-388 and HL-60 growth.

1.4.6 Tetrazine derivatives for anticorrosion applications

Some heterocyclic compounds containing nitrogen atoms are good corrosion inhibitors for many metals and alloys in various aggressive media⁸⁶. Lagrenée and co-workers have investigated the inhibition effect of 3,6-bis(2-methoxyphenyl)-1,2-dihydro-1,2,4,5-tetrazine (2-MDHT, **60**, Figure 15) on the corrosion of mild steel in acidic media, by weight loss and various electrochemical techniques. Results reveal that this organic compound is a very good inhibitor, and is able to reduce the corrosion of steel under acidic conditions.



60
Figure 15. Molecular structure of 2-MDHT.

Generally speaking, due to their intrinsic electron-deficient property, tetrazines can participate in a variety of reactions, especially in S_NAr reaction and inverse electron demand Diels-Alder reaction. 1,2,4,5-Tetrazines have already been very widely utilised for the highly effective synthesis of natural products, ligands, NLO materials, highly energetic materials, bioactive compounds, building blocks, etc. Such applications of 1,2,4,5-tetrazines continue to increase rapidly in number, and a review describing the advances and applications in 1,2,4,5-tetrazine chemistry over the last ten years has just been published on the internet at the end of the composition of this manuscript⁸⁷. However, the potential of tetrazines in sensor applications has seldom been noticed and not explored yet till now. In our consideration, the combination of all these properties of tetrazine—good redox reversibility, fluorescence in some cases (which will be discussed in Chapter 3), and high electron affinity—could lead to the development of a new class of molecular sensors toward anions and electron-rich compounds.

References

- 1 J. Sauer, 1,2,4,5-Tetrazines. In *Comprehensive Heterocyclic Chemistry*; A. J. Boulton, Volume Ed.; A. R. Katritzky, C. W. Rees, E. F. Scriven, Eds.; Pergamon Press: **1996**; Vol. 2, pp 901-955.
- 2 A. R. Katritzky, *Handbook of Heterocyclic Chemistry*, Pergamon Press, G. B. **1986**.
- 3 J. Waluk, J. Spanget-Larsen, E. W. Thulstrup, *Chem. Phys.* **1995**, 200, 201.
- 4 W. Kaim, *Coord. Chem. Rev.* **2002**, 230, 127.
- 5 M. A. El Sayed, *J. Chem. Phys.* **1963**, 38, 2834.
- 6 R. Gleiter, V. Schehlmann, J. Spanget-Larsen, H. Fischer, F. A. Neugebauer, *J. Org. Chem.* **1988**, 53, 5756.
- 7 J. Spanget-Larsen, E. W. Thulstrup, J. Waluk, *Chem. Phys.* **2000**, 254, 135.
- 8 A. Pinner, *Ber.* **1893**, 26, 2128; **1894**, 27, 984.
- 9 D. L. Boger, S. M. Weinreb, *Hetero Diels-Alder Methodology in Organic Synthesis*; Academic Press: **1997**.
- 10 U. Schirmer, B. Wuerzer, N. Meyer, F. A. Neugebauer, H. Fischer, DE Patent No. 3508214, **1986**; *Chem. Abstr.* **1987**, 106, 45718.
- 11 W. Zambach, R. Naef, S. Trah, A. Jeanguenat, M. Eberle, A. Steiger, WO Patent Appl. 0078739, **2000**; *Chem. Abstr.* **2001**, 134, 71613.
- 12 D. E. Chavez, M. A. Hiskey, *J. Energ. Mater.* **1999**, 174, 357-377.
- 13 H.-H. Licht, H. Ritter, *J. Energ. Mater.* **1994**, 12, 223-235.
- 14 M. A. Hiskey, D. E. Chavez, D. Naud, U.S. Patent 6458227, **2002**; *Chem. Abstr.* **2001**, 137, 265190.
- 15 F. Bédioui, J. Devynck, C. Bied-Charreton, *J. Mol. Cat. A : Chem.* **1996**, 92, 1411.
- 16 G. Bidan, B. Divisia-Blohorn, M. Lapkowski, J. M. Kern, J. P. Sauvage, *J. Am. Chem. Soc.* **1992**, 114, 598.
- 17 R. P. Kingsborough, T. M. Swager, *Progress in Inorg. Chem.* **1999**, Vol. 48, (K. D. Karlin Ed.), J. Wiley and Sons.
- 18 J. P. Lang, H. Kawaguchi, K. Tatsumi, *Inorg. Chem.* **1997**, 36, 6447.
- 19 A. Weissberger (Consulting Editor), *The chemistry of heterocyclic compounds, a series of monographs: The 1,2,3- and 1,2,4- triazines, tetrazines and pentazines, chapter 5: The 1,2,,4,5-tetrazine*. Interscience publishers, Inc., New york, **1956**.

-
- 20 R. Wiley, C. Jarboe, Jr., F. Hayes, *J. Org. Chem.* **1957**, *2*, 835.
- 21 P. Audebert, M. Saoud, F. Miomandre, S. Sadki, M. C. Vernière, P. Hapiot, *New J. Chem.* **2004**, *28*, 387.
- 22 P. Audebert, F. Miomandre, S. Sadki, G. Clavier, *Electrochem. Commun.* **2004**, *6*, 144.
- 23 R. N. Butler, F. L. Scott, and R. D. Scott, *J. Chem. Soc. C* **1970**, 2510.
- 24 V. W. Skorianetz, E. sz. Kováts, *Helv. Chim. Acta* **1971**, *54*, 1923.
- 25 V. W. Skorianetz, E. sz. Kováts, *Helv. Chim. Acta* **1972**, *55*, 1405.
- 26 R. J. Stollé, *Prakt. Chem.* **1906**, *73*, 277.
- 27 K.-P. Hartmann and M. Heuschmann, *Tetrahedron* **2000**, *56*, 4213.
- 28 S. C. Fields, M. H. Parker, W. R. Erickson, *J. Org. Chem.* **1994**, *59*, 8284.
- 29 M. D. Coburn, G. A. Buntain, B. W. Harris, M. A. Hiskey, K. -Y. Lee and D. G. Ott, *J. Heterocycl. Chem.* **1991**, *28*, 2049.
- 30 D. E. Chavez and M. A. Hiskey, *J. Energ. Mater.* **1999**, *17*, 357.
- 31 D. E. Chavez, R. D. Gilardi, M. A. Hiskey, *Angew. Chem. Int. Ed.* **2000**, *39*, 1791.
- 32 D. E. Chavez and M. A. Hiskey, *J. Heterocycl. Chem.*, **1998**, *35*, 1329.
- 33 C. -H. Lin, E. Lieber and J. P. Horwitz, *J. Am. Chem. Soc.* **1954**, *76*, 427.
- 34 M. D. Helm, A. Plant, J. P. A. Harrity, *Org. Biomol. Chem.* **2006**, *4*, 4278.
- 35 J. Sandstrom, *Acta Chem. Scand.* **1961**, *15*, 1575.
- 36 D. L. Boger, S. M. Sakya, *J. Org. Chem.* **1988**, *53*, 1415.
- 37 D. L. Boger, M. J. Zhang, *J. Am. Chem. Soc.* **1991**, *113*, 4230.
- 38 D. L. Boger, R. P. Schaum, R. M. Garbaccio, *J. Org. Chem.* **1998**, *63*, 6329.
- 39 U. Schirmer, B. Wuerzr, N. Meyer, F. A. Neugebauer, H. Fischer, Ger Offen, DE3508214-A, **1986**; *Chem. Abstr.* 106: 45718p.
- 40 Z. Novák, B. Bostai, M. Csékei, K. Lőrincz, A. Kotschy, *Heterocycles* **2003**, *60*, 2653.
- 41 D. M. Schrader, Y. C. Jean, *Positron and Positronium Chemistry*; Elsevier: Amsterdam, **1988**.
- 42 O. E. Mogensen, *Positron Annihilation in Chemistry*; Springer-Verlag: Berlin, **1995**.
- 43 B. Lévy, A. Kotschy and Z. Novák, *J. Phys. Chem. A* **2004**, *108*, 1753.
- 44 M. C. Wilkes, *J. Heterocycl. Chem.* **1991**, *28*, 1163.
- 45 F. A. Neugebauer, C. Krieger, H. Fischer, R. Siegel, *Chem. Ber.* **1983**, *116*, 2261.

-
- 46 D. Hunter, D. G. Neilson, *J. Chem. Soc., Perkin Trans. 1* **1984**, *1*, 2779.
- 47 F. A. Neugebauer, R. Siegel, *Chem. Ber.* **1985**, *118*, 2157.
- 48 D. Hunter, D. G. Neilson, T. J. R. Weakley, *J. Chem. Soc., Perkin Trans. 1* **1985**, *1*, 2709.
- 49 J. Faragó, Z. Novák, G. Schlosser, A. Csámpai, A. Kotschy, *Tetrahedron* **2004**, *60*, 1991.
- 50 Z. Novák, A. Kotschy, *Org. Lett.* **2003**, *5*, 3495.
- 51 R. A. Carboni, R. V. Lindsey, *J. Am. Chem. Soc.* **1959**, *81*, 4342.
- 52 D. L. Boger, *Tetrahedron* **1983**, *39*, 2869.
- 53 D. L. Boger, *Chem. Rev.* **1986**, *86*, 781.
- 54 D. L. Boger, *Chemtracts—Org. Chem.* **1996**, *9*, 149.
- 55 D. L. Boger, S. N. Weinreb, *Organic Chemistry—A Series of Monographs*, **1986**, *Vol. 47: Hetero Diels-Alder Methodology in Organic Synthesis, Chapter 10*, 300-357.
- 56 J. L. Han and C. W. Ong, *Tetrahedron* **2006**, *62*, 8169.
- 57 G. Özer, N. Saracoglu, A. Menzek, M. Balci, *Tetrahedron* **2005**, *61*, 1545.
- 58 A. Kotschy, Z. Novák, Z. Vincze, D. M. Smith and G. Hajós, *Tetrahedron Lett.* **1999**, *40*, 6313.
- 59 Z.-K. Wan, G. H. C. Woo, J. K. Snyder, *Tetrahedron* **2001**, *57*, 5497.
- 60 R. E. Sammelson, M. M. Olmstead, M. J. Haddadin, and M. J. Kurth, *J. Org. Chem.* **2000**, *65*, 9265.
- 61 L. I. Robins, R. D. Carpenter, J. C. Fettinger, M. J. Haddadin, D. S. Tinti, and M. J. Kurth, *J. Org. Chem.* **2006**, *71*, 2480.
- 62 M. Girardot, R. Nomak, and J. K. Snyder, *J. Org. Chem.* **1998**, *63*, 10063.
- 63 T. J. Sparey and T. Harrison, *Tetrahedron Lett.* **1998**, *39*, 5873.
- 64 J. W. Wijnen, S. Zavarise, J. B. Engberts and M. Charton, *J. Org. Chem.* **1996**, *61*, 2001.
- 65 R. Hoogenboom, B. C. Moore, and U. S. Schubert, *J. Org. Chem.* **2006**, *71*, 4903.
- 66 S. M. Sakya, K. K. Groskopt, *Tetrahedron Lett.* **1997**, *38*, 3805.
- 67 A. Hamasaki, R. Ducray, and D. L. Boger, *J. Org. Chem.* **2006**, *71*, 185.
- 68 J. Sauer and D. K. Heldmann, *Tetrahedron* **1998**, *54*, 4297.
- 69 S. F. Mason, *J. Am. Chem. Soc.* **1959**, 1263.
- 70 C. Adamo, V. Barone, *Chem. Phys. Lett.* **2000**, *330*, 152.

-
- 71 S. Ryu, R. M. Stratt, K. K. Baeck, and P. M. Weber, *J. Phys. Chem. A* **2004**, *108*, 1189.
- 72 D. V. Brumbaugh, J. E. Kenny and D. H. Levy, *J. Chem. Phys.* **1983**, *78*, 3415.
- 73 C. A. Haynam, D. V. Brumbaugh and D. H. Levy, *J. Chem. Phys.* **1984**, *80*, 2256.
- 74 P. M. Weber, J. T. Buontempo, F. Novak, S. A. Rice, *J. Chem. Phys.* **1988**, *88*, 6082.
- 75 P. M. Weber, S. A. Rice, *J. Chem. Phys.* **1988**, *88*, 6120.
- 76 I. Janowska, F. Miomandre, G. Clavier, P. Audebert, J. Zakrzewski, K. H. Thi, and I. Ledoux-Rak, *J. Phys. Chem. A* **2006**, *110*, 12971.
- 77 B. L. Schottel, H. T. Chifotides, M. Shatruk, A. Chouai, L. M. Pérez, J. Bacsá, and K. R. Dunbar, *J. Am. Chem. Soc.* **2006**, *128*, 5895.
- 78 M. V. Huynh, M. A. Hiskey, D. E. Chavez, D. L. Naud, and R. D. Gilardi, *J. Am. Chem. Soc.* **2005**, *127*, 12537.
- 79 D. E. Chavez, M. A. Hiskey, and R. D. Gilardi, *Org. Lett.* **2004**, *6*, 2889.
- 80 M. B. Talawar, R. Sivabalan, N. Senthilkumar, G. Prabhu, S. N. Asthana, *J. Hazard. Mater. A* **2004**, *113*, 11.
- 81 H. Neunhoeffer, *Comprehensive Heterocyclic Chemistry, I*; A. R. Katritzky, Ed.; Pergamon: Frankfurt, **1984**; *Vol. 3*, 531.
- 82 J. Sauer, *Comprehensive Heterocyclic Chemistry, I*; A. J. Boulton, Ed.; Elsevier: Oxford, **1996**; *Vol. 6*, 901.
- 83 L. M. Werbel, D. J. Mcnamara, *J. Heterocycl. Chem.* **1979**, *16*, 881.
- 84 W.-X. Hu, G.-W. Rao and Y.-Q. Sun, *Bioorg. Med. Chem. Lett.* **2004**, *14*, 1177.
- 85 G.-W. Rao and W.-X. Hu, *Bioorg. Med. Chem. Lett.* **2006**, *16*, 3702.
- 86 F. Zucchi, G. Trabanelli, G. Brunoro, *Corros. Sci.* **1992**, *33*, 1135.
- 87 N. Saracoglu, Recent Advances and Applications in 1,2,4,5-Tetrazine Chemistry, *Tetrahedron* (**2007**), doi: 10.1016/j.tet.2007.02.051

Chapter 2 Development of anion and electron-rich compound sensors

2.1 Supramolecular chemistry and receptors

Molecules which interact with one another through noncovalent forces (hydrogen bonding, π - π stacking, van der Waals interactions and electrostatic interaction) in organized assemblies to perform useful functions are termed supramolecules (Figure 1). They are found in their most refined form in biological systems.

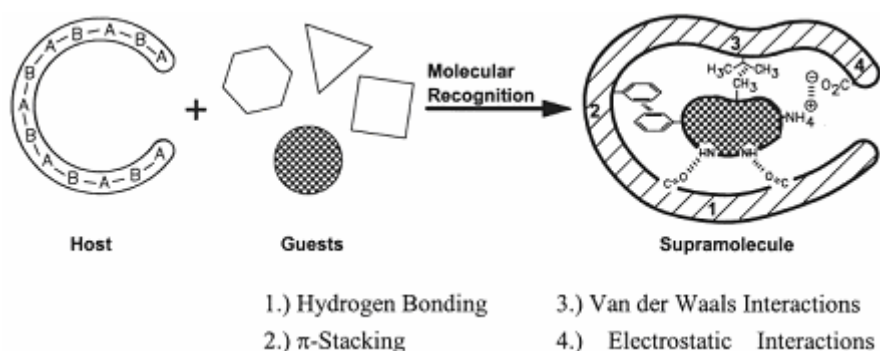


Figure 1. Molecular recognition and supramolecular bonding.

A receptor is a species that can select one of many possible binding partners and form a complex that is stabilized by supramolecular interactions as mentioned above.

Advances in supramolecular chemistry have given rise to the preparation of a great deal of molecular receptors which bear adequate functional groups to establish noncovalent interactions with molecular substrates. The research and the design of such receptor molecules has an important and increasing impact in different fields, such as analytical and medicinal chemistry, and in the development of catalytic substances mimicking enzymes, etc. In comparison to cation receptors, research of anion or neutral organic molecule receptors is a relatively new field, but has already become an established area in supramolecular chemistry.

2.2 Optical (colorimetric, fluorescent) sensors and electrochemical sensors

Generally speaking, sensors are developed from receptors. Usually the structure of a sensor is a combination of a complexing part (acting as a receptor) and a sensing part. The complexation of guest species with receptors can be monitored either by optical (colorimetric or fluorescent) changes or by changes in electrochemical behaviours (resistance, conductivity, current, potential, capacity¹, etc.), on which optical sensors and electrochemical sensors are designed and function, respectively.

2.2.1 Fluorescent molecular sensors

2.2.1.1 Brief introduction of fluorescence

Fluorescence is a particular case of luminescence. The mode of excitation is absorption of a photon, which brings the absorbing species into an electronic excited state. The emission of photons accompanying de-excitation is then called luminescence (fluorescence, phosphorescence, or delayed fluorescence), which is one of the possible physical effects resulting from interaction of light with matter.

The Perrin-Jablonski diagram (Figure 2) is convenient for visualizing in a simple way the possible processes: photon absorption, internal conversion, fluorescence, intersystem crossing, phosphorescence, delayed fluorescence and triplet-triplet transitions. The singlet electronic states are denoted S_0 (fundamental electronic state), S_1 , S_2 , etc., and the triplet states, T_1 , T_2 , etc.. Vibrational levels are associated with each electronic state. Since the absorption is very fast ($\sim 10^{-15}$ s, Table 1) with respect to all other processes, there is no concomitant displacement of the nuclei according to the Franck-Condon principle, and the vertical arrows corresponding to absorption start from the 0 (lowest) vibrational energy level of S_0 because the majority of molecules are in this level at room temperature. Absorption of a photon can bring a molecule to one of the vibrational levels of S_1 , S_2 , etc.. The subsequent de-excitation process consisting in the emission of photons accompanying the $S_1 \rightarrow S_0$ relaxation is called fluorescence. Generally fluorescence emission occurs from S_1 and therefore its characteristics (except polarization) do not depend on the excitation wavelength. The 0-0 transition is usually the same for absorption and fluorescence, but the fluorescence spectrum is located at higher wavelengths (lower energy) than the absorption spectrum because of the energy loss in the excited state due to vibrational relaxation.

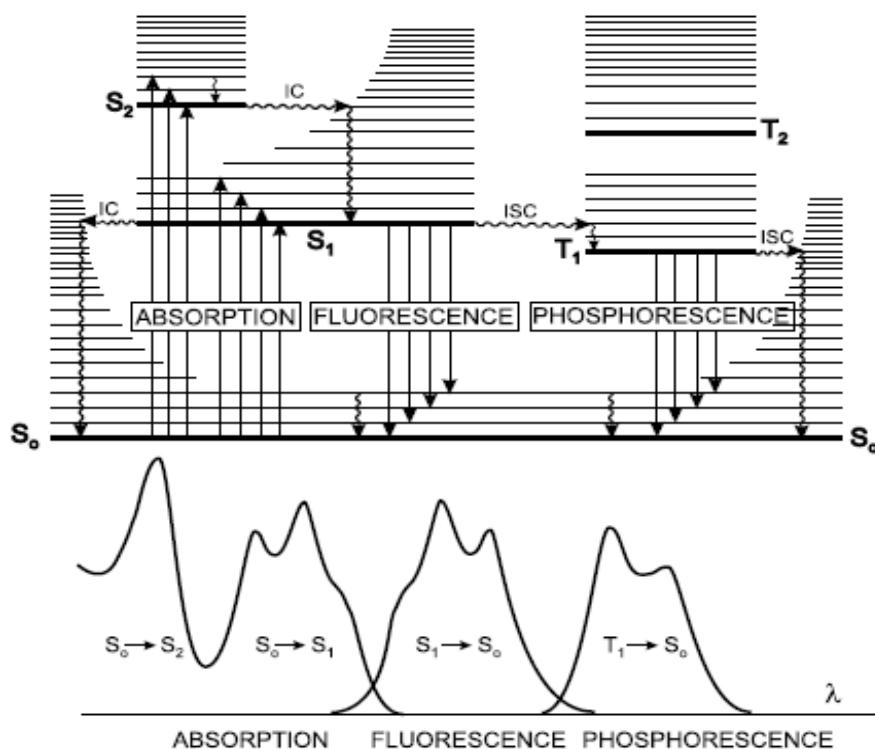


Figure 2. Perrin-Jablonski diagram and illustration of the relative positions of absorption, fluorescence and phosphorescence spectra. IC: Internal conversion, a non-radiative transition between two electronic

states of the same spin multiplicity. In solution, this process is followed by a vibrational relaxation towards the lowest vibrational level of the final electronic state. ISC: Intersystem crossing, a non-radiative transition between two isoenergetic vibrational levels belonging to electronic states of different multiplicities.

Table 1. Characteristic times of each process

CHARACTERISTIC TIMES	
absorption	10^{-15} s
vibrational relaxation	10^{-12} - 10^{-10} s
lifetime of the excited state S_1	10^{-10} - 10^{-7} s \rightarrow fluorescence
intersystem crossing	10^{-10} - 10^{-8} s
internal conversion	10^{-11} - 10^{-9} s
lifetime of the excited state T_1	10^{-6} - 1 s \rightarrow phosphorescence

2.2.1.2 Fluorescent molecular sensors

A fluorescent molecular sensor consists of a fluorophore as the signaling part, which acts as a signal transducer that converts the information of the presence of an analyte into an optical signal expressed as the changes in the fluorescence characteristics.

A large amount of fluorescent molecular sensors are designed and synthesized, because, firstly, there are high demands in analytical chemistry, clinical biochemistry, medicine chemistry, environment, etc.; secondly, a huge number of chemical and biochemical analytes can be detected by fluorescence methods: cations (H^+ , Li^+ , Na^+ , K^+ , Ca^{2+} , Mg^{2+} , Zn^{2+} , Pb^{2+} , Al^{3+} , Cd^{2+} , etc.), anions (halide ions, citrates, carboxylates, phosphates, ATP, etc.), neutral molecules (sugars, e.g. glucose, etc.) and gases (O_2 , CO_2 , NO , etc.); thirdly, fluorescent molecular sensors offer distinct advantages such as high sensitivity, high selectivity, short response time, local observation (by fluorescence imaging spectroscopy), and the possibility for remote sensing (combining with optical fibers). The great improvement in the sensitivity and the spatial or temporal resolution of instruments also promoted successfully the application of fluorescent sensors in various fields.

Valeur has classified the fluorescent molecular sensors into three classes (Figure 3)²:

Class 1: fluorophores that undergo quenching upon collision with an analyte;

Class 2: fluorophores that can reversibly bind an analyte, of which the fluorescence can be either quenched (CEQ type: Chelation Enhancement of Quenching) or enhanced (CEF type: Chelation Enhancement of Fluorescence) upon binding;

Class 3: fluorophores linked, via a spacer or not, to a receptor. The design of such sensors, which are based on molecule or ion recognition by a receptor, requires special care in order to fulfil the criteria of affinity and selectivity, which are relevant to the field of supramolecular chemistry. The changes in photophysical properties of the fluorophore upon interaction with the bound analyte are due to the perturbation of photoinduced processes by the latter (electron transfer, charge transfer, energy transfer, excimer or exciplex formation or disappearance, etc.) Again, fluorescence can be quenched or enhanced.

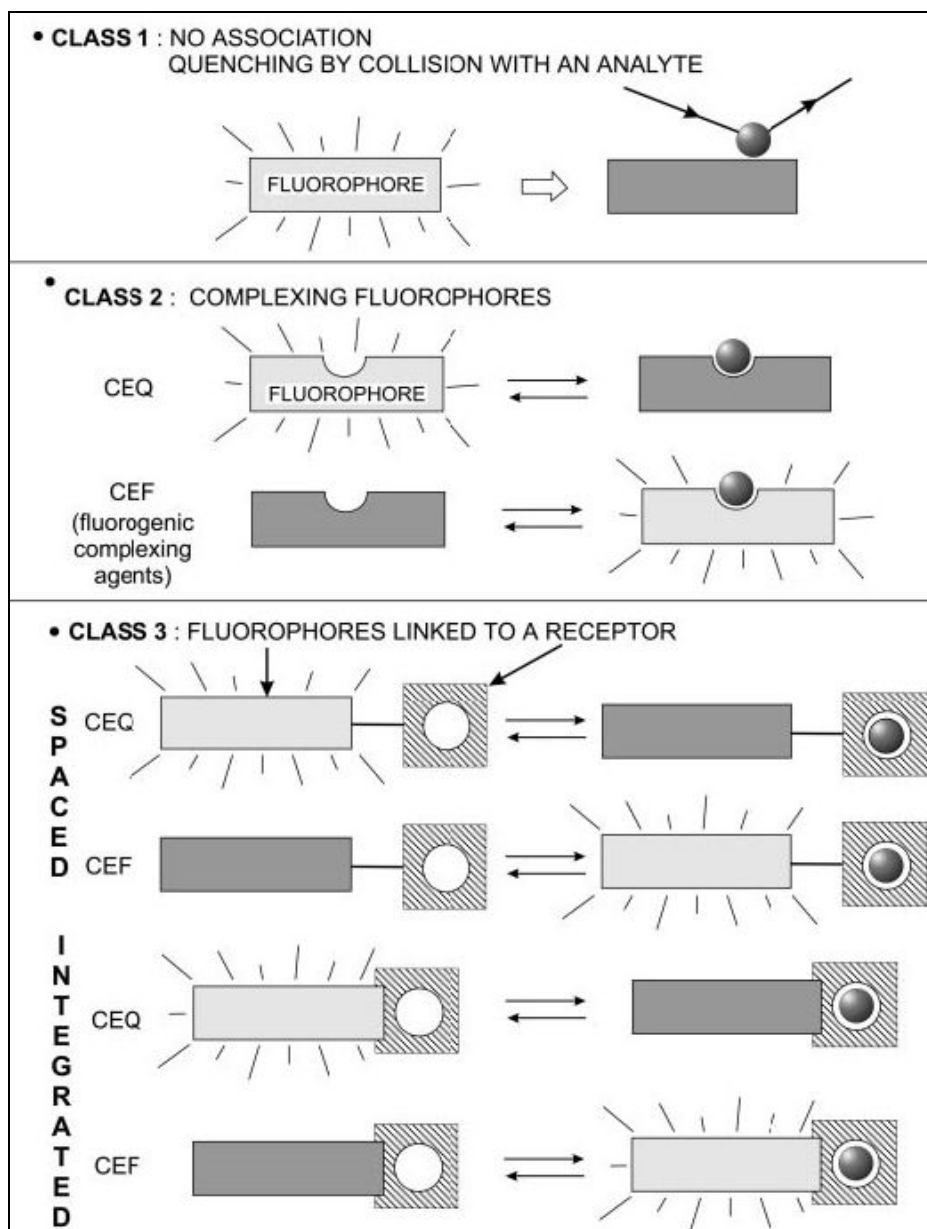


Figure 3. Main classes of fluorescent molecular sensors classified by Valeur.

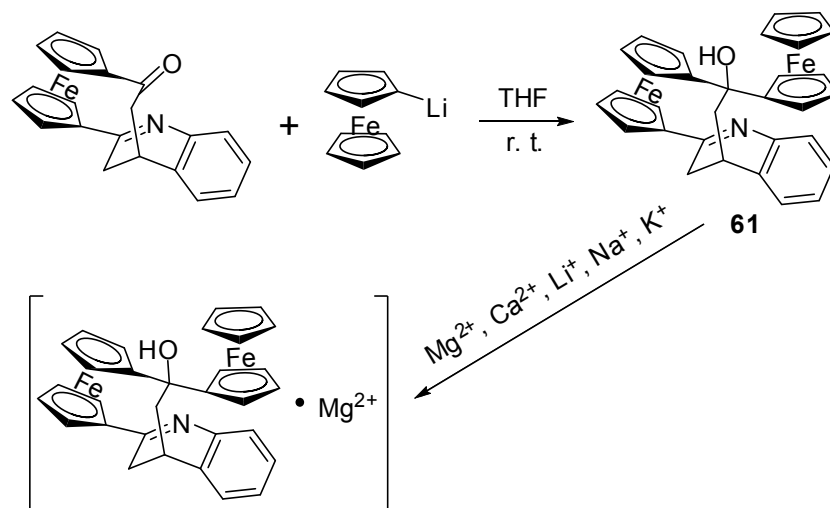
2.2.2 Electrochemical sensors

Electrochemical sensors are based on changes of electrochemical behaviour once the complex between redox-active receptor and analyte is formed³. The changes in electrochemical behaviour can be used to monitor the complexation of guest species, which is also considered as the process of molecular recognition.

For example, ferrocene derivatives, mostly those which are substituted with macrocyclic ligands, are prototype molecules which have proved to be especially versatile as ion sensors⁴⁻⁷. Cation binding at an adjacent receptor site of a ferrocene-based host induces a positive shift in the redox potential of the ferrocene/ferrocenium

couple, either by through-bond and/or through-space electrostatic interactions, interference or conformational change⁸.

Molina and colleagues⁹ have synthesized a diferrocene derivative **61**, in which two ferrocene redox-active moieties are in proximity to the cation-binding dihydroquinoline site through an aza-substituted bridge (Scheme 1). This molecule, containing a ferrocenophane architecture with another ferrocenyl substituent, functions as a highly selective electrochemical sensor for Mg^{2+} ion, while not showing any response to Ca^{2+} or alkaline ions. The response of **61** to Mg^{2+} can be clearly detected by electrochemical techniques even in the presence of a large amount of other metal ions.



Scheme 1. Synthesis of an electrochemical sensor for the selective detection of Mg^{2+} .

Yua *et al*¹⁰ described an electrochemical sensor for an electrochemically inactive compound using β -CD immobilized on a poly(N-acetylaniline) film modified electrode as a molecular host, in which 1,4-hydroquinone (HQ) was chosen as a probe. The target analyte cinchonine (CCN) is electrochemically inactive within the potential range studied and capable to form a strong complex with β -CD. In the presence of CCN, the decrease in HQ peak current is directly proportional to the amount of CCN, which provides a basis for the sensitive, fast and simple electrochemical CCN's sensing. The study of competitive inclusion processes also enables a better understanding of cyclodextrin-based supramolecular chemistry and the design of novel assay methodology for electrochemically inactive guest molecules.

In the search of a novel sensor to detect the presence of formaldehyde (HCOH), a common environmental pollutant with serious toxicity^{11, 12}, Chengbu Liu *et al*¹³ developed a boron-doped (B-doped) single-walled carbon nanotube (SWCNT) presenting high sensitivity to HCOH. The relevant sensing mechanism is attributed to the sensitive conductance change of SWCNT caused by charge transfer between SWCNTs and HCOH molecules which affects the electronic transport properties of SWCNT.

2.3 Anion sensors

2.3.1 Roles of anions

The design and synthesis of systems that are capable of sensing various anions are currently of major interest because of the important roles that anions play in physiological and environmental systems¹⁴⁻¹⁸.

Anions are ubiquitous throughout biological systems and play essential roles. For example, chloride is an important electrolyte in maintaining potentials across cell membranes, and the misregulation of its transport through cell membranes by chloride channels is the cause of cystic fibrosis¹⁹. Transport of chloride as HCl by the prodigiosins through biological lipid bilayer membranes has been shown to uncouple lysosomal vacuolar-type ATPases²⁰. In fact DNA, which carries genetic information of organism, is a polyanion. A majority of enzyme substrates and co-factors are also anionic. For example, the anionic carboxypeptidase A is an enzyme coordinating to the C-terminal carboxylate group of polypeptides by the formation of an arginine-aspartate salt bridge and catalyzing the hydrolysis of this residue.

Many anions are also of great importance as agricultural fertilizers and industrial raw material²¹, as well as a significant influence factor for environment. For example, phosphorous, a key nutrient in living organisms is involved in several biological and environmental processes, but extensive input of phosphate due to over fertilization and from industrial and domestic waste water pollution results in eutrophication, a process that is often accompanied by growth of toxic algae^{22, 23}. Pollutant anions have also been linked to carcinogenesis, for example, the metabolites of nitrate. The production of pertechnetate during the reprocessing of nuclear fuel (and its subsequent discharge into the seas and oceans) is also a matter of environmental concern.

2.3.2 Difficulties in anion recognition and sensing

Although molecular recognition of anionic species plays a pivotal role in a large number of chemical and biological processes, practical detection of anions has continued to be a more challenging issue than the detection of cations, which has been fully developed for almost 40 years²⁴⁻²⁸.

The difficulty in designing anion receptors comes from several aspects. First of all, anions are larger than isoelectronic cations and therefore have a lower charge to radius ratio²⁹, which means electrostatic binding interactions are less effective than they would be for the smaller cation (Table 2).

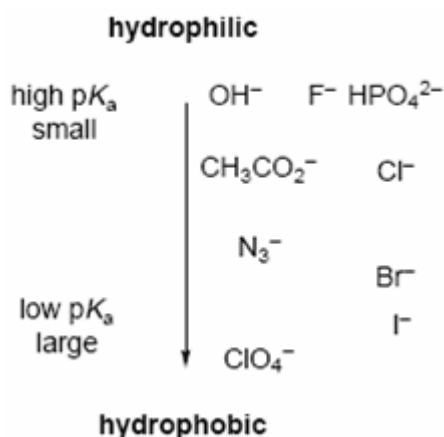
Table 2. A comparison of the radii of isoelectronic cations and anions.

Cation	r (Å)	Anion	r (Å)
Na ⁺	1.16	F ⁻	1.19
K ⁺	1.52	Cl ⁻	1.67
Rb ⁺	1.66	Br ⁻	1.82
Cs ⁺	1.81	I ⁻	2.06

Secondly, anions may be sensitive to pH values, for they are protonated at low pH and so lose their negative charge, hence receptors must function within the pH window of their target anion³⁰.

Additionally, solvent effects also play a crucial role in controlling anion binding strength and selectivity. Electrostatic interactions generally dominate in anion solvation, and hydroxylic solvents in particular form strong hydrogen bonds with anions. Thus a potential anion receptor must effectively compete with the solvent environment, in which the anion recognition event takes place. Usually a neutral receptor that binds anions solely through ion-dipole interactions only associates with anions in aprotic solvents, whereas a charged receptor binds to highly solvated (hydrated) anions in protic solvent media.

Hydrophobicity can also influence the selectivity of a receptor. The Hofmeister Series orders anions by their hydrophobicity and therefore degree of aqueous solvation (Scheme 2)³¹. Hydrophobic anions are generally bound more strongly in hydrophobic binding sites.



Scheme 2. The Hofmeister Series order of hydrophilic/hydrophobic anions.

Last but not the least, anionic species have a wide range of geometries (Figure 4), therefore a higher degree of design may be required to make receptors complementary to their anionic guest.

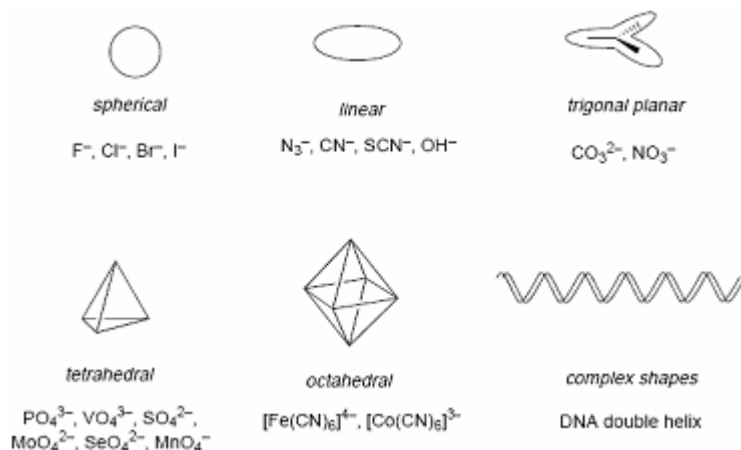


Figure 4. The structure variety of anions.

2.3.3 Developments in research for anion receptors and sensors

Despite all the difficulties discussed above, a lot of developments have been achieved in anionic recognition and sensing since the pioneering work of Lehn³² and Schmidtchen³³, who have first developed sophisticated positively charged concave receptors capable of including inorganic anions. Figure 5 shows their representative receptor-anion complexes. In the case of **a**³⁴, the rod-like azide anion is included in the ellipsoidal cavity containing six ammonium groups; while in **b**³⁵, the spherical iodide anion is included within the spherical cavity containing four tetraalkyl ammonium groups. In both cases, the positively charged groups are positioned strategically within the internal framework of receptor, and selectivity derives from the matching of the geometrical features—shape, size—of receptor's cavity with the anion. Since then, a new branch of chemistry developed, which has been defined as anion coordination chemistry³⁶.

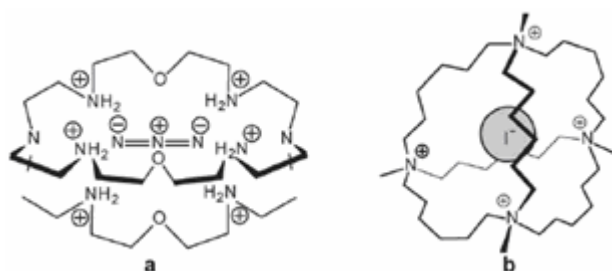
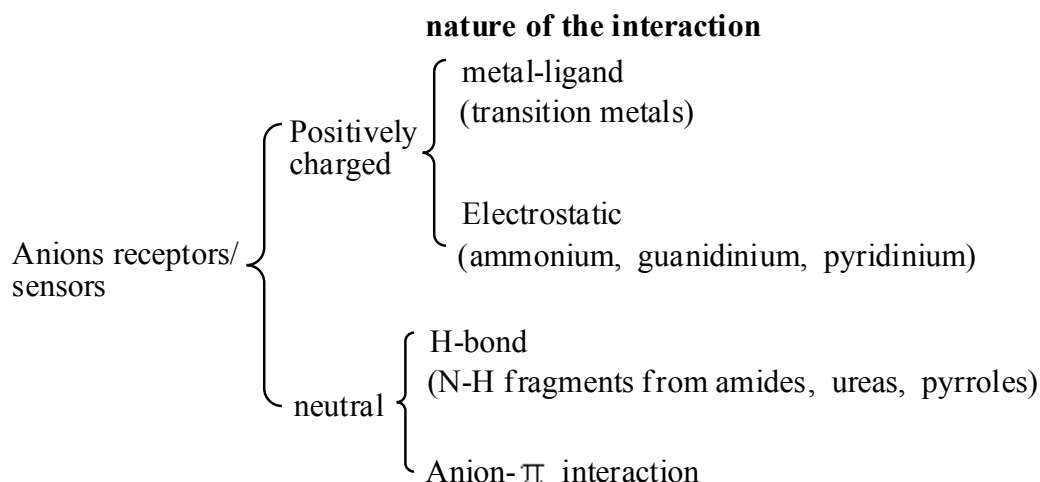


Figure 5. Prototypes of concave positively charged receptors suitable for anion inclusion.

By far, synthetic receptors for anions are usually based on macrocyclic polyammonium/guanidinium, amides, urea/thiourea and functionalized calixarenes.

Similar to the classical coordination chemistry of metals, anion coordination chemistry is based on non-covalent interactions, and an anion establishes multi-point interactions with its receptor (either positively charged or neutral), as a metal ion with its ligands. As a consequence, some concepts and paradigms of metal coordination chemistry, for example the chelate effect or the macrocyclic effect, apply well to anion coordination chemistry. Sensors derived from receptors can be positively charged, from the presence of ammonium/tetraalkylammonium fragments, or

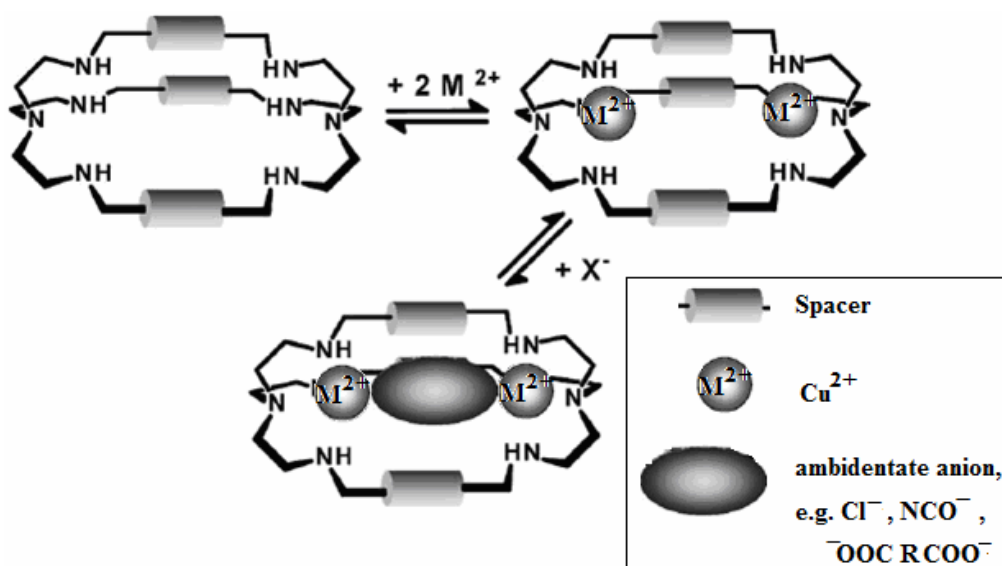
incorporate metal ions. Sensors can be neutral, too; in that case, they should interact with the anion through hydrogen bonding and should contain H-bond donor groups, essentially N–H fragments from amides and ureas. Luigi Fabbrizzi³⁷ classified anion receptors/sensors on the basis of the nature of the interaction, to which we added another class of interaction—anion- π interaction (Scheme 3).



Scheme 3. Classification of anion-sensor interactions.

2.3.3.1 Anion sensors based on metal–ligand interaction

Positive charges within receptor's cavity can be provided by transition metal ions (e.g. Cu(II)), which offer a binding site to one donor atom of the envisaged anion. Metal–ligand interactions are relatively strong and in most cases more than compensate the endoergonic terms associated to anion desolvation. As a consequence, receptors containing transition metal ions ensure selective anion recognition in water. For example, the Fabbrizzi's group³⁷ has synthesized some dicopper(II) bistren cryptates, which are ideal receptors for ambidentate anions capable to bridge the two Cu(II) centres (Figure 6):



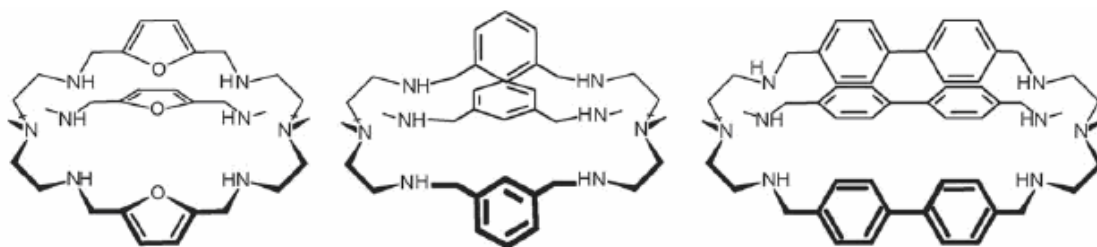
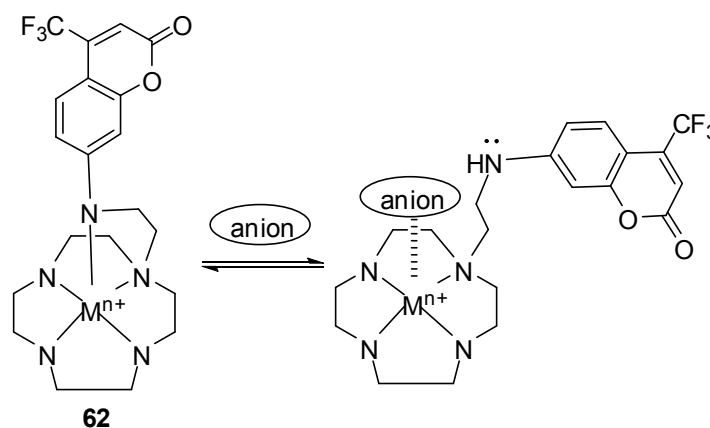


Figure 6. Inclusion process of an anion into a bistren dimetallic cage, and some examples of bistren cryptates.

The size of the ellipsoidal cavity and consequent inclusion selectivity for anions can be modulated by varying the length of the spacers linking the two tren subunits. The selective recognition of halides, polyatomic anions, aromatic and aliphatic dicarboxylates can be realized.

While most currently known anion sensors work only in organic solutions, sensors for biological applications are required to function in neutral aqueous solutions. Kikuchi *et al.*³⁸ have designed a novel fluorescent anion sensor which could be applied in aqueous solution (Scheme 4).



Scheme 4. Design concept of a fluorescent sensor of anions. M^{n+} is a metal ion that can be chelated stably by cyclen.

The sensor molecule **62**-Cd(II) contains a 7-amino-4-trifluoromethylcoumarin as a fluorescent reporter and Cd(II)-cyclen (1,4,7,10-tetraazacyclododecane) as an anion host. In neutral aqueous solution, Cd^{II} of **62**-Cd(II) is coordinated by the four nitrogen atoms of cyclen and the aromatic amino group of coumarin. When various anions are added to a buffer solution (pH 7.4) containing **62**-Cd(II), the analyte displaces the aromatic group of coumarin from the sphere of coordination of Cd(II), causing a change of the emission spectrum. While pyrophosphate and citrate are detected with high sensitivity, fluoride and perchlorate produce no response. Some organic anions such as ATP and ADP also give strong signals, indicating the potential for biochemical and analytical applications. The same sensing principle could also be widely applicable to the sensing of other molecules.

2.3.3.2 Anion sensors based on electrostatic interaction

Quarternary ammonium and guanidinium are often-used groups in the construction of anion sensors to produce electrostatic interaction with anions.

Schmidtchen's group produced in an elegant work the macrotricyclic quaternary ammonium hosts **63** and **64** (Figure 7), which can be used as receptors to form complexes with a variety of anionic guests in water³⁹. The crystal structure of the complex of **63** with an internal iodide was obtained and the driving force is the strong electrostatic interactions of iodide ion with four quaternary ammonium groups.

Frontera and co-workers⁴⁰ have designed and synthesized a new tripodal receptor based on squaramide-ammonium unit (**65**, Figure 7), which is able to form stable complexes with tricarboxylate anions. Hydrogen bonding is also involved in the formation of the complex. They have evaluated its binding properties with several guests, and determined its association constants. A sensing ensemble of the receptor **65** with fluorescein is able to be applied for the determination of citrate in highly competitive media.

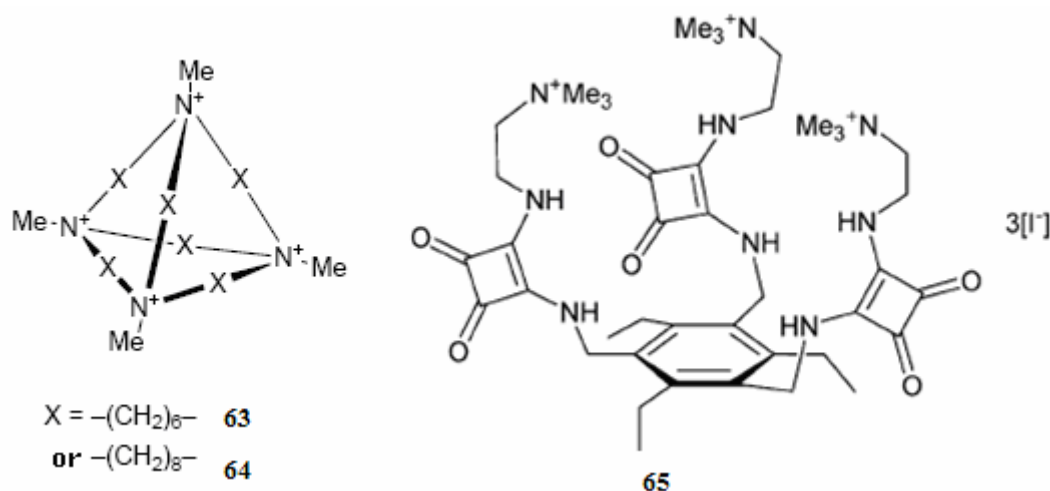


Figure 7. Macrotricyclic quaternary ammonium hosts for receptor applications (**63**, **64**) and new tripodal receptor based on squaramide-ammonium unit (**65**).

Since these electrostatic interaction-based anion sensors are positively charged and are therefore associated with counterions, in many cases a competition for the anion-binding site between the counterions and the analyte may occur. To overcome this disadvantage, many neutral sensors based on hydrogen bonding are designed and synthesized.

2.3.3.3 Anion sensors based on hydrogen bonding

The binding of anions to neutral receptors is of special significance; first, to avoid the competing counterion complexes present if cationic hosts are used, and second, the selectivity is highest in neutral receptors due to the dominance of directional interactions. For instance, the high specificity of neutral, anion binding proteins is due to a recognition site where the anion guest is bonded simply via multiple hydrogen bonds⁴¹. Obviously, each nonbonded interaction is weaker than coulombic interactions present in positively charged receptors; however an enough number of nonbonded interactions can lead to selective neutral receptors for anions.

The interaction firstly considered for a neutral molecular sensor with an anion is hydrogen bonding. In particular, the receptor must act as an H-bond donor and the anion as an H-bond acceptor. Suitable fragments for H-bond donation are OH and NH. Due to the higher electronegativity of oxygen, the O-H bond is more polarized, from

which results that OH is a more powerful H-bond donor than N-H. However, molecules containing ureas, amides, and pyrrole groups have proven to be effective and selective anion-binding agents⁴².

For example, urea derivatives, one of the most classical and first investigated NH containing receptors, are able to donate two hydrogen bonds to Y-shaped anions such as acetate, to give an H-bonded complex, whose structure is shown in Figure 8. A variety of receptors containing one or more urea subunits have been designed and tested for anion recognition and sensing over the past decade. Recently, the crystal and molecular structure of complex **66** has been reported, which indicates that acetate establishes two directional H-bonds with the two-NH fragments of the urea subunit, and the N(urea)-O(acetate) distances (2.69 and 2.77 Å) position the interaction among ‘moderate’ hydrogen bonds, whose nature is mainly electrostatic. This example emphasizes the directionality of the bifurcate hydrogen bonding interaction with the acetate ion.

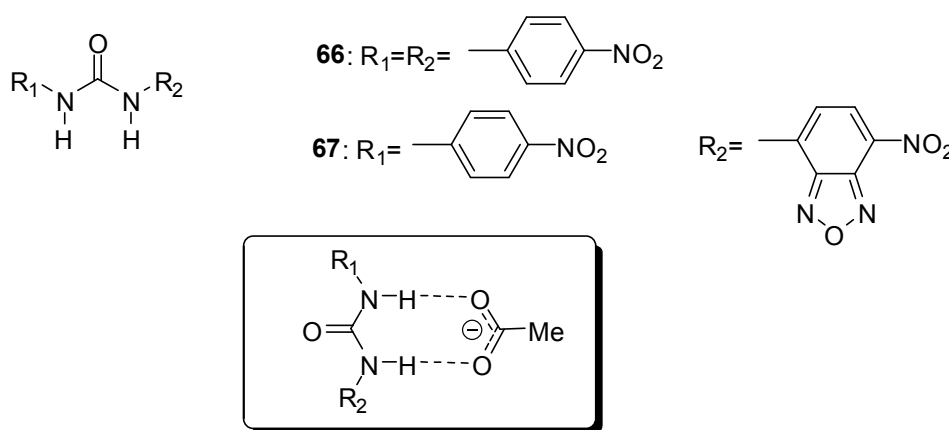


Figure 8. The H-bond complex between a urea based receptor and acetate.

Unlike ureas which bind Y-shaped anions in a parallel hydrogen-bonding array, another NH containing receptors, amidopyrroles, offer a convergent hydrogen-bonding array suited to bind a single atom in an anion (Figure 9)⁴².

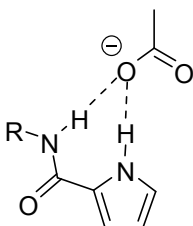


Figure 9. Convergent hydrogen-bonds of amidopyrrole with anion.

2.3.3.4 Anion- π interactions and anion sensors based on multiple non-covalent interactions involving π - π stacking interaction or anion- π interaction

Aromatic rings, for complexation purposes, have been intuitively regarded as sources of electron density and were thus expected to interact repulsively with anions for a long time. However, in 1997 and 1999, Dougherty⁴³, Besnard⁴⁴ and Alkorta and co-workers⁴⁵ have produced theoretical evidences of electrostatic bonding between hexafluorobenzene and the heteroatom in molecules such as H₂O, HCN, and HF wherein the negative end of the dipole is directed toward the C₆ axis of the ring

(Figure 10). *Ab initio* calculations reveal a significant binding interaction between water and hexafluorobenzene in a geometry that points the oxygen lone pairs directly into the face of the π system. The geometry is as anticipated from electrostatic arguments emphasizing the substantial quadrupole moment of the aromatic.

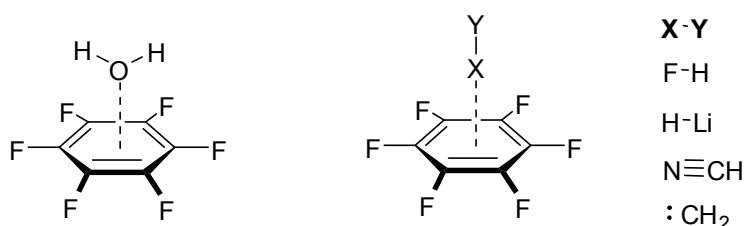


Figure 10. Binding interaction between small molecules and hexafluorobenzene.

Then in 2002, Mascial and colleagues⁴⁶ have demonstrated the basis for unprecedented noncovalent bonding between anions and the aryl centroid of electron-deficient aromatic rings, by an *ab initio* study of the interaction between 1,3,5-triazine and the fluoride, chloride, and azide ions at the MP2 level of theory (Figure 11). Minima are also located corresponding to C-H \cdots X hydrogen bonding, reactive complexes for nucleophilic attack on the triazine ring, and π -stacking interactions (with azide). Trifluoro-1,3,5-triazine also participates in aryl centroid complexation and forms nucleophilic reactive complexes with anions.

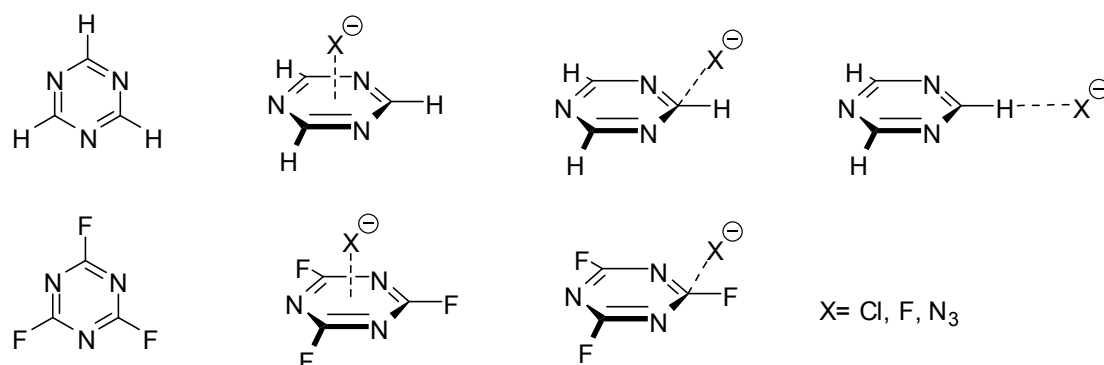


Figure 11. Noncovalent bonding between anions and electron-deficient aromatic rings.

This is the first theoretical demonstration of an interaction between a formally negatively charged species and the π system of an aromatic ring, and complex energies suggest that the aryl centroid-anion bond should be applicable as noncovalent design principle, and the triazine ring incorporated as a new anion recognition module in cyclophane chemistry.

Almost at the same time, D. Quiñero and colleagues⁴⁷ have for the first time used the term “anion- π interaction” to describe the interaction between the permanent quadrupole of C_6F_6 and anions, during their research on the interactions between anions (H^- , F^- , Cl^- , Br^- , NO_3^- , CO_3^{2-}) and hexafluorobenzene. In these complexes the anions are positioned over the benzene ring along the C_6 axis. The results derived from crystallographic structures and theoretical calculations reveal the existence of anion- π interactions which are energetically favorable, and this new nonbonding interaction has been studied by using a topological analysis of the electron density and MIPp calculations.

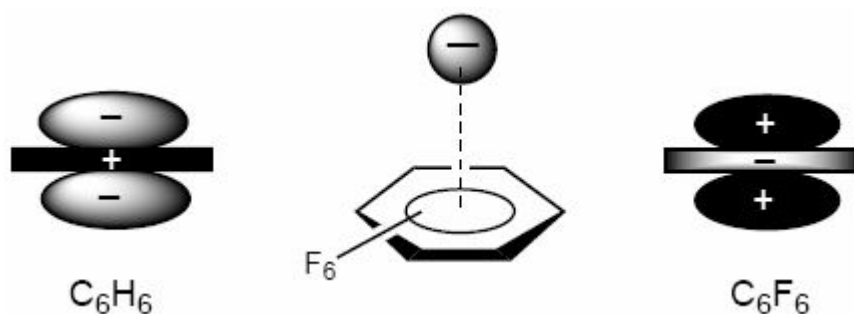


Figure 12. Representations of the quadrupole moments of benzene (left) and hexafluorobenzene (right), and the anion- π interaction (middle).

D. Quiñero and colleagues⁴⁸ have also carried out *ab initio* calculations on complexes between 1,3,5-trinitrobenzene (TNB) and anions (H⁻, F⁻, Cl⁻, Br⁻), where the anions are positioned over the ring along the C₃ axis. This study combines crystallographic and computational evidences to demonstrate an attractive interaction between the anion and the π -cloud of TNB. This interaction is rationalized based on the important role of the quadrupole moment of TNB and the anion-induced polarization. In addition, the study has been extended to 1,3,5-trifluorobenzene (TFB), which possesses a very small quadrupole moment. As a result, minimum energy complexes have been found between TFB and both anions and cations due to the stabilization obtained from the ion-induced polarization.

Untill now, the potential applications of these electron-deficient π systems of aromatic rings for the construction of molecular sensors have only been demonstrated by theoretical evidences, and very rare experimental examples of molecular sensor design involving anion- π interactions have been reported.

2.4 Sensors for electron-rich compounds*

2.4.1 General strategy used for detecting neutral analytes: π - π stacking

The general and often-used strategy for the construction of sensors of neutral compounds involves the establishment of π - π stacking between analyte and receptor. For example, the favorable interactions in the benzene-hexafluorobenzene complex have already been studied, including the face-to-face stacking in its crystal structure⁴⁹. A detailed analysis carried out by Williams stresses the important role of the large, permanent quadrupoles of the two molecules, which are similar in magnitude but of opposite sign (Figure 12)⁵⁰. The importance of the quadrupole moment for understanding intermolecular interactions of aromatic systems has been rationalized⁵¹⁻⁵³, and theoretical studies of the possible interaction of the π -electron cloud of C₆F₆ with several small electron donor molecules have been published previously⁵⁴⁻⁵⁶.

Penelle and Rotello⁵⁷ have created a molecular sensor employing π -stacking and lipophilic environment for efficient and rapid recognition of hexachlorobenzene in water, by careful engineering of a thin, molecularly imprinted polymer film

* Sensors for small gaseous molecules (electronic nose) are excluded from this thesis.

attached to a quartz crystal microbalance. Efficient imprinting was obtained in these films by controlling the heterogeneity of crosslinking in the polymer network and using appropriate electron-rich complements to the electron-deficient hexachlorobenzene (Figure 13). A comparison of the signals arising from two sensors, coated with imprinted and blank films respectively, unambiguously distinguishes hexachlorobenzene from small molecules of similar sizes and structures (anisole, benzene, chlorobenzene, and cyclohexane). The investigated sensors demonstrate both high selectivity and sensitivity (down to 10^{-12} mol.L⁻¹), while exhibiting an exceptionally fast response time (~10 s).

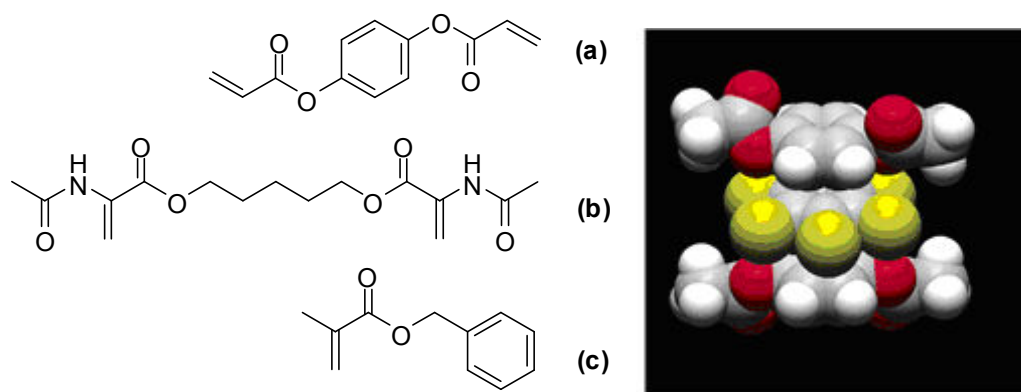


Figure 13. Chemical structures of the monomeric components used in the film fabrication (a, b, c), and predicted structure of the 2:1 π -stacked complex between 1,4-diacetoxybenzene and hexachlorobenzene within the polymer matrix (Amber force field).

Calixpyrroles, an easy-to-make class of neutral macrocycles, has attracted intensive interest in molecular recognition chemistry in recent years. Sessler and co-workers stated that calixpyrroles are effective and selective receptors for anions as well as neutral substrates^{58,59}. Both optical and electrochemical sensors based on calixpyrroles can be constructed for the recognition and sensing of anionic and neutral analytes. Multiple hydrogen bonding interactions between calixpyrrole and substrate are major binding contributions, while a subsidiary interaction mode using the periphery of calixpyrrole as an electron-rich site for binding either metals or neutral molecule species through metal- π , π - π stacking, or π -H interactions, which helps to stabilize the complex, has also been described. Shao⁶⁰ synthesized a new class of calix[4]pyrroles **69-72** (Figure 14), which can form a 1:1 non-covalent, charge-transfer molecular complex with chloranil (**68**) in CHCl₃, indicating that these molecules could find applications in the detection of neutral electron-deficient molecules.

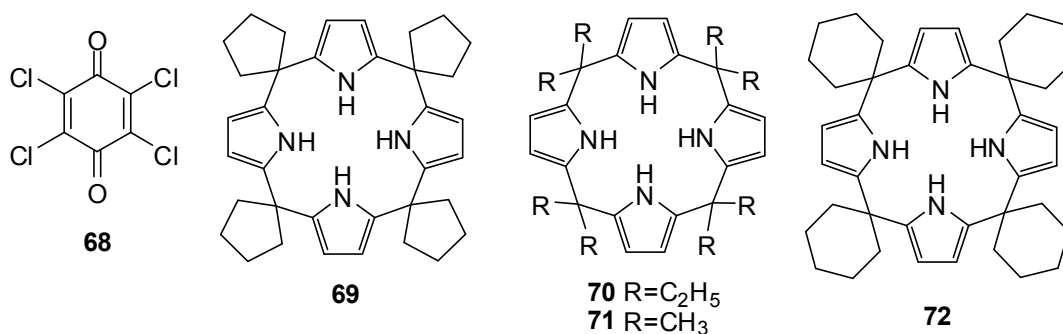
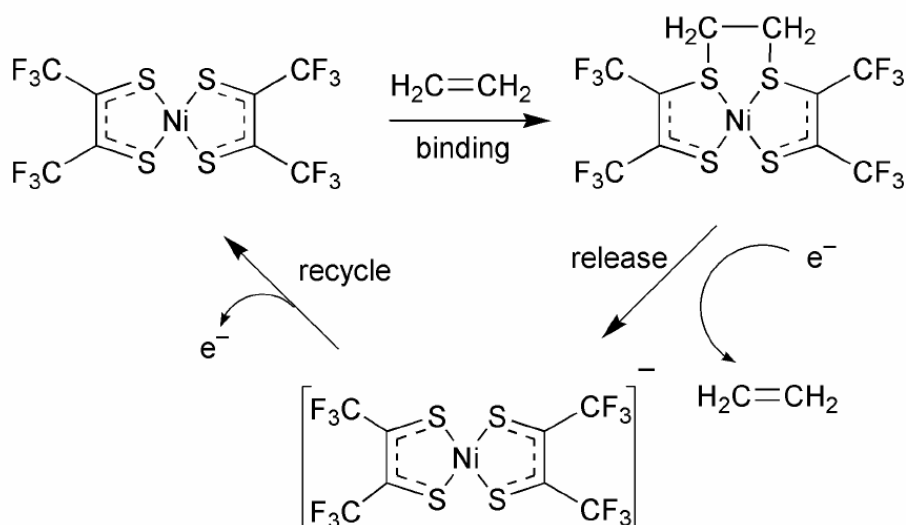


Figure 14. Calixpyrroles for recognition of neutral analytes.

2.4.2 Redox-switched binding

Electrochemical oxidation or reduction can influence or trigger a range of physicochemical properties in a molecular system, which are often termed redox switches (or electroswitches). The binding process can also be redox switched, if the binding affinity of a receptor or host molecule towards a substrate or guest is changed upon its oxidation or reduction. The change in redox potential upon complexation enables the binding process to be read out electrochemically and leads to the possibility of developing electrochemical sensors for a range of substrates. The interactions between redoxactive compounds and organic compounds including neutral ones have already been summarized by Tucker and Collinson⁶¹.

For example, a nickel dithiolene complex was shown to bind olefins in a reversible manner through a redox-switch cycle⁶². The complex bound the olefin in its neutral form with the olefin adding across two sulfur atoms. This process could be followed electrochemically by cyclic voltammetry studies in DM which revealed that the reversible one-electron reduction wave of the nickel dithiolene was markedly affected by the addition of excess alkene. Reduction appeared to diminish the stability of the adduct to such an extent that the olefin was rapidly released from the complex, which could then be oxidized back to the starting material (Scheme 5). Such a process appears to be a viable method of separating and purifying ethene from gas streams containing impurities such as CO, H₂S and ethyne which do not interact with the complex.



Scheme 5. A redox switch cycle for ethene separation.

2.4.3 Rare examples of sensors for electron-rich compounds

Detection of electron-rich compounds is of important significance, especially in environmental monitoring and pollutant controlling. Many organic pollutant molecules comprise electron-rich parts such as benzene, naphthalene and other aromatic rings including heteroaromatic rings. Yet examples for sensing such electron-rich compounds are surprisingly rare, for most fluorophores and electroactive groups in sensor molecules are also electron-rich, and thus generally specific non-bonding interactions between analyte and sensor could hardly be established.

As a known example, 4-Chlorophenol (4-CP) is one of a family of chlorophenols (CPs) which as a group represents a severe pollution problem to both aquatic and terrestrial ecosystems⁶³. Combining high-intensity ultrasound with a mechanically and chemically robust boron-doped diamond electrode, Compton and co-workers⁶⁴ have successfully developed an aqueous 4-chlorophenol voltammetric sensor. The surface regeneration abilities of power ultrasound through cavitation erosion of electrodeposited 4-chlorophenol by-products, facilitates a reproducible, insonated limiting-current oxidative signal in dilute acid conditions, with increased mass-transport offering enhanced sensitivity. A limit of detection of 1 mM and a linear range of 1–300 mM are achieved.

References

- 1 C. Ziegler, W. Gopel, H. Hammerle, H. Hatt, G. Jung, L. Laxhuber, H.-L. Schmidt, S. Schutz, F. Vogtle, A. Zell, *Biosens. Bioelectron.* **1998**, *13*, 539.
- 2 B. Valeur, *Molecular Fluorescence: Principles and Applications*, Wiley-VCH Verlag GmbH, **2001**, 274.
- 3 P. D. Beer, P. A. Gale, *Angew. Chem. Int. Ed.* **2001**, *40*, 486.
- 4 J. C. Medina, T. T. Goodnow, M. T. Rojas, J. L. Atwood, B. C. Lynn, A. E. Kaifer, G. W. Gokel, *J. Am. Chem. Soc.* **1992**, *114*, 10583.
- 5 P. D. Beer, Z. Cheng, M. G. B. Drew, J. Kingston, M. Ogden, P. Spencer, *J. Chem. Soc. Chem. Commun.* **1993**, 1046.
- 6 H. Plenio, H. El-Desoky, J. Heinze, *Chem. Ber.* **1993**, *126*, 2403.
- 7 H. Plenio, C. Aberle, *Organometallics* **1997**, *16*, 5950.
- 8 P. D. Beer, P. A. Gale, G. Z. Chen, *J. Chem. Soc. Dalton Trans.* **1999**, 1897.
- 9 J. L. Lopez, A. Turraga, A. Espinosa, M. D. Velasco, P. Molina, *Chem. Eur. J.* **2004**, *10*, 1815.
- 10 Y. Yang, X. Yang, H. -F. Yang, Z.-M. Liu, Y. -L. Liu, G. -L. Shen, R. -Q. Yu, *Anal. Chim. Acta* **2005**, *528*, 135.
- 11 M. Agathos, H. A. Bernecker, *Derm. Beruf. Umwelt.* **1982**, *30*, 43.
- 12 D. W. Cockcroft, V. H. Hoepfner, *Dolovich J. Chest.* **1982**, 82.
- 13 R. Wang, D. Zhang, Y. Zhang, and C. Liu, *J. Phys. Chem. B* **2006**, *110*, 18267.
- 14 F. P. Schmidtchen, M. Berger, *Chem. Rev.* **1997**, *97*, 1609.
- 15 T. S. Snowden, E. V. Anslyn, *Curr. Opin. Chem. Biol.* **1999**, *3*, 740.
- 16 P. D. Beer, P. A. Gale, *Angew. Chem. Int. Ed. Engl.* **2001**, *40*, 486.
- 17 J. L. Sessler, J. M. Davis, *Acc. Chem. Res.* **2001**, *34*, 989.
- 18 R. Martínez-Máñez, F. Sancenón, *Chem. Rev.* **2003**, *103*, 4419.
- 19 F. M. Ashcroft, *Ion Channels and Disease*; Academic Press: San Diego, CA, **2000**.
- 20 R. A. Manderville, *Curr. Med. Chem. –Anticancer Agents* **2001**, *1*, 195.
- 21 *Ullmann's Encyclopedia of Industrial Chemistry*, 6th ed.; Wiley VCH: New York, **1999**.
- 22 P. J. Worsfold, L. J. Gimbert, U. Mankasingh, O. N. Omaka, G. Hanrahan, P. Gardolinski, P. M. Haygarth, B. L. Turner, M. J. Keith-Roach, I. D. McKelvie, *Talanta* **2005**, *66*, 273.

-
- 23 G. Hanrahan, T. M. Salmassi, C. S. Khachikian, K. L. Foster, *Talanta* **2005**, *66*, 435.
- 24 R. H. Yang, W. H. Chan, A. W. M. Lee, P. F. Xia, H. K. Zhang, K. A. Li, *J. Am. Chem. Soc.* **2003**, *125*, 2884.
- 25 H. Huang, K. Wang, W. Tan, D. An, X. Yang, S. Huang, Q. Zhai, L. Zhou, Y. Jin, *Angew. Chem. Int. Ed.* **2004**, *43*, 5635.
- 26 K. Hanaoka, K. Kikuchi, H. Kojima, Y. Urano, T. Nagano, *J. Am. Chem. Soc.* **2004**, *126*, 12470.
- 27 Z. Xu, Y. Xiao, X. Qian, J. Cui, D. Cui, *Org. Lett.* **2005**, *7*, 889.
- 28 P. Chen, B. Greenberg, S. Taghavi, C. Romano, D. vander Lelie, C. He, *Angew. Chem., Int. Ed.* **2005**, *44*, 2715.
- 29 R. D. Shannon, *Acta Crystallogr. Sect. A* **1976**, *32*, 751.
- 30 S. Mangani, M. Ferraroni, in *Supramolecular Chemistry of Anions* (Eds.: A. Bianchi, K. Bowman-James, et al.), WILEYVCH, New York, **1997**, p. 63.
- 31 F. Hofmeister, *Arch. Exp. Pathol. Pharmacol.* **1888**, *24*, 247.
- 32 E. Graf, J.-M. Lehn, *J. Am. Chem. Soc.* **1976**, *98*, 6403.
- 33 F. P. Schmidtchen, *Angew. Chem. Int. Ed. Engl.* **1977**, *89*, 751.
- 34 B. Dietrich, J. Guilhem, J.-M. Lehn, C. Pascard, E. Sonveaux, *Helv. Chim. Acta* **1984**, *67*, 91.
- 35 F. P. Schmidtchen, G. Müller, *J. Chem. Soc. Chem. Commun.* **1984**, 1115.
- 36 K. Bowman-James, *Acc. Chem. Res.* **2005**, *38*, 671.
- 37 V. Amendola, M. Bonizzoni, D. Esteban-Gómez¹, L. Fabbrizzi, M. Licchelli, F. Sancenón, A. Taglietti, *Coord. Chem. Rev.* **2006**, *250*, 1451.
- 38 S. Mizukami, T. Nagano, Y. Urano, A. Odani, and K. Kikuchi, *J. Am. Chem. Soc.* **2002**, *124*, 3920.
- 39 F. P. Schmidtchen, *Chem. Ber.* **1981**, *114*, 597.
- 40 A. Frontera, J. Morey, A. Oliver, M. N. Pinã, D. Quinõnero, A. Costa, P. Ballester, P. M. Deyà, and E. V. Anslyn, *J. Org. Chem.* **2006**, *71*, 7185.
- 41 F. A. Quioco, J. S. Sack, N. K. Vyas, *Nature* **1987**, *329*, 561.
- 42 P. A. Gale, *Acc. Chem. Res.* **2006**, *39*, 465.
- 43 J. P. Gallivan, D. A. Dougherty, *Org. Lett.* **1999**, *1*, 103.
- 44 Y. Danten, T. Tassaing, M. Besnard, *J. Phys. Chem. A* **1999**, *103*, 3530.
- 45 I. Alkorta, I. Rozas, J. Elguero, *J. Org. Chem.* **1997**, *62*, 4687.

-
- 46 M. Maascal, A. Armstrong, M. Bartberger, *J. Am. Chem. Soc.* **2002**, *124*, 6274.
- 47 D. Quiñonero, C. Garau, C. Rotger, A. Frontera, P. Ballester, A. Costa, P. M. Deyà, *Angew. Chem. Int. Ed.* **2002**, *41*, 3389.
- 48 D. Quiñonero, C. Garau, A. Frontera, P. Ballester, A. Costa, P. M. Deyà, *Chem. Phys. Lett.* **2002**, *359*, 486.
- 49 J. H. Williams, J. K. Cockcroft, A. N. Fitch, *Angew. Chem. Int. Ed. Engl.* **1992**, *31*, 1655.
- 50 J. H. Williams, *Acc. Chem. Res.* **1993**, *26*, 593.
- 51 P. Hobza, H. L. Selzle, E. W. Schlag, *J. Am. Chem. Soc.* **1994**, *116*, 3500.
- 52 F. Cozzi, R. Ponzini, R. Annunziata, M. Cinquini, J. S. Siegel, *Angew. Chem. Int. Ed. Engl.* **1995**, *34*, 1019.
- 53 H. Adams, F. J. Carver, C. A. Hunter, J. C. Morales, E. M. Seward, *Angew. Chem. Int. Ed. Engl.* **1996**, *35*, 1542.
- 54 I. Alkorta, I. Rozas, J. Elguero, *J. Org. Chem.* **1997**, *62*, 4687.
- 55 J. P. Gallivan, D. A. Dougherty, *Org. Lett.* **1999**, *1*, 103.
- 56 Y. Danten, T. Tassaing, M. Besnard, *J. Phys. Chem. A* **1999**, *103*, 3530.
- 57 K. Das, J. Penelle, and V. M. Rotello, *Langmuir* **2003**, *19*, 3921.
- 58 P. A. Gale, J. L. Sessler, V. Kral', V. Lynch, *J. Am. Chem. Soc.* **1996**, *118*, 5140.
- 59 P. A. Gale, P. Jr. Anzenbacher, J. L. Sessler, *Coord. Chem. Rev.* **2001**, *222*, 57.
- 60 S. Shao, Y. Guo, L. He, S. Jiang and X. Yu, *Tetrahedron Lett.* **2003**, *44*, 2175.
- 61 J. H. R. Tucker and S. R. Collinson, *Chem. Soc. Rev.* **2002**, *31*, 147.
- 62 K. Wang and E. I. Stiefel, *Science* **2001**, *291*, 106.
- 63 J. C. Merriman, D. H. J. Anthony, J. A. Kraft, R. J. Wilkinson, *Chemosphere* **1991**, *23*, 1605.
- 64 A. J. Saterlay, J. S. Foord, R. G. Compton, *Electroanalysis* **2001**, *13*, 1065.

Chapter 3 Tetrazine derivatives for sensor applications

3.1 Interaction of tetrazines with anions/electron-rich compounds—anion- π interaction/ π - π interaction

The research on tetrazines for sensor applications is still an undeveloped field; and the binding ability of *s*-tetrazines has not been noticed until very recently.

The interesting work of Dunbar's group^{1, 2} has for the first time offered experimental evidences of anion binding ability of *s*-tetrazines, by reporting a one-pot, high-yield synthesis of metallacyclophanes from 3,6-bis(2-pyridyl)-*s*-tetrazine (**50**) and $M(\text{CH}_3\text{CN})_6^{2+}$ ($M=\text{Ni}, \text{Co}, \text{Zn}$). The reaction is templated by the counterion (BF_4^- , SbF_6^-) which is fundamental to the formation of the metallacyclophane. Two examples, retrieved from the Cambridge Structural Database, are shown in Figure 1. In the first example (**a**), the encapsulated anion BF_4^- resides in the void space in the center of the cavity of the molecular square, π -interacting with the four electron deficient *s*-tetrazine rings. In the second one (**b**), the anion used in the reaction is SbF_6^- and the result is the formation of a molecular pentagon; again the anion has short contacts with the five aromatic *s*-tetrazine rings.

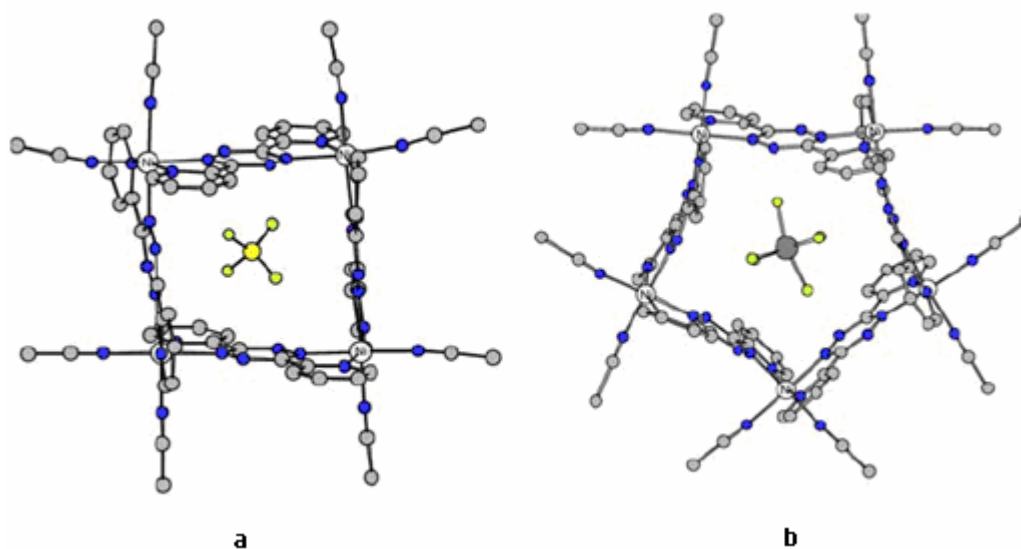


Figure 1. a. Crystal structure of $[\text{Ni}_4(\mathbf{50})_4(\text{CH}_3\text{CN})_8]^{8+}$ with encapsulated $[\text{BF}_4]^-$ ion; b. Crystal structure of $[\text{Ni}_5(\mathbf{50})_5(\text{CH}_3\text{CN})_{10}]^{10+}$ with encapsulated $[\text{SbF}_6]^-$ ion.

They have also carried reactions of **50** with a series of other solvated first-row transition metals $M(\text{II})$ ($M= \text{Mn}, \text{Fe}, \text{Cu}$), and obtained the respective cyclic products³. The formation of the various metallacyclophanes is influenced by the choice of metal ions, anions, and solvents. Short distances are also noted between the centroids of the tetrazine rings to the O/F atoms of the encapsulated anions rather than interactions with the cationic metal centers, which indicate clearly the anion- π interactions as a stabilizing factor in the present cyclic structures.

The anion- π interaction (see **Chapter 2**) has also been demonstrated by Frontera's group in the study of interactions between anions and hexafluorobenzene⁴ or 1,3,5-trinitrobenzene⁵, and by Maascal *et al.*⁶ during their study of interactions between anions and electron-deficient *s*-triazine aromatic rings.

More recently, Frontera's group⁷ has reported the results of high level *ab initio* calculations computed for several complexes (Figure 2) of anions with urea (**73a-c**), squaramide (**74a-c**) and the electron deficient aromatic ring of *s*-tetrazine (**75a-c**) to better understand the binding forces entangled in both hydrogen bond and anion- π interactions. The computed binding energies of complexes of *s*-tetrazine with anions were compared with those of urea and squaramide which are well known binding units for building neutral anion receptors. Furthermore, molecular electrostatic potential (MEP) and molecular interaction potential maps without and with polarization (MIP and MIPp, respectively) for all the anion acceptors used (urea, squaramide and *s*-tetrazine) were calculated and carefully inspected in order to evaluate the contribution of the different components (electrostatic, polarization, van der Waals forces or charge-transfer effects) to the total binding energy of the mentioned interactions. The results derived from their calculations confirmed that *s*-tetrazine is a good candidate to be a new binding unit for designing and synthesizing new cyclophane type receptors suitable for the recognition of anions. Moreover, the physical nature of the interactions of *s*-tetrazine with anions, demonstrated by MIPp calculations, indicated that the polarization and electrostatic terms dominate the interaction.

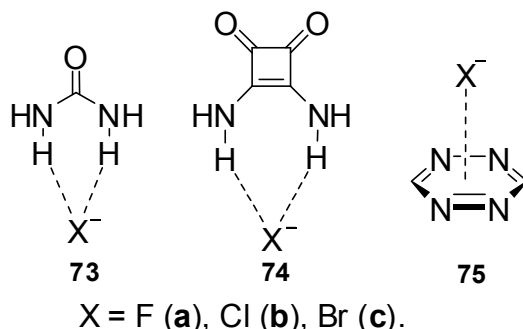


Figure 2. Anion complexes of urea, squaramide and *s*-tetrazine.

3.2 Development of tetrazines in sensor applications: the previous work in Audebert's group

Although some crystallographic structures found in the CSD confirm the π -interaction of anions with the aromatic ring of the *s*-tetrazine derivatives, and experimentally, anions have been used to template the synthesis of *s*-tetrazine-based metallacyclophanes, the capability of binding anions or electron-rich compounds of *s*-tetrazine has not yet been used in the molecular recognition of anions till now. During their research Audebert *et al.* have noticed that some tetrazines have fluorescent properties, which was also mentioned once by one research group before⁸. Otherwise little attention was given on the fluorescence property of tetrazines.

In previous work conducted by Audebert *et al.*⁹, several tetrazine compounds, chloromethoxy-*s*-tetrazine (**76**), dimethoxy-*s*-tetrazine (**52**), chloronaphthoxy-*s*-tetrazine (**77**) and a new bridged tetrazine 1,4-bis(chloro-*s*-tetrazinyloxo)butane (**78**) have been synthesized (Figure 3), and their electrochemical and photochemical properties have been investigated.

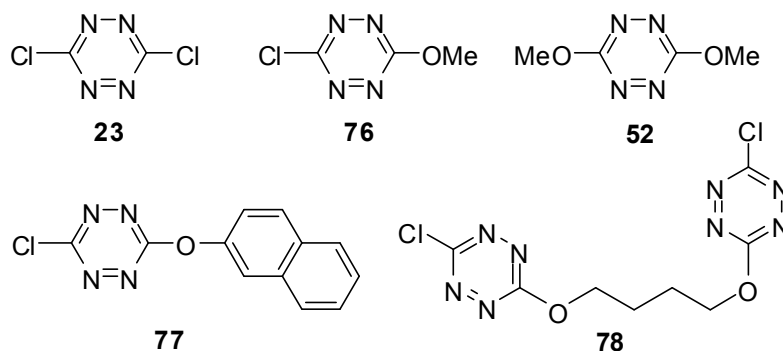


Figure 3. Tetrazines synthesized by Audebert *et al.*

The electrochemical study was performed to investigate the potential ability of the anion radical of chlorotetrazines to cleave into a tetrazinyl radical and a chloride ion, and to check the sensitivity of the reduction potential to chemicals, especially electron-rich compounds, since it had been already suggested in the literature⁷, that tetrazines should be able to coordinate to fluoride ions, and hence there is a possibility that the redox potential could be affected by the addition of halide ions or electron-rich aromatic compounds.

The results of electrochemistry measurements show that all the tetrazine compounds investigated are reducible, giving well defined, fully reversible cyclic voltammograms (CVs), as depicted on Figure 4. CVs are reversible whatever the chlorine content. Apparently the tetrazine ring is electrodeficient enough to prevent a chlorine atom to be expelled from the anion radical.

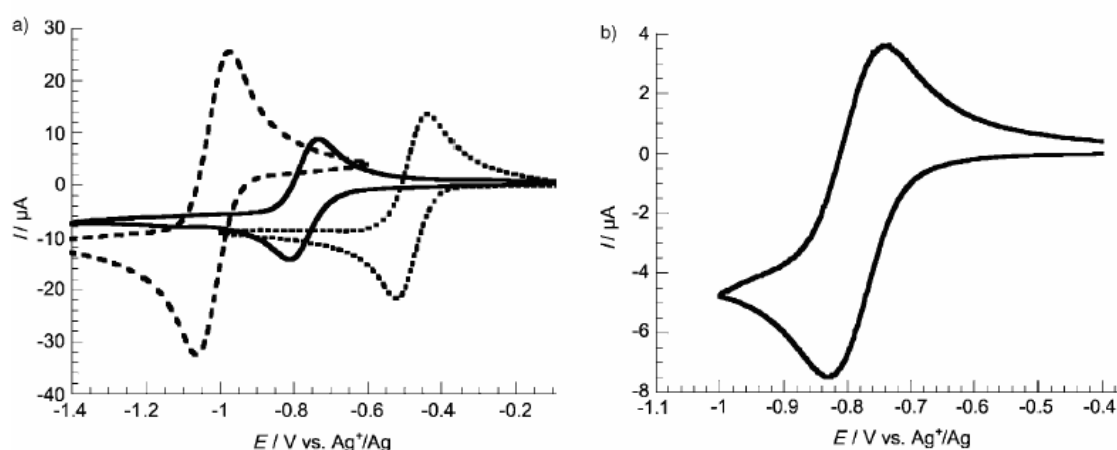


Figure 4. CV of a) **23**(- - - -), **52**(- · - · -), **76**(————); and b) **78** in dichloromethane (+ TBAP) on glassy carbon electrode at 0.1 Vs^{-1} . CV of compound **77** is similar to **52** and was not displayed for clarity purpose.

Some attempts were made to investigate the influence of halides added (all of which have been tested) and electron-rich substances (phenol, anisole and triphenylamine) on the redox potential of the tetrazine (dichloro-*s*-tetrazine was chosen as the model substrate). No potential shift was observed, as it should have been the case, if the formation of a somewhat stabilized adduct between the neutral tetrazine and the electron-rich added compound had occurred. However, in the case of acidic aromatic compounds such as phenol and especially 4-nitrophenol, a positive shift of the reduction potential of the tetrazine, as well as a strong decrease of the reoxidation current has been observed, which gives evidence for an efficient proton transfer between the basic anion radical of the tetrazine compound and the phenolic moiety.

Geometry optimisation has been completed and the results show that all of the tetrazines investigated are completely planar, confirming a good electronic interaction between the cycle and its substituents (Figure 5).

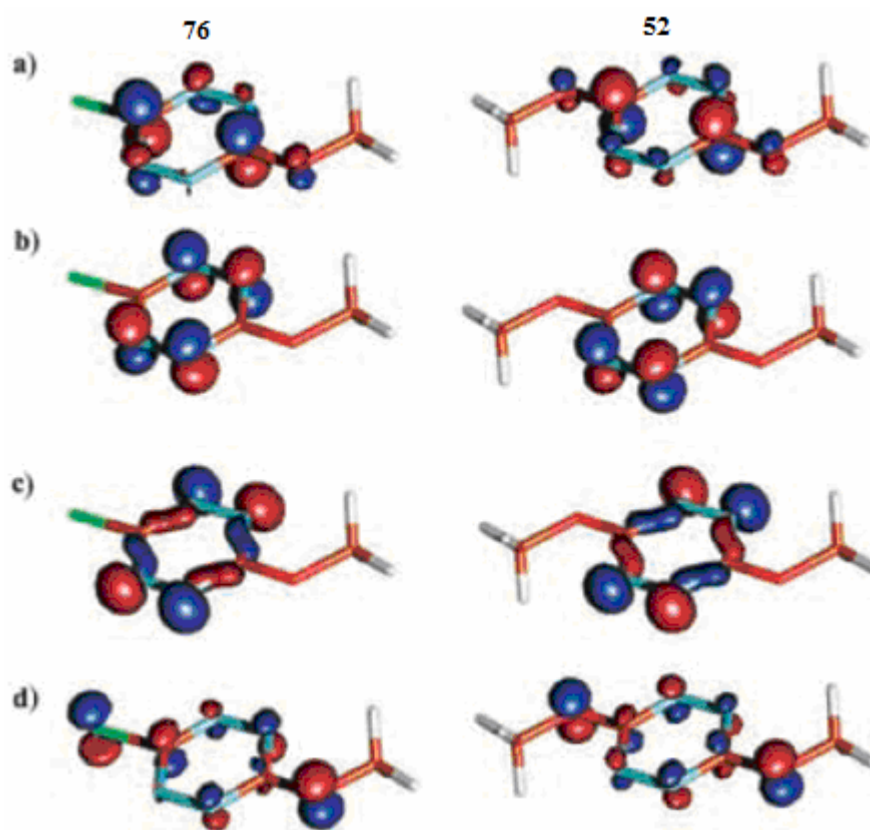


Figure 5. Plots of HOMO (c), LUMO (b) and the two next ones HOMO-1 (d) and LUMO+1 (a) for compound **76** (left column) and **52** (right column).

The absorption spectra of these compounds all show two major absorption areas, located around 500-550 nm and 260-370 nm, respectively (Figure 6, Table 1). The fluorescence spectra of these tetrazines have been recorded both in solution (Figure 7) and in the crystalline state (Table 2). The fluorescence decays (Figure 8) have also been investigated and show long lifetimes (several tens of ns) with monoexponential behavior, as expected for small molecules in solution if only one population of molecules is encountered. Compound **77** shows a biexponential behavior with a very short lifetime, which might be due to the contribution of the naphthalene moiety. For symmetric molecules dichlorotetrazine **23** and

dimethoxytetrazine **52**, lifetimes are all in the same range (50 to 60 ns) and quantum yields are close. On the contrary, the chloromethoxytetrazine **76** shows a three times higher quantum yield and a very long lifetime. This very unusual behavior is interesting in view of potential sensor applications.

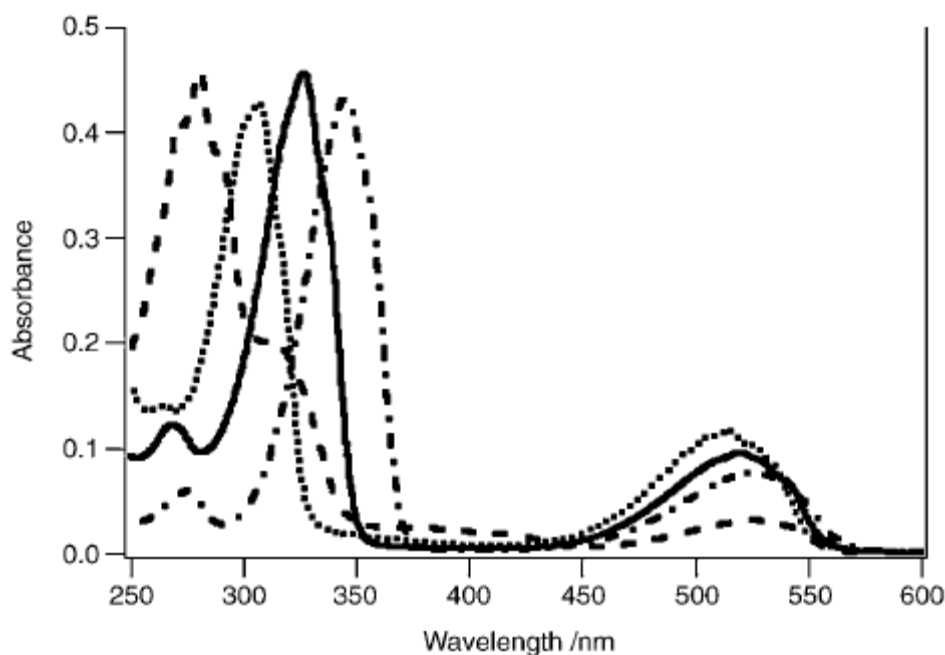


Figure 6. Absorption spectra of compounds **23** (.....), **76** (—), **52** (—•—•—•), and **78** (- - -) in dichloromethane.

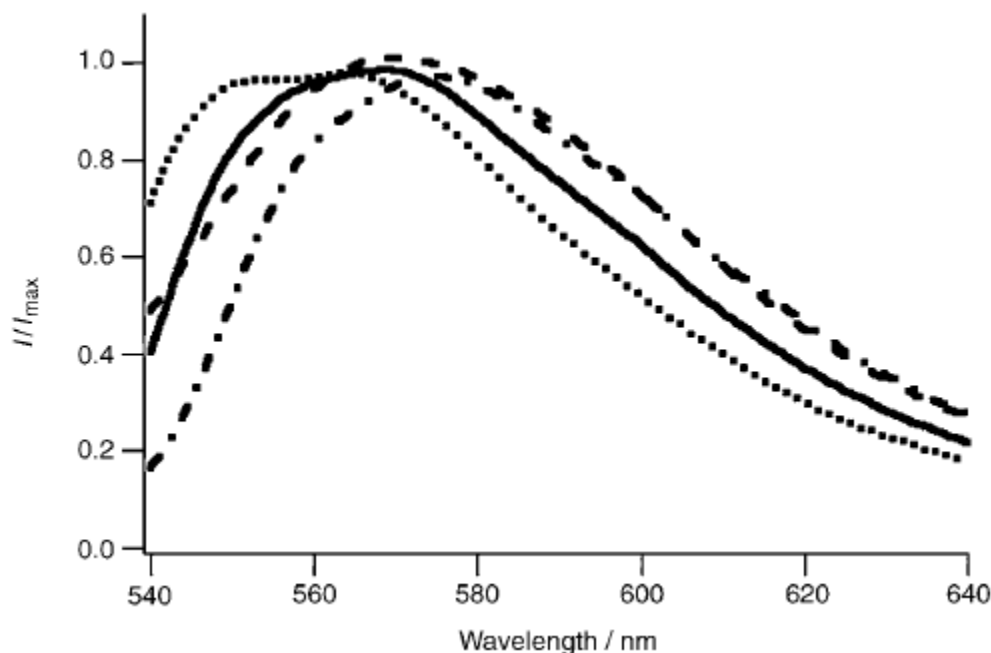


Figure 7. Fluorescence emission spectra of compounds **23** (.....), **76** (—), **52** (—•—•—•), and **78** (- - -) in dichloromethane. Excitation wavelength: 495 nm.

Table 1. Spectroscopic data of tetrazine **23**, **76**, **52** and **78**.

Compound	λ_{\max}^{abs} (nm)	λ_{\max}^{em} (nm)	ϵ_{abs} (L.mol ⁻¹ .cm ⁻¹)	Lifetime (ns)	Φ_F
23	307-515	551-567	460	58	0.14

76	269-327-520	567	1900	160	0.38
52	275-345-524	575	663	49	0.11
77	281-523	338 ^a 567 ^b	573	120; 6 ^c	0.004
78	270-328-521	572	1170		0.36

[a] Excitation at 281 nm. [b] Excitation at 524 nm. [c] Biexponential decay.

Table 2. Maximum emission wavelenths and lifetimes of tetrazines in the powder state (excitation wavelenths at 495 nm).

Compound	λ_{\max}^{abs} (nm)	Lifetime (ns)
23	555	17.8
76	560	19.1
52	569	16.0
77	563	0.7 ^a
78	559.5	12.6 ^b 8-9 ^c

[a] Multiexponential. [b] Monoexponential (excitation at the crystal centre). [c] Multiexponential (excitation at the crystal edge).

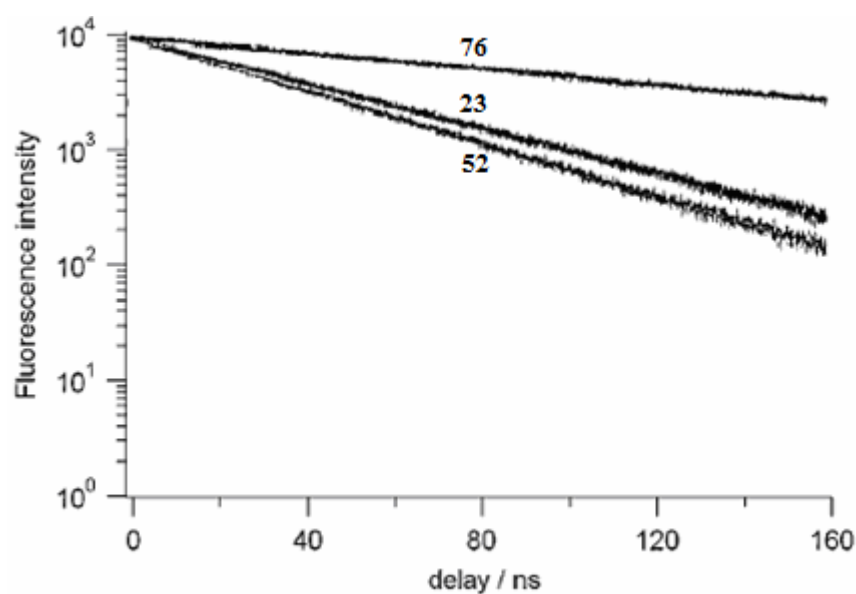


Figure 8. Fluorescence decays of tetrazines **23**, **52**, **76** in dichloromethane (excitation wavelenths 495nm).

In order to investigate the possible use of these molecules as sensor agents, the fluorescence quenching was also studied by adding electron-rich rings of either aprotic compounds such as anisole or tertiary amines or protic compounds such as phenol or 4-nitrophenol. The tetrazine **78** was selected as potential “tweezer” for donor substrates, because it can possibly act as a two-sided acceptor. In all cases the electron-rich aromatic compounds have been shown to quench the fluorescence of the tetrazine excited state in the visible range and electron transfer seems to be the most efficient way of fluorescence quenching.

To sum up, all these tetrazines are reversibly electroactive, with redox potentials shifting cathodically with the donor character of substituent; all these

tetrazines are also fluorescent with maximum emission wavelengths in the range 550-575 nm. Some of them show very long fluorescence lifetimes (a few tens of ns) and remain fluorescent in the solid state without major changes in the spectral features, which place them certainly among the smallest crystalline organic fluorophores in the visible range ever prepared. Moreover, the fluorescence of these tetrazine derivatives can be efficiently quenched by the presence of electron-rich compounds like triphenylamine or anisole, which make them very promising molecules for sensor applications.

3.3 Molecular designing for sensors

The preliminary investigations show that 1,2,4,5-tetrazines are very promising candidates for the construction of fluorescent or electrochemical molecular sensors for anions and electron-rich compounds. Some experimental results concerning the fluorescence rules of tetrazines were also obtained:

- *s*-Tetrazine is weakly fluorescent;
- Aromatic *s*-tetrazines are not fluorescent;
- Several *s*-tetrazines substituted by heteroatoms are fluorescent (Figure 9):

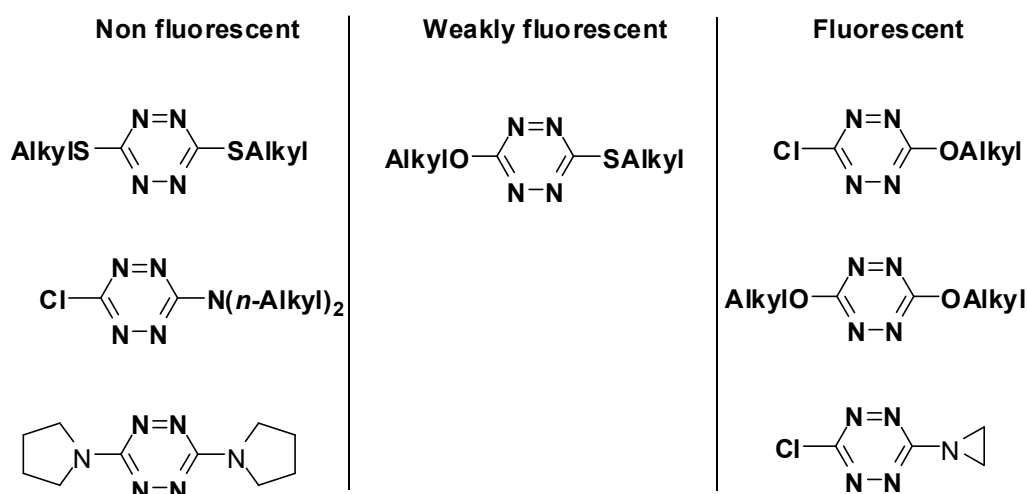


Figure 9. Some experimental results concerning the fluorescence rules of tetrazines.

Therefore, based on these results, a series of molecular sensors containing tetrazine segments as both binding units and sensing units were designed (Figure 10):

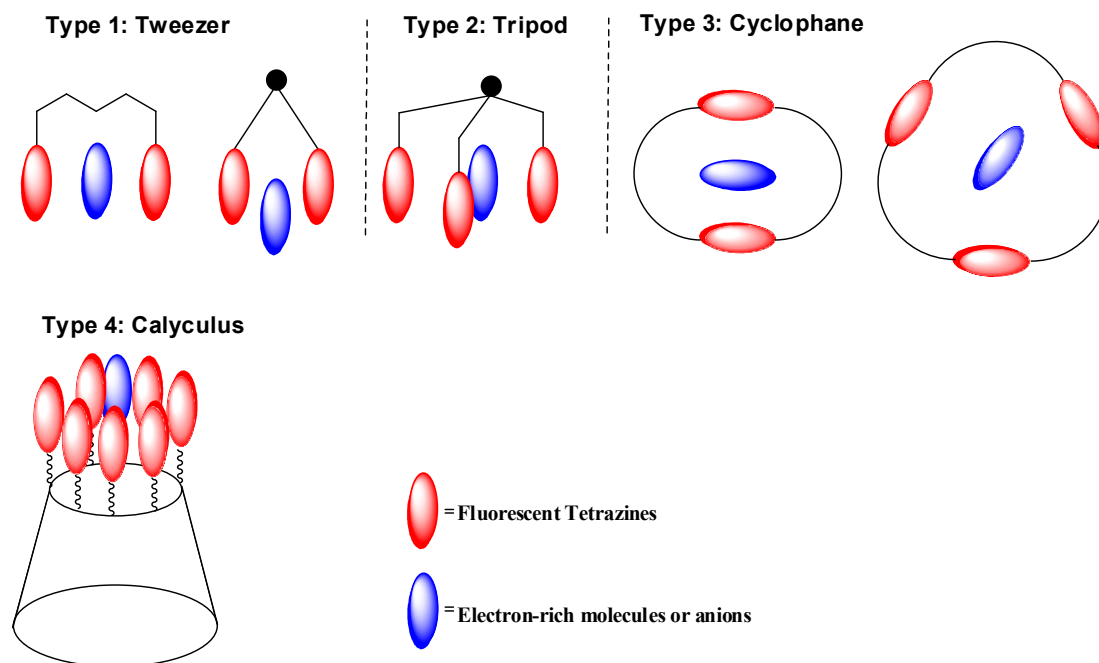


Figure 10. Molecular design of different types of sensors.

For the type 1, the first “tweezer” prepared before has a flexible alkyl chain, which seems to be not very efficient to “bind” the anions or electron-rich molecules, as indicated by electrochemistry studies. Therefore, besides the enlargement of “tweezers” with flexible chains, we have also designed some tweezers with rigid backbones (**82-84**, Figure 11, molecules in bold style in this figure and the subsequent ones were synthesized successfully):

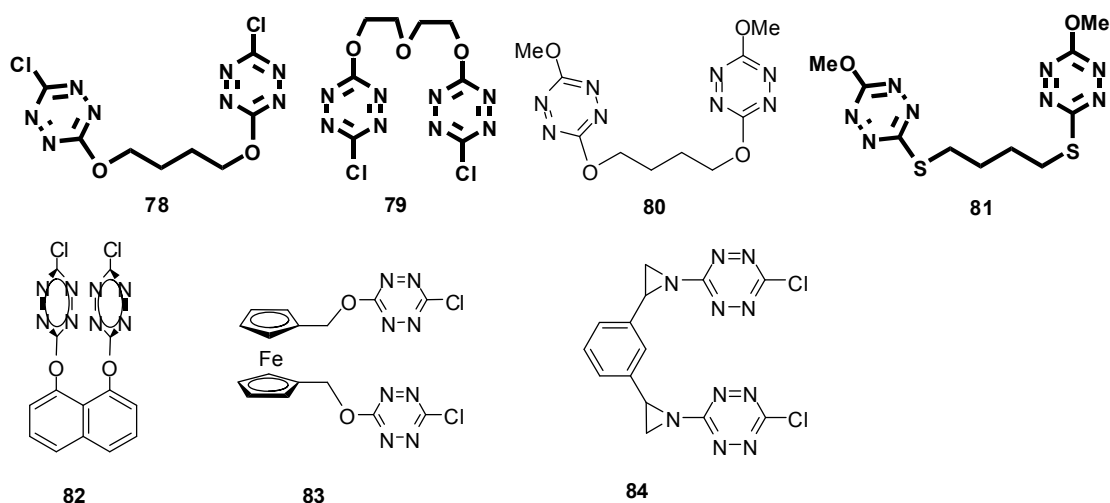


Figure 11. Synthetic targets of “Tweezers”.

For the type 2, tripod sensors, three molecules were designed based on readily available triols triethanolamine and 2-(bromomethyl)-2-(hydroxymethyl)propane-1,3-diol (Figure 12):

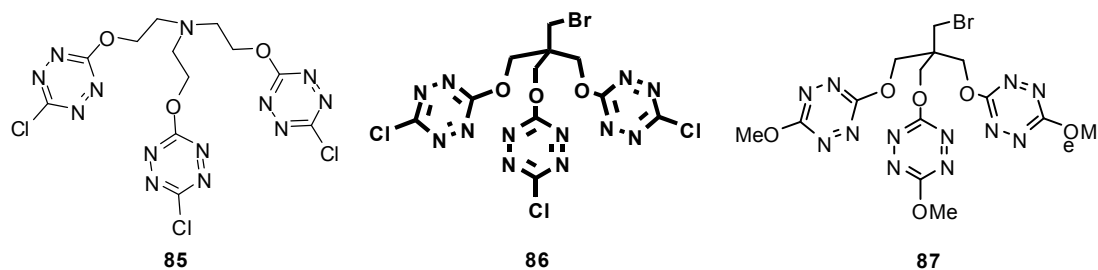


Figure 12. Tripod-sensor targets.

Cyclophanes capable of both complexation and detection of a guest are the field of active research¹⁰ because of the expected enhanced sensing abilities from the presence of a cage-like structure. However, the complexation of anions or electron-rich molecules remains a difficult task because of the lack of suitable receptors and particularly of neutral ones. Therefore it was a natural challenge to try to prepare a cyclophane containing several tetrazines which could lead to the formation of complexes with anions or electron-rich molecules. Taking advantage from the various properties of tetrazines, we might then detect the presence of a guest by fluorescence and release it reversibly by electrochemistry. Therefore several cyclophane molecular targets have been set up for this purpose (Figure 13):

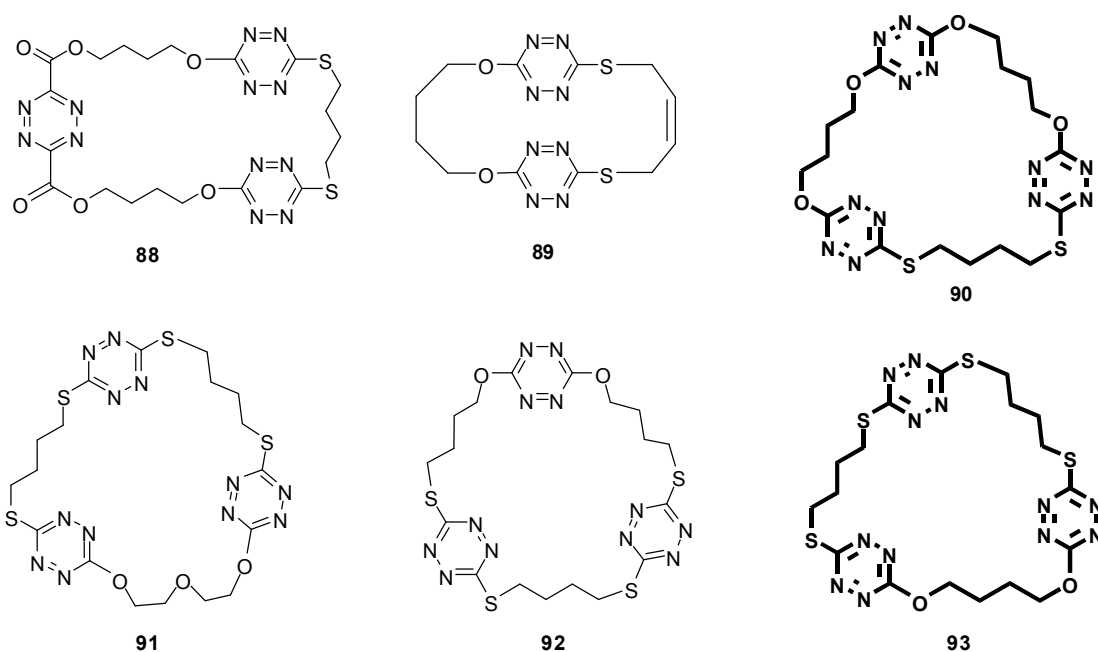


Figure 13. Cyclophane-tetrazine targets.

α -, β - and γ -cyclodextrins (CDs) are toroidal molecules containing six, seven and eight D-glucopyranose units, respectively. The internal diameters of the cavities are approximately 5, 6.5 and 8.5 Å, respectively, and the depth is about 8 Å (Figure 14).

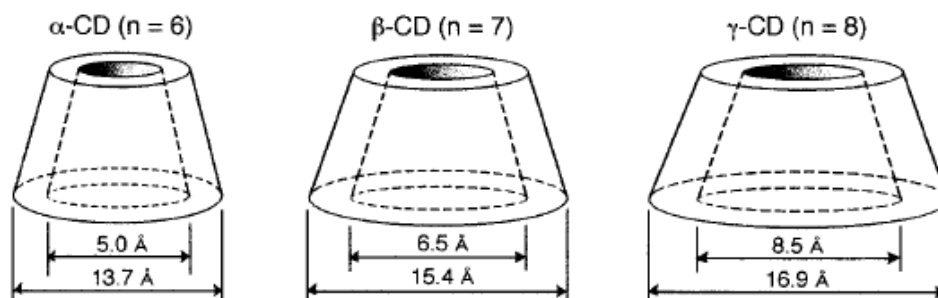


Figure 14. Schematic representation of α -, β - and γ -cyclodextrins (CDs).

To increase the affinity and the selectivity of the quenching, it remained to favour the proximity of the tetrazine to the quencher. We reasoned that CDs, with their size-adaptable internal hydrophobic cavity¹¹, could especially fit this purpose by favouring the inclusion in their midst of substrates of the appropriate dimension, while the others would remain in solution and, therefore, participate much less efficiently to the quenching. Multichromophoric CD derivatives have been reported as photocatalytic devices that mimic the photosynthetic light-harvesting antenna¹², for nonlinear optics¹³ or to detect different cationic species^{14, 15}. Sensing of small molecules like aromatic hydrocarbons, quinones and steroids has become possible with metalocyclodextrins by attaching lanthanide or ruthenium binding units to the cyclodextrin¹⁶. The transfer of the excitation energy amongst chromophores in cyclodextrins has been studied: for instance, energy transfer to excimers¹⁷ or to embedded chromophores^{18, 19} and red-edge effects²⁰ have been characterized and quantified. But the chromophores used, naphthalene derivatives, absorb and emit light at wavelengths that do not fit to the specification of modern light sources and detectors. Tetrazines are the smallest dyes able to absorb and emit around 500 nm. Besides their electron attracting character, the intrinsic chemistry of the dichlorotetrazine is especially suited to achieve the proximity between the sensing tetrazine ring and the cyclodextrin cavity, because this particular molecule was anticipated to react directly with the OH functional groups of cyclodextrin. Therefore, cyclodextrins functionalized by fluorescent tetrazine rings (Type 4, Figure 15) are set up as synthetic targets for the calycular type of receptors.

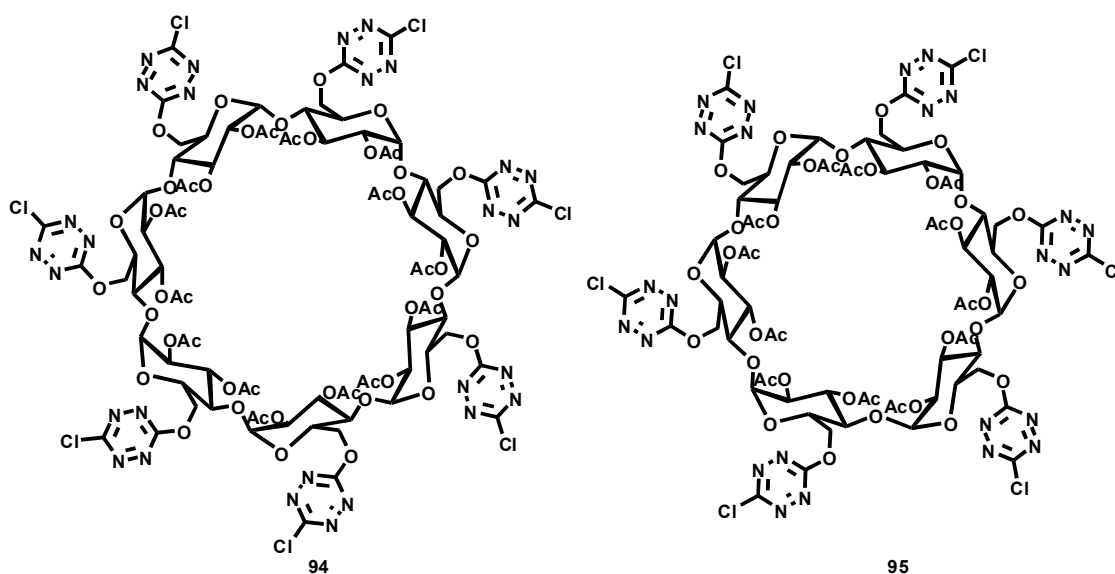
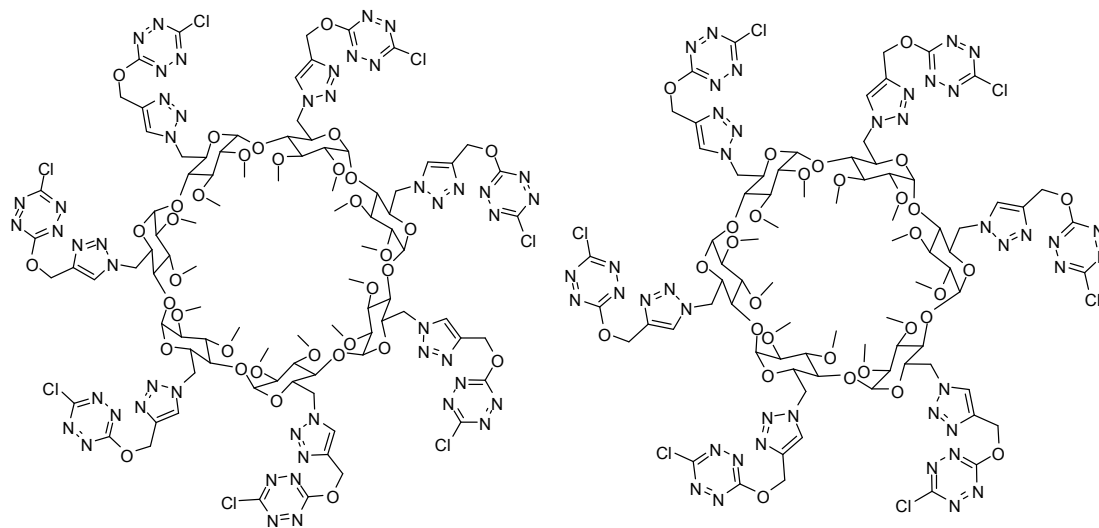


Figure 15. CD-tetrazine targets.

Since “click chemistry” is generally considered to be very efficient and reliable in the construction of new molecular structures, and has already been widely applied in organic synthesis (see **Chapter 4**), cyclodextrins functionalized by fluorescent tetrazine rings through “click reaction” are also set up as synthetic targets (Figure 16).



96

97

Figure 16. CD-tetrazine targets using click chemistry.

References

- 1 C. S. Campos-Fernandez, R. Clerac, K. R. Dunbar, *Angew. Chem. Int. Ed.* **1999**, *38*, 3477.
- 2 C. S. Campos-Fernandez, R. Clerac, J. M. Koomen, D. H. Russell, K. R. Dunbar, *J. Am. Chem. Soc.* **2001**, *123*, 773.
- 3 C. S. Campos-Fernandez, B. L. Schottel, H. T. Chifotides, J. K. Bera, J. Bacsá, J. M. Koomen, D. H. Russell, and K. R. Dunbar, *J. Am. Chem. Soc.* **2005**, *127*, 12909.
- 4 D. Quiñonero, C. Garau, C. Rotger, A. Frontera, P. Ballester, A. Costa, P. M. Deyà, *Angew. Chem. Int. Ed.* **2002**, *41*, 3389.
- 5 D. Quiñonero, C. Garau, A. Frontera, P. Ballester, A. Costa, P. M. Deyà, *Chem. Phys. Lett.* **2002**, *359*, 486.
- 6 M. Maascal, A. Armstrong, M. Bartberger, *J. Am. Chem. Soc.* **2002**, *124*, 6274.
- 7 C. Garau, D. Quiñonero, A. Frontera, A. Costa, P. Ballester, P. M. Deyà, *Chem. Phys. Lett.* **2003**, *370*, 7.
- 8 F. Gückel, A. H. Maki, F. A. Neugebauer, D. Schweitzer, H. Vogler, *Chem. Phys.* **1992**, *164*, 217.
- 9 P. Audebert, F. Miomandre, G. Clavier, M.-C. Vernières, R. Renault-Méallet, S. Badré, *Chem. Eur. J.* **2005**, *11*, 5667.
- 10 J. -M. Lehn, *Science*, **2002**, *295*, 2400.
- 11 J. Szejtli, *Chem. Rev.* **1998**, *98*, 1743.
- 12 P. F. Wang, L. Jullien, B. Valeur, J. S. Filhol, J. Canceill and J. M. Lehn, *New J. Chem.* **1996**, *20*, 895.
- 13 E. Rekaí, J. B. Baudin, L. Jullien, I. Ledoux, J. Zyss and M. Blanchard-Desce, *Chem. Eur. J.* **2001**, *7*, 4395.
- 14 P. Choppinet, L. Jullien and B. Valeur, *J. Chem. Soc., Perkin Trans. 2* **1999**, 249.
- 15 R. Heck, F. Dumarcay and A. Marsura, *Chem. Eur. J.* **2002**, *8*, 2438.
- 16 J. M. Haider and Z. Pikramenou, *Chem. Soc. Rev.* **2005**, *34*, 120.
- 17 M. N. Berberan-Santos, J. Canceill, J. C. Brochon, L. Jullien, J. M. Lehn, J. Pouget, P. Tauc and B. Valeur, *J. Am. Chem. Soc.* **1992**, *114*, 6427.
- 18 L. Jullien, J. Canceill, B. Valeur, E. Bardez, J. P. Lefevre, J. -M. Lehn, V. MarchiArtzner and R. Pansu, *J. Am. Chem. Soc.* **1996**, *118*, 5432.

-
- 19 M. N. Berberan-Santos, P. Choppinet, A. Fedorov, L. Jullien and B. Valeur, *J. Am. Chem. Soc.* **2000**, *122*, 11876.
- 20 M. N. Berberan-Santos, J. Pouget, B. Valeur, J. Canceill, L. Jullien and J. M. Lehn, *J. Phys. Chem.* **1993**, *97*, 11376.

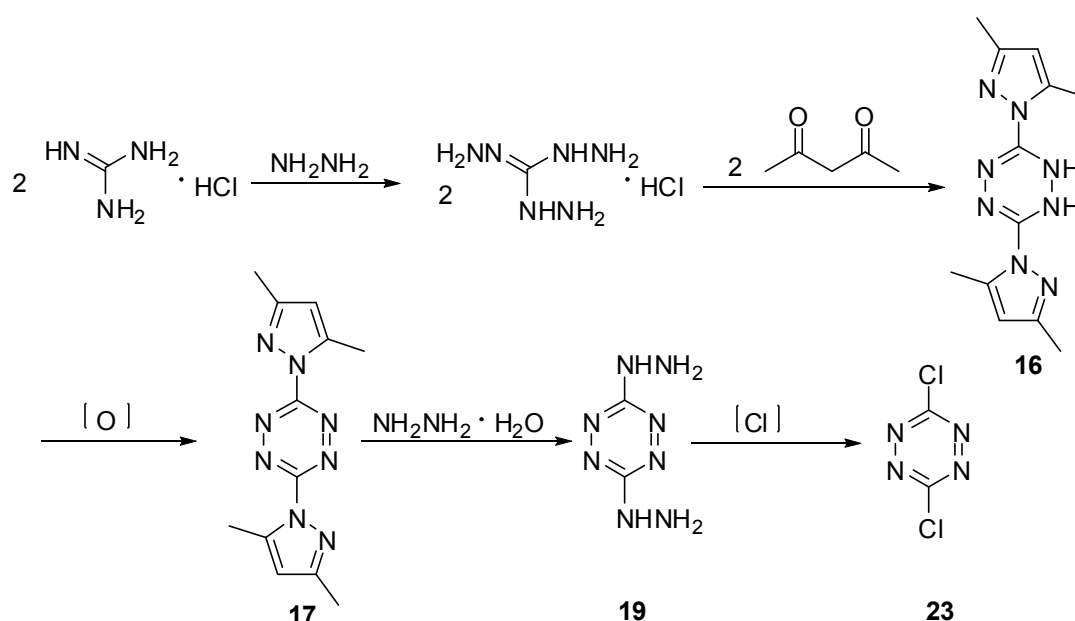


Chapter 4 Synthesis: results and discussion

4.1 Preparation of 3,6-dichloro-1,2,4,5-tetrazine (7)

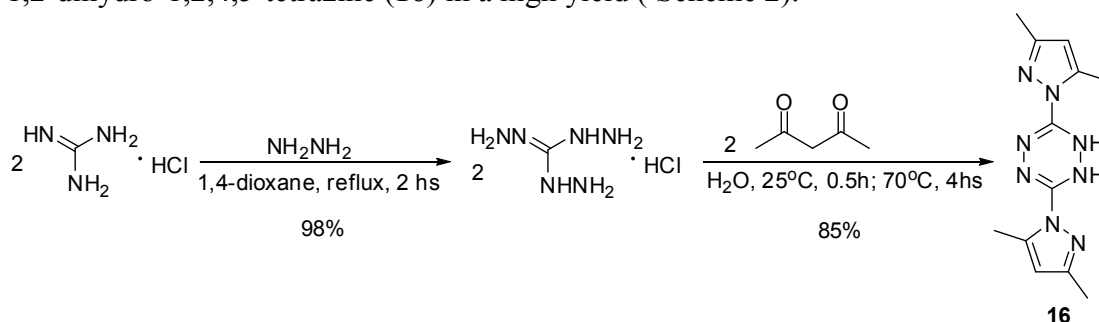
3,6-Dichloro-1,2,4,5-tetrazine, because of its high reactivity toward various nucleophiles as already mentioned before (**Chapter 1.3.1**), is used as starting material for the preparation of a variety of 3,6-substituted tetrazines. Therefore a facile preparation for a large quantity of dichloro-*s*-tetrazine should be established.

The dichloro-*s*-tetrazine (**23**) was obtained in our laboratory firstly by the method described by Hiskey¹ (Scheme 1).



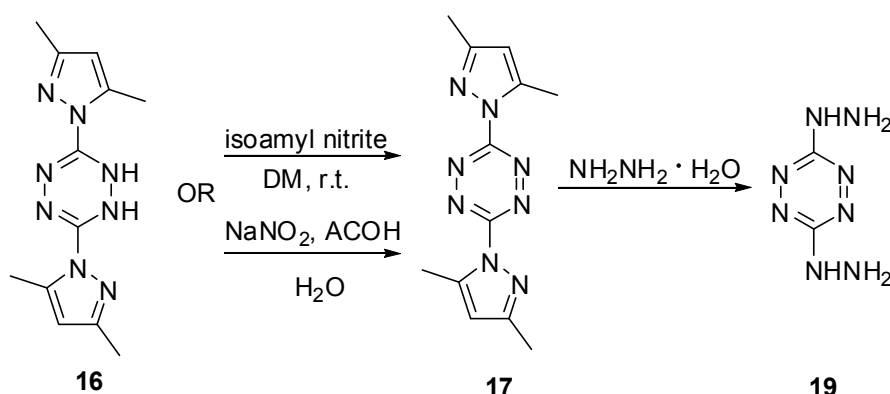
Scheme 1. Preparation of dichloro-*s*-tetrazine.

First of all, guanidine hydrochloride was refluxed with hydrazine in dioxane to give triaminoguanidine monohydrochloride in high yield, which is then condensed with two equivalent of 2,4-pentanedione to afford 3,6-bis(3,5-dimethylpyrazol-1-yl)-1,2-dihydro-1,2,4,5-tetrazine (**16**) in a high yield (Scheme 2).



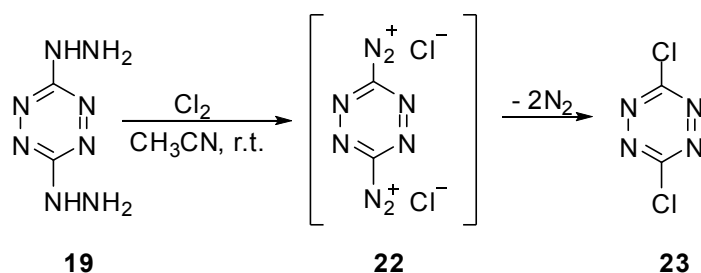
Scheme 2. Preparation of **16**.

The dihydro-tetrazine **16** can then be oxidized easily by isoamyl nitrite to give **17**. The yield of oxidation is high, but the alkyl alcohol generated from the oxidation makes the work-up procedures slightly inconvenient. Thus we developed a new method for the oxidation of dihydro-tetrazine: by using NaNO_2 combined with acetic acid, the oxidation went smoothly in water. After the reaction, the pure product **17** could be obtained after washing with a dilute solution of potassium carbonate. The bis-dimethylpyrazolyl-*s*-tetrazine (**17**) was then refluxed with hydrazine in a short time to give 3,6-dihydrazino-1,2,4,5-tetrazine (**19**) (Scheme 3).



Scheme 3. Preparation of **19**.

The bis-dihydrazino-tetrazine (**19**) was easily converted to 3,6-dichloro-1,2,4,5-tetrazine (**23**) via the diazonium salt (**22**) by oxidation with chlorine gas (Scheme 4). In our lab² we noticed that it was important, first to freshly prepare the bis-hydrazino-tetrazine (**19**), second, to ensure an important flux of chlorine with a strong agitation, because of the side reactions that might occur between the starting compound and **23**. The best way is to insure a large chlorine inlet and a powerful magnetic stirrer, so that the reaction is complete in 7-10 min; longer reaction time leads to the formation of by-products which are insoluble in acetonitrile. The reaction is over when the solution becomes clear.

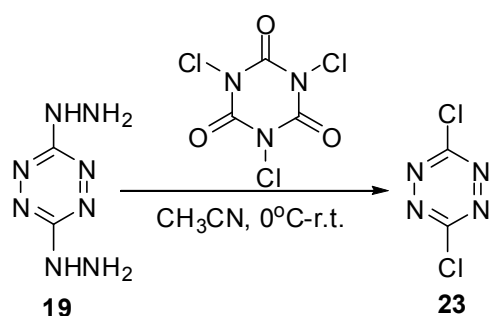


Scheme 4. Chlorination of **19** by chlorine gas.

The dichloro-*s*-tetrazine obtained upon evaporation of acetonitrile solution is usually pure enough for most synthetic procedures. However, in some cases small amounts of decomposed products of **23** or by-products from the chlorination step might influence the subsequent reactions, leading to low yield or even no reaction. In these cases a short column chromatography using DM as eluent is necessary to purify the dichloro-*s*-tetrazine.

However, using chlorine gas for chlorination of tetrazine is still inconvenient. Very recently, we noticed and realized a new chlorination method firstly reported by

Helm and colleagues³: in presence of a solid chlorination agent, trichloroisocyanuric acid, the bis(hydrazino)-*s*-tetrazine is converted smoothly to dichloro-*s*-tetrazine, thus the use of more dangerous, less controllable gaseous chlorine is avoided (Scheme 5).

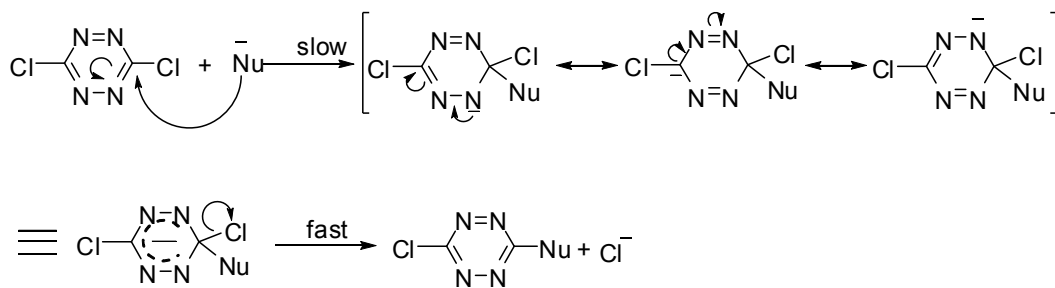


Scheme 5. Chlorination of **19** using trichloroisocyanuric acid.

4.2 Attempts to synthesize novel tweezer molecular sensors

4.2.1 S_NAr reaction of tetrazines

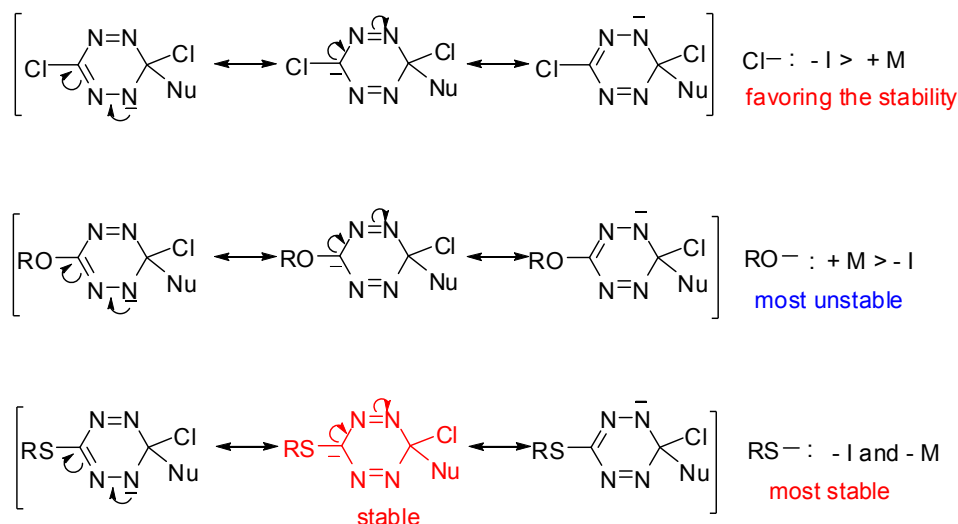
As already mentioned before, 3,6-dichloro-1,2,4,5-tetrazine is readily to undergo aromatic nucleophilic substitution with a variety of nucleophiles, because chlorine acts as a good leaving group and at the same time, a strong $-I$ group that enhances the electron deficiency of the tetrazine ring, thus facilitating the nucleophilic attack on the ring. The mechanism of S_NAr reaction of dichloro-*s*-tetrazine is described in Scheme 6:



Scheme 6. S_NAr mechanism of dichloro-*s*-tetrazine.

Once a chlorine is substituted by a heteroatom such as an oxygen or a sulfur, the reactivity of the tetrazine ring toward another nucleophilic attack is changed, which can be explained by the stability of the intermediate. This stability is different with respect to the different nucleophiles (Scheme 7). Sulfur atom, due to the ability of its empty low lying d orbitals to form $d-\pi$ conjugation with the adjacent carbon bearing a negative charge, is able to stabilize the negative charge on the tetrazine ring to a large extent, and chlorine, with electron-donating mesomeric effect ($+M$ effect) and much stronger electron-withdrawing inductive effect ($-I$ effect), is also able to stabilize effectively the negative charge on the tetrazine ring of the intermediate. On the contrary, oxygen, because of its stronger electron-donating mesomeric effect compared with its electron-attracting inductive effects, can hardly stabilize the negative charge, and makes the alkoxychlorotetrazines more resistant to undergo

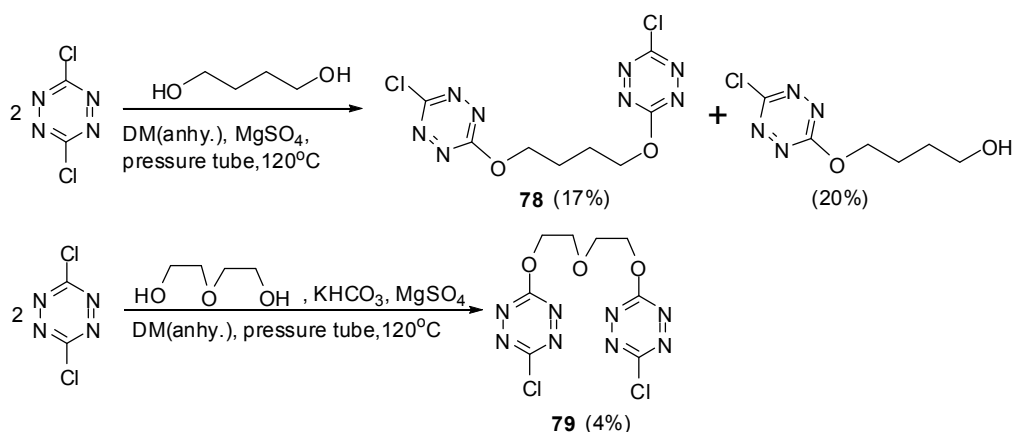
substitution reactions with nucleophiles. In fact it is this additional stabilization brought by RS⁻ on the reaction intermediate that makes RS-Tz-Cl even more prone than Cl-Tz-Cl to undergo substitution with thiols, leading directly to the disubstituted product RS-Tz-SR even when dichloro-*s*-tetrazine is in a large excess. However, under carefully controlled reaction conditions, this kind of disubstitution can be reduced to a minimum, and thus molecules like **98** can be obtained in a rather good yield (Scheme 11, **98**).



Scheme 7. Stability differences of intermediates in substitution of tetrazine Cl-Tz-Cl, RO-Tz-Cl and RS-Tz-Cl.

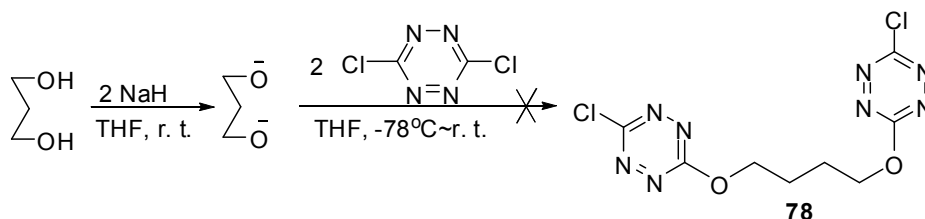
4.2.2 Tweezers with flexible chains

Dichloro-*s*-tetrazine reacts readily with methanol to give chloromethoxy-*s*-tetrazine almost quantitatively at room temperature, while when reacting with 1,4-butanediol, high temperature and excess of dichloro-*s*-tetrazine is needed. Even so the second hydroxyl of diol is difficult to react with another molecule of dichloro-*s*-tetrazine, and lots of mono-substituted products (4-(6-chloro-1,2,4,5-tetrazin-3-yloxy)butan-1-ol) are isolated, even after a long reaction time (Scheme 8). Use of a pressure tube did not improve markedly the yield, and the result was even worse when another diol such as diethyleneglycol was used in the reaction.



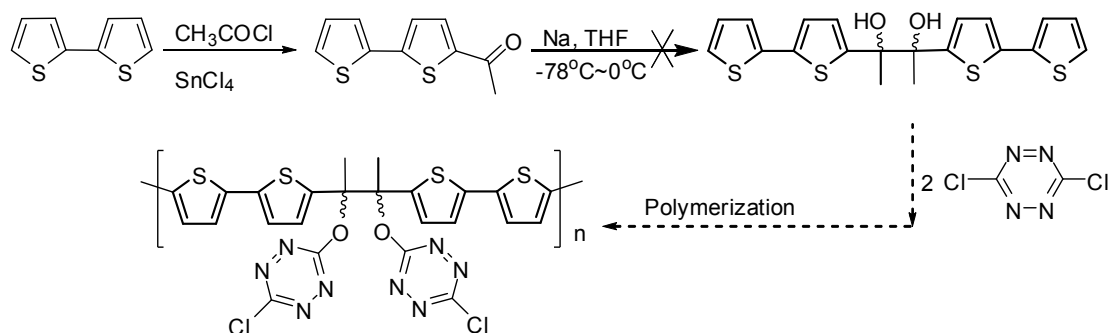
Scheme 8. Synthesis of flexible "tweezers".

The attempts to use 1,4-dianions to react with dichloro-*s*-tetrazine all failed and only led to decomposition of all tetrazines (Scheme 9).



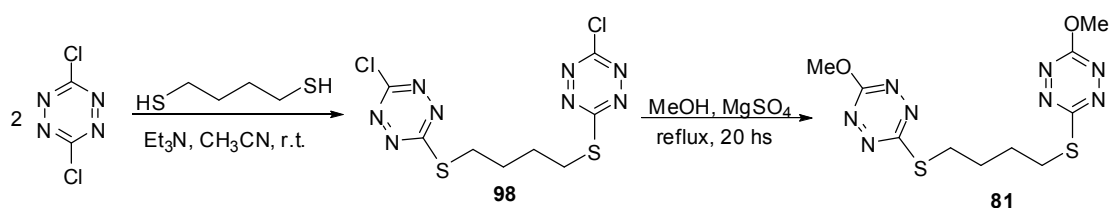
Scheme 9. Reaction of **23** with dianion.

Another attempt to obtain a series of “tweezers” attached on a polymer chain through polymerization of bithiophene also failed, because of the difficulty in preparation of 2,3-di(2,2'-bithiophen-5-yl)butane-2,3-diol through the coupling of acetyl bithiophene (Scheme 10).



Scheme 10. Attempt to prepare polymer tweezers.

1,4-Dithiol, as a stronger nucleophile, reacts much more easily with dichloro-*s*-tetrazine, and has a strong tendency to react further with the mono-substituted tetrazine to give products containing dithio-tetrazine segments even in the presence of excess dichloro-*s*-tetrazine. On the other hand, the chlorothio- derivatives can easily react further with methanol to give unsymmetric tetrazines (Scheme 11).



Scheme 11. Reaction of **23** with dithiol and subsequent substitution with methanol.

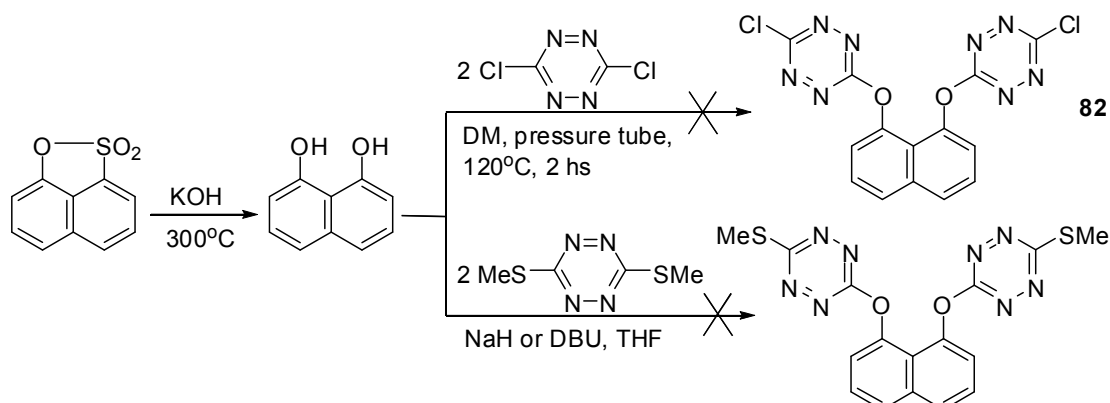
4.2.3 Tweezers with rigid frameworks

All attempts to synthesize tweezer molecular sensors with rigid frameworks failed. However we detailed here some attempts.

4.2.3.1 Reactions of tetrazines with dihydroxynaphthalene

In the presence of dichloro-*s*-tetrazine, 1,8-dihydroxynaphthalene was all consumed but no new tetrazine products were formed, possibly because it is easy to be oxidized by dichlorotetrazine under the reaction conditions. When dimethylthio-*s*-

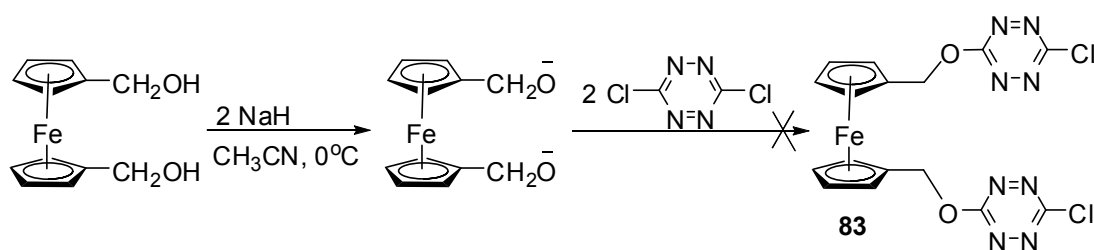
tetrazine was reacted with 1,8-dihydroxynaphthalene, again no reaction took place but both reactants could be mostly recycled (Scheme 12).



Scheme 12. Reactions of tetrazines with 1,8-dihydroxynaphthalene.

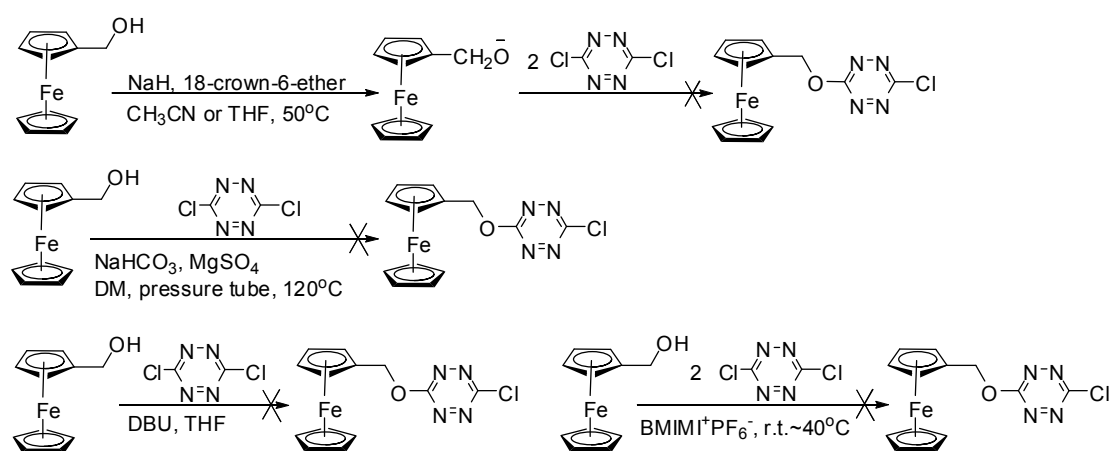
4.2.3.2 Reactions with ferrocenemethanol

Firstly the dianion of ferrocenedimethanol was used to react with dichloro-*s*-tetrazine and failed (Scheme 13). All the tetrazine decomposed after the addition of dianion.



Scheme 13. Attempt to prepare 83.

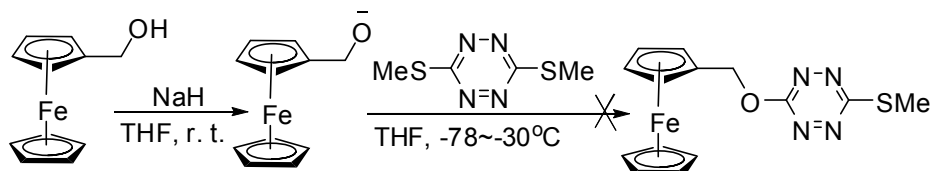
Since ferrocenemethanol is much less expensive and much more readily available, it was tested instead of ferrocenedimethanol to react with dichloro-*s*-tetrazine under various conditions but all failed (Scheme 14).



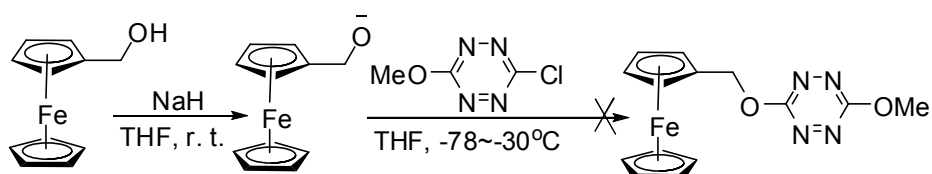
Scheme 14. Reactions of ferrocenemethanol with 23.

Considering that dimethylthio-*s*-tetrazine (**29**) is more stable, and easier to undergo substitution with nucleophiles, it was tested to react with ferrocenemethanol,

but also failed to give the expected product. Most of the ferrocenemethanol could be recycled after the reaction, while all dimethylthio-*s*-tetrazine decomposed (Scheme 15). Chloromethoxy-*s*-tetrazine was also tested for the reaction, and decomposed fully under the reaction condition (Scheme 16).

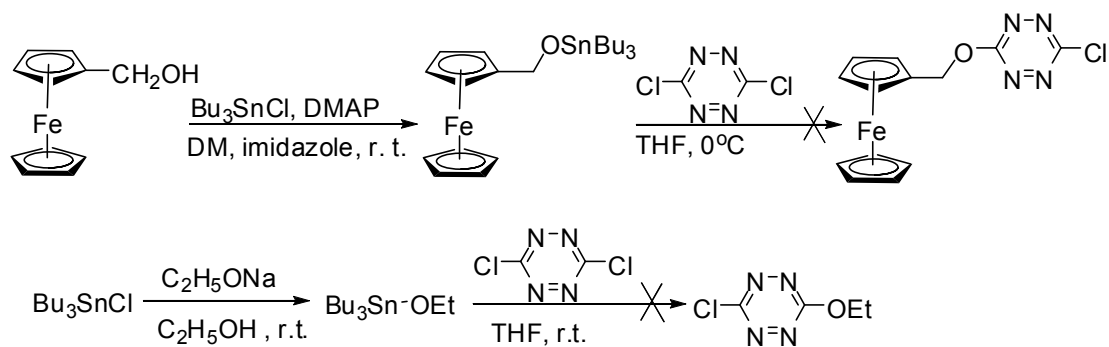


Scheme 15. Reaction of ferrocenemethanol with 29.



Scheme 16. Reaction of ferrocenemethanol with 76.

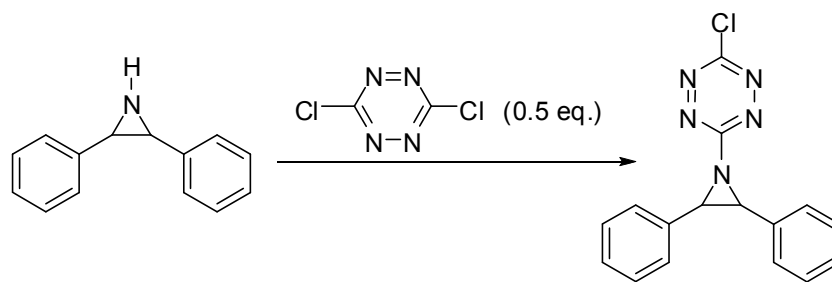
Tributylferrocenemethoxytin and tributylethoxytin were also prepared and reacted with dichloro-*s*-tetrazine, since the oxygen in the Sn-O bond was supposed to be much “softer” than in alkoxy anions. However under the reaction conditions the dichloro-*s*-tetrazine all decomposed, and no new tetrazine compounds was produced (Scheme 17). We assumed that the possible reason is that ferrocenes are very electroactive compounds and are easy to undergo one electron oxidation, leading to ferroceniums. Again, dichloro-*s*-tetrazine acts as a good oxidant to undergo reduction-oxidation reaction with ferrocenes, instead of substitution with OH groups.



Scheme 17. Reactions of 23 with organic tin compounds.

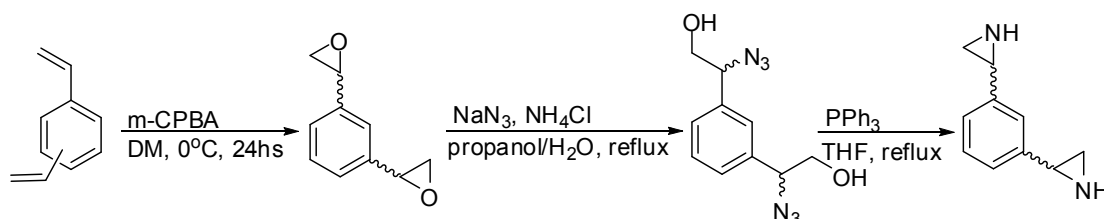
4.2.3.3 Reactions with phenyl diaziridines

During the previous work in our laboratory, we have already synthesized 3-chloro-6-(2,3-diphenylaziridin-1-yl)-1,2,4,5-tetrazine and observed its strong fluorescence (Scheme 18). This inspired us to design and synthesize fluorescent “tweezer” sensors based on aziridine-tetrazine. Therefore two methods were tried to prepare the phenyl di-aziridines to react with dichloro-*s*-tetrazine.



Scheme 18. Preparation of 3-chloro-6-(2,3-diphenylaziridin-1-yl)-1,2,4,5-tetrazine.

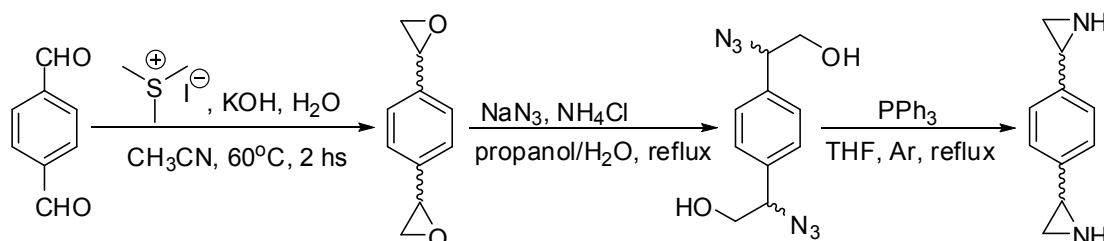
Firstly, the starting compound 1,3-divinylbenzene, obtained from Aldrich as a mixture of 80% of 1,3-divinylbenzene, 15% of 1,4- and 1,2-divinylbenzene and 5% of alkyl-styrene, was oxidized with *m*-CPBA to give a mixture which contained mostly several isomers of 1,3-di(oxiran-2-yl)benzene ((*R,R*), (*S,S*) and (*R,S*)). The mixture of di-oxyranes was then refluxed with NaN_3 and NH_4Cl in propanol/ H_2O to give a mixture of isomers of di-azidoalcohol, which was then condensed in the presence of triphenylphosphine to afford all the possible isomers of 1,3-di(aziridin-2-yl)benzene ((*R,R*), (*S,S*) and (*R,S*)) (Scheme 19).



Scheme 19. Preparation of di-aziridine from 1,3-divinylbenzene.

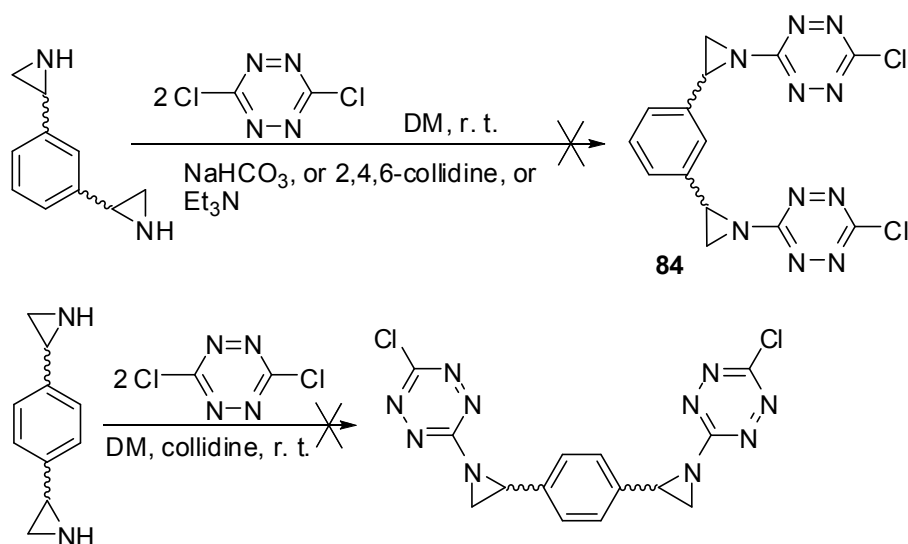
The products obtained from every step were always mixture of isomers, with small amount of impurities derived from *para*- or *ortho*- isomers of divinylbenzene, according to the analysis of $^1\text{H-NMR}$ and $^{13}\text{C-NMR}$. Moreover, the isolation and purification of the final products was very tedious and caused lots of loss of products because of the high polarity of phenyl di-aziridines.

To minimize the quantity of impurities derived from starting compound, we have tried another method for the preparation of phenyl diaziridine (Scheme 20). The terephthalaldehyde was reacted with trimethylsulfonium iodide to give 1,4-di(oxiran-2-yl)benzene as a mixture of isomers ((*R,R*), (*S,S*), (*R,S*)), which reacted with NaN_3 to afford the azido alcohol, then condensed in presence of PPh_3 to give a mixture of isomers of 1,4-di(aziridin-2-yl)benzene as a viscous liquid, which is soluble in DMF but not in DM, EA or acetone.



Scheme 20. Preparation of di-aziridine from terephthalaldehyde.

Unfortunately all the attempts to react diaziridine with dichloro-*s*-tetrazine only led to decomposition of all tetrazine (Scheme 21). Considering the fact that the mono-aziridine—2,3-diphenylaziridine reacts when in large excess, with dichloro-*s*-tetrazine to give the expected monosubstituted tetrazine, the failure of the reaction of di-aziridine with dichlorotetrazine could be ascribed to the presence of another aziridine group, which probably traps the HCl produced from the first substitution, and thus couldn't attack the second molecule of dichloro-*s*-tetrazine and might lead to the decomposition of the whole monosubstituted molecule.

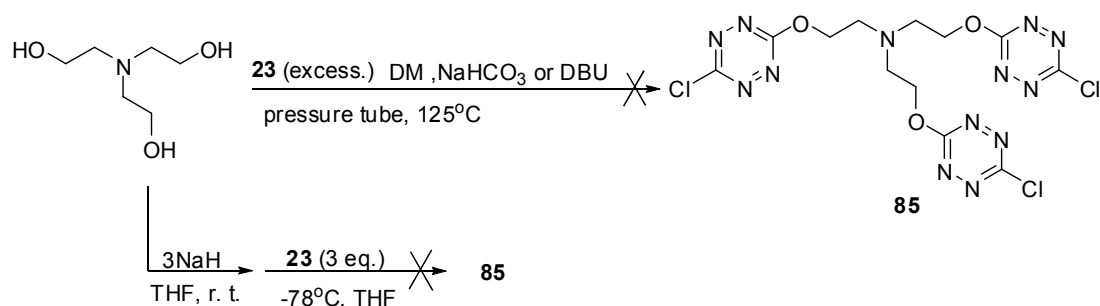


Scheme 21. Attempt to prepare diaziridine-tetrazines.

4.3 Synthesis of tripod molecular sensors

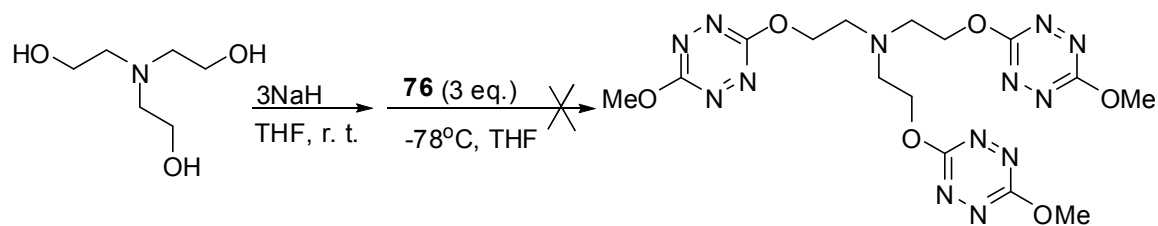
4.3.1 Using triethanolamine

The reactions of triethanolamine with dichloro-*s*-tetrazine were carried out under various conditions as a first attempt to prepare tripod but all failed (Scheme 22). The possible reason is that the nitrogen on the triethanolamine might capture the HCl produced by the substitution of dichloro-*s*-tetrazine, stopping the subsequent substitution or leading to the decomposition of the product. Otherwise in the presence of trialkoxide anions, the dichloro-*s*-tetrazine was all decomposed because of the too harsh conditions.



Scheme 22. Reactions of triethanolamine with dichloro-*s*-tetrazine.

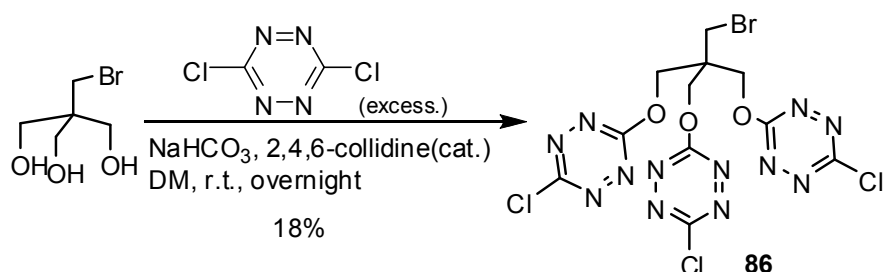
Chloromethoxy-*s*-tetrazine was also tried to react with the tri-anion of triethanolamine (Scheme 23). Only traces of dimethoxy-*s*-tetrazine was isolated.



Scheme 23. Reaction of triethanolamine with chloromethoxy-*s*-tetrazine (76).

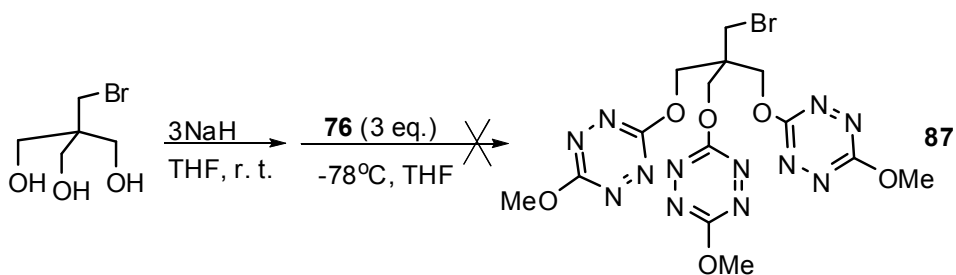
4.3.2 Using 2-(bromomethyl)-2-(hydroxymethyl)propane-1,3-diol as triol

As already mentioned before, when only NaHCO₃ or KHCO₃ were used as base for the reaction of diol with dichloro-*s*-tetrazine, high temperature and long reaction time were obligatory to ensure the second OH to react, and even so a considerable quantity of mono-tetrazine product could be isolated. This is because they are inorganic bases hence hardly soluble in organic solvents like dichloromethane. So it acts as an absorbent for HCl more than a catalyst for the substitution. Considering as well that the use of alkoxy-dianions is too harsh and leads to decomposition of tetrazines in most cases, we turned to 2,4,6-collidine which is an often-used organic base with no nucleophilicity. We added a catalytic amount of it and the reaction went smoothly to give the expected trisubstituted product (Scheme 24).



Scheme 24. Preparation of tripod-tetrazine **86**.

Using the same method, the yield for the reaction of 1,4-diol with dichloro-*s*-tetrazine was also greatly improved. However, the method used for monosubstitution of dichloro-*s*-tetrazine can not be applied for the further substitution of chloroalkoxy-*s*-tetrazine, since the reactivity of the latter is greatly decreased, and the alkoxide needs to be prepared before the substitution. Unfortunately the reaction of the trialkoxide with chloromethoxy-*s*-tetrazine only gave traces of dimethoxy-*s*-tetrazine as product, the mechanism of which might be that the trialkoxide attacks the chloromethoxy-*s*-tetrazine on the methoxy side to release a methoxide, which then attacks another molecule of chloromethoxy-*s*-tetrazine to give dimethoxy-*s*-tetrazine as a final product (Scheme 25).

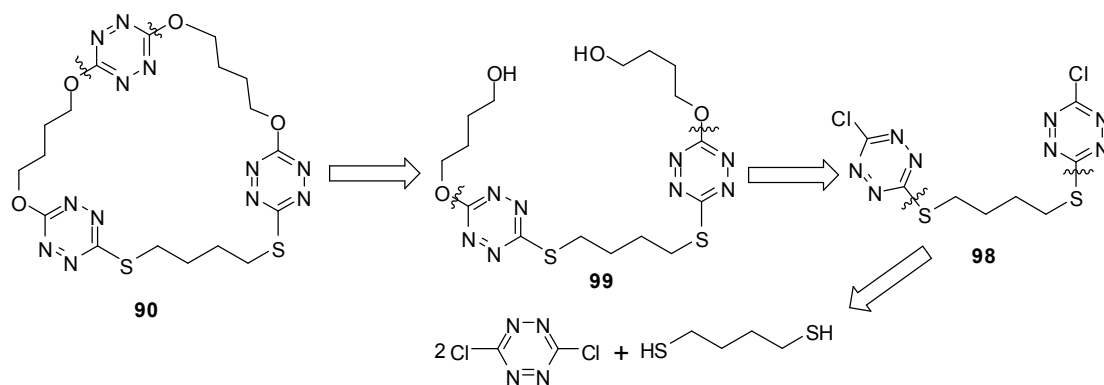


Scheme 25. Attempt to prepare tripod-tetrazine **87**.

4.4 Synthesis of cyclophane molecular sensors

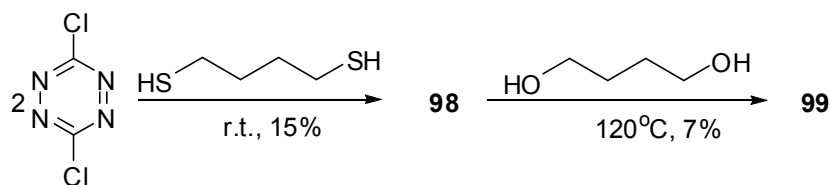
4.4.1 The first cyclophane-tetrazine

The first attempt to synthesize cyclophane-tetrazine **90** was carried out early before our discovery of using 2,4,6-collidine as catalyst for triple substitutions of triol with dichloro-*s*-tetrazine, and the low yield of the reaction of 1,4-diol with two molecules of dichloro-*s*-tetrazine was still a problem. Therefore we decided to firstly react 1,4-dithiol with two molecules of dichloro-*s*-tetrazine, which could give much better yield. The retrosynthetic scheme was thus established (Scheme 26):



Scheme 26. Retrosynthesis analysis of cyclophane-tetrazine **90**.

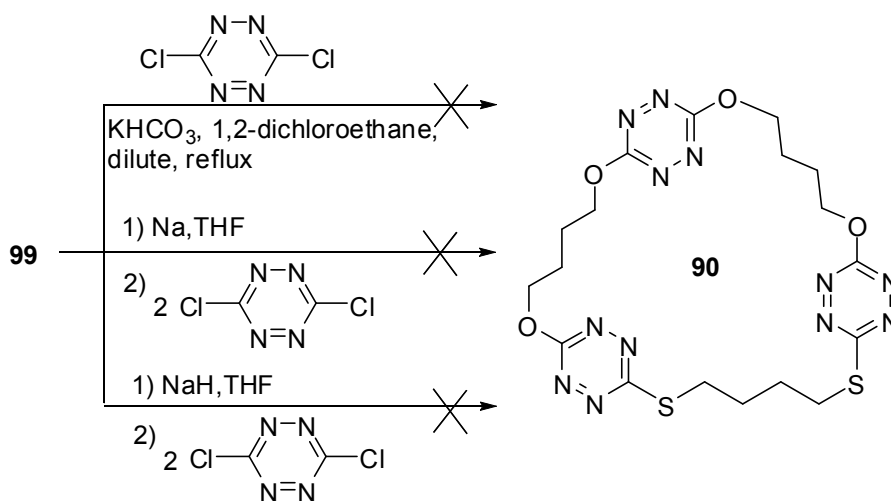
Slow addition of a solution of butyl dithiol into dichloro-*s*-tetrazine solution afforded bis-tetrazine **98** in good yield, which then reacted with excessive butyl diol to give the tetrazine-diol **99** (Scheme 27). The tetrazine-diol, with two terminal hydroxyl groups, was expected to undergo double nucleophilic substitutions with one molecule of dichloro-*s*-tetrazine to give the final cyclophane.



Scheme 27. Synthesis of **99**.

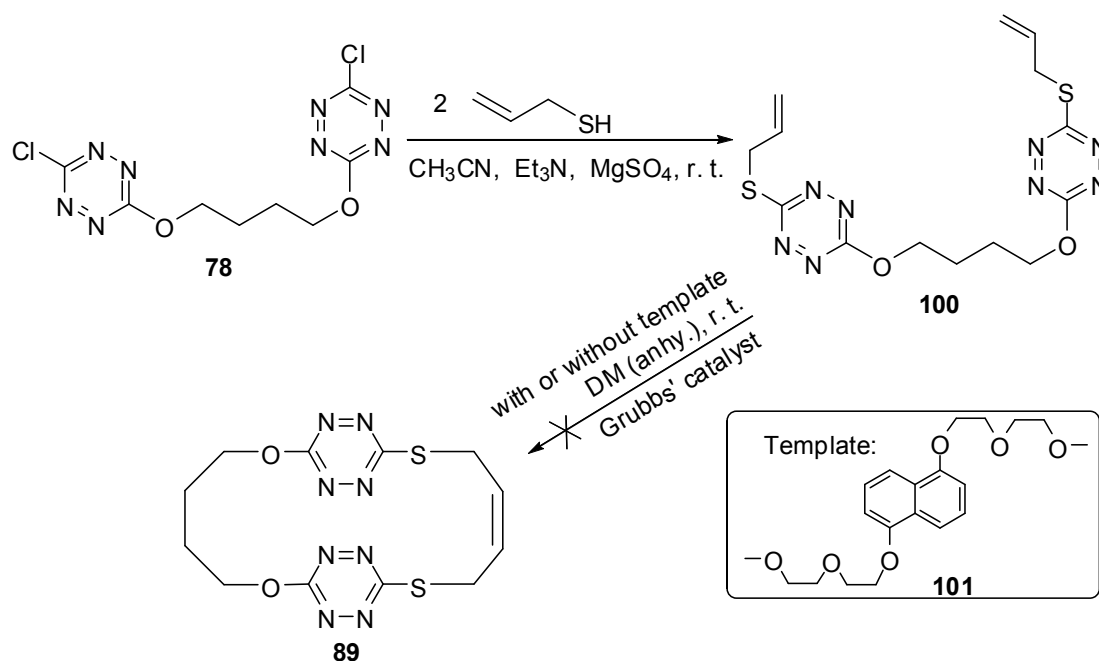
However, since the substitution by one oxygen atom reduces greatly the activity of the tetrazine for the second nucleophilic substitution, as already mentioned

before, many attempts for the last ring closure step ended up as a failure (Scheme 28). The results indicated that using OTzO formation as a ring closure step was not appropriate, and thus other ring closure reactions under mild conditions should be considered.



Scheme 28. Attempts for ring closure.

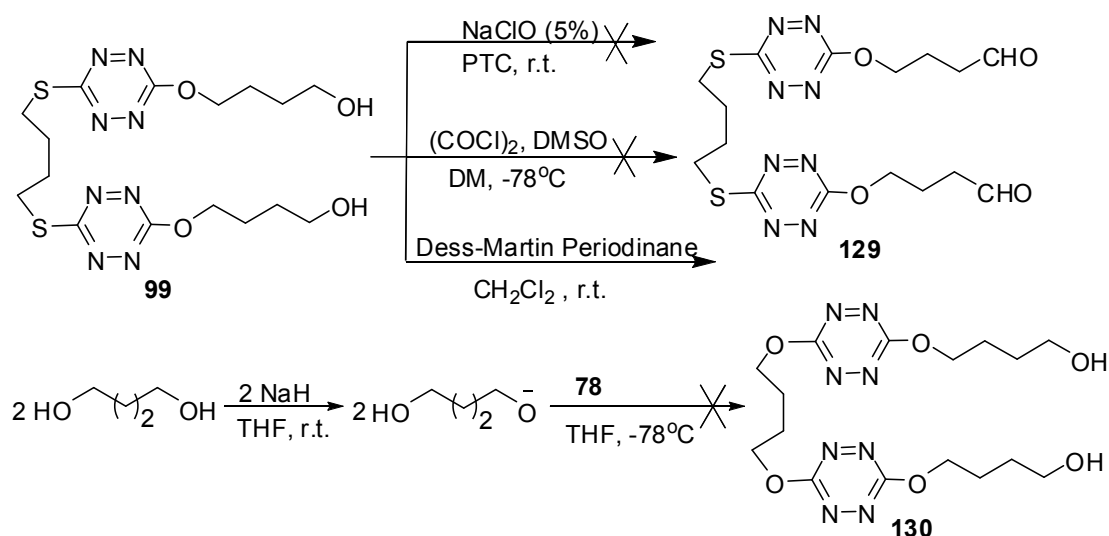
We then considered using other methods for ring closure. The bis-tetrazine **78** reacted with 2 equivalent of prop-2-ene-1-thiol to give 1,4-bis(6-(allylthio)-1,2,4,5-tetrazin-3-yloxy)butane (**100**), which contains two terminal alkenyl groups and should undergo readily RCM (ring closure metathesis) reaction in the presence of Grubbs' 1st generation catalyst. However, to our surprise, neither RCM nor intermolecular metathesis took place, whether with or without addition of electron-rich compound **101** as template molecule (Scheme 29).



Scheme 29. Attempt of RCM.

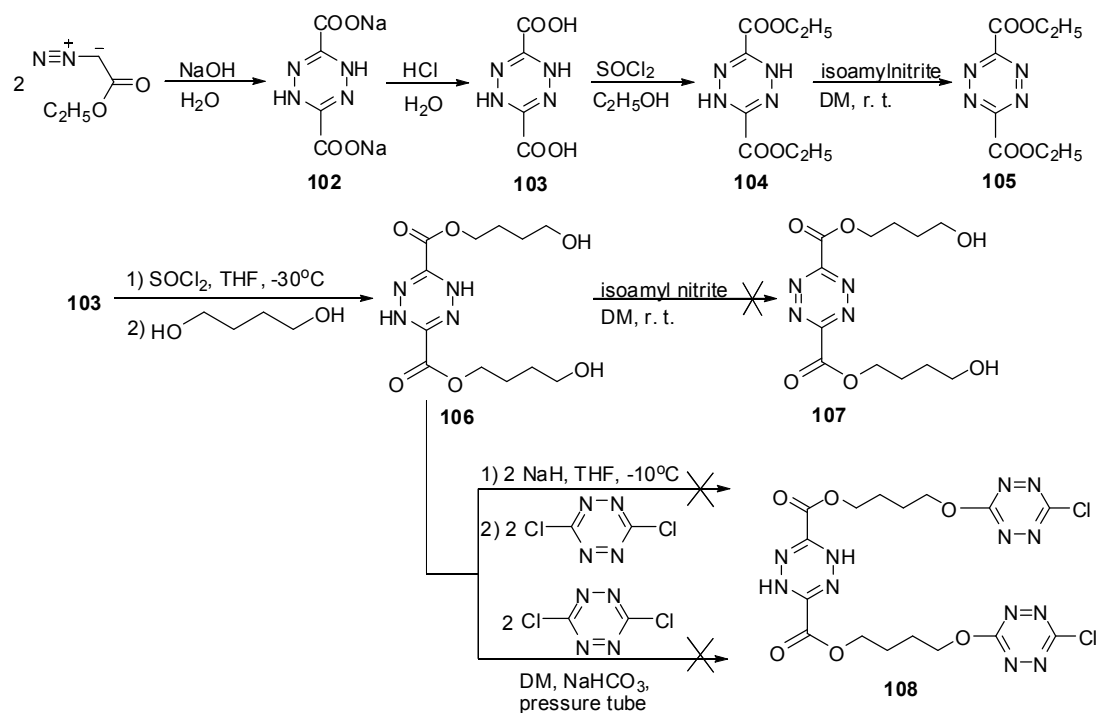
We have also explored the possibility of using McMurry reaction for the ring closure step. For this purpose the model compound **99** was firstly prepared and

oxidized to give di-aldehyde **129** with Dess-Martin periodinane. However, since the diol **130** containing O-Tz-O subunits could not be obtained, and also considering that the McMurry reaction is carried out under harsh conditions (TiCl₃/K), we gave up trying on this synthetic route (Scheme 30).



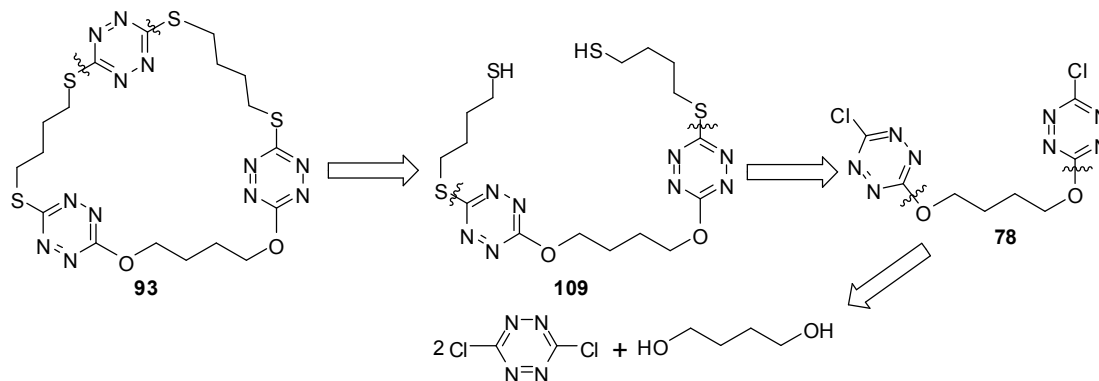
Scheme 30. Preparation for McMurry reaction.

Bis-carboxylate tetrazines were also prepared, and their potentiality for construction of cyclophanes was examined. It is interesting to notice that the diethyl 1,4-dihydro-1,2,4,5-tetrazine-3,6-dicarboxylate **104**, is oxidized readily with isoamyl nitrite, while another bis-dicarboxylate dihydro-tetrazine with two hydroxyl groups, bis(4-hydroxybutyl) 1,4-dihydro-1,2,4,5-tetrazine-3,6-dicarboxylate (**106**), couldn't be oxidized under the same condition to give aromatic tetrazine ring. The possible hydrogen bonding between the NH of tetrazine ring and the oxygen of hydroxyl group might be responsible for it (Scheme 31).



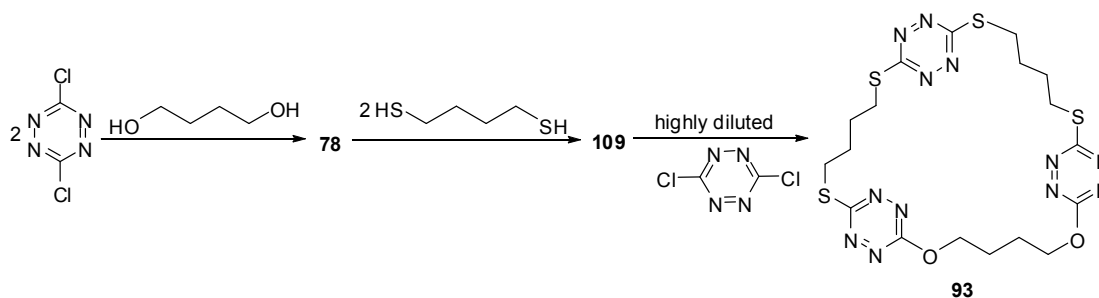
Scheme 31. Synthesis and application of bis-carboxylate tetrazines.

Since we have already noticed that dichloro-*s*-tetrazine has a strong tendency to undergo disubstitution with thiols, we then considered using the reaction of dithiol with dichloro-*s*-tetrazine as the ring closure step, and thus we adjusted the structure of target molecule, and established another retrosynthetic approach (Scheme 32).



Scheme 32. Retrosynthetic analysis of cyclophane-tetrazine **93**.

The adjusting was proved to be very efficient. The cyclophane **93** was obtained in three steps from dichloro-*s*-tetrazine (Scheme 33) in a moderate overall yield. The substitution with sulphur was found to be more effective than with oxygen, as reported in analogous cases. The ring closure occurs with a satisfactory 40% yield in high dilution conditions. Single crystal X-ray structure (Figure 1) could be successfully obtained, and shows that the cyclic structure is mainly driven by the tendency of the alkyl chains to adopt an all *trans*- conformation. Therefore, the tetrazine rings are more or less coplanar to the mean plane of the macrocycle instead of facing toward the center of the cavity.



Scheme 33. Synthesis of cyclophane-tetrazine **93**.

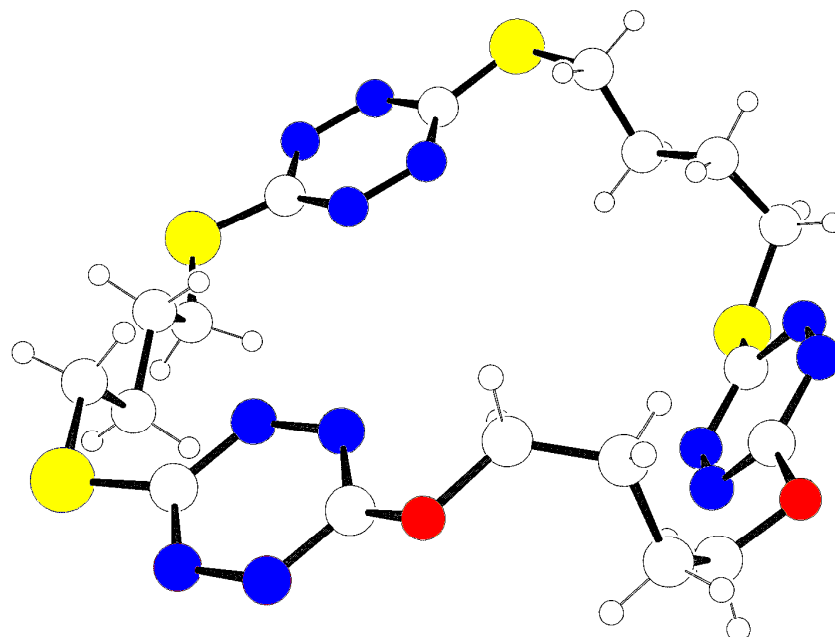
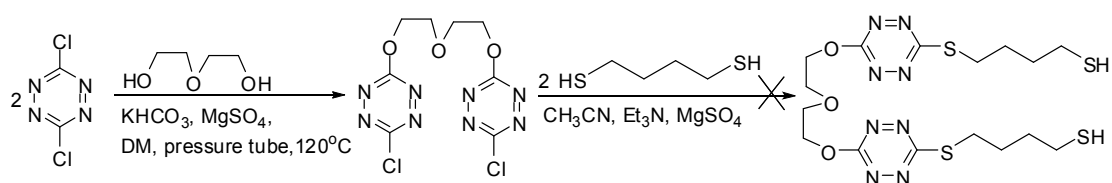


Figure 1. Crystal structure of cyclophane (**93**) containing 3 tetrazines (S yellow, O red and N blue).

This is the first example of a cyclophane molecule based on tetrazine moieties designed for electron-donating entities recognition. Unfortunately this cyclophane is weakly fluorescent, although interactions between its anion-radical and phenol derivative are evidenced subsequently through spectroscopic and electrochemical measurements.

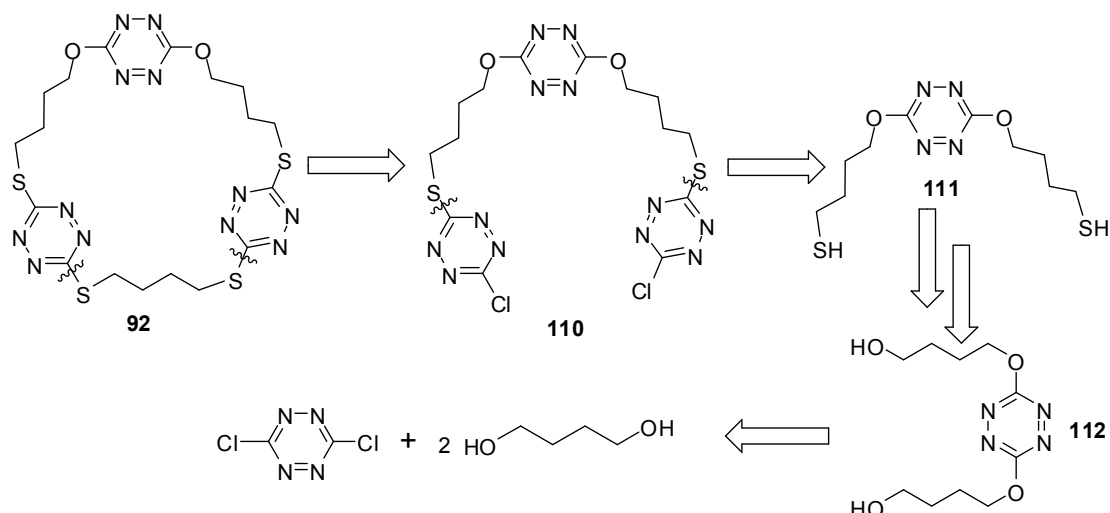
The utilization of diethyleneglycol instead of 1,4-butanediol as diol to construct a larger cyclophane was tried once and failed, possibly because of the water absorbed by acetonitrile during too long reaction time (Scheme 34). We didn't continue on this target and concentrated our efforts on the construction of another cyclophane containing at least one O-Tz-O segment, which is strongly fluorescent according to our experience (the fluorescence quantum yield of dimethoxytetrazine in DM is about 0.11).



Scheme 34. Attempt to prepare cyclophane-tetrazine **91**.

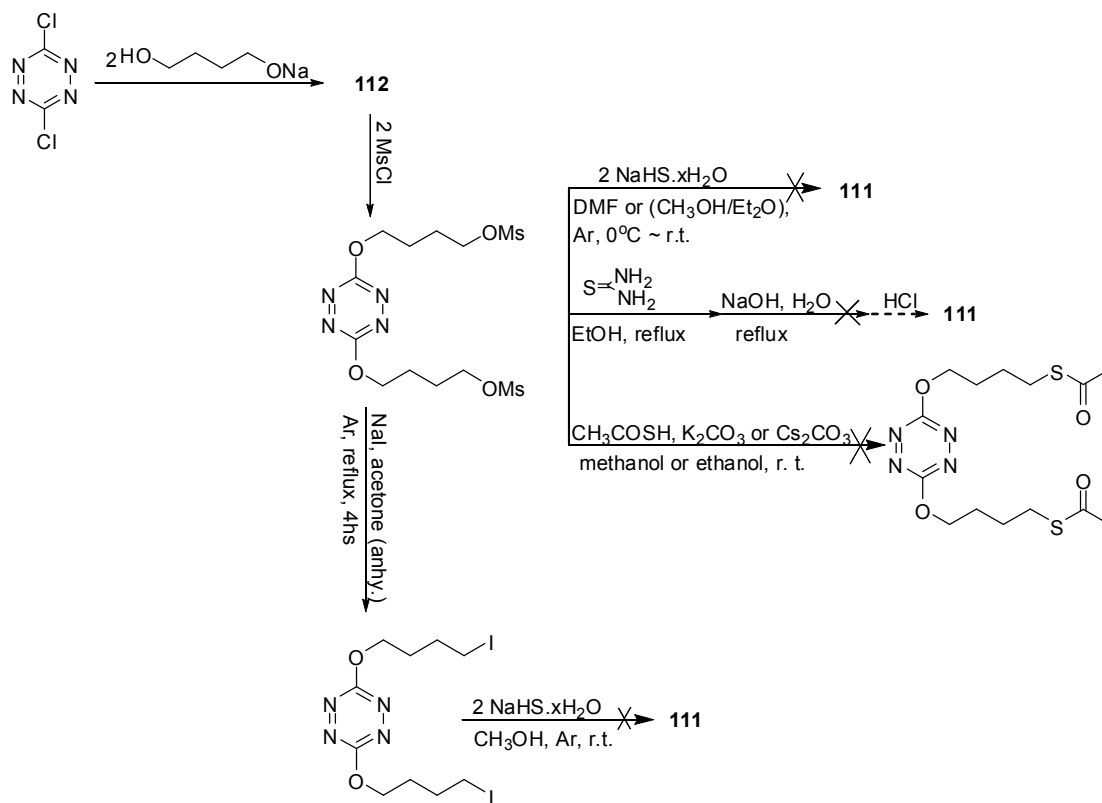
4.4.2 Attempt to synthesize cyclophane-tetrazine **92**

Using OTzO formation as a ring closure step is not appropriate due to the difficulty of disubstitution of dichloro-*s*-tetrazine with hydroxyl group, as already proved in the first attempt to prepare a cyclophane-tetrazine. Therefore we considered preparing the OTzO part of the molecule at the very beginning, then introducing the terminal thiol groups through FGI (Functional group interchange) (Scheme 35):



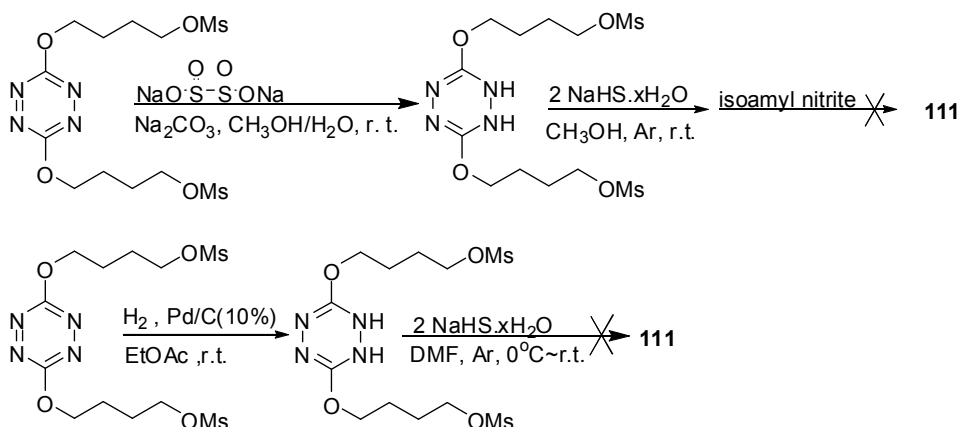
Scheme 35. Retrosynthesis for cyclophane-tetrazine **92**.

Dichloro-*s*-tetrazine reacted with two equivalents of mono-anions of 1,4-diol at low temperature to give the tetrazine-diol **112** in moderate yield. The two pendant OH groups were reacted with methanesulfonyl chloride to produce two OMs leaving groups quantitatively. However the synthetic route was obstructed by the difficulty to introduce two thiol groups in the terminal positions. All attempts to substitute the two terminal OMs groups by SH ended up with nucleophilic attacks on tetrazine ring leading to its decomposition (Scheme 36).



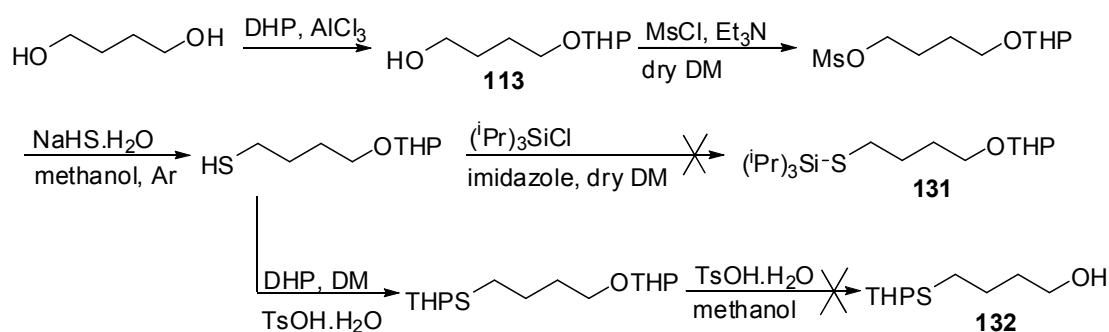
Scheme 36. Attempts to prepare **111**.

We also tried to reduce the tetrazine ring to 2H-tetrazine in order to reduce its electrophilicity before the substitution, but this last step failed as well (Scheme 37).

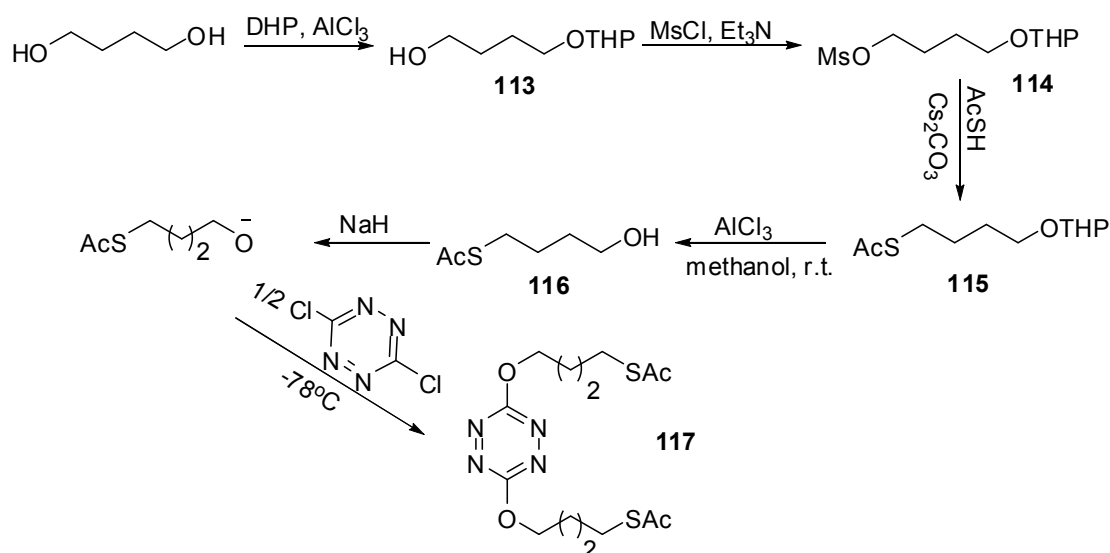


Scheme 37. Attempts to prepare **111** through reduction-substitution.

Since the functional transformations of hydroxyl to thiol with a tetrazine ring existing in the molecule were unsuccessful, we therefore considered preparing an alkyl chain comprising an alcohol at one end and a protected thiol at the other. Since the attempts to prepare triisopropylsilyl-protected thiol alcohol **131** or THP-protected thiol alcohol **132** all failed at the last step (Scheme 38), we decided to prepare an acetyl protected one. Thus 1,4-diol was reacted with a half equivalent of DHP in the presence of AlCl_3 to give mono protected diol **113**, which was reacted with methanesulfonyl chloride to produce **114** containing a leaving group MsO, which was then substituted by ethanethioate to give **115**. After deprotection of THP with AlCl_3 and methanol, the alcohol containing an acetyl protected thiol **116** was obtained, which was then deprotonized by NaH and reacted readily with dichloro-*s*-tetrazine to give the tetrazine **117** with two protected terminal thiols (Scheme 39).

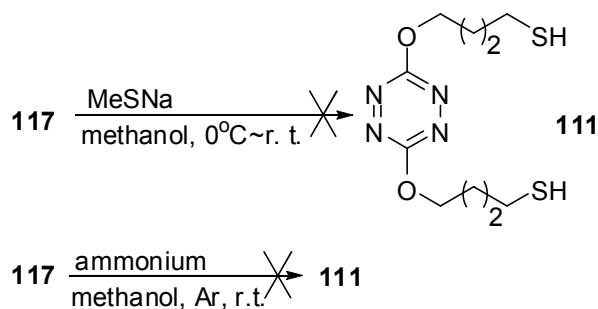


Scheme 38. Attempts to prepare triisopropylsilyl-protected or THP-protected alcohols.



Scheme 39. Synthesis of tetrazine with protected thiol groups.

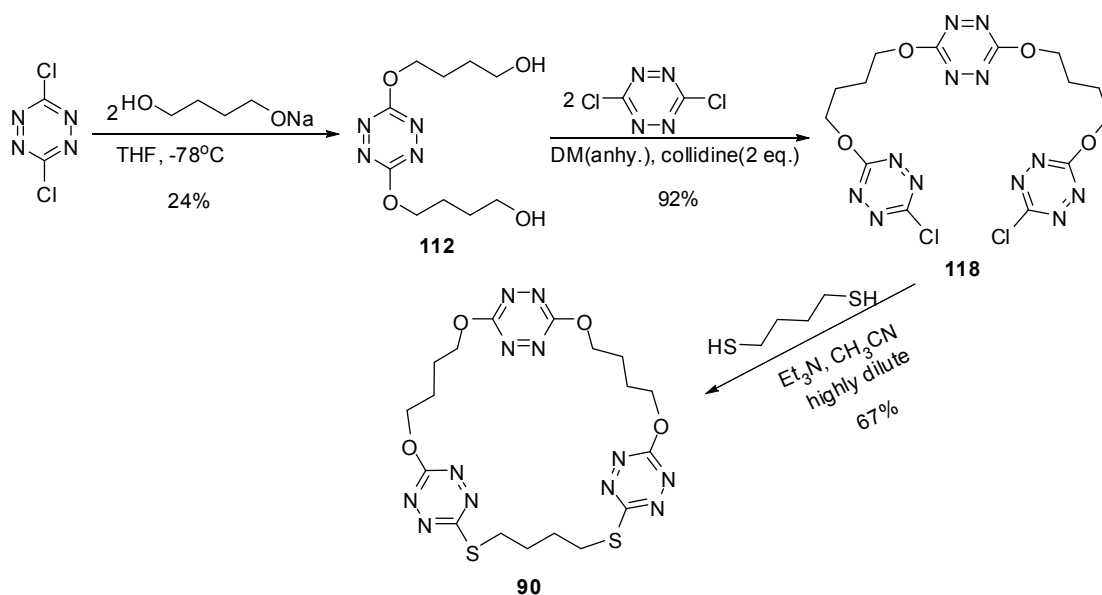
However, when we tried to deprotect the acetyl groups with MeSNa, the MeS anion attacked again the tetrazine ring. The rapid vanishing of the red color, which is characteristic for most tetrazine derivatives, indicated the decomposition of tetrazine ring or aza-addition to the ring. Deprotection of acetyl group with ammonium also ended up with decomposition of most of the tetrazines (Scheme 40).



Scheme 40. Attempts to deprotect **117**.

4.4.3 Reconsideration of cyclophane-tetrazine **90**

All the attempts to prepare the intermediate tetrazine-dithiol **111** failed. However, after many trials of reactions between alcohols and tetrazines in presence of different bases (Na_2CO_3 , NaHCO_3 , K_2CO_3 , Et_3N , DBU, etc.), we discovered that 2,4,6-collidine is a good catalyst as well as a base for the introduction of alcohols on dichloro-*s*-tetrazine, especially for polyols. We then reconsidered the first target cyclophane **90** and developed a new synthetic route, which succeeded finally (Scheme 41).



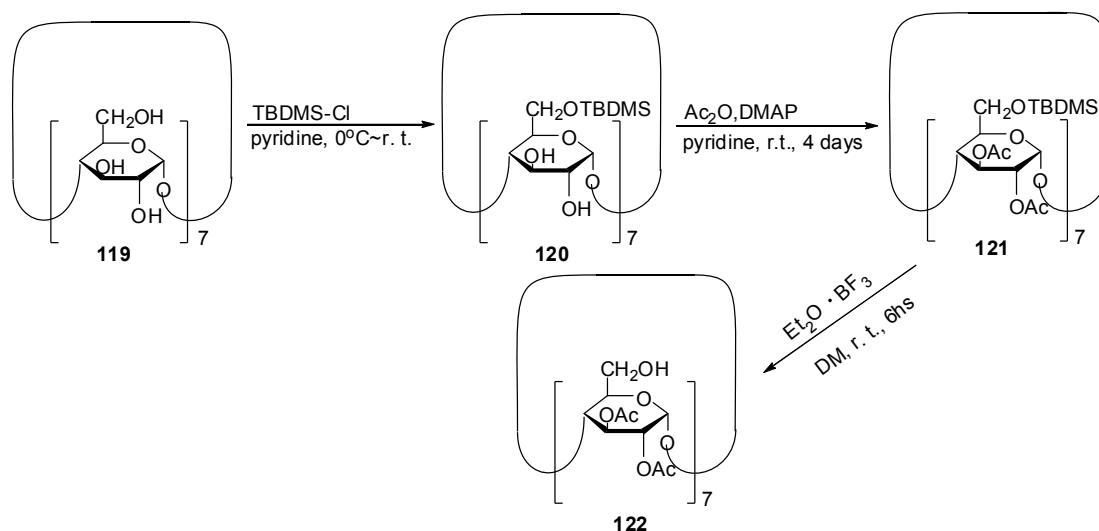
Scheme 41. Synthesis of cyclophane-tetrazine **90**.

The mono-anion of 1,4-diol was reacted with a half equivalent of dichloro-*s*-tetrazine to give the tetrazine-diol **112**, which was reacted smoothly with another two equivalent of dichloro-*s*-tetrazine to give 3,6-bis(4-(6-chloro-1,2,4,5-tetrazin-3-yloxy)butoxy)-1,2,4,5-tetrazine (**118**) at room temperature. Ring-closing with 1,4-dithiol under highly dilute condition afforded the new cyclophane-tetrazine **90** containing an O-Tz-O moiety in good yield (67%).

4.5 Synthesis of calycular molecular sensors—new multichromophoric cyclodextrin functionalized by fluorescent tetrazine rings.

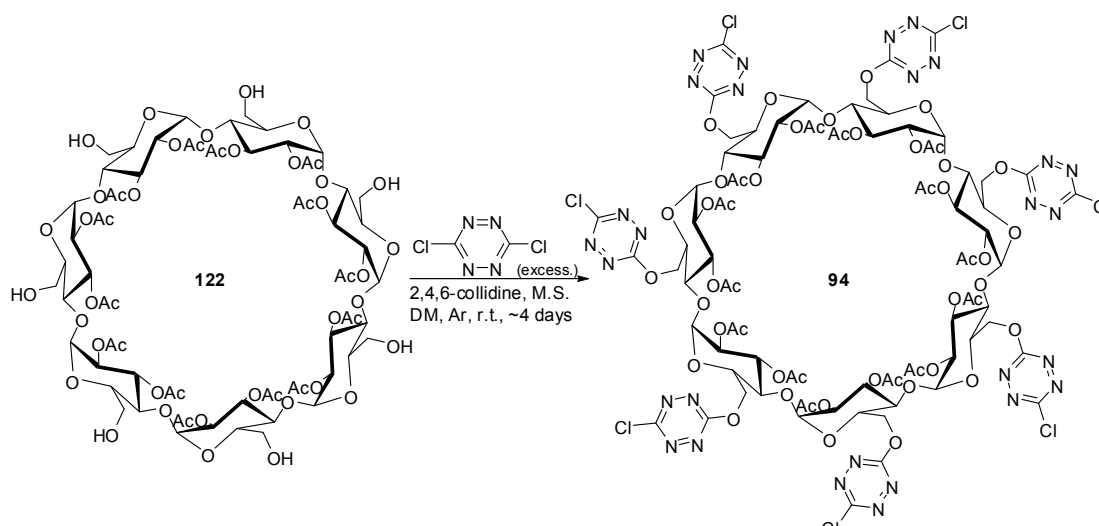
4.5.1 Attachment of tetrazines onto cyclodextrins via S_NAr reactions.

The preparation of 2,3-peracylated β -cyclodextrin **122** was straightforward: first the primary hydroxyls of **119** (on the upper face of the cyclodextrin cone) are selectively protected with TBDMS, followed by the protection of the two secondary hydroxyl (on the bottom of the cone) with acetyl to afford **121**, and after selectively removing the TBDMS groups, the 2,3-peracylated cyclodextrin **122** was obtained in an overall high yield (Scheme 42).



Scheme 42. Preparation of **122**.

Three methods were tried to link seven tetrazines onto the β -CD ring: when NaHCO_3 was used as base, only a complicated mixture of tetrazine-containing products was obtained, indicating the deprotection of secondary hydroxyls and subsequent reaction with dichloro-*s*-tetrazine; when 2,4,6-collidine was used as base and without molecular sieves, the target molecule could be obtained but in low yield; with collidine as base and addition of molecular sieves, a yield of more than 50% could be achieved (Scheme 43). Considering that there are seven substitutions of hydroxyl with dichloro-*s*-tetrazine, the yield for each introduction of tetrazine onto **122** is up to 91%, which indicates that 2,4,6-collidine and anhydrous environment are crucial for the success of the 7-fold substitution.

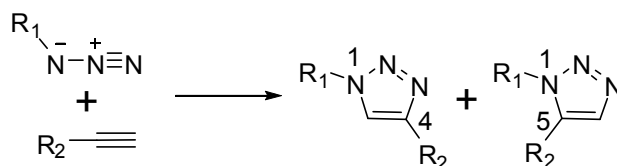


Scheme 43. Reaction of **122** with dichlorotetrazine.

The 2,3-peracetylated multichromophoric α -cyclodextrin functionalized by six fluorescent tetrazine rings was obtained by the same method as for the β -analogue. The yield of the last step is up to 50%, which means that an average yield of 89% can be achieved for each substitution.

4.5.2 Attempt to attach tetrazines via “click chemistry”

“Click chemistry” was firstly proposed by Sharpless and coworkers⁴ in order to accelerate the synthesis of drug-like molecules, which sets up a set of criteria to define reliable reactions: giving products stereoselectively in high yields, producing inoffensive byproducts, low to no sensitivity to oxygen and water, utilizing readily available starting materials, and having a thermodynamic driving force of at least 20 kcal·mol⁻¹. Preferably, the reactions should be conducted in benign solvents and chromatography is not used for purification of reaction products. Two types of click reactions that have influenced drug discovery are the nucleophilic opening of strained ring systems⁵ and 1,3-dipolar cycloadditions⁶. Of particular interest is the Huisgen [3 + 2] cycloaddition between a terminal alkyne and an azide to generate substituted 1,2,3-triazoles (Scheme 44). This reaction has been termed the “cream of the crop” of click reactions and has found application in various facets of drug discovery.

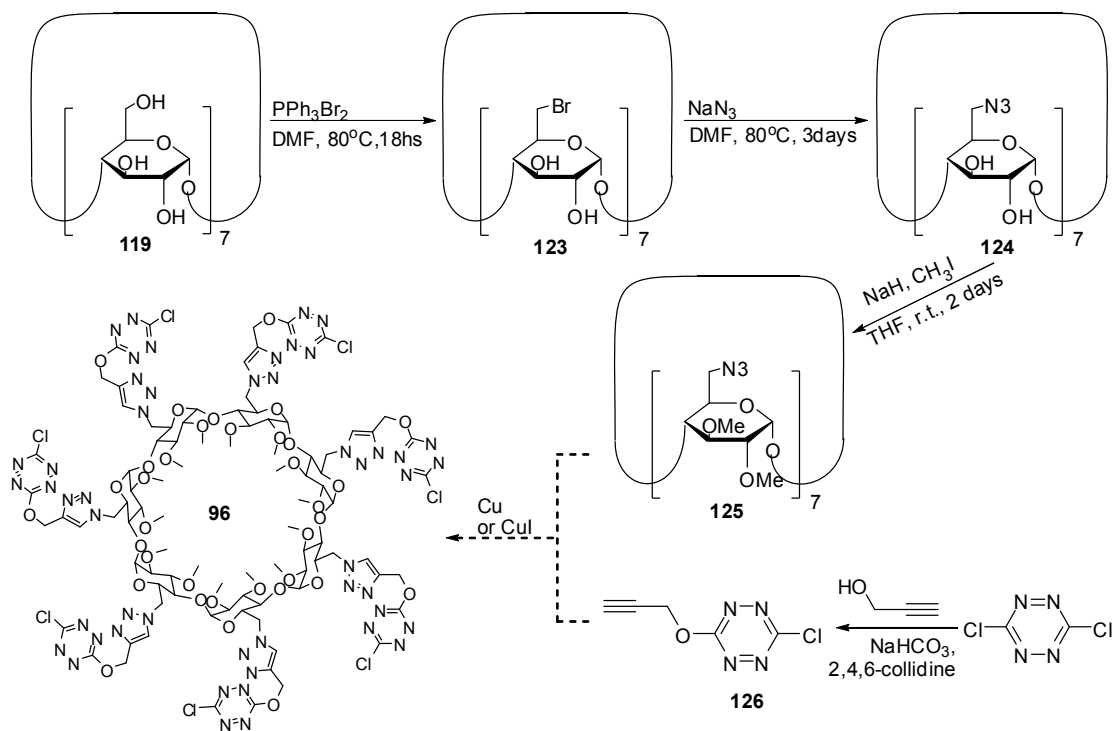


Scheme 44. 1,2,3-Triazole formation via Huisgen 1,3-dipolar cycloaddition.

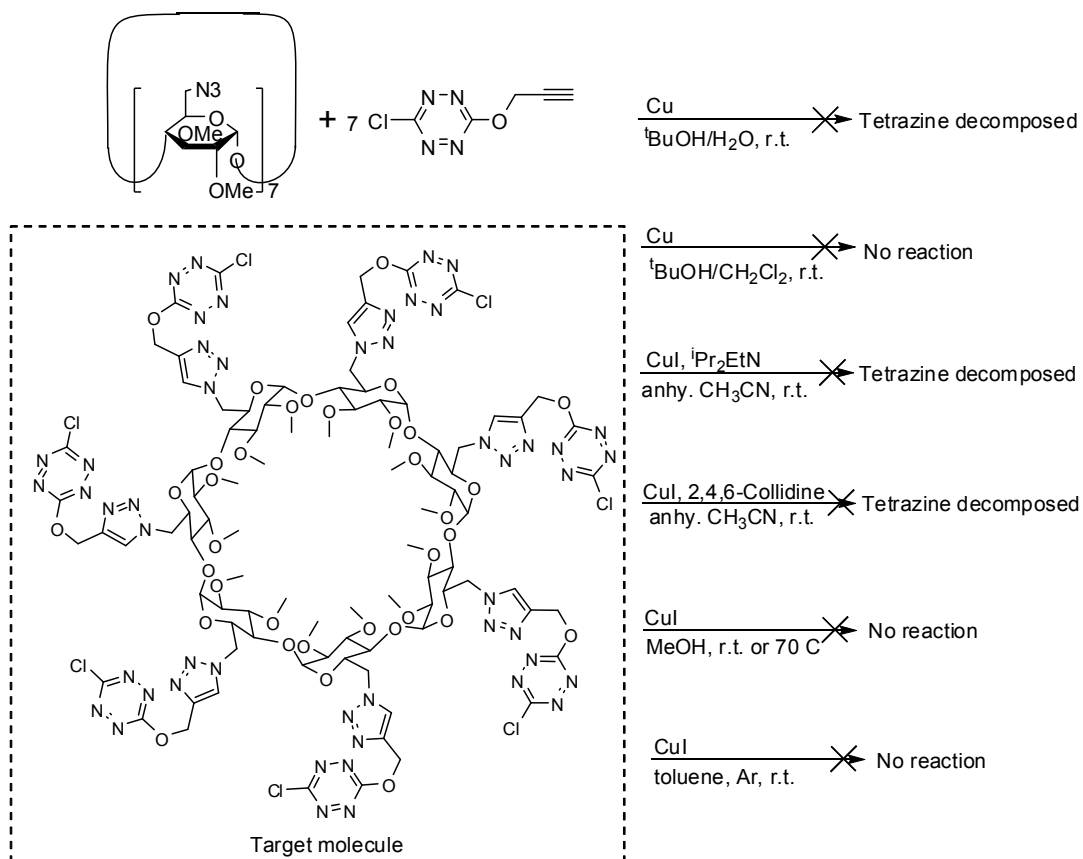
The reaction generates a mixture of 1,4- and 1,5-disubstituted triazoles, and various attempts to control the regioselectivity have been reported without much success until the discovery of the copper(I)-catalyzed reaction in 2002, which exclusively yields the 1,4-disubstituted 1,2,3-triazole^{7,8}. Several copper(I) salts such as CuI and CuOTf·C₆H₆, can be employed but the reactions generally must be run with acetonitrile as co-solvent, require a nitrogen base, and sometimes generate unwanted diacetylene and bis-triazole by-products. The *in situ* reduction of copper(II) salts such as CuSO₄·5H₂O with sodium ascorbate in aqueous alcoholic solvents allows the formation of 1,4-triazoles at room temperature in high yield with less than 2 mol % catalyst loading. Primary, secondary, and tertiary substituted azides as well as aromatic azides can be utilized. Numerous terminal acetylene components participate in the transformation and the reaction is compatible with various functional groups such as esters, acids, alkenes, alcohols, and amines. The copper-catalyzed reaction was also expanded later by Yamamoto and coworkers⁹ using a bimetallic catalyst so that 1,4,5-substituted triazoles could be obtained from seemingly internal alkynes. Due to the reliability and generality of the copper(I)-catalyzed azide-alkyne cycloaddition to generate N-heterocyclic links, the reaction has been utilized for various aspects, from drug discovery, *in vivo* enzyme activity-profiling to discovery of novel chemical materials.

Therefore we considered utilizing this type of reliable “click reaction” to attach the seven tetrazines onto the CD ring (Scheme 45). The 2,3-permethyl-β-cyclodextrin-azide (**125**) was obtained via bromination-azidation-methylation of β-cyclodextrin, and the 3-chloro-6-(prop-2-ynoxy)-1,2,4,5-tetrazine (**126**) was obtained through the substitution of propargyl alcohol with dichloro-*s*-tetrazine in high yield. However, for the last step of attachment, many attempts have ended up as a failure (Scheme 46). The dichloro-*s*-tetrazine couldn't stand for a long time in the

presence of base or water in the “click” conditions, while without base, no reaction took place.



Scheme 45. Attempt to synthesize β -CD-tetrazine through "Click chemistry".



Scheme 46. “Click reaction” under different conditions.

References

-
- 1 D. E. Chavez, M. A. Hiskey, *J. Energ. Mater.* **1999**, *17*, 357.
 - 2 P. Audebert, F. Miomandre, G. Clavier, M. –C. Vernière, S. Badré, R. Méallet-Renault, *Chem. Eur. J.* **2005**, *11*, 5667.
 - 3 M. D. Helm, A. Plant, J. P. A. Harrity, *Org. Biomol. Chem.* **2006**, *4*, 4278.
 - 4 H. C. Kolb, M. G. Finn, K. B. Sharpless, *Angew. Chem. Int. Ed.* **2001**, *40*, 2004.
 - 5 R. B. Henerson, J. S. Fruton, In *Heterocyclic Compounds*. R. C., Elderfield, Ed.; Wiley & Sons, Inc.: London, **1950**, *Vol. 1*.
 - 6 R. Huisgen, 1,3-Dipolar Cycloadditions – Introduction, Survey, Mechanism. In *1,3-Dipolar Cycloaddition Chemistry*. Padwa, A, Ed.; Wiley: New York, **1984**, pp.1-176.
 - 7 V. Rostovtsev, L. G. Green, V. V. Fokin, K. B. Sharpless, *Angew. Chem. Int. Ed.* **2002**, *41*, 2596.
 - 8 C. W. Tornøe, C. Christensen, M. Meldal, *J. Org. Chem.* **2002**, *67*, 3057.
 - 9 S. Kamijo, J. J. Tienan, Y. Yamamoto, *Tetrahedron Lett.* **2004**, *45*, 689.



Chapter 5 UV/Visible absorption, fluorescence and electrochemical studies

5.1 Introduction of fluorescence quenching: Stern-Volmer equation and Rehm-Weller equation

A molecule (M), once in the excited state (M^*) after absorption of a photon, can return to the ground state (S_0), by emission of fluorescence, or through other de-excitation pathways (Figure 1)¹: internal conversion, intersystem crossing, intramolecular charge transfer and conformational change. Interactions in the excited state with other molecules may also compete with de-excitation: electron transfer, proton transfer, energy transfer, excimer or exciplex formation. Most of the main intermolecular photophysical processes responsible for de-excitation of molecules, involve a fast transfer process from a donor to an acceptor: electron transfer, proton transfer or energy transfer.

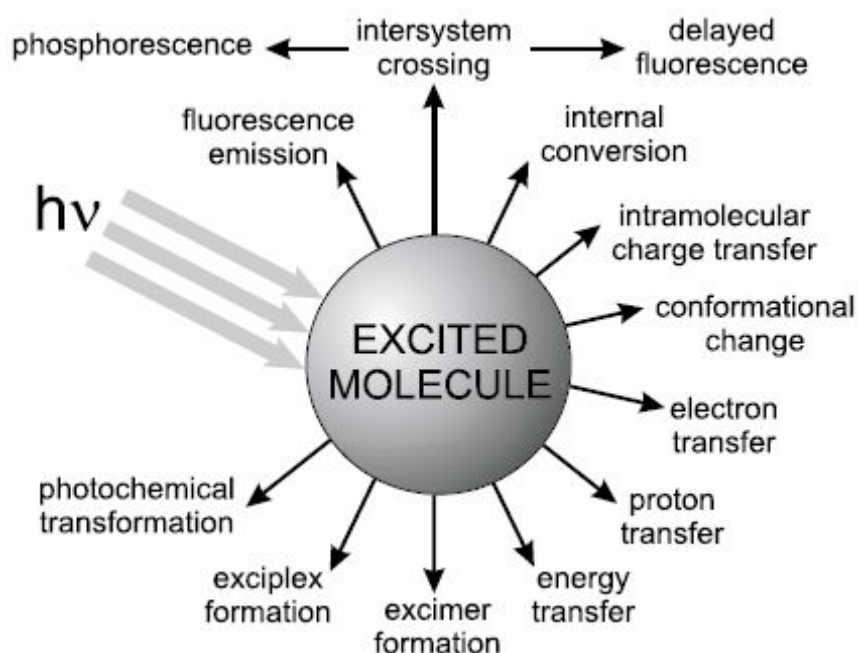


Figure 1. De-excitation pathways for an excited molecule.

If these de-excitation pathways take place on a time-scale during which the molecules stay in the excited state (10^{-10} - 10^{-7} s), they may compete with fluorescence emission. The characteristics of fluorescence (spectrum, quantum yield, and lifetime) can be affected by any excited state process involving interactions of the excited molecule with its close environment, and then can provide information on such a microenvironment.

If the presence of a molecule Q decreases the fluorescence quantum yield, leading to the loss of fluorescence intensity, the molecule is called a quencher, and the process is called fluorescence quenching, whatever the nature of the competing

intermolecular process for molecules in the excited state (M^*). The fluorescence characteristics (decay time and/or fluorescence quantum yield) of M^* are affected by the presence of Q, as a result of competition between the intrinsic de-excitation and other intermolecular processes.

The quenching mechanism can be either static or dynamic. If the fluorescence quenching is dynamic (a diffusion-controlled reaction), the observed rate constant for quenching is time-dependent, and the well known Stern-Volmer Equation (Equation 1) is used to describe the quenching in steady-state experiments¹:

$$\left(\frac{I_0}{I}\right) - 1 = k_q \cdot \tau_0 \cdot [Q]$$

Equation 1. Stern-Volmer Equation.

where I and I_0 are the steady-state intensities in presence and absence of quencher Q, respectively; k_q is the quenching constant; τ_0 is the lifetime of M^* in the absence of Q; and [Q] is the quencher concentration. Generally, the ratio I_0/I is plotted against the quencher concentration [Q], so that the Stern–Volmer plot can be obtained according to the equation. If the variation is found to be linear, the slope gives the Stern–Volmer constant k_{sv} ($k_{sv} = k_q \cdot \tau_0$), and k_q can be calculated if the excited-state lifetime in the absence of quencher (τ_0) is known.

If the fluorescence quenching is static, there are two possibilities: either there is an existence of a sphere of effective quenching, or there is a formation of a ground-state non-fluorescent complex. In the former case, the quencher Q is in large excess so that there is a high probability that M^* and Q are in proximity so that the interaction is significant at the time of excitation. Therefore no mutual approach during the excited-state lifetime is required. When the probability of finding a quencher molecule within the encounter distance with a molecule M^* is less than 1, this situation is relevant to static quenching. In this case the ratio I_0/I is not linear and shows an upward curvature at high quencher concentrations, according to the Equation 2:

$$\frac{I_0}{I} = \exp(V_q N_a [Q])$$

Equation 2. Equation for static quenching when Q is in large excess.

where V_q is the volume of a sphere (called the sphere of effective quenching, active sphere or quenching sphere) surrounding the fluorophore M, N_a is Avogadro's number, and [Q] is the quencher concentration.

In the latter case, a ground-state non-fluorescent complex is formed. The excited-state lifetime of the uncomplexed fluorophore M is unaffected, which is in contrast to dynamic quenching. The fluorescence intensity of the solution decreases upon addition of Q, but the fluorescence decay after pulse excitation is unaffected. If the ratio of fluorophore and quencher in the complex is 1:1, and considering that the fluorescence intensities are proportional to the concentrations (which is valid in dilute solutions), the relationship between the fluorescence intensities and the quencher concentration can be expressed according to the Equation 3:

$$\frac{I_0}{I} - 1 = K_s [Q]$$

Equation 3. Equation for static quenching when there is a formation of a ground-state non-fluorescent complex.

where K_s is the stability constant of the complex. A linear relationship is thus obtained, as in the case of the Stern-Volmer plot, but there is no change in excited-state lifetime for static quenching, whereas in the case of dynamic quenching the ratio I_0/I is proportional to the ratio τ_0/τ of the lifetimes.

Photoinduced electron transfer (PET) is often responsible for fluorescence quenching, which is involved in many organic photochemical reactions. The oxidative and reductive properties of molecules can be enhanced in the excited state, and the variations in standard free enthalpy ΔG^0 for the corresponding reactions can be expressed according to the Rehm–Weller Equation¹:

$$\Delta G^0 = E(D/D^+) - E(A/A^-) - E_{0-0} - \frac{e^2}{\epsilon_r \cdot r}$$

Equation 4. Rehm–Weller Equation.

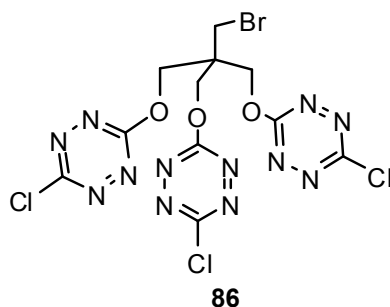
where e is the electron charge, ϵ_r the dielectric constant of the solvent and r is the distance between the donor and acceptor, $E(D/D^+)$ represents the redox potential of electron donor, and $E(A/A^-)$ the redox potential of the electron acceptor. The Equation yields the free energy for the electron transfer between the two compounds. Usually it is impossible to get the exact value of r , and thus it is assumed to be equal to the sum of the donor and acceptor radii.

For a specified acceptor, the $E(A/A^-)$ and E_{0-0} are fixed, and $e^2/(\epsilon_r \cdot r)$ is constant, therefore ΔG^0 can be expressed as a linear function of the redox potential of donors ($E_{ox}^0(D)$), which is a simplified Rehm-Weller equation (Equation 5):

$$\frac{\Delta G^0}{R.T} = -\text{Log}(k_q) = a \cdot E_{ox}^0(D) + b$$

Equation 5. The simplified Rehm-Weller equation.

5.2 Spectroscopic and electrochemical study for tripod-tetrazine (86)



5.2.1 Absorption and fluorescence studies

The UV-vis. absorption spectrum of the tripod-tetrazine **86** was recorded in dichloromethane solution (Figure 2). It is similar to that of chloroalkoxy-*s*-tetrazines (compounds **76** or **78**, Chapter 3.2, Figure 6). The strong band at 323 nm can be attributed to a π - π^* allowed transition while the one at 518 nm corresponds to an n - π^* transition, which is responsible for its color in the visible range. The position of the UV band is strongly dependant on the electron donor or acceptor character of the substituents on the tetrazines as already demonstrated with all the tetrazines synthesized in our laboratory^{2, 11}.

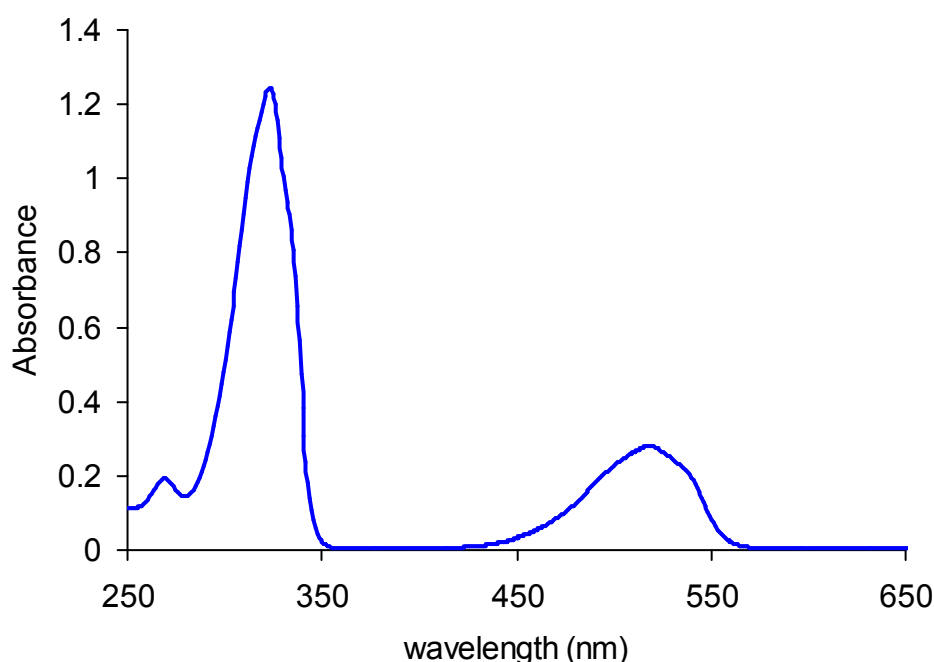


Figure 2. Absorption spectrum of **86** in DM (C: 0.16 mM).

The shape of the fluorescence spectra of **86** is typical of tetrazine derivatives (Figure 3). The position of the maximum is in accordance with those already observed for chloroalkoxy-*s*-tetrazine derivatives: 565nm for tripod-tetrazine **86**, and 567nm and 572nm for chloromethoxy-*s*-tetrazine **76** and 1,4-bis(chloro-*s*-tetrazinyloxy)butane **78** (Chapter 3.2, Figure 7), respectively. As observed for

unsymmetrically substituted tetrazines studied in our laboratory, the fluorescence quantum yield is good (0.29) and the fluorescence lifetime is long (150 ns, Table 1), making it a promising candidate as fluorescent molecular sensor for anions or neutral electron-rich molecules.

Furthermore, the comparison of the fluorescence excitation and UV-vis. spectra (Figure 3) shows that they are identical in shape and position, and the fluorescence excitation spectrum is the mirror image of the emission one, which indicate that the emitting species is the same as the absorbing one. Hence it can be concluded that despite their close proximity in the molecule, the three tetrazines of the tripod molecule are not interacting one with each other. This is further confirmed by the fact that time resolved fluorescence decay presents only one characteristic lifetime (Table 1) which is close to the one observed for the monomeric tetrazine **76** (160 ns).

Table 1. Main spectral data of tripod-tetrazine **86** in DM.

Compound	λ_{\max}^{abs} (nm)	ϵ_{abs} (L.mol ⁻¹ .cm ⁻¹)	λ_{\max}^{em} (nm)	Φ_F	Lifetime (ns)
Tripod-tetrazine (86)	518	1802	565	0.29	150
	323	7963			
	269	1251			

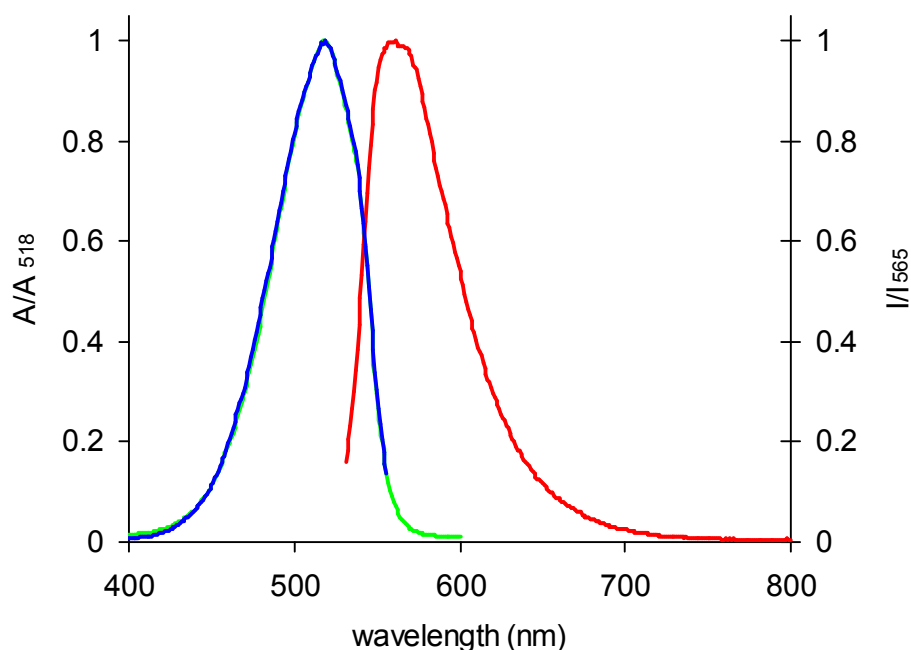


Figure 3. Normalized fluorescence emission (—), fluorescence excitation (—) and UV-vis. absorption (—) spectra of tripod-tetrazine **86** in DM.

5.2.2 Fluorescence quenching of tripod-tetrazine

In order to investigate the ability of **86** to act as a fluorescent sensor agent, fluorescence quenching studies were carried out by addition of electron-rich aromatics: tetrathiafulvalene (TTF), triphenylamine (TPA), tris(4-bromophenyl)amine, pyrrole and trimethoxybenzene (Figure 4), and the corresponding Stern-Volmer slopes (k_{SV}) were obtained (Table 2). The results show that TTF is the most efficient quencher for **86**.

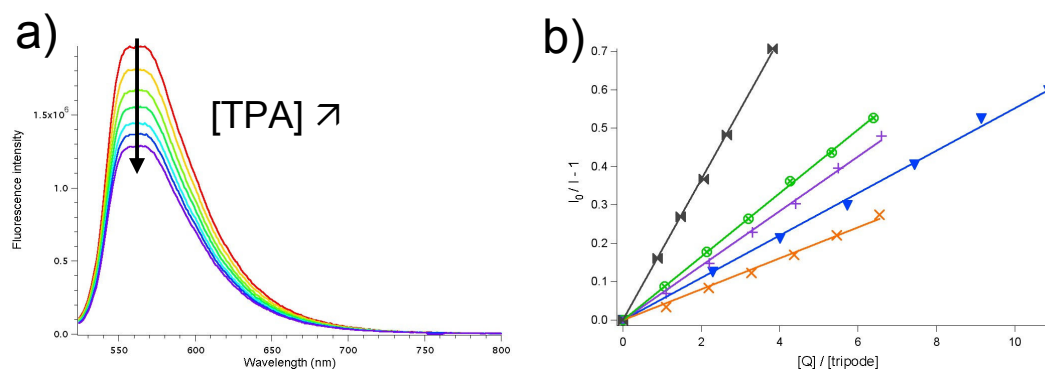


Figure 4 a) Modification of fluorescence spectra of **86** in DM, upon addition of TPA from 0.06 mM (1 eq.) to 0.36 mM (6 eq.);
 b) Stern-Volmer plots for the quenching of **86** with TTF (—■—), triphenylamine (—●—), tri(4-bromophenyl)amine (—▲—), pyrrole (—▲—) and 1,3,5-trimethoxybenzene (—×—).

Table 2. Stern Volmer constant (k_{SV}) for tripod-tetrazine **86** with the different tested quenchers.

Quencher	slope: k_{SV} ($L \cdot mol^{-1}$)	$k_q^{(a)}$ ($L \cdot mol^{-1} \cdot s^{-1}$)	E_{ox}^0 (V vs SCE)
Tetrathiafulvalene (TTF)	2897.9	$19.32 \cdot 10^9$	0.38
Triphenylamine (TPA)	1485.9	$9.83 \cdot 10^9$	1.04
Tris(4-bromophenyl)amine	1271.9	$8.48 \cdot 10^9$	1.07
Pyrrole	988.1	$6.59 \cdot 10^9$	1.31
1,3,5-trimethoxybenzene	711.2	$4.74 \cdot 10^9$	1.56

a) Dynamic quenching mechanism is postulated here to calculate the k_q .

The differences in quenching for the tested molecules can be attributed to their electron donor strength which is directly related to their oxidation potential. We can then connect the observed k_q to the corresponding E_{ox}^0 according to the Equation 5. The plot is linear (Figure 5) which confirms that the quenching is due to an electron transfer from the aromatic donor to the accepting tetrazine in its excited state.

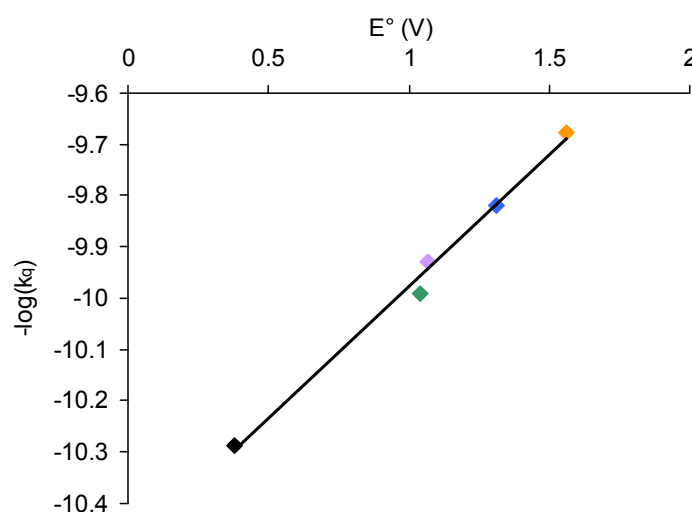


Figure 5 Rehm-Weller plot for **86**, R^2 : 0.992.

The quenching of **86** by tetrathiafluvalene (TTF) was also studied by time resolved fluorescence in order to decipher its mechanism. The results show that the fluorescence of the tripod-tetrazine is efficiently quenched (Figure 6). As the quantity of TTF increases, the initial fluorescence intensity of the fluorescence decay keeps nearly constant (the small drop is less than 5% and is due to fluctuation of laser intensity), while the lifetime becomes shorter and shorter but still monoexponential (*i.e.* unique); this indicates that the mechanism of quenching is dynamic and not static.

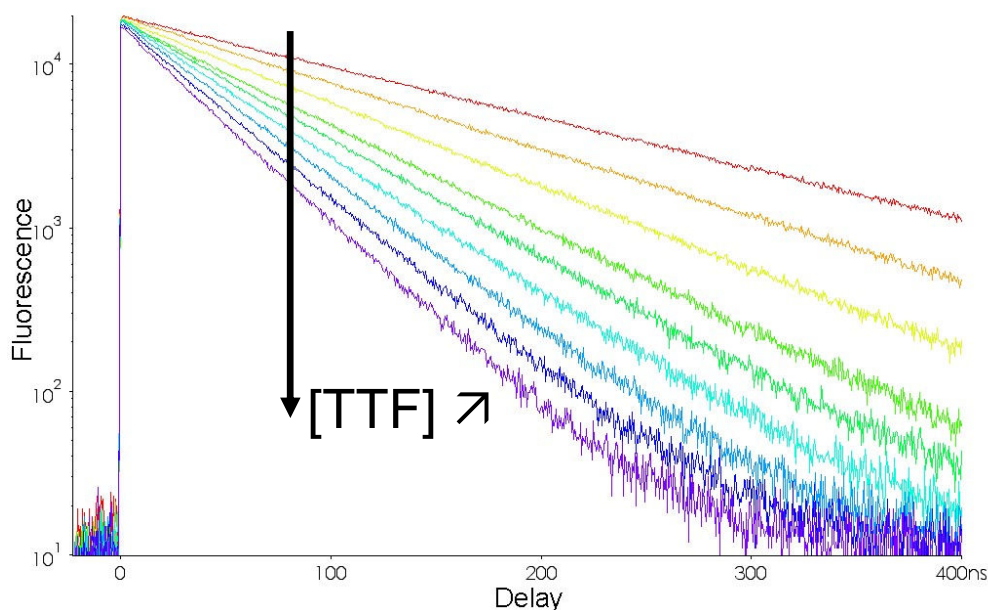


Figure 6. Fluorescence decay variation of tripod-tetrazine **86** in DM upon addition of TTF from $0.15 \cdot 10^{-3} \text{ mol.L}^{-1}$ to $1.1 \cdot 10^{-3} \text{ mol.L}^{-1}$.

Figure 7 shows the Stern-Volmer plot derived from Figure 6 for tripod-tetrazine **86** in the presence of TTF in dichloromethane. In this case, in Equation 4, the variation of intensity ($\frac{I_0}{I}$) is replaced by the relative change in lifetime ($\frac{\tau_0}{\tau}$).

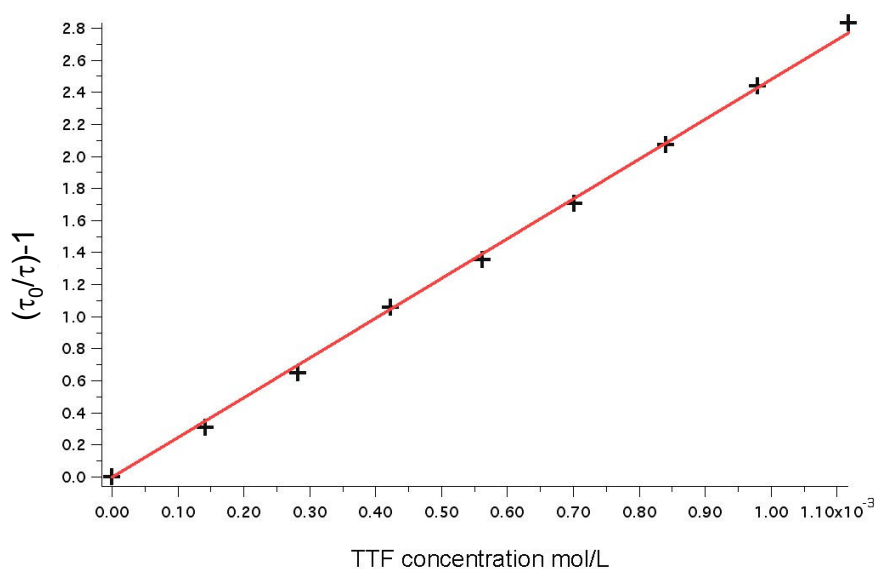


Figure 7. Stern-Volmer plot of **86** as function of TTF concentration.

The slope was found to be $2480 \text{ L}\cdot\text{mol}^{-1}$ which is in the same order to the one found from the steady state fluorescence (Table 2), confirming further that the quenching mechanism is dynamic.

5.2.3 Preliminary electrochemical studies of tripod-tetrazine

We have also investigated the influence of addition of different electron-rich compounds on the redox behaviour of the tripod-tetrazine. When 0.5 eq. of resorcinol was added into the solution of **86**, the redox current was dramatically decreased so that the redox peak were no more distinct, hence it is difficult to observe if the redox potential was shifted or not (Figure 8). The redox current was even completely lost when 1 eq. of resorcinol was added. As for comparison, the CV of the tripod-tetrazine **86** is quite reversible in presence of 1 eq. of bithiophene (BTH), and the redox current could be observed even when 5 eq. of BTH was added, although largely decreased (Figure 9). The addition of (*N*-methyl pyrrole) NMP also influences the CV current of **86** significantly. The redox peaks were no more noticeable after 2 equivalents of NMP were added. However, in all cases the redox potential of **86** seems to be stable, and is not influenced by the addition of electron-rich aromatics.

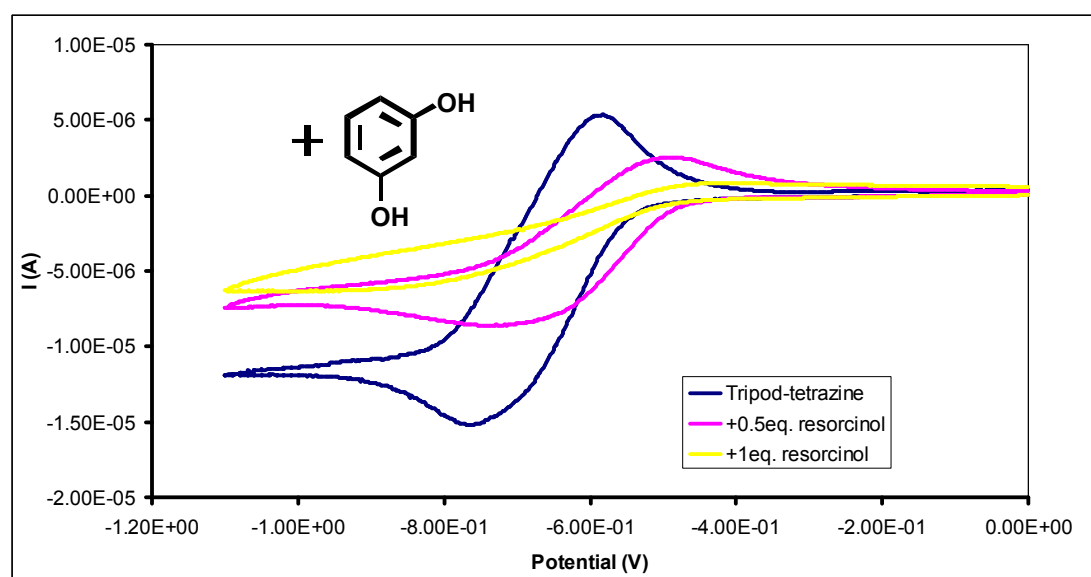


Figure 8. Variation of the cyclic voltammogram of tripod-tetrazine **86** with addition of resorcinol. Scan rate: $50 \text{ mV} \cdot \text{s}^{-1}$. $E_{p,c}$: -0.765 V , $E_{p,a}$: -0.582 V . Reference: Ag wire.

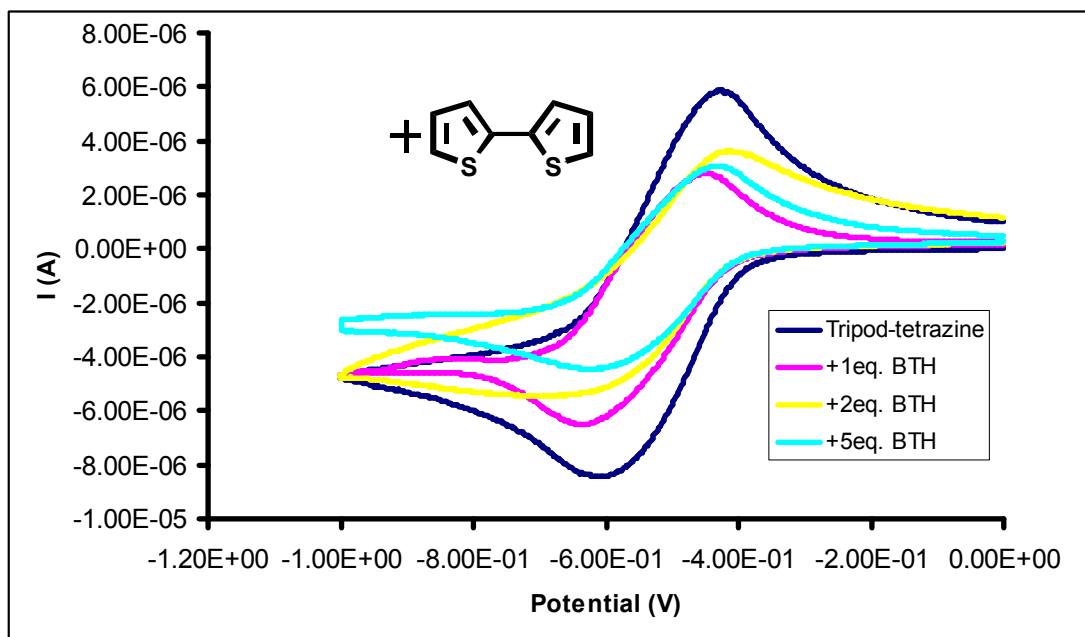


Figure 9. Variation of the cyclic voltammogram of tripod-tetrazine **86** with addition of BTH. Scan rate: $50 \text{ mV} \cdot \text{s}^{-1}$. Reference: Ag^+/Ag .

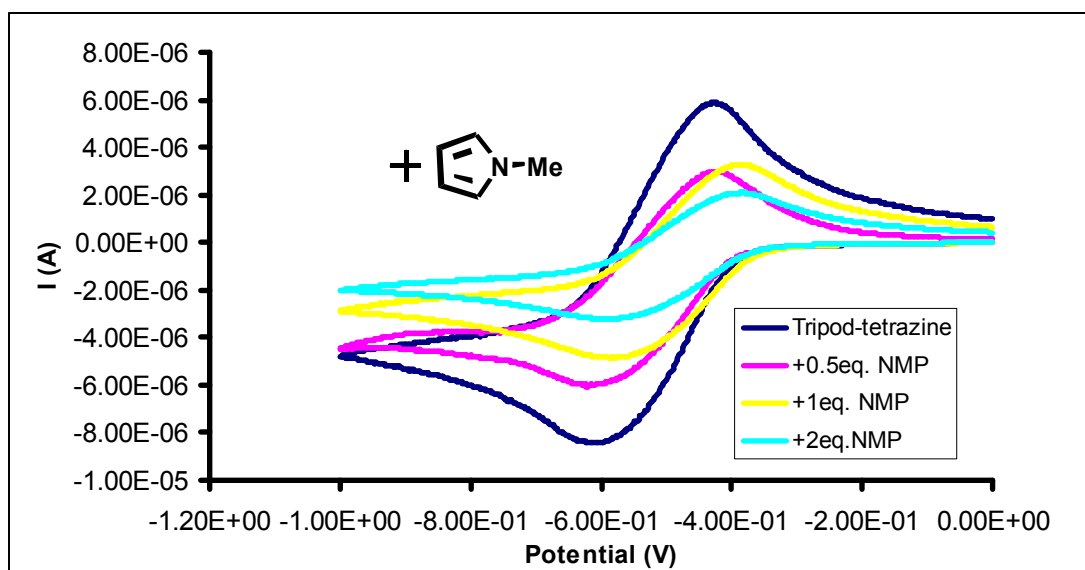


Figure 10. Modification of the cyclic voltammogram of tripod-tetrazine **86** with addition of NMP. Scan rate: $50 \text{ mV} \cdot \text{s}^{-1}$.

5.3 Spectroscopic and electrochemical studies for the first cyclophane (**93**)

The choice of 1,4-butanediol as a spacer was motivated by the fact that it introduces an oxygen atom right on the tetrazine ring, and -OR type substituents have been recognized to insure the existence of fluorescence properties in the tetrazine systems, since the n orbital remains lying higher than the π orbital (indeed it is the $n-\pi^*$ transition which generates fluorescence). Compounds **133** and **112** were prepared for comparison (Figure 11).

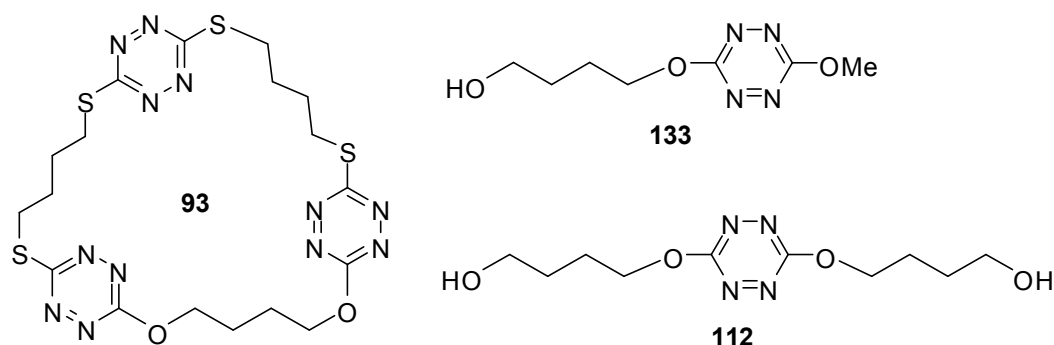


Figure 11 Cyclophane **93** and model compounds **112** and **133**

5.3.1 Spectroscopic study

The absorption spectrum of cyclophane-tetrazine **93** is similar to that of linear tetrazines substituted by alkylthio and alkoxy groups (Figure 12, Table 3). The band at 403 nm can be attributed to a $\pi-\pi^*$ transition while the one at 529 nm corresponds to an $n-\pi^*$ transition. Indeed, the position of the first band is common to all sulphur-substituted tetrazines and is strongly red-shifted when compared to the bis-alkoxytetrazines, since $\pi-\pi^*$ transitions are known to present such a shift when the substituent is more electron-donor². Accordingly, the energy of the $n-\pi^*$ transition is less influenced by substitution on the tetrazine ring, so this band is found in a small range of wavelengths (510-530 nm) for all compounds. Absorption and fluorescence spectra of **133** and **112** are the same, and identical to the ones of dimethoxy-*s*-tetrazine³ as it could be expected, showing no effect at all of the hydroxy terminal groups, even on the fluorescence. The shape of the fluorescence spectra of **93** is typical of tetrazine derivatives. The position of the maximum is in accordance with the fluorescence of linear tetrazines derivatives containing alkylthio and alkoxy substituents. As for all the sulphur-substituted tetrazines studied before⁴, the fluorescence quantum yield is unfortunately very low. Therefore, it was not possible to conduct satisfactory studies of its behavior in the presence of possible quenchers like anions or electron-rich molecules.

Table 3. Maximal absorption and emission wavelengths, molar extinction coefficient and fluorescence quantum yield for compounds **93**, **133** and **112**.

Compound	$\lambda_{\text{max}}^{\text{abs}}$ (nm)	ϵ_{abs} (L.mol ⁻¹ .cm ⁻¹)	$\lambda_{\text{max}}^{\text{em}}$ (nm)	Φ_{F}
93	529	1200	585	0.002
	403	2100		
133	526	Not determined	572	0.10
	347			
112	528	Not determined	575	0.09
	348			

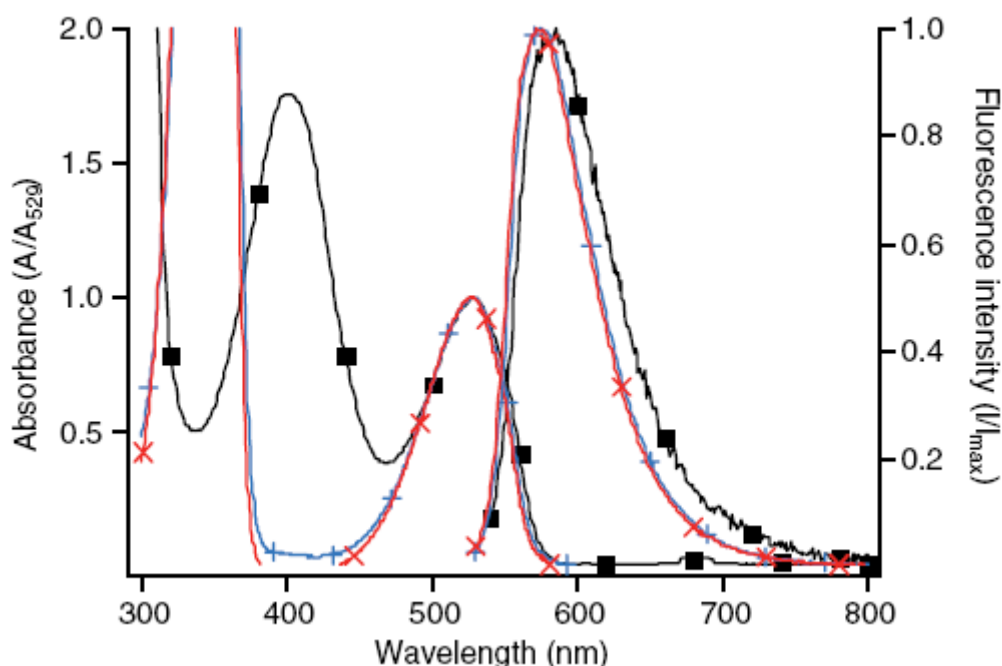


Figure 12. Absorption and fluorescence spectra of **93** (black line, ■), **133** (red line, ×) and **112** (blue line, +) in dichloromethane solution.

5.3.2 Electrochemistry study

The electrochemical behavior of tetrazine compounds **133** and **112** has been investigated in dichloromethane. Both compounds exhibit similar redox behavior with a well-defined reversible reduction wave at -1.11 V and -1.21 V vs. Ag/Ag⁺, respectively. These potential values fit perfectly well with the one of dimethoxy-*s*-tetrazine, showing that substitution of methoxy groups by butanedioxy ones induces only an insignificant cathodic shift, and especially that no influence of the acidity of the hydroxy terminal groups takes place.

The cyclophane **93** has a straightforward electrochemical behavior analogous to tetrazines substituted by heteroatoms. Despite the presence of three tetrazines, among which one is slightly different from the two others, a single peak is featured with a redox potential at *ca.* -1.12 V vs. Ag/Ag⁺. All three tetrazines are reduced together, since otherwise further electron transfer would be visible at lower potentials. This is also in apparent agreement with the approximate number of electrons

transferred, although this is less easy to estimate, due to uncertainties on the actual diffusion coefficient. The comparison of the reduction peak current for **93** with the oxidation peak current of ferrocene used as a standard, leads to a number of exchanged electrons that falls between 2 and 3 for the cyclophane tetrazine, depending on the size assumed for the solvated compound. Nevertheless this point proves that the electron exchange of the tetrazine rings is rather fast at the timescale used for CV.

5.3.3 Sensitivity of the electrochemical response to added organic compounds

We have checked the sensitivity of the redox process of **93** to several electron-rich molecules; especially, we were curious to check if a 3-fold symmetry donor would change the electrochemical response of the 3-fold symmetric tetrazine cyclophane, despite the electrochemistry has been shown to be less sensitive than fluorescence in similar cases³.

Four compounds have been tested: naphthalene (which does not have the appropriate symmetry, but seemingly fits with the cyclophane cavity), 1,3,5-trihydroxymethylbenzene, and triethanolamine, which both possess the complementary symmetry, although with a different steric hindrance. Finally, we also investigated the influence of resorcinol (1,3-dihydroxybenzene), which possesses two OH- groups at 120° one another, on the electrochemistry of compound **112**. The case of resorcinol is interesting since it possesses two reactive groups that can match the two hydroxy groups of **112**, and it is also the most acidic among the tested compounds.

While naphthalene was found not to influence the electrochemical response of the tetrazines in the cyclophane, the two other compounds have an effect on the redox potential of the cyclophane (Figure 13). However, conversely to what one would expect, the stronger complexing agent seems to be the anion-radical, since the peak potentials happen to be shifted in the positive range. The benzenetrimethanol displays the larger effect, since it probably fits much better the cyclophane cavity than the smaller triethanolamine. As a reverse peak is observed without current loss even at low scan rates, this is therefore a reversible complexation mechanism, and not a proton transfer which would lead to an irreversible evolution of the electrochemical behavior of the cyclophane. This analysis is moreover confirmed by the behavior of **133** and **112**, which do not display any visible influence of their hydroxy terminal groups on their electrochemical properties. The effect observed with the 3-fold symmetry compounds is thus probably due to H-bonding interactions with the anion-radical of the tetrazine, rather than a simple proton transfer effect. In order to confirm the absence of the formation of a complex in the neutral state, a NMR titration of cyclophane **93** was conducted in the presence of benzenetrimethanol in d₃-acetonitrile. No variation of the peaks position of the cyclophane could be detected upon addition of increasing amounts of benzenetrimethanol.

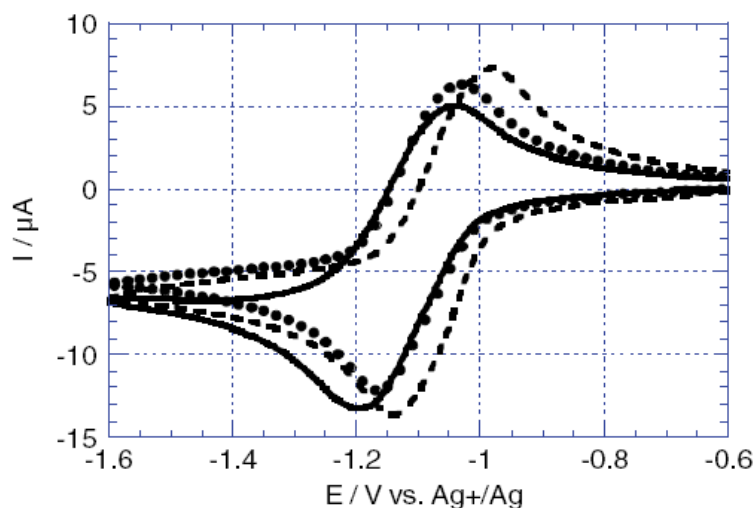


Figure 13. CVs of cyclophane **93** (ca. 5 mmol.L⁻¹) in CH₂Cl₂ + TBAP on glassy carbon electrode at 0.05 V/s: alone (full line); +2 eq. of triethanolamine (dots); +1eq. of 1,3,5-trihydroxymethylbenzene (dashed line).

As a comparison, the response of tetrazine **112** in the presence of resorcinol was also examined. The Figure 14 represents the evolution of the CV of tetrazine **112** in the presence of increasing amounts of resorcinol. The behavior is most interesting because not only the reversibility of the tetrazine reduction is gradually lost, but in addition there is simultaneously an increase in the reduction currents and a shift in the redox potentials. This is indicative of an irreversible reaction of the anion-radical in the presence of the added substrate. To check whether the interaction occurs between resorcinol and compound **112** or its anion-radical, UV-Vis absorption measurements were performed upon addition of resorcinol to the solution of **112**. No shift in the absorption maximum wavelength was observed up to addition of 25 eq. of resorcinol. This result was further confirmed by NMR titration of **112** in the presence of resorcinol in d₃-acetonitrile. No variation of the spectra of the tetrazine could be detected in the presence of increasing quantities of resorcinol. Therefore, we can conclude that interactions take place between resorcinol and the anion-radical of **112**, involving proton transfer. Besides the reoxidation of the protonated species can be seen at higher potential (ca. -300 mV) on the CV.

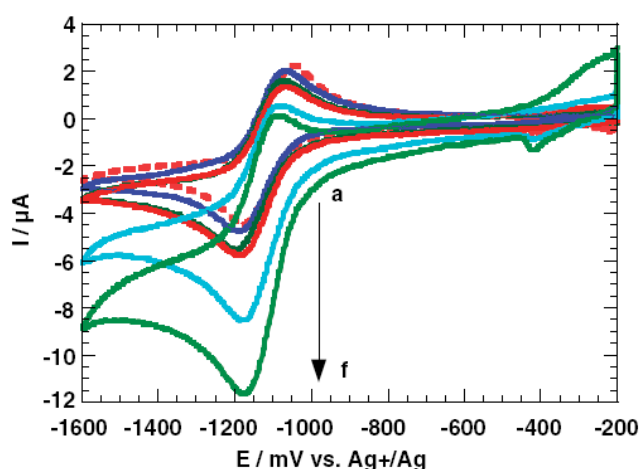
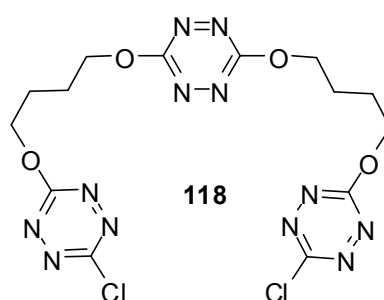


Figure 14. CVs of the reduction of **112** (ca. 2 mmol.L⁻¹) in dichloromethane (+TBAP) after addition of increasing amounts of resorcinol (dissolved in acetonitrile): (a) 0 eq. (dashed line); (b) 0.5 eq.; (c) 1 eq.; (d) 1.5 eq.; (e) 3.5eq.; and (f) 4.5 eq. Currents are corrected for dilution effects.

The spectroscopic and electrochemical properties of the first cyclophane molecule based on tetrazine moieties were explored, and compared with several new tetrazines. The cyclophane was designed for electron-donating entities recognition, and the electrochemical response of it can be sensitive to electron-rich and hydroxyl substituted compounds. This demonstrates the utility of tetrazine as a new building block for the synthesis of receptors for electron-rich molecules.

5.4 Discussion of fluorescence of new cyclophane-tetrazine **90** and tetrazines **118** and **128**

5.4.1 Trimer-tetrazine **118**



5.4.1.1 Absorption and fluorescence studies of **118**

The absorption and fluorescence spectra of the compound before cyclization, 3,6-bis(4-(6-chloro-1,2,4,5-tetrazin-3-yloxy)butoxy)-1,2,4,5-tetrazine (**118**), were both recorded in DM (Figure 15). It displays two very strong bands in the UV region (269 nm and 330 nm, Table 4), the latter corresponding to the π - π^* allowed transition, the peak value of which is between the ones for Cl-Tz-O (327 nm) and O-Tz-O (343 nm). Therefore this band is most probably the merge of two absorptions from Cl-Tz-O and O-Tz-O, respectively. The much less intense band in the visible region (522 nm), corresponding to the n - π^* transition, is a common character for most tetrazine derivatives and responsible for the color of the compound.

Compound **118** is strongly fluorescent, which is not surprising, since the three tetrazine moieties that it possesses are all fluorescent according to our preliminary results. The fluorescence spectrum in solution is also shown Figure 15 illuminating the spectral shape and position of the band. The fluorescence characters are more like dimethoxy-*s*-tetrazine (Chapter 3, compound **52**), rather than chloromethoxy-*s*-tetrazine (compound **76**). For example, the values found for fluorescence lifetime and quantum yield (τ_0 =59 ns, Φ_F =0.126) are in the same range as those of dimethoxy-*s*-tetrazine (τ_0 =49 ns, Φ_F =0.11). However, both the fluorescence lifetime and quantum yield are markedly decreased compared to chloromethoxy-*s*-tetrazine (τ_0 =160 ns, Φ_F =0.38).

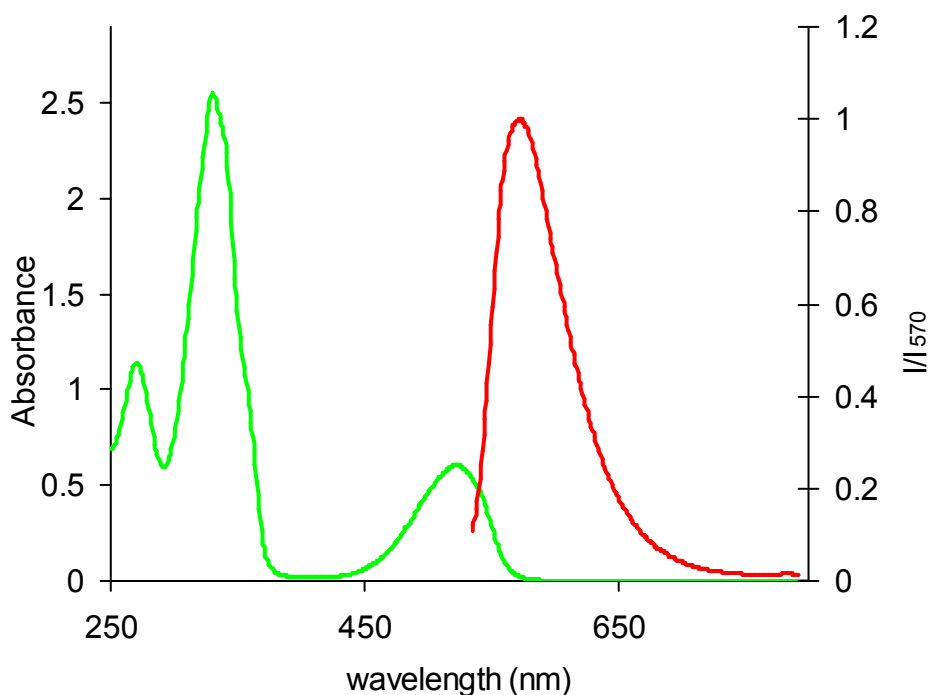


Figure 15. Absorption (—) and fluorescence (—) spectra of **118**.

Table 4. Spectral data of **118**.

Compound	λ_{\max}^{abs} (nm)	ϵ_{abs} (L·mol ⁻¹ ·cm ⁻¹)	λ_{\max}^{em} (nm)	Φ_F	Lifetime (ns)
118	522	2097	570	0.126	59
	330	8510			
	269	3888			

5.4.1.2 Fluorescence quenching of tetrazine **118**

The fluorescence quenching of **118** was carried out in the presence of different electron-rich quenchers: triphenylamine (TPA), tris(4-bromophenyl)amine, pyrrole and 1,3,5-trimethoxybenzene. Figure 16(a) shows the modification of fluorescence spectra of **118** upon addition of TPA, which represents the typical change of fluorescence intensity during the addition of quenchers, and was used to obtain the Stern-Volmer plots (Figure 16(b)), according to the Stern-Volmer Equation (see Equation 1).

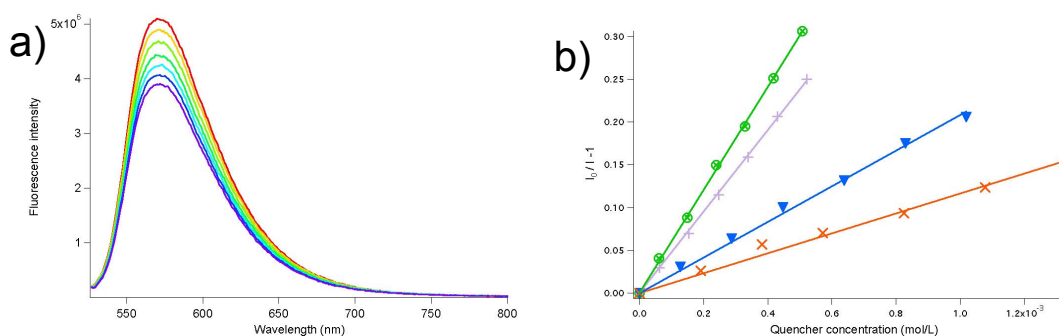


Figure 16 a) Modification of fluorescence spectra of **118** upon addition of triphenylamine (TPA); b) Stern-Volmer plots for the quenching of **118** with triphenylamine (—), tri(4-bromophenyl)amine (—), pyrrole (—) and 1,3,5-trimethoxybenzene (—).

The Stern-Volmer slopes (k_{SV}) for the four quenchers are presented in Table 5, along with their quenching constant k_q . Obviously the two triaryl amines, triphenylamine and tris(4-bromophenyl)amine quench the fluorescence of **118** much more efficiently than pyrrole or trimethoxybenzene.

It should be noticed that, in the presence of the same quencher, the structures of different sensor molecules influence greatly the quenching efficiency. For example, in presence of TPA, the k_{SV} for **118** is $603.1 \text{ L}\cdot\text{mol}^{-1}$, while for tripod-tetrazine **86**, it is much higher ($1485.9 \text{ L}\cdot\text{mol}^{-1}$, see Table 2), which illustrates that TPA quenches the fluorescence of tripod-tetrazine **86** much more efficiently than it does for **118**. This probably indicates that in the case of TPA, the tripodal structure of **86** is more favorable than the opened, chain structure of **118** to attain the proximity between sensor and quencher, thus facilitating the sensing process. The same effect was also observed in the case of tris(4-bromophenyl)amine, pyrrole, and 1,3,5-trimethoxybenzene as quenchers, where the k_{SV} values for tripod-tetrazine **86** are all much larger than those for **118**.

Table 5 Stern-Volmer constant (k_{SV}) for compound **118** with different quenchers.

Quencher	slope: $k_q \cdot \tau_0$ ($\text{L}\cdot\text{mol}^{-1}$)	$k_q^{(a)}$ ($\text{L}\cdot\text{mol}^{-1}\cdot\text{s}^{-1}$)	E_{ox}^0 (V vs SCE)
Triphenylamine (TPA)	603.1	$10.22 \cdot 10^9$	1.04
Tris(4-bromophenyl)amine	475.6	$8.06 \cdot 10^9$	1.07
Pyrrole	250.3	$3.53 \cdot 10^9$	1.31
1,3,5-trimethoxybenzene	208.01	$1.93 \cdot 10^9$	1.56

a) Assuming a dynamic quenching.

As in the case of fluorescence quenching of tripod-tetrazine **86**, a linear relationship between the oxidative potentials of quenchers (E_{ox}^0) and variations of free energy ($\Delta G^0 = -RT \log k_q$) is again obtained (Figure 17) according to the simplified Rehm-Weller equation (Equation 5), confirming that it is through an electron transfer mechanism that these electron-rich compounds quench the fluorescence of **118**.

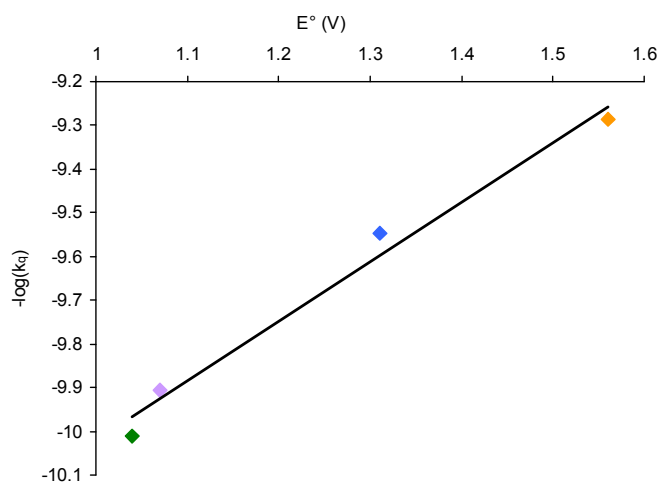
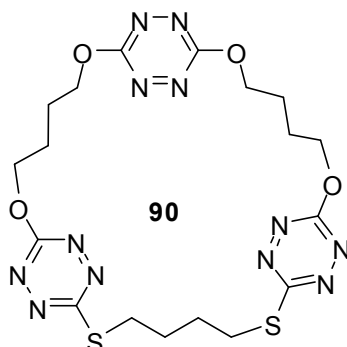


Figure 17 Rehm-Weller plot for **118**; R^2 : 0.983.

5.4.2 Cyclophane-tetrazine **90**



5.4.2.1 Absorption and fluorescence study of **90**

The absorption spectrum of the cyclophane-tetrazine **90** is shown in Figure 18. The two bands around 350 nm and 397 nm are in the region corresponding to π - π^* transitions. The absorption band at 528 nm is characteristic for nearly all 3,6-heteroatomsubstituted tetrazine compounds, which all show an absorbance band in this region corresponding to an n - π^* transition.

The new cyclophane **90** was designed and synthesized in view of improving the fluorescence quantum yield compared to the first cyclophane **93**. However, once cyclized, the compound was found to be only weakly fluorescent on TLC plate during the synthetic procedures. Study of the fluorescence spectrum also confirmed the weak fluorescence (Figure 18). The fluorescence quantum yield is unfortunately only about 0.006 in dichloromethane (Table 6), higher but close to that of the first cyclophane **93** ($\Phi_F = 0.002$).

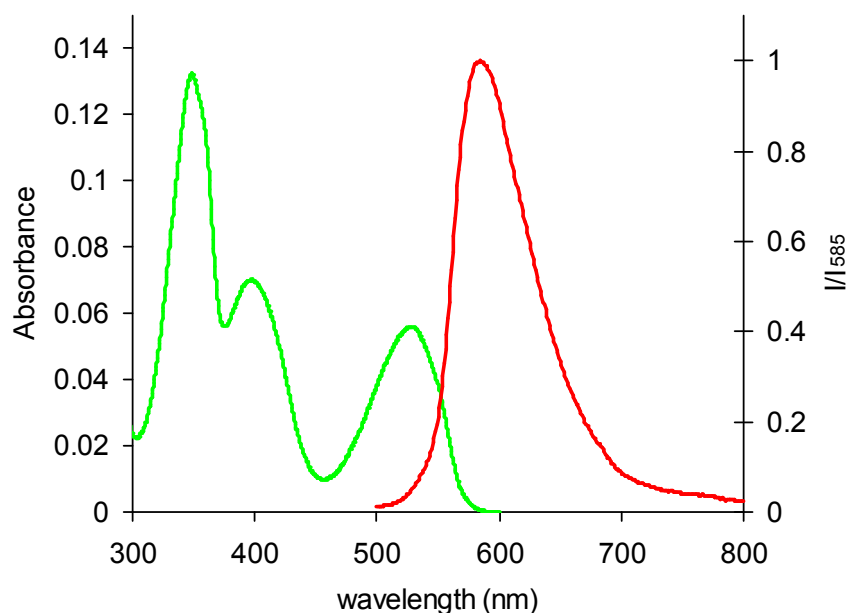


Figure 18. Absorption (—) and fluorescence (—) spectra of cyclophane-tetrazine **90** in DM (C: 0.034 mM).

Table 6. Spectral data of cyclophane-tetrazine **90**.

Compound	λ_{\max}^{abs} (nm)	ϵ_{abs} ($\text{L}\cdot\text{mol}^{-1}\cdot\text{cm}^{-1}$)	λ_{\max}^{em} (nm)	Φ_{F}	Lifetime (ns)
90	528	1647	585	0.006	$\tau_1 = 2.7 \pm 0.1$ (99.6%)
	397	2098			$\tau_2 = 38.3 \pm 0.8$ (0.4%)
	350				$\overline{\tau}_0 = 4.6$
	257				

The solvent effect on absorption and fluorescence was investigated. The absorbance and fluorescence maxima of **90** in different solvents are almost identical, with differences of less than 7 nm between each other. This is because it corresponds to the $n-\pi^*$ transition, which is insensitive to the environment. On the other hand, the fluorescence quantum yields of the cyclophane-tetrazine **90** vary slightly in different solvents: the highest Φ_{F} (0.0144) is obtained when ethanol is used as solvent (Table 7). We tried to rationalize this variation by comparing them to known solvent parameters: Hildebrand solubility parameter (δ), dielectric constant (ϵ_r), dipole moment (μ), and electrostatic factor ($\text{EF} = \epsilon_r \times \mu$). Unfortunately no linear correlation could be drawn.

Table 7. Solvent effects on photophysical properties of the new cyclophane-tetrazine **90**.

Solvent	λ_{\max}^{abs} (nm)	λ_{\max}^{em} (nm)	Φ_{F}
Dichloromethane	528	577	0.0063
Acetonitrile	522	576	0.0042
Ethanol	528	582	0.0144
Chloroform	529	578	0.0049
Dioxane	524	578	0.0088
1,2-Propylene carbonate	522	576	0.0053

5.4.2.2 Fluorescence quenching of cyclophane-tetrazine **90**

Although the fluorescence quantum yield of cyclophane-tetrazine **90** is low, the quenching effect could still be observed with the electron-rich compound TPA (Figure 19, Table 8). Compared to the tripod-tetrazine (**86**) and trimer-tetrazine (**118**), although the k_{SV} of **90** is smaller because of its much shorter lifetime, the quenching constant k_{q} is 2 times larger than that of tripod-tetrazine and trimer-tetrazine, indicating that the ring structure of cyclophane is much more favorable than the open-formed tripod structure or linear trimer structure to attain the sensor-quencher proximity leading to a relative efficient fluorescence quenching.

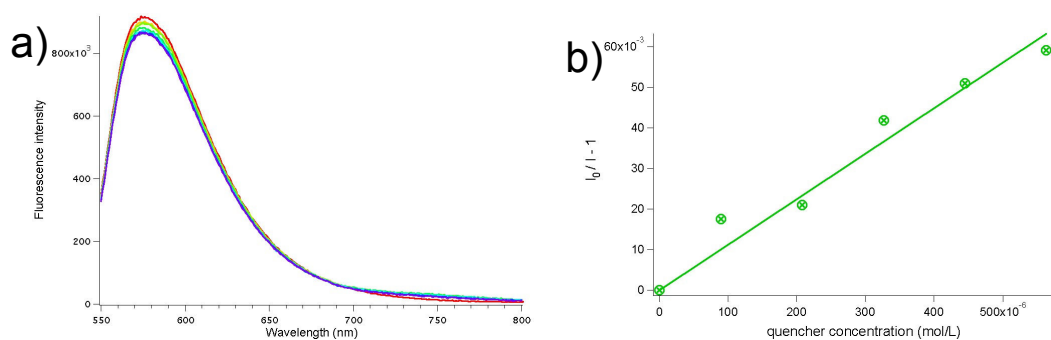
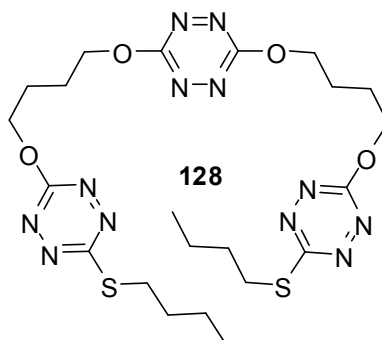
**Figure 19.** Fluorescence quenching of **90** with TPA: a) changes of fluorescence intensity upon addition of TPA; b) Stern-Volmer plot of quenching in presence of TPA.

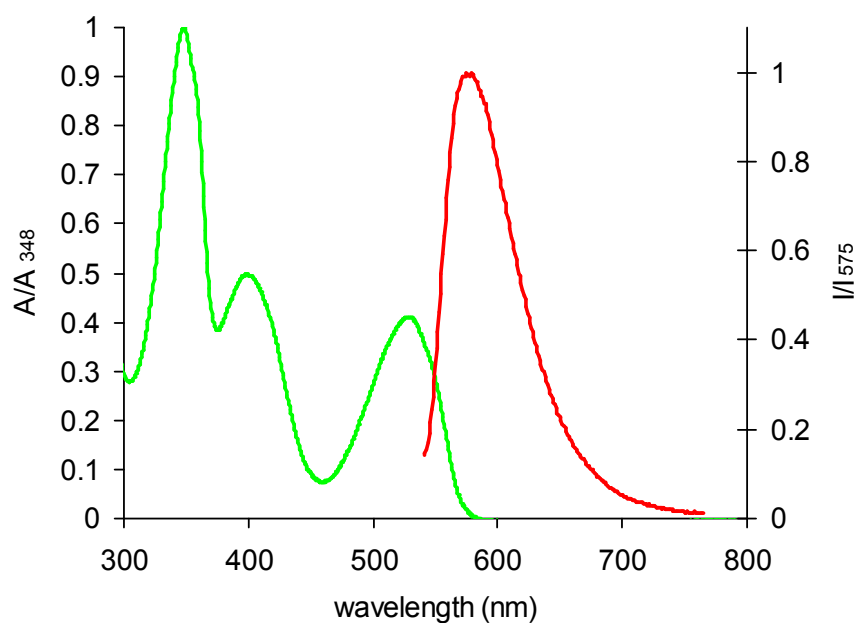
Table 8. Values of quenching effect (k_{SV} and k_q) of **90** in presence of TPA.

Quencher	slope: $k_{SV} = k_q \cdot \tau_0$ ($L \cdot mol^{-1}$)	k_q ($L \cdot mol^{-1} \cdot s^{-1}$)
TPA	102.4	$22.2 \cdot 10^9$

5.4.3 Tetrazine 128



To investigate the reason of the weak fluorescence of the cyclophane-tetrazine **90**, compound **128** was synthesized as an open-form analogue, and its absorption and fluorescence spectra were recorded in DM for comparison (Figure 20).

**Figure 20.** Absorption (—) and emission (—) spectra of **128**.**Table 9.** Spectral data of **128**.

Compound	λ_{max}^{abs} (nm)	λ_{max}^{em} (nm)	Φ_F	Lifetime (ns)
128	529	575	0.006	10
	399			
	348			
	259			

The absorption spectrum of the open-form analogue **128** is identical to the cyclophane-tetrazine **90**. The maxima of every absorption band for each compound are almost the same, with differences of less than 2 nm (Table 9). Compound **128** is also weakly fluorescent, and its fluorescence spectrum is almost the same to that of cyclophane **90**. These results confirmed that the loss of fluorescence of the cyclophane-tetrazine **90** is coming not from the cyclic structure, but from the introduction of thiol substituents on the tetrazines.

5.4.4 Molecular modeling and fluorescence properties

The novel cyclophane **90** containing an O-Tz-O moiety is only weakly fluorescent, which was surprising at the very beginning because dimethoxy-*s*-tetrazine is very fluorescent. Thus we tried to explain these results by modeling 3,6-disubstituted-1,2,4,5-tetrazines using the Gaussian03 software⁵ at the B3LYP level of theory and 6-31+G(d) base.

In a first step, a fluorescent tetrazine and a non fluorescent one were compared. The main feature which was observed is that there is a clear inversion of the two highest occupied orbitals between the two tetrazines (Figure 21). In the case of the fluorescent one, the HOMO (Highest Occupied Molecular Orbital) is an n type one and the HOMO-1 is π type. The situation is reversed for the non fluorescent one.

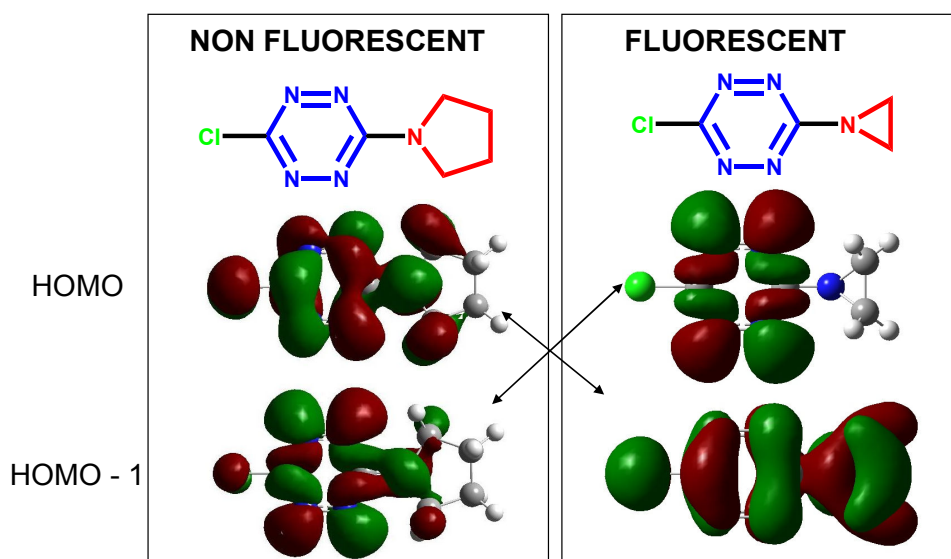


Figure 21 Comparison of the highest occupied orbitals for a fluorescent and a non fluorescent tetrazine

This trend was further confirmed when all the tetrazines obtained were modeled using the same method (Figure 22).

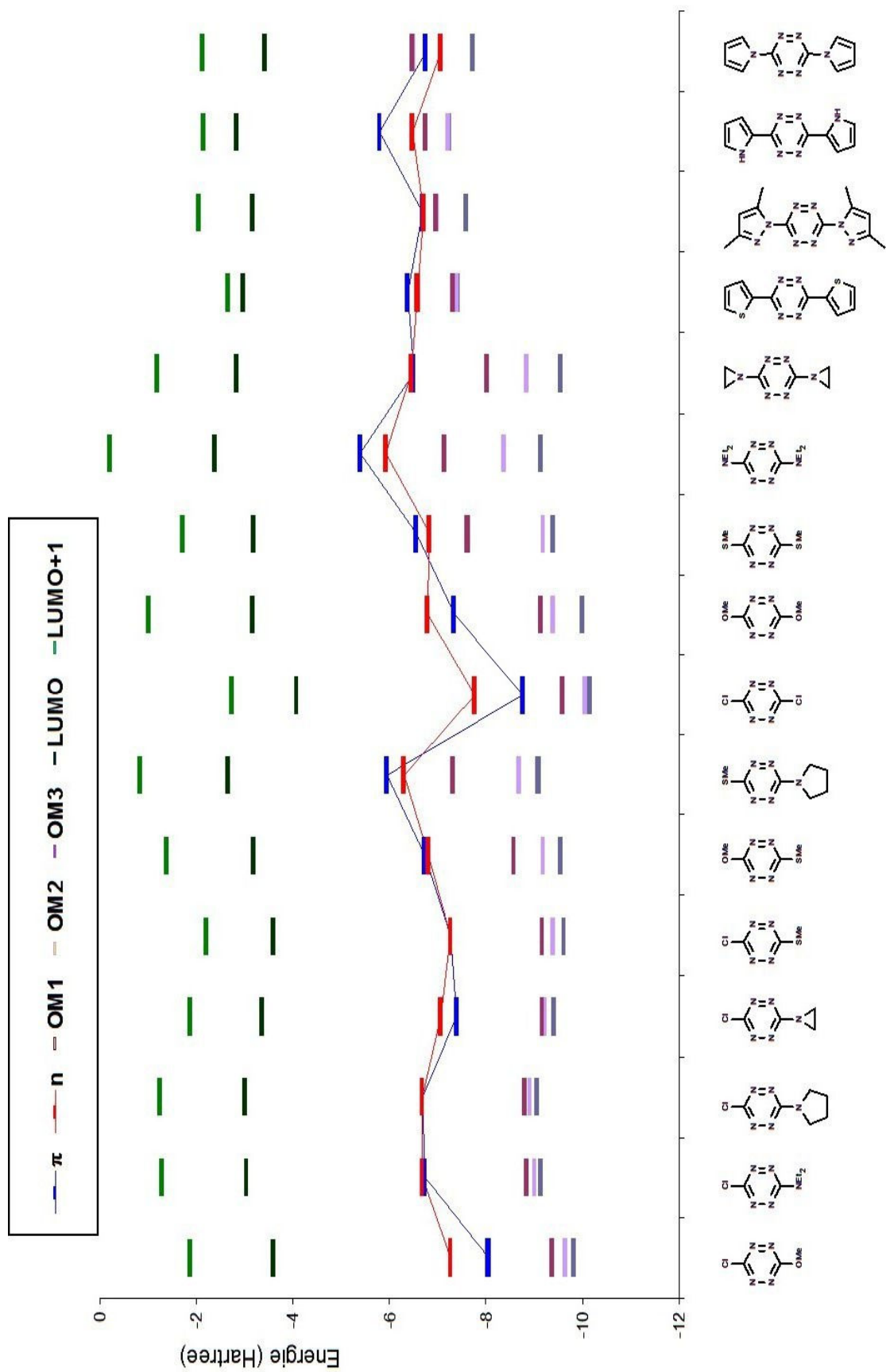


Figure 22 Energy diagram of the frontier orbitals of the tetrazine obtained in our laboratory

Combination of the results of these calculations and the observations from our experiments indicates clearly that when the HOMO is of n type the molecule is fluorescent. This is the case for dialkoxy- or chloroalkoxy-*s*-tetrazines (Figure 22). The molecule is not fluorescent when the HOMO has a π character, which is the case for dimethylthiol-*s*-tetrazine or tetrazine substituted by aromatics. While in the case of 3-alkoxy-6-alkylthiol-*s*-tetrazines, for example 3-methoxy-6-methylthiol-*s*-tetrazine which is weakly fluorescent, the energy level of HOMO-1 (n orbital) is nearly degenerated with that of HOMO (π orbital) yielding a weak fluorescence.

Then we compared the energy differences of LUMO and HOMO for model tetrazines substituted by two chlorines, chlorine/oxygen, chlorine/sulfur, oxygen/sulfur, two oxygens and two sulfurs (Table 10, Figure 23). We found out that for O-Tz-O and S-Tz-O, their LUMO energies are almost at the same level, while the HOMO energy level of S-Tz-O is slightly higher than that of O-Tz-O, which makes the HOMO-LUMO energy gap smaller than that of O-Tz-O. Therefore, if they coexist in a same molecule like cyclophane **90**, the first transition will take place on the S-Tz-O moiety after the absorption of a photon. This is confirmed further by the calculations of molecular orbitals of **90**, which show clearly that both its HOMO and HOMO-1 are located on each of the S-Tz-O moieties, respectively, and both show distinct π character with a small contribution of n type which explains the weak fluorescence observed (Figure 24).

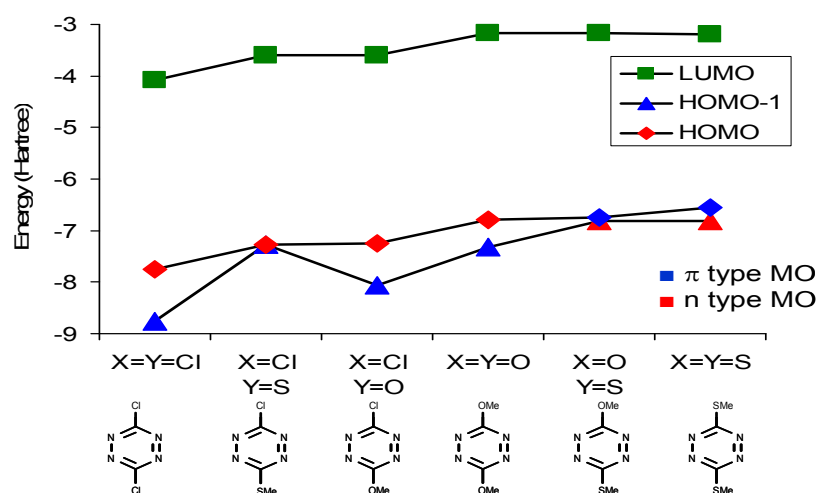
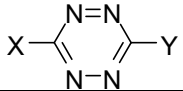


Figure 23. Comparison of energy levels of different tetrazines

Table 10. Comparison of energy levels (in Hartree) of HOMO, HOMO-1 and LUMO of 3,6-heteroatomsubstituted tetrazines.

	HOMO-1	HOMO	LUMO
X=Y=Cl	-8.7540264	-7.76227536	-4.07450736
X=Cl Y=S	-7.27592544	-7.26286176	-3.592512
X=Cl Y=O	-8.05348656	-7.25877936	-3.58924608
X=Y=O	-7.33090176	-6.79501872	-3.16086624
X=O Y=S	-6.81570288	-6.7373208	-3.177468
X=Y=S	-6.8230512	-6.55878384	-3.18263904

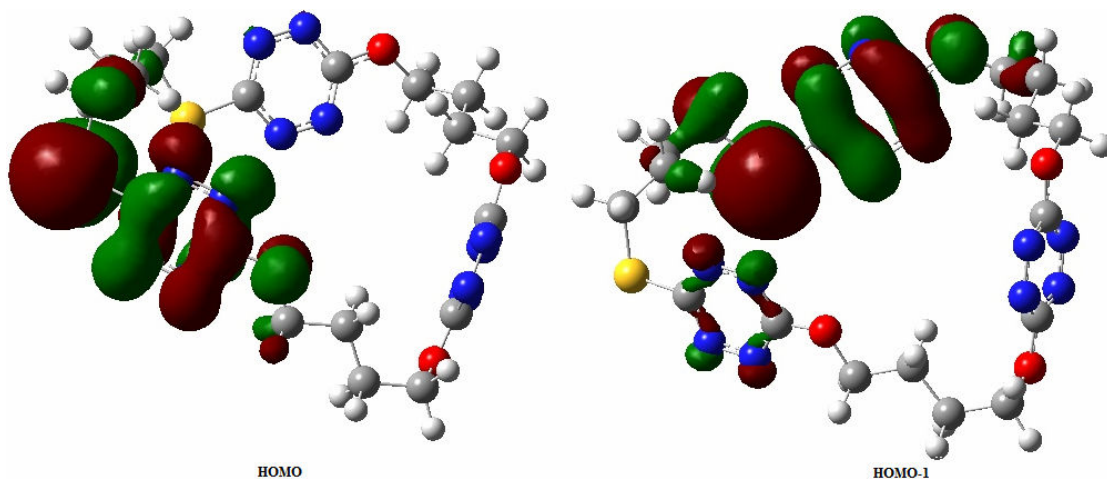


Figure 24. HOMO and HOMO-1 of cyclophane **90**. Red: oxygen; yellow: sulfur; blue: nitrogen.

In fact the features of absorption and fluorescence spectra of other multi-tetrazine derivatives can also be clarified by molecular modeling calculations. For example, the fact that the fluorescence of trimer-tetrazine **118** is more like dimethoxy-s-tetrazine rather than chloromethoxy tetrazine (see Chapter 5.4.1), can be explained by the calculation results on energy levels of molecular orbital for a series of tetrazines, which demonstrate that the HOMO-LUMO energy gap of O-Tz-O is slightly lower than that of the Cl-Tz-O (Table 10, Figure 23), which guarantees the first $n-\pi^*$ transition to take place on O-Tz-O moiety. Calculations on the energy levels of molecular orbitals also show clearly that the HOMO of **118**, from which the transition takes place leading to the fluorescence, is completely located on the middle O-Tz-O moiety, while the HOMO-1 and HOMO-2 are located on each Cl-Tz-O side moieties.

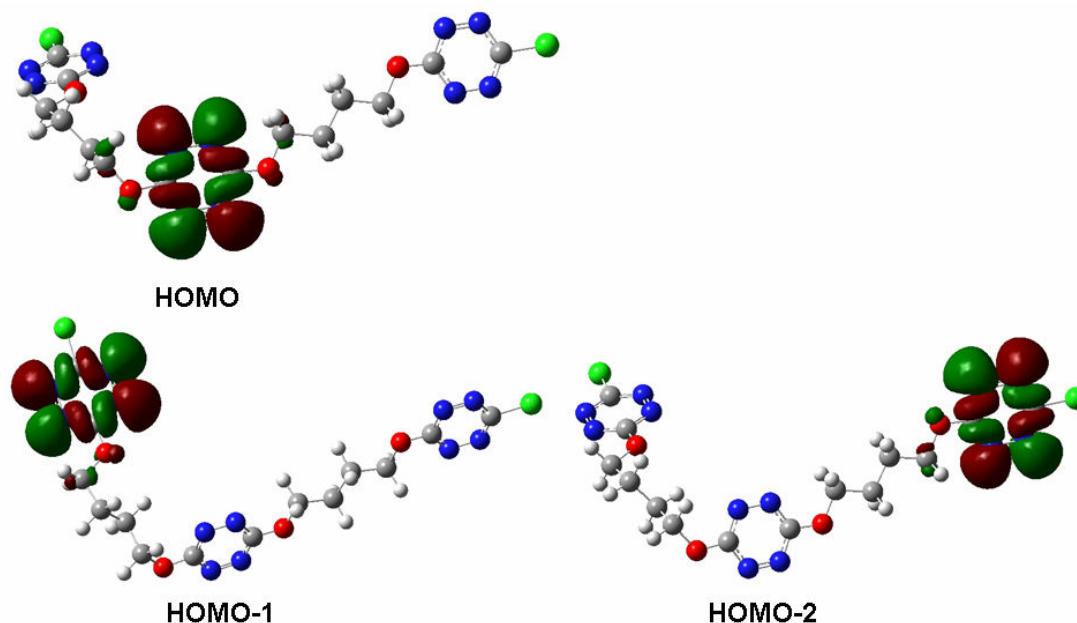


Figure 25. HOMO, HOMO-1 and HOMO-2 of trimer-tetrazine **118**. Red: oxygen; green: chlorine; blue: nitrogen.

5.5 Fluorescence and electrochemical study of β -CD-tetrazine

5.5.1 Absorption and fluorescence studies

We have performed fluorescence studies on β -CD-tetrazine (**94**), both in dichloromethane (Figure 26) and methanol (Figure 27). The fluorescence spectra of the β -CD-tetrazine show characteristics close to the ones of the generic chloromethoxy-*s*-tetrazine (**76**). Fluorescence lifetime and fluorescence yield depend both on the molecule and on the solvent (Table 11).

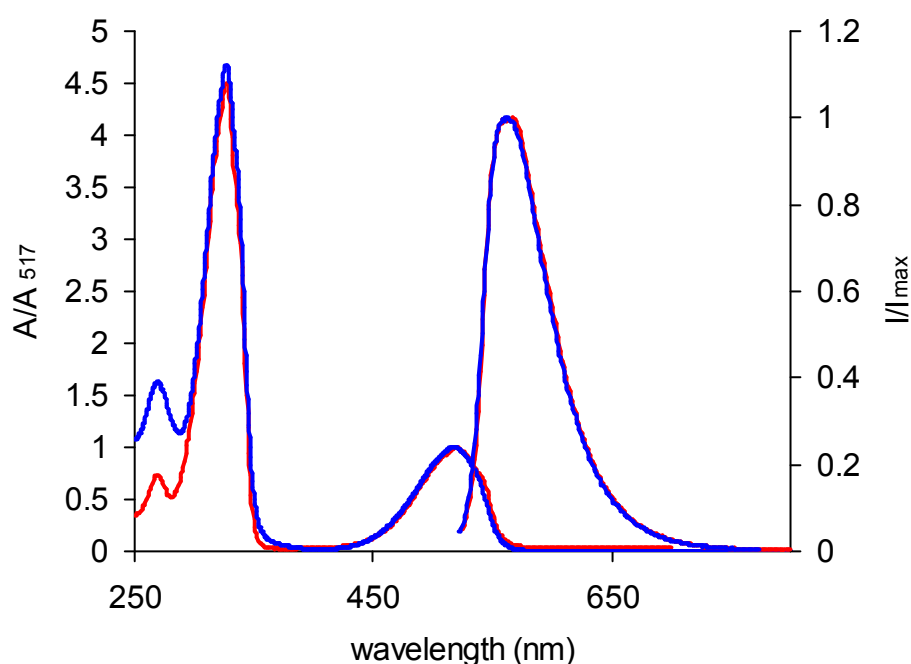


Figure 26. Absorption (left) and fluorescence (right) spectra of **76** (—) and β -CD-tetrazine **94** (—) in dichloromethane.

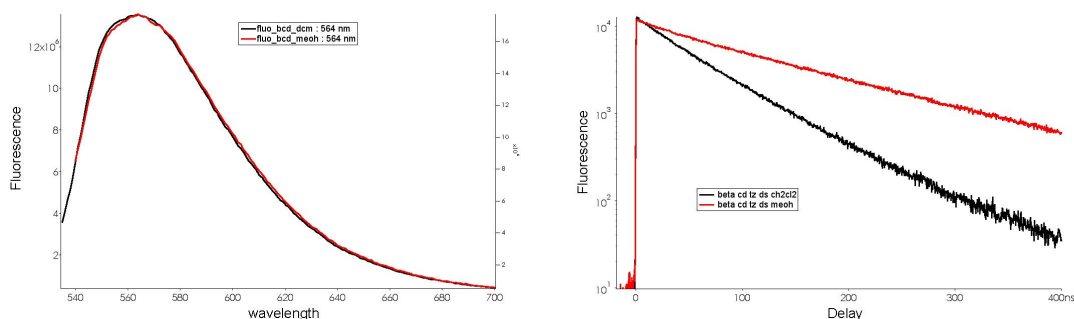


Figure 27 Steady state (left) and time resolved (right) fluorescence of **94** in DM (black) and MeOH (red)

Table 11. Spectroscopic characteristics of β -CD-tetrazine (**94**) vs. chloromethoxy-*s*-tetrazine (**76**).

	λ_{abs} (nm)	λ_{em} (nm)	ϵ_{abs} ($\text{L}\cdot\text{mol}^{-1}\cdot\text{cm}^{-1}$)	$\Phi_{\text{F}}^{(a)}$	τ_{o} (ns)
76 in DM	269, 327, 520	567	1900	0.35	160
94 in DM	266, 327, 517	563	3675	0.12	66 (0.68) 33 (0.32)
76 in MeOH	290, 325, 511	563	-	0.23	150
94 in MeOH	265, 325, 512	564	-	0.23	138 (0.86) 28 (0.14)

a) Reference: Rhodamine 6G in ethanol, $\Phi_{\text{F}}=0.95$

The fluorescence rate was measured from the fluorescence yield and lifetime. It is close to $2 \times 10^6 \text{ s}^{-1}$ for all compounds since the fluorescence rate is only slightly affected by environment effects. We observe that the average fluorescence lifetime and quantum yield of tetrazines bound to cyclodextrin are smaller than or equal to that of the free dye. It may be due to interactions between neighbouring fluorophores on the same cyclodextrin moiety. Indeed, the fluorescence lifetime of **76** is 160 ns in dichloromethane and 19 ns in crystals. These interactions are stronger in dichloromethane where they reduce the fluorescence lifetime and yield by a factor of two. These differences in lifetime and quantum yield may reflect a closer distance between the tetrazine substituents in dichloromethane compared to methanol.

5.5.2 Fluorescence quenching of β -CD-tetrazine

The fluorescence quenching has been studied in the presence of an electron donor, TTF (tetrathiafulvalene), for both compounds. The choice of TTF was made because it fits correctly the cyclodextrin cavity ($\sim 5 \text{ \AA}$), and it has a weak affinity for polar solvents (Figure 28):

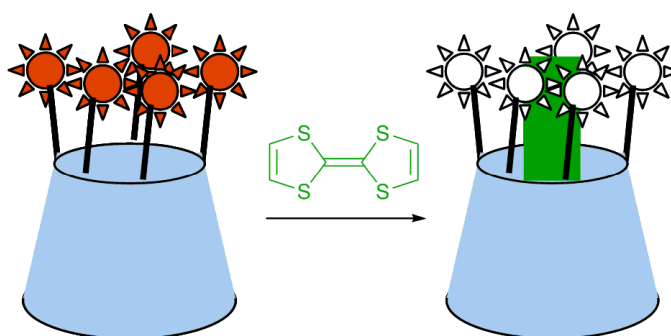


Figure 28. Principle of fluorescence quenching of β -CD-tetrazine by TTF.

The fluorescence of tetrazine **76** is quenched by TTF via electron transfer in dichloromethane (Figure 29). As time-resolved fluorescence lifetime decreases, it shows that a dynamic quenching occurs¹. From the time resolved measurements a slope of the Stern-Volmer plot $k_{\text{SV}}=3200 \text{ mol}^{-1}\cdot\text{L}$ is measured. This gives a quenching rate (k_{q}) of $2 \cdot 10^{10} \text{ L}\cdot\text{mol}^{-1}\cdot\text{s}^{-1}$. In dichloromethane, the fluorescence of β -CD-tetrazine **94** is also quenched by TTF (Figure 29, Figure 30). The quenching was measured

both in intensity and in lifetime. The Stern-Volmer plot is linear with a smaller slope of $858 \text{ L}\cdot\text{mol}^{-1}$ (Figure 29, Table 12). A value of $798 \text{ L}\cdot\text{mol}^{-1}$ is derived from lifetime variations. This confirms the value of the quenching rate and the predominance of the dynamic quenching for β -CD-tetrazine in dichloromethane. In methanol, fluorescence quenching starts with TTF concentration corresponding to a ratio β -CD-tetrazine: TTF of 1:0.2 (Figure 30, b). As long as the ratio is smaller than 1:1, a drop of the “zero-delay” amplitude is observed and the fluorescence lifetime does not change. This means that static quenching occurs probably because of the entrapment of the quencher in the cavity of the cyclodextrin in this lipophobic solvent. At higher ratio (Figure 30, b), the lifetime decreases, corresponding to a dynamic quenching, because the cavity is saturated, and additional quenching occurs with quenchers dispersed in solution around the functionalized cyclodextrine. Bithiophene (BTH) also quenches the fluorescence of **94**, although much less efficiently compared to the quencher TTF (Table 12).

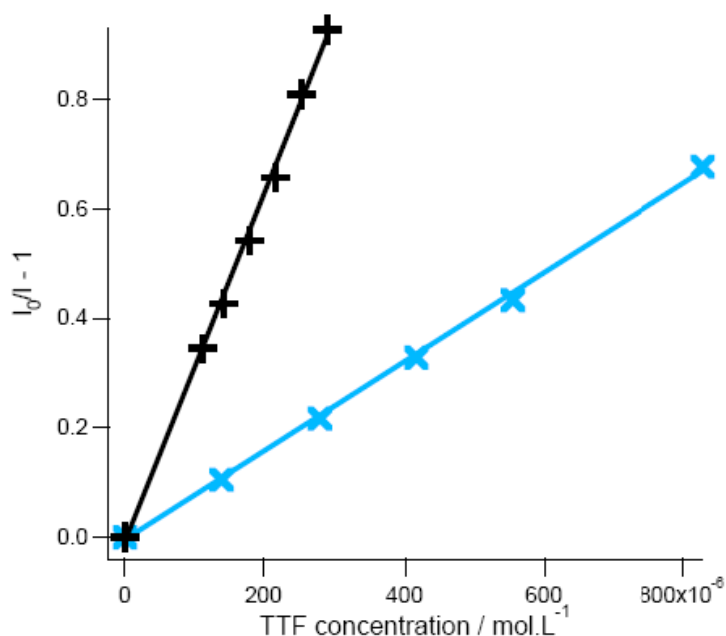


Figure 29. Stern-Volmer plots for the quenching of the fluorescence of **76** (black, +) and **94** (blue, x) by TTF in DM.

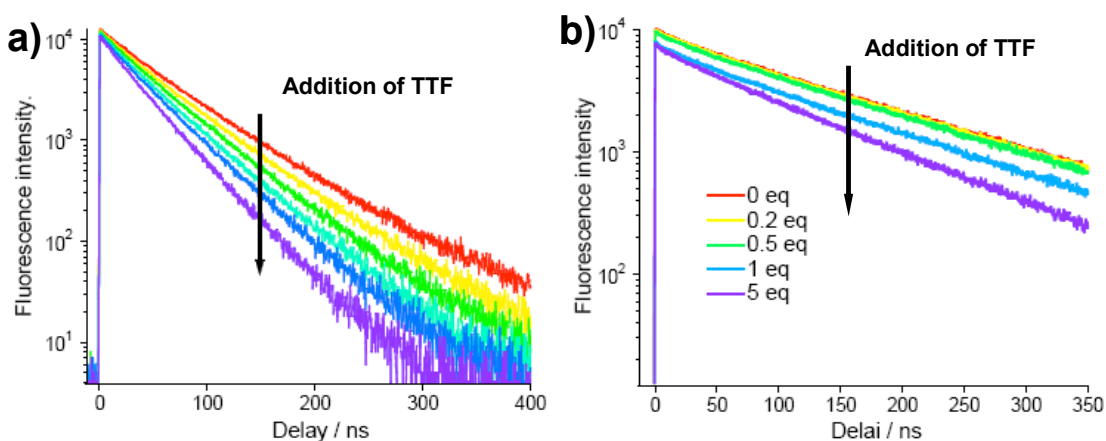


Figure 30. Fluorescence decays of β -CD-tetrazine in presence of TTF. a) in DM, ratio β -CD-tetrazine: TTF 1:4.5 to 1:26, b) in methanol, ratio 1:0.2 to 1:5. The intensity drop observed in methanol is characteristic of a static quenching between **94** and TTF.

Table 12. The Stern-Volmer slopes and quenching constants of **94** in presence of TTF and BTH in DM.

Quencher	slope: k_{SV} ($L.mol^{-1}$)	k_q ($\times 10^9$)
Tetrathiafulvalene (TTF)	858.2	14.37
Bithiophene (BTH)	312.3	5.23

The results from fluorescence experiments show that the fluorescence of β -CD-tetrazine can be efficiently quenched by an aromatic molecule with the adequate size in lipophobic environments. This should open the field to efficient quenching in polymer films, and maybe in the future to the fabrication of new and selective sensing devices based on tetrazines.

5.5.3 Electrochemical study of β -CD-tetrazine

Figure 31 shows the cyclic voltammogram for the β -CD-tetrazine, which displays one reduction peak with good reversibility. The reduction potential is -0.88 V, which is almost in the same range of chloro-oxygen substituted tetrazines previously prepared (- 0.77 V, see Chapter 3.2), but slightly lower. Furthermore, the peak difference of 200mV is indicative of a scattering in several discrete but close together redox potentials for the seven tetrazines. This is likely due to the entropic factor linked to the number of equivalent tetrazines in close proximity on the same molecule.

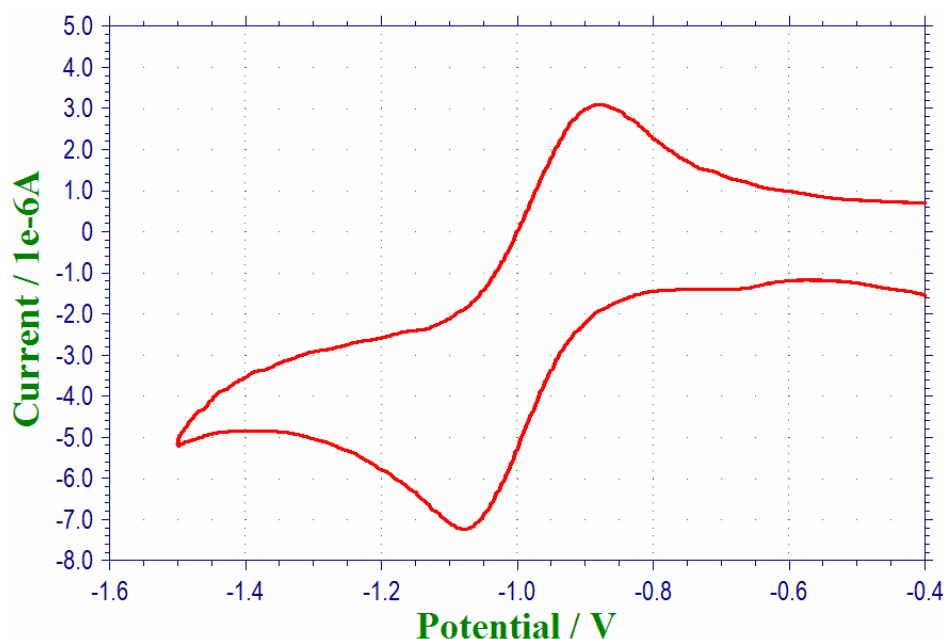


Figure 31. Cyclic voltammogram of β -CD-tetrazine **94** in DM. Scan rate: 100 mV.s^{-1} . E_{pa} : -0.878 V, E_{pc} : -1.075 V.

To investigate the interaction between **94** and electron-rich compounds, the *N*-methyl pyrrole (NMP) was added into the DM solution of β -CD-tetrazine **94**. Figure 32 demonstrates clearly that the addition of NMP influences the electrochemical response of the tetrazines on the β -CD ring. The reduction potential peaks shifted gradually to the positive range with the increasing amount of NMP,

while the oxidation ones also shifted gradually to the positive range. These phenomena indicate that an interaction takes place between **94** and NMP. The nature of this interaction is not easy to understand with these preliminary results.

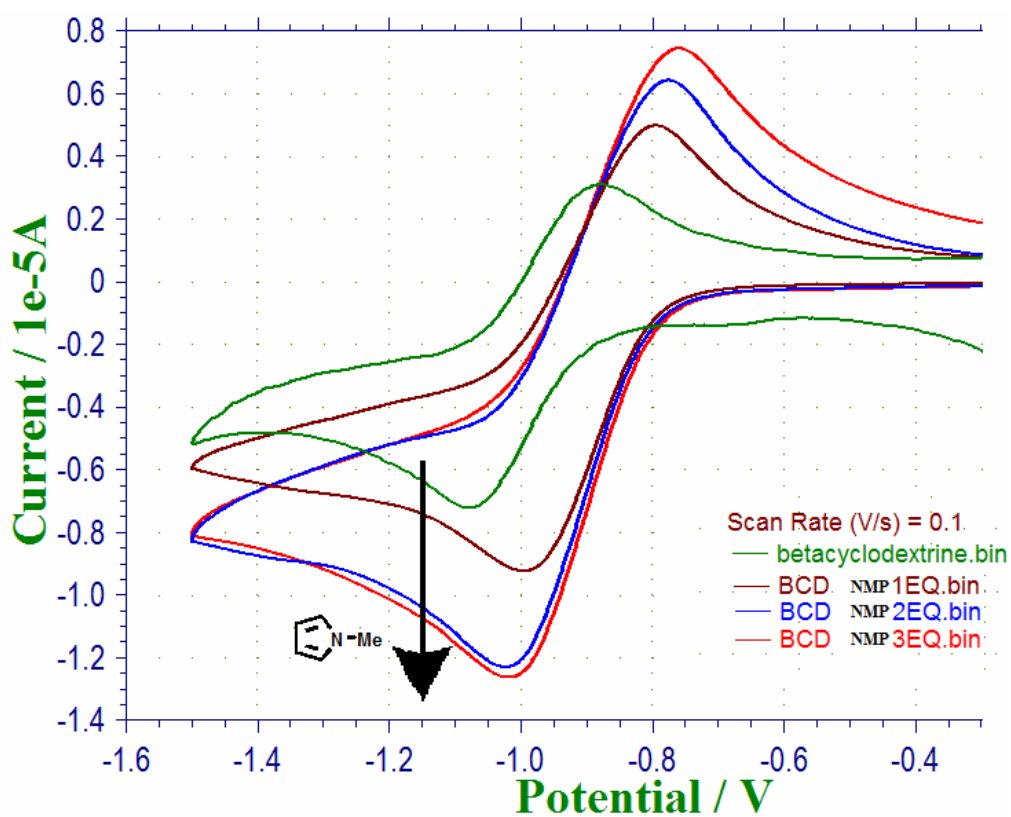


Figure 32. Titration of **94** by NMP in DM. Addition of NMP: 1eq., 2eq., 3eq. Scan rate: 100 mV.s⁻¹. Working electrode: Glass carbon.

5.6 α -CD-tetrazine (**95**)

5.6.1 Absorption and fluorescence studies of **95**

The absorption spectrum of **95** is identical to **94** (Figure 33). The maxima for each absorption band are almost the same, with differences of 1-2 nms (Table 13). The strong absorption band around 328 nm corresponds to the π - π^* allowed transition of Cl-Tz-O, and the less intense band in the visible region (519 nm) corresponds to the n - π^* transition which is responsible for the red color. The fluorescence quantum yield of **95** in dichloromethane is in the same range as that of **94**, but slightly lower (0.10 for **95** to 0.12 for **94**).

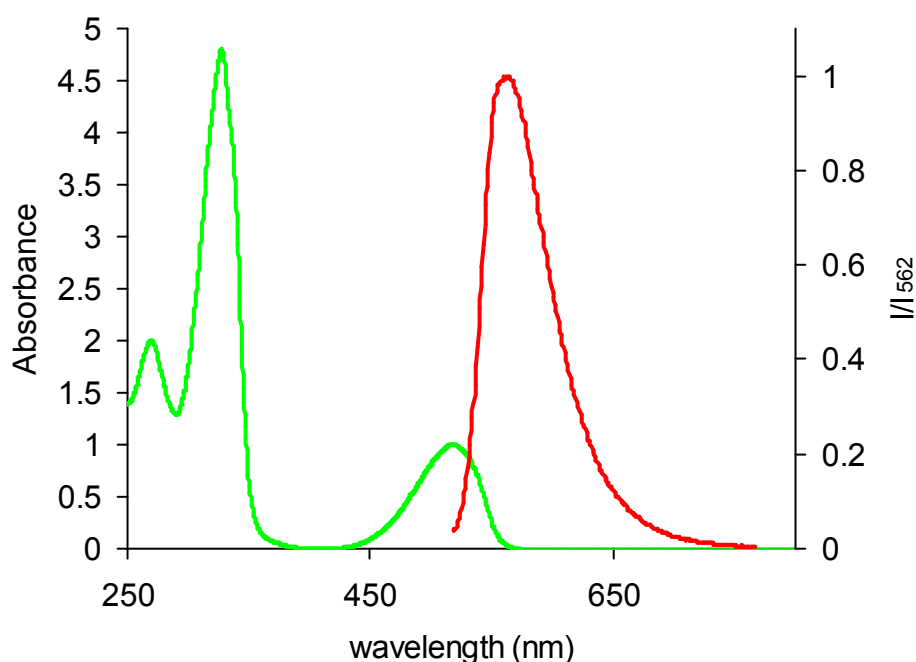


Figure 33. Absorption (—) and fluorescence (—) spectra of α -CD-tetrazine **95** in DM (C: 0.296 mM).

Table 13. Spectral data of **95** in DM.

Compound	λ_{\max}^{abs} (nm)	ϵ_{\max}^{abs} (L.mol ⁻¹ .cm ⁻¹)	λ_{\max}^{em} (nm)	Lifetime ^(a) (ns)	Φ_F
α CD-tetrazine (95)	519	3379			
	328	16760	562	50 ^(b)	0.100
	270	6708			

a) An average lifetime of 142.5 ns (biexponential) was found in MeOH. b) Biexponential decay.

5.6.2 Fluorescence quenching

Fluorescence quenching of **95** by TTF was carried out, both in methanol (Figure 34) and in DM (Figure 36). In both cases a linear relationship is found when plotting the Stern-Volmer equation (Figure 35, Figure 37). The k_{sv} is much larger in methanol than in DM in the presence of TTF as quencher, which indicates that the

quencher is more prone to enter into the lipophilic cavity of α -CD-tetrazine in polar environment, leading to a more efficient fluorescence quenching for **95**.

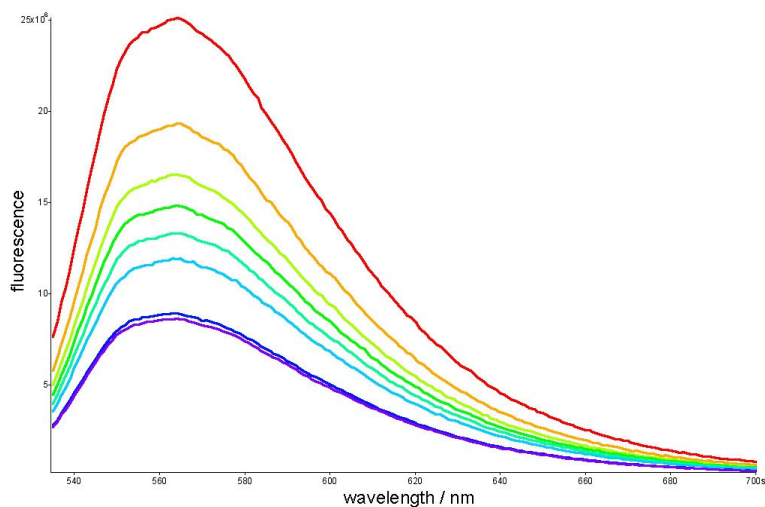


Figure 34. Fluorescence quenching of α -CD-tetrazine with TTF in methanol.

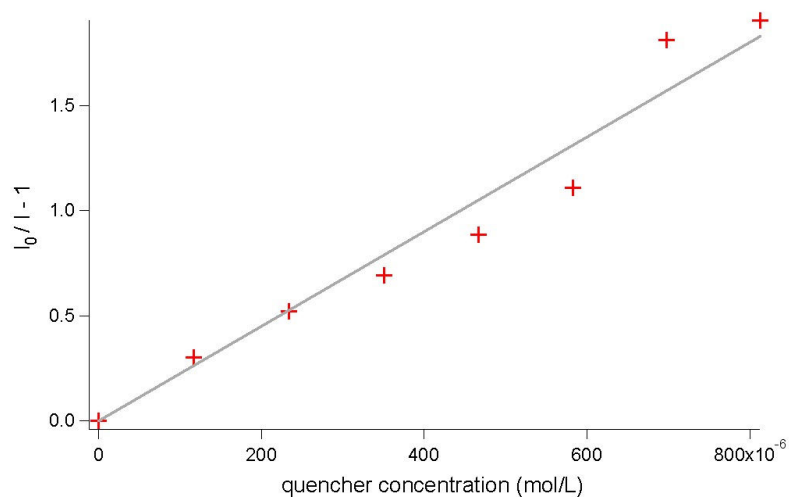


Figure 35. Stern-Volmer plot of α -CD-tetrazine with TTF in methanol. Stern-Volmer plot $k_{SV} = 2254 \pm 100$ ($R^2 = 0.98$)

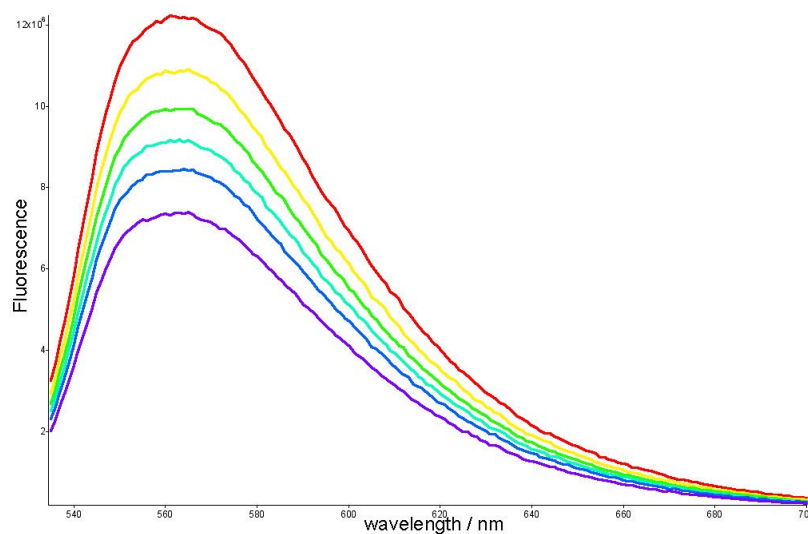


Figure 36. Fluorescence quenching of α -CD-tetrazine with TTF in dichloromethane.

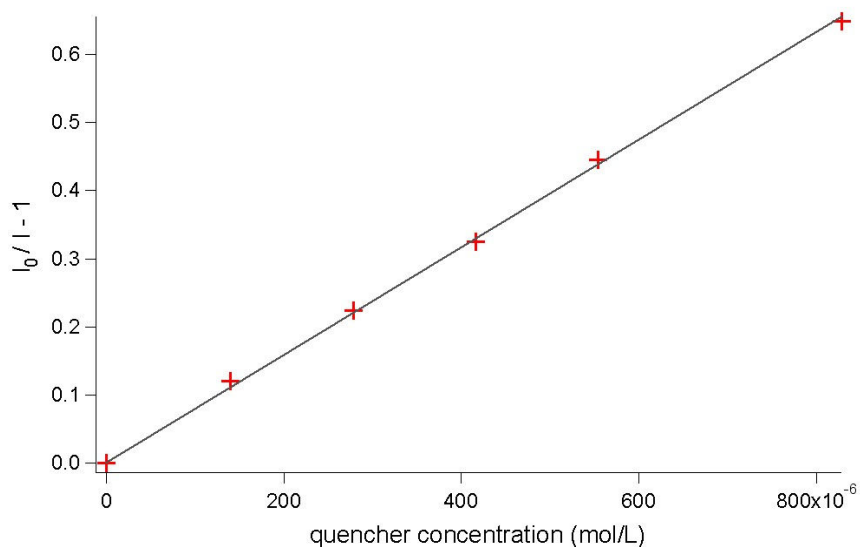


Figure 37. Stern-Volmer plot of α -CD-tetrazine with TTF in dichloromethane. Stern-Volmer plot $k_{SV} = 791 \pm 6$ ($R^2 = 0.999$), $k_q = 15.8 \times 10^9$.

5.6.3 Electrochemical study

The cyclic voltammetry was performed in dichloromethane using a 1 mm diameter Pt working electrode. Interestingly the α -CD-tetrazine shows only one fully reversible reductive peak in the range 0 to -1.8 V, indicating that the six tetrazines on the α -CD ring are identical, and are all reduced simultaneously at the same potential (Figure 38). This behavior is very different from that of its analogue β -CD-tetrazine. The standard reduction potential is -0.84 V, which is very close to the first reduction potential of the β -CD-tetrazine (-0.82 V), indicating that the proximity of the tetrazines does not influence their redox potential in this case.

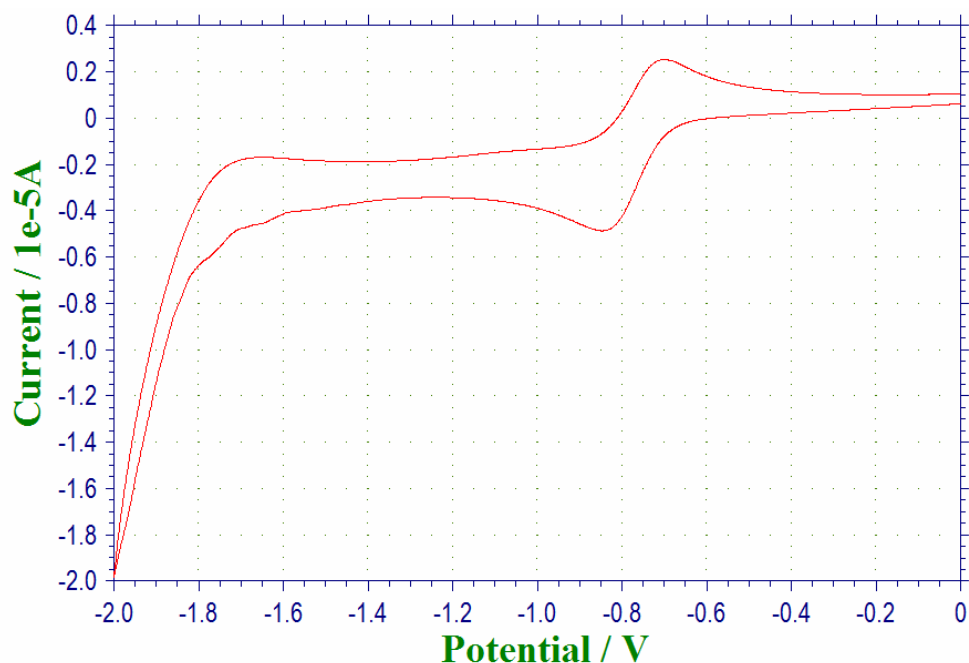


Figure 38. Cyclic voltammogram of α -CD-tetrazine **95** in DM. Scan rate: $100 \text{ mV} \cdot \text{s}^{-1}$. E_{pc} : -0.8392 V, E_{pa} : -0.7032 V.

Titration of α -CD-tetrazine **95** with NMP in DM was also carried out to investigate the possibility to form the complex. As shown in Figure 39, the cyclic voltammogram does not show any obvious shift of the reduction potential or current loss. The CV remains mostly reversible during the addition of NMP, even when the quantity of NMP is in large excess (5 eq.). This result indicates that, unlike the β -CD-tetrazine that forms a stable 1:1 complex with NMP, the α -CD-tetrazine could not form the complex with NMP, the reason of which might be the smaller cavity of **95** compared to the β -CD one's. Titration of **95** with toluene gave the same result (Figure 40).

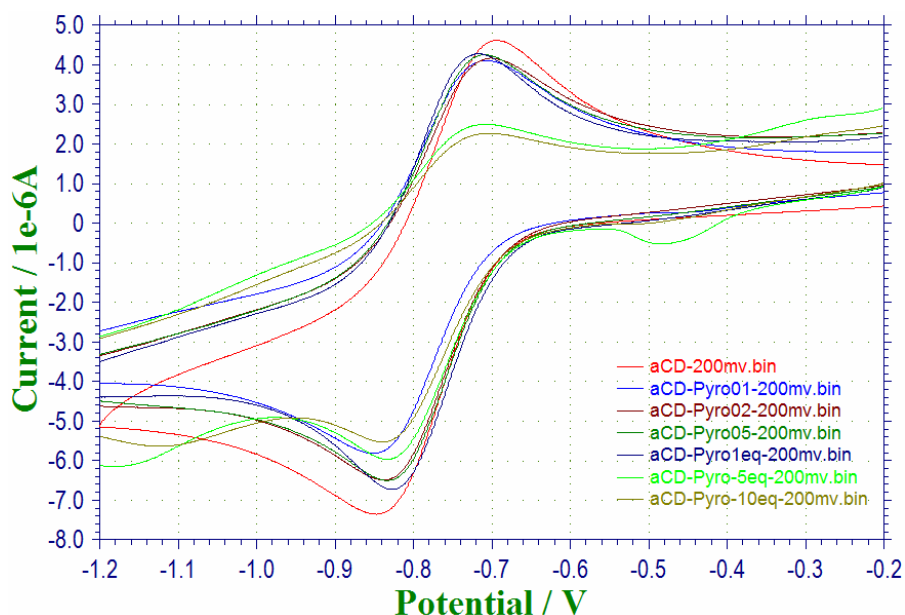


Figure 39. Titration of α -CD-tetrazine **95** by NMP in DM.

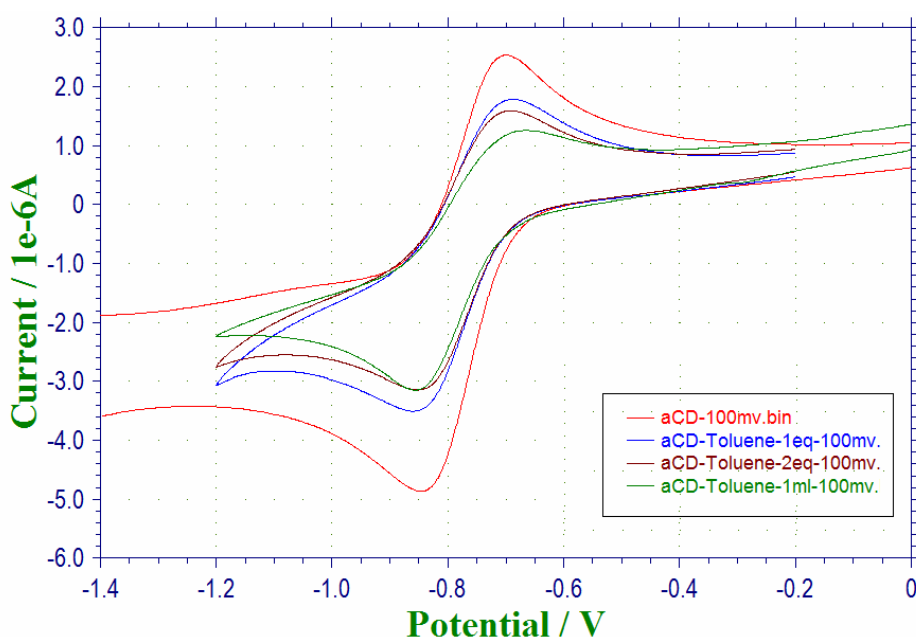


Figure 40. Titration of α -CD-tetrazine **95** by toluene in DM.

References

-
- 1 B. Valeur, *Molecular Fluorescence: Principles and Applications*, 1st edition, Wiley-VCH, Weinheim, **2001**.
 - 2 P. Audebert, S. Sadki, F. Miomandre, G. Clavier, M. C. Vernières, M. Saoud, P. Hapiot, *New J. Chem.* **2004**, 28, 387.
 - 3 P. Audebert, F. Miomandre, G. Clavier, M.-C. Vernières, R. Renault-Méallet, S. Badré, *Chem. Eur. J.* **2005**, 11, 5667.
 - 4 D. Garreau, J. M. Savéant, *J. Electroanal. Chem.* **1975**, 50, 1.
 - 5 Gaussian 03, Revision C.02, M. J. Frisch, G. W. Trucks, H. B. Schlegel, G. E. Scuseria, M. A. Robb, J. R. Cheeseman, J. A. Montgomery, Jr., T. Vreven, K. N. Kudin, J. C. Burant, J. M. Millam, S. S. Iyengar, J. Tomasi, V. Barone, B. Mennucci, M. Cossi, G. Scalmani, N. Rega, G. A. Petersson, H. Nakatsuji, M. Hada, M. Ehara, K. Toyota, R. Fukuda, J. Hasegawa, M. Ishida, T. Nakajima, Y. Honda, O. Kitao, H. Nakai, M. Klene, X. Li, J. E. Knox, H. P. Hratchian, J. B. Cross, C. Adamo, J. Jaramillo, R. Gomperts, R. E. Stratmann, O. Yazyev, A. J. Austin, R. Cammi, C. Pomelli, J. W. Ochterski, P. Y. Ayala, K. Morokuma, G. A. Voth, P. Salvador, J. J. Dannenberg, V. G. Zakrzewski, S. Dapprich, A. D. Daniels, M. C. Strain, O. Farkas, D. K. Malick, A. D. Rabuck, K. Raghavachari, J. B. Foresman, J. V. Ortiz, Q. Cui, A. G. Baboul, S. Clifford, J. Cioslowski, B. B. Stefanov, G. Liu, A. Liashenko, P. Piskorz, I. Komaromi, R. L. Martin, D. J. Fox, T. Keith, M. A. Al-Laham, C. Y. Peng, A. Nanayakkara, M. Challacombe, P. M. W. Gill, B. Johnson, W. Chen, M. W. Wong, C. Gonzalez, and J. A. Pople, Gaussian, Inc., Wallingford CT, 2004.



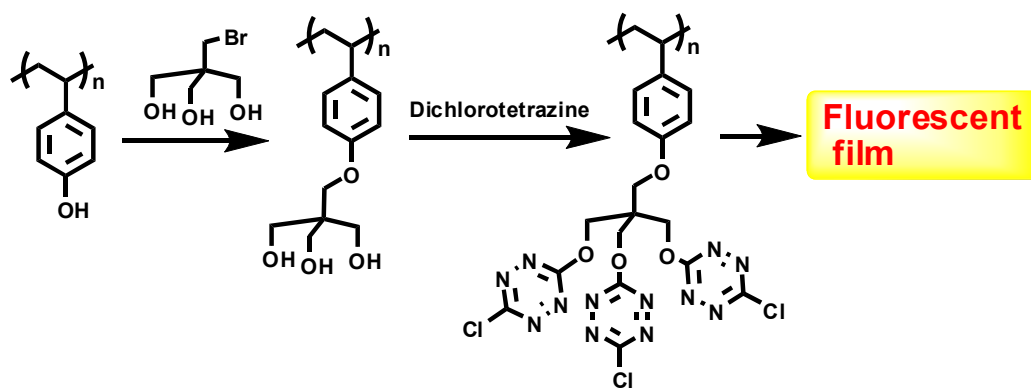
General conclusion and perspectives:

A series of *s*-tetrazine derivatives towards molecular sensors for anions and electron-rich compounds were designed, using tetrazine moieties as both binding units and sensing units, including tweezer-tetrazines, tripod-tetrazines, cyclophane-tetrazines, and calycular tetrazines. Among them the attempts using 1,8-dihydroxynaphthalene, ferrocenedimethanol and phenyl diaziridines as rigid tweezer frames all failed. However, a tripod-tetrazine (**86**) was obtained successfully after the improvement of reaction conditions of dichloro-*s*-tetrazine (**23**) with polyols by a careful scanning of the bases employed. Attempts to synthesize cyclophane **92** failed because of the difficulty to introduce terminal thiols onto the tetrazine derivatives, and other attempts to obtain the cyclophane-tetrazines through RMC or McMurry reactions were also tried and failed. However two cyclophanes, **90** and **93**, were finally obtained, and the single crystal structure of **93** was also obtained. β -cyclodextrin and α -cyclodextrin were used to construct the calycular tetrazine derivatives (**94**, **95**), both of which were obtained in good yield under the optimized condition for S_NAr reactions of dichloro-*s*-tetrazine (**23**) with polyols.

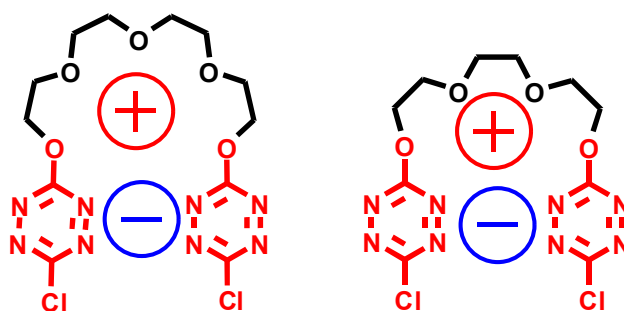
Fluorescence studies show that the fluorescence of **86**, **90**, **94** and **95** can be efficiently quenched by electron-rich compounds such as TPA, tris(4-bromophenyl)amine, pyrrole, TTF and 1,3,5-trimethoxybenzene. Electrochemical studies also indicate the interactions between these tetrazine derivatives and electron-rich compounds. The fluorescence quenching mechanisms were also investigated in some cases, and a dynamic quenching was found in the case of **86** with TTF. Moreover, a linear relationship between k_q and E_{ox}^0 is found for **86** in presence of different electron-rich quenchers, confirming that the quenching is due to an electron transfer from the aromatic donor to the accepting tetrazine in its excited state. Calculations on molecular orbitals were also carried out to investigate the relationship between molecular structures and fluorescence properties, and the weak fluorescence of the two cyclophane-tetrazines can be explained by their HOMO-LUMO characters and positions. Electrochemical studies of **86**, **90**, **94** and **95** were also performed and the results show that the electrochemical responses are sensitive to the addition of electron-rich compounds, indicating the interactions between them.

At the present time, a more detailed electrochemical investigation for the interaction between these new tetrazine derivatives and electron-rich molecules and anions is still going on, and an in-depth investigation for the complexation using NMR techniques is underway.

At the same time, the methodology for tetrazine reactions developed in this thesis is being applied to the synthesis of a fluorescent polymer:



Furthermore, a series of new tetrazine derivatives containing a polyol chain can be designed based on the method developed. The polyol frame is expected to be able to catch a cation, which can then bind an anion together with the tetrazines attached on each side. In this way the interactions with anions are expected to be largely enhanced, and also able to be adjusted by the choice of cations. The synthesis of the two molecules below is already finished and the electrochemical and fluorescence studies are on the plan.



Further developments will include grafting of tetrazines on metallic and silica nanoparticles, attachment to photochromic compounds or two photons absorbent...

Chapter 6 Experimental Section

General procedures

Synthesis

All chemicals were purchased from Aldrich or Acros and were used as received. All solvents for synthesis were synthetic grade. Anhydrous solvents were freshly distilled before use according to published procedures¹. All column chromatographies (CC) were performed on silica gel 60 (0.040-0.063 mm), silica gel SDS (Société de Documentation et Synthèse, Peypin, Bouches du Rhône). Analytical thin layer chromatographies (TLC) were performed on silica gel 60F254 (60/15µm) on aluminum plates (SDS), and detected by UV (254 nm). The deuterated solvents were purchased from SDS. NMR spectra were recorded on a Bruker 300 spectrometer. Chemical shifts are given in ppm related to the protonated solvent as internal reference (¹H: CHCl₃ in CDCl₃, 7.26 ppm, CHD₂SOCD₃ in CD₃SOCD₃, 2.49 ppm; ¹³C: ¹³CDCl₃ in CDCl₃, 77.14 ppm, ¹³CD₃SOCD₃ in CD₃SOCD₃, 39.6 ppm); coupling constants (J) in Hz. Mass spectrometry (chemical ionization with NH₃) was performed on a MS Engin 5989B mass spectrometer in the laboratory of the Institut Lavoisier de Versailles (UMR 8180), Université de Versailles Saint-Quentin-en-Yvelines. Single crystal X-ray diffraction was done by Jérôme Marot at the Institut Lavoisier de Versailles (UMR 8180), Université de Versailles Saint-Quentin-en-Yvelines.

Fluorescence

All solvents were of spectroscopic grade.

Steady-state spectroscopy

A U.V.-vis. Varian CARY 500 spectrophotometer was used. Excitation and emission spectra were measured on a SPEX Fluorolog-3 (Jobin-Yvon). A right-angle configuration was used. Optical density of the samples was checked to be less than 0.1 to avoid reabsorption artefacts.

Time-resolved spectroscopy

The fluorescence decay curves were obtained with a time-correlated single-photon-counting method using a titanium-sapphire laser (82 MHz, repetition rate lowered to 4 MHz thanks to a pulse-peaker, 1 ps pulse width, a doubling crystals is used to reach 495 nm excitation) pumped by an argon ion laser². The Levenberg-Marquardt algorithm was used for non-linear least square fit³. In order to estimate the goodness of the fit, the weighted residuals were calculated⁴. In the case of single photon counting, they are defined as the residuals, i.e.

1 W. L. E. Armarego, C. L. L. Chai, *Purification of laboratory chemicals, 5th edition*, Butterworth-Heinemann, an imprint of Elsevier Science, **2003**.

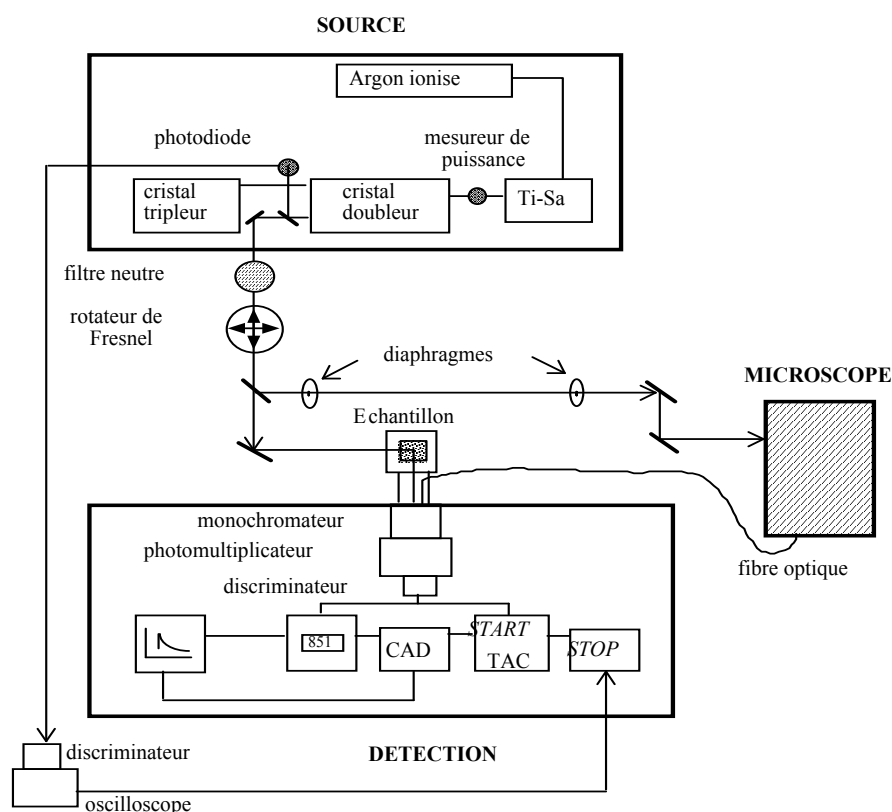
2 L. Schouffet, P. Denjean, R. B. Pansu, *J. Fluoresc.* **1997**, *7*, 155-165.

3 K. A. Levenberg, *Appl. Math II*, **1944**, *2*, 164.

4 *J. Fluoresc.* **2005**, *15*, 377-413.

the difference between the measured value and the fit, divided by the square root of the fit. χ^2 is equal to the variance of the weighted residuals. A fit was said good for χ^2 values between 0.8 and 1.2.

Apparatus for fluorescence experiments:

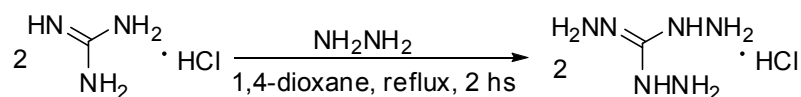


Electrochemistry

Electrochemical studies were performed using dichloromethane (SDS, anhydrous for analysis) as a solvent, with *n*-tetrabutylammonium perchlorate (Fluka, puriss.) as a supporting electrolyte. The substrate concentration was ca. 1 mM (accurate values are given in the figure caption). A 1 mm diameter Pt electrode was used as the working electrode, along with a Ag/Ag⁺ (10⁻² M) reference electrode and a Pt wire counter electrode. The cell was connected to a PAR 272 potential state monitored by a PC computer. The reference electrode was checked vs. ferrocene as recommended by IUPAC. In our case, E⁰(Fc⁺/Fc) = 0.046 V. All solutions were deaerated by argon bubbling prior to each experiment.

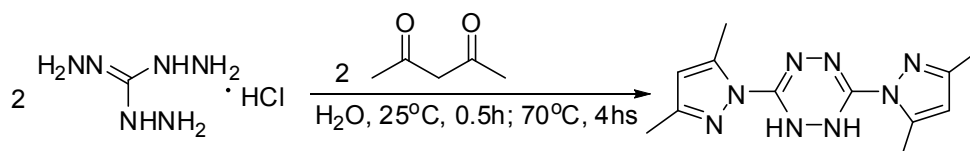
6.1 Preparation of 3,6-dichloro-1,2,4,5-tetrazine.

6.1.1 Preparation of triaminoguanidine monohydrochloride.



To a slurry of guanidine hydrochloride (26.1 g, 0.267 mol) in 150 mL of dioxane was added hydrazine monohydrate (45 mL, 0.91 mol) with stirring. The mixture was heated to reflux for 2 hours, then cooled to r. t.. The solids were collected by filtration, washed with dioxane and dried at 70°C overnight to give pure triaminoguanidine monohydrochloride (35.6 g, 95%).

6.1.2 Preparation of 3,6-bis(3,5-dimethylpyrazol-1-yl)-1,2-dihydro-1,2,4,5-tetrazine (**16**).



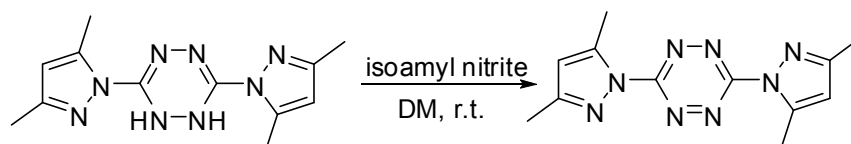
To a solution of triaminoguanidine monohydrochloride (35.6 g, 0.253 mol) in 200 mL of water was added 2,4-pentanedione (52.5 mL, 0.506 mol, 2 eq.) dropwise with stirring at r. t.. After the addition was complete the mixture was stirred at r. t. for 0.5 hour and at 70°C for 4 hours, during which time a yellow solid precipitated from the solution. The solids were filtered from the cooled solution, washed with water, and dried in vacuo over P₂O₅ to give dihydro-tetrazine **16** (27.5 g, 79.9%).

¹H NMR (300MHz, CDCl₃) δ 8.06(s, 2H), 5.97(s, 2H), 2.49(s, 6H), 2.22(s, 6H)

¹³C NMR (75MHz, CDCl₃) δ 150.11, 145.92, 142.45, 110.01, 13.95, 13.62

6.1.3 Preparation of 3,6-bis(3,5-dimethylpyrazol-1-yl)-1,2,4,5-tetrazine (**17**).

Method 1. Using isoamyl nitrite

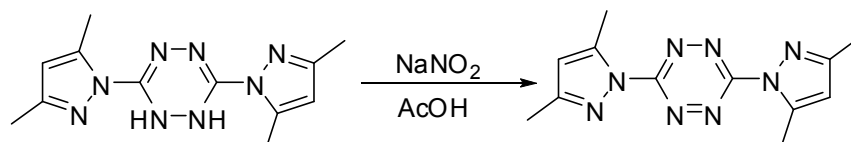


Isoamyl nitrite (36 mL, 2.6 eq.) was added by syringe into a solution of 3,6-bis(3,5-dimethylpyrazol-1-yl)-1,2-dihydro-1,2,4,5-tetrazine (27.5 g, 0.101 mol) in 290 mL of DM at r. t. while stirring. The mixture was stirred for 1 hour, then bubbled with N₂ to expel the volatiles. The solvents and other volatiles were removed by evaporation to give tetrazine **17** as a red solid (26.9 g, 99%).

¹H NMR (300MHz, CDCl₃) δ 6.19 (s, 1H), 2.71 (s, 3H), 2.39 (s, 3H)

¹³C NMR (75MHz, CDCl₃) δ 159.22, 154.39, 143.69, 111.81, 14.58, 13.78

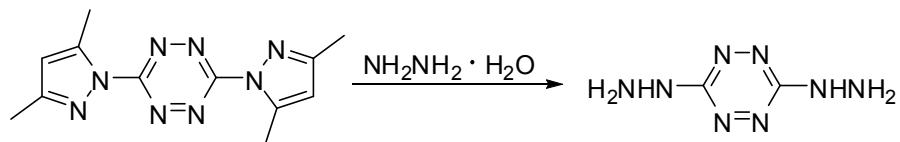
Method 2. Using NaNO₂ and AcOH



In a 1L 2necked round bottom flask, prepare a solution of sodium nitrite (26.2g, 0.38mol) in 588mL of water and add 60mL of dichloromethane. Lower the temperature at 0°C and add 3,6-bis(3,5-dimethylpyrazol-1-yl)-1,2-dihydro-s-tetrazine (37g, 0.136 mole). Add dropwise acetic acid (18.67mL, 0.326 mol). After gas evolution stopped, separate the

organic layer and extract the aqueous layer with dichloromethane (3 x 100mL). The organic layers are reunited, washed to neutrality with a 5% aqueous solution of potassium carbonate, dried over calcium chloride and filtered. The product **17** is obtained by evaporation of the solvent under reduced pressure.

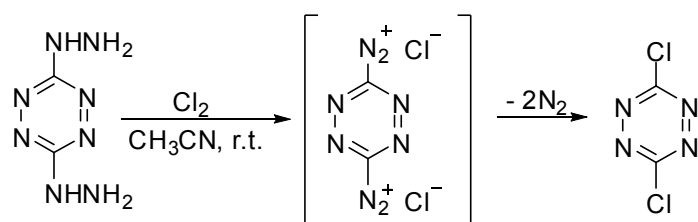
6.1.4 Preparation of 3,6-dihydrazino-1,2,4,5-tetrazine (**19**).



Hydrazine monohydrate (5.54 mL, 0.112 mol) was added slowly by syringe into a solution of 3,6-bis(3,5-dimethylpyrazol-1-yl)-1,2,4,5-tetrazine (15.2 g, 0.056 mol) in 100 mL of acetonitrile while stirring. The mixture was refluxed for 0.5 hour, then cooled to room temperature. The solids were filtered and washed with a small amount of acetonitrile. The product **19** is unstable (explosive) and should not be dried fully. Due to its insolubility, it is not characterized and used as such in the next step.

6.1.5 Preparation of 3,6-dichloro-1,2,4,5-tetrazine (**23**).

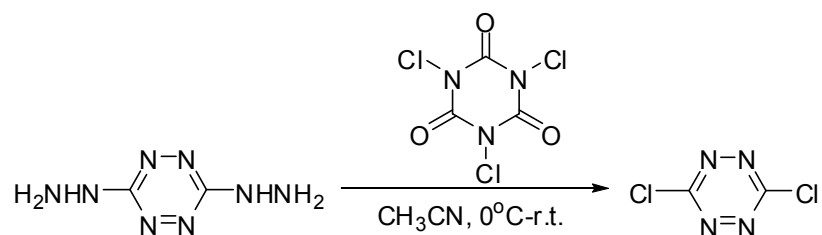
Method 1. Using chlorine gas



Into a suspension of freshly prepared 3,6-dihydrazino-1,2,4,5-tetrazine (**19**) (5.2 g, 0.037 mol) in 40 mL of acetonitrile cooled with an ice bath was bubbled chlorine gas under a strong agitation. The mixture became homogeneous after 10 min, and the chlorine gas was subsequently removed by bubbling N_2 into the solution. After evaporation of the solvent the 3,6-dichloro-1,2,4,5-tetrazine was obtained as a bright red solid which can be sublimated (5.0 g, 90%). The product obtained is usually pure enough for most synthetic purpose and a short column chromatography (silica, DM) can be carried out for further purification.

^{13}C NMR (75MHz, CDCl_3) δ 168.2

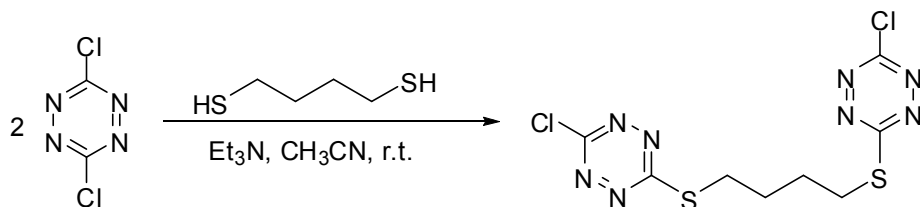
Method 2. Using trichloroisocyanuric acid



To a slurry of 3,6-di(hydrazino)-1,2,4,5-tetrazine (12.5 g, 0.088 mol) in acetonitrile (350 mL) at 0°C was added dropwise over 30 minutes a solution of trichloroisocyanuric acid (40.8 g, 0.18 mol) in acetonitrile (250 mL). After the addition was finished the reaction vessel

was allowed to warm to room temperature and stirred for 20 minutes. The white insoluble precipitate was removed by filtration and the volatiles removed from the resulting orange solution in vacuo to give crude 3,6-dichloro-1,2,4,5-tetrazine as an orange solid. Same purification as previous gave pure **23** (6.785 g, 51%) as an orange powder.

6.2 Preparation of 1,4-bis(6-chloro-1,2,4,5-tetrazin-3-ylthio)butane (**98**).

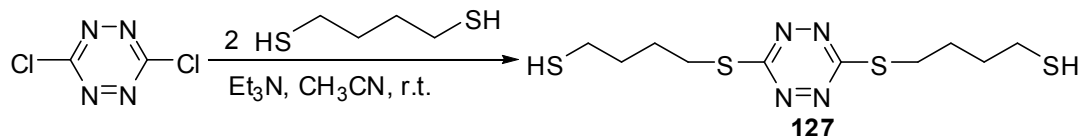


1,4-dithiol (0.4 g, 3.3 mmol) and triethylamine (0.93 mL, 6.6 mmol) were mixed in 30 mL acetonitrile in a dropping funnel and were added slowly into the solution of dichloro-*s*-tetrazine (1.0 g, 6.6 mmol) in 10 mL of acetonitrile at room temperature. After the addition the mixture was stirred for another 2 hours until TLC indicated the reaction was over (1:5 EA/PE). The solids were filtered, washed with ether, and the filtrate was evaporated. After a column chromatography (silica, 1:6 ethyl acetate/ petroleum ether) 0.18 g of product **98** was obtained as a red solid (15%).

$^1\text{H NMR}$ (300MHz, CDCl_3) δ 3.37(m, 4H), 2.02(m, 4H)

$^{13}\text{C NMR}$ (75MHz, CDCl_3) δ 175.67, 165.64, 30.02, 27.52

6.3 Preparation of 3,6-di(1,4-dithiol-1-)-1,2,4,5-tetrazine (**127**)

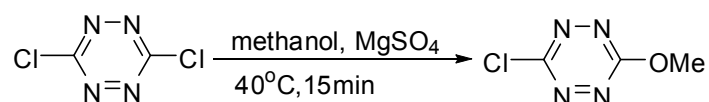


To a solution of 1,4-dithiol (1.6 mL, 13.3 mmol, 2 eq.) and triethylamine (1.9 mL, 13.3 mmol, 2 eq.) in 10 mL of acetonitrile was added slowly the solution of dichloro-*s*-tetrazine (1.0 g, 6.6 mmol) in 30 mL of acetonitrile at room temperature. After the addition the mixture was stirred for another 2 hours, then filtered. The filtrate was evaporated and the residue passed through a column chromatography (silica, 1:3 ethyl acetate/ petroleum ether) to give 0.8 g of compound **127** as a red powder (38%).

$^1\text{H NMR}$ (300MHz, CDCl_3) δ 6.72(s, 2H), 2.88(t, 4H, $J=6.9\text{Hz}$), 2.50-2.47(m, 4H), 1.77-1.62(m, 8H)

$^{13}\text{C NMR}$ (75MHz, CDCl_3) δ 149.79, 32.66, 31.02, 27.79, 23.91

6.4 Preparation of 3-chloro-6-methoxy-1,2,4,5-tetrazine (**76**)



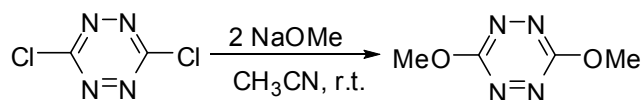
To a solution of dichloro-*s*-tetrazine (1.0 g, 6.62 mmol) in 100 mL of methanol was added 0.5 g MgSO_4 . The mixture was stirred and warmed slowly to 40 °C. After 15 min TLC indicated the reaction was finished (1:8 ethyl acetate/petroleum ether). The solids were filtered and washed twice with DM, and the filtrate was evaporated. After a short column

chromatography (silica, 1:8 ethyl acetate/ petroleum ether) a red fluorescent solid was obtained which is easy to sublimate (0.5 g, 50%).

^1H NMR (300MHz, CDCl_3) δ 4.33(s, 3H)

^{13}C NMR (75MHz, CDCl_3) δ 167.06, 164.61, 57.5

6.5 Preparation of 3,6-dimethoxy-1,2,4,5-tetrazine (52)

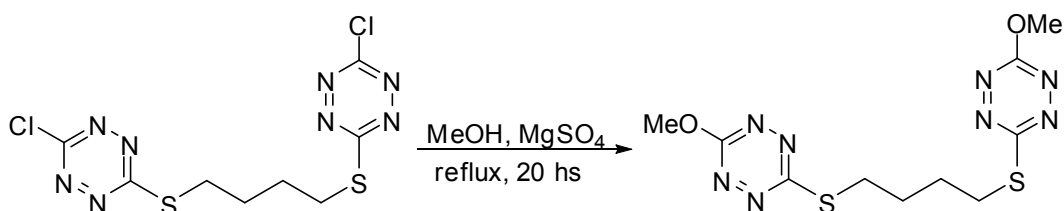


To a solution of dichloro-*s*-tetrazine (0.31 g, 2 mmol) in 4 mL of anhydrous acetonitrile was added dropwise the solution of NaOMe in methanol (0.1 g Na dissolved in 5 mL of anhydrous methanol) and the mixture was stirred at room temperature for 2 hours, after which 3 drops of water was added to quench the reaction. After a short column chromatography (silica, 1:10 ethyl acetate/ petroleum ether) 0.03 g pink solid was obtained which is very fluorescent and easy to sublimate (10%).

^1H NMR (300MHz, CDCl_3) δ 4.23(s, 3H)

^{13}C NMR (75MHz, CDCl_3) δ 166.55, 56.82

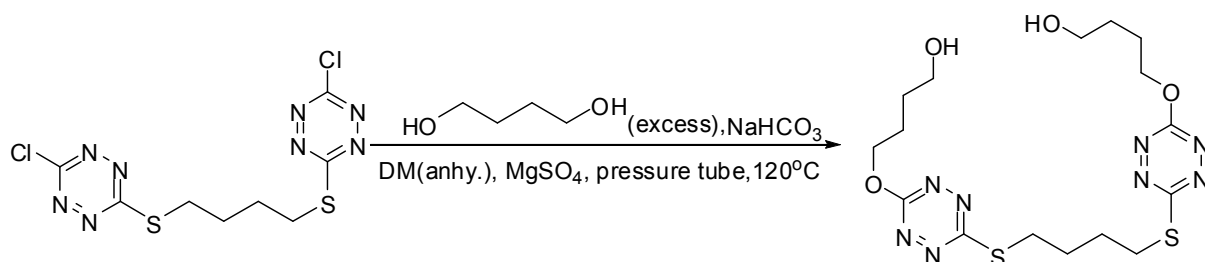
6.6 Preparation of 1,4-bis(6-methoxy-1,2,4,5-tetrazin-3-ylthio)butane (81)



1,4-bis(6-chloro-1,2,4,5-tetrazin-3-ylthio)butane (94 mg, 0.27 mmol) and MgSO_4 (0.5 g) were added into 50 mL of methanol and the mixture was refluxed under Ar atmosphere for 20 hours. After filtration of the solids the filtrate was evaporated and the residue was passed through a column chromatography (silica, 3:10 ethyl acetate/ petroleum ether). After evaporation of the solvents 46mg of red solid was obtained which is not fluorescent on TLC (50%).

^1H NMR (300MHz, CDCl_3) δ 4.24(s, 6H), 3.35-3.30(m, 4H), 2.03-1.96(4H)

6.7 Preparation of 4,4'-(6,6'-(butane-1,4-diylbis(sulfaneydiyl))bis(1,2,4,5-tetrazine-6,3-diyl))bis(oxy)dibutan-1-ol (99)



To a 20-mL pressure tube were added 143 mg (0.41mmol) 1,4-bis(6-chloro-1,2,4,5-tetrazin-3-ylthio)butane, 0.365 mL (10 eq.) of 1,4-butanediol, 34 mg (0.4 mmol) NaHCO_3 , 0.3

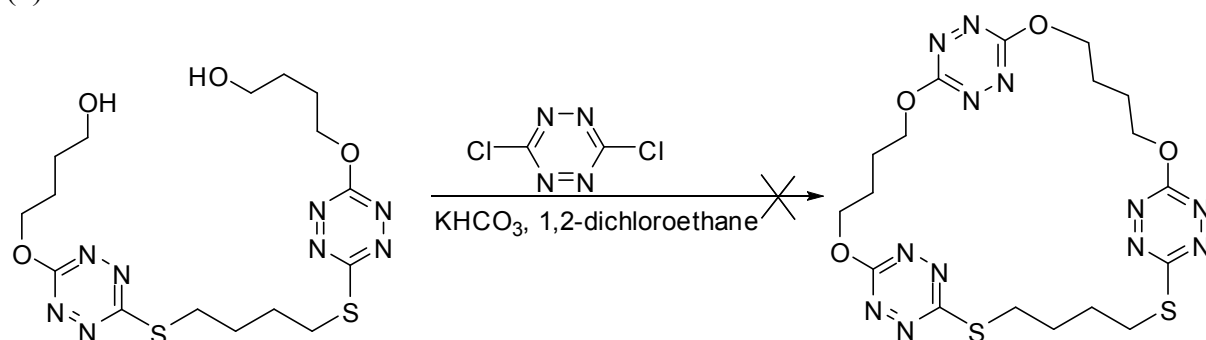
g MgSO₄, and 6 mL of dichloromethane. The mixture was stirred and heated to 120 °C for 2 hours, then cooled to room temperature. After a column chromatography (silica, ethyl acetate) 13 mg di-substituted product was obtained as a red solid (7%).

¹H NMR (300MHz, CDCl₃) δ 4.63(t, 4H, J=6.3Hz), 3.76(t, 4H, J=6.3Hz), 3.33(m, 4H), 2.10-1.98(m, 8H), 1.83-1.60(m, 4H), 1.60(br., 2H)

¹³C NMR (75MHz, CDCl₃) δ 171.16, 165.92, 69.53, 62.21, 30.11, 28.82, 27.90, 25.11

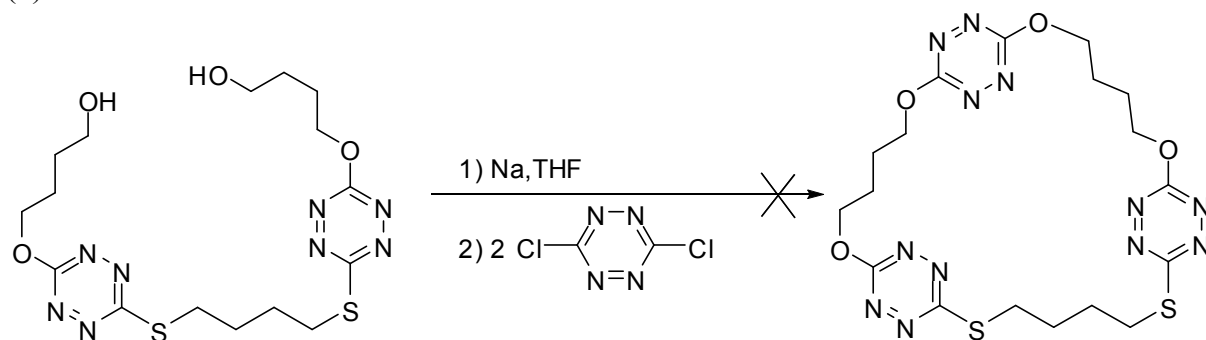
6.8 Attempts to synthesize cyclophane-tetrazine **90**

(1)



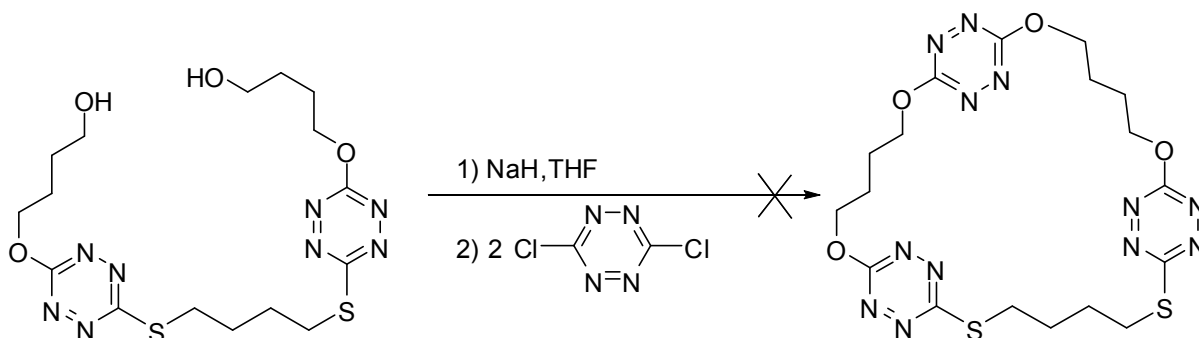
To a 500-mL 3-necked round bottom flask equipped with a N₂ inlet, a magnetic stirring bar, a condenser and an oil bath, 50 mg tetrazine-diol **99** (0.1 mmol) and 200 mL of dichloroethane were added, and the solution was heated to reflux. The solution of dichloro-*s*-tetrazine (17 mg, 0.1 mmol) in 30 mL of dichloroethane was added dropwise. The mixture was refluxed for 5 hours, and TLC indicated no new compound was formed, while most of the dichloro-*s*-tetrazines were consumed, and most of the tetrazine-diol remained.

(2)



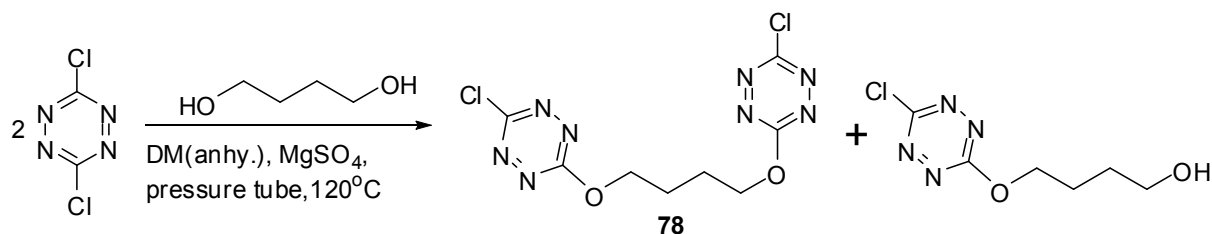
20 mg tetrazine-diol **99** (0.04 mmol) was dissolved in 20 mL of anhydrous THF under Ar atmosphere. Na (2 mg, 0.08 mmol) was added and the mixture was refluxed for 0.5 hour, during which time a red solid was formed and precipitated from THF. A solution of dichloro-*s*-tetrazine (7 mg, 1 eq.) in 20 mL of THF was added slowly into the mixture while stirring. After usual work-up procedure TLC (ethyl acetate) indicated most of the tetrazine-diol remained.

(3)



4 mg NaH (60% in oil, 2 eq.) was added into a solution of 22 mg tetrazine-diol **99** (0.044 mmol) in 50 mL of THF at room temperature. The mixture was stirred for 0.5 hour, and a solution of dichloro-*s*-tetrazine (7 mg, 1 eq.) in 20 mL of THF was added dropwise. After stirring overnight TLC indicated no new compounds, while the tetrazine-diol remained and all dichloro-*s*-tetrazine decomposed.

6.9 Preparation of 1,4-bis(6-chloro-1,2,4,5-tetrazin-3-yloxy)butane (**78**)



Dichloro-*s*-tetrazine (1.10 g, 7.28 mmol), 1,4-butanediol (0.26 mL, 2.9 mmol), MgSO₄ (0.5 g), 10 mL of anhydrous dichloromethane and a magnetic stirring bar were added into a 20-mL pressure tube. The tube was sealed and heated to 120 °C for 2 hours, then cooled to room temperature. The solids were filtered out and washed with dichloromethane. The filtrates were combined and evaporated. After a short column chromatography (silica, DM→1:20 methanol/DM) 0.16 g disubstituted product **78** (17%) and 0.12 g monosubstituted product (20%) were obtained.

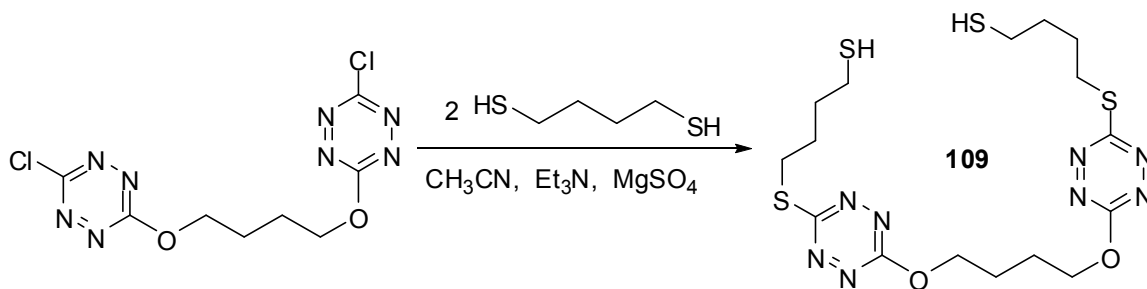
78: ¹H NMR (300MHz, CDCl₃) δ 3.75(t, 4H, J=5.88Hz, OCH₂), 1.79(t, 4H, J=6.31Hz, OCH₂CH₂)

¹³C NMR (75MHz, CDCl₃) δ 166.7(C of tetrazine), 164.3 (C of tetrazine), 70.9 (OCH₂), 28.7 (OCH₂CH₂)

MS (EI), *m/z*: 318 ([M]⁺, calc. 318)

Mono-substituted product: ¹H NMR (300MHz, CDCl₃) δ 4.67(t, 2H, J=6.2Hz, OCH₂), 3.71(t, 2H, J=6.3Hz, CH₂-OH), 2.26(br., 1H, OH), 2.05-2.00(m, 2H, OCH₂CH₂), 1.79-1.74(m, 2H, HOCH₂CH₂)

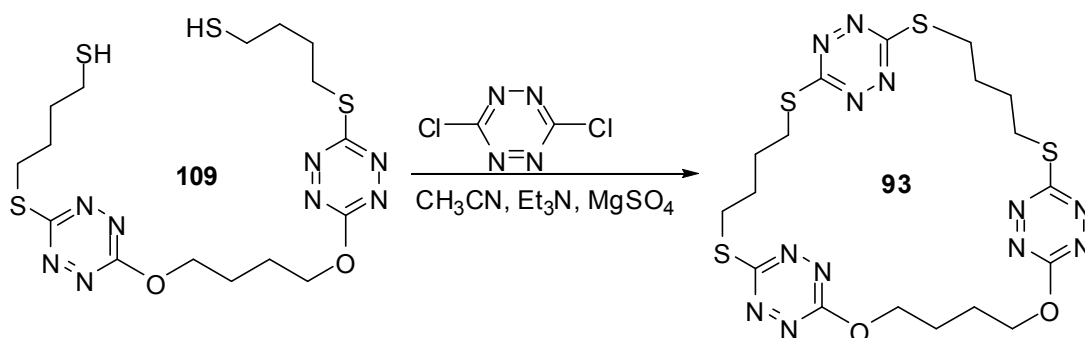
6.10 Preparation of 4,4'-(6,6'-(butane-1,4-diylbis(oxy))bis(1,2,4,5-tetrazine-6,3-diyl))bis(sulfaneydiyl)dibutane-1-thiol (**109**)



To a solution of 1,4-dithiol (0.33 mL, 6 eq.) and triethylamine (0.14 mL, 2 eq.) in 20 mL of anhydrous CH_3CN was added dropwise a solution of 0.15 g 1,4-bis(6-chloro-1,2,4,5-tetrazin-3-yloxy)butane (0.5 mmol) in 50 mL of acetonitrile. The addition was finished in 3 hours, after which time the solution was stirred for another 1 hour. After filtration of the solids the filtrate was evaporated and the residue was passed through a column chromatography (silica, 1:2 ethyl acetate/ petroleum ether) to give a red solid which is not fluorescent on TLC (0.1 g, 44%).

^1H NMR (300 MHz, CDCl_3) δ 4.70-4.65(m, 4H), 3.29(t, 4H, $J=7.2\text{Hz}$), 2.59(m, 4H), 2.19-2.17(m, 4H), 1.93-1.90(m, 4H), 1.82-1.78(m, 4H), 1.38(t, 2H, $J=8.1\text{Hz}$, SH)

6.11 Synthesis of cyclophane-tetrazine 93

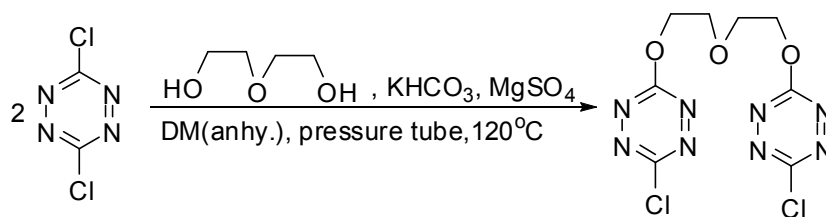


To a mixture of 100 mL of acetonitrile, 0.04 mL of triethylamine (2.5 eq.), and 0.3 g MgSO_4 , a solution of tetrazine-dithiol (0.1 g, 0.2 mmol) in 50 mL acetonitrile and a solution of dichloro-*s*-tetrazine (0.031 g, 0.2 mmol) in 50 mL of acetonitrile were added at the same speed through syringe in 2 hours. The mixture was stirred for another 1 hour, and the solids were filtered. The filtrate was evaporated and the residue was passed through a column chromatography (silica, 1:3 ethyl acetate/ petroleum ether) to give the cyclophane as a red solid which is not fluorescent on TLC plate (46 mg, 40%).

^1H NMR (300 MHz, CDCl_3) δ 4.72 (t, 4H, $J=3.3\text{Hz}$), 3.30-3.35 (m, 8H), 2.15-2.19 (m, 4H), 1.95-2.00 (m, 4H)

^{13}C NMR (75 MHz, CDCl_3) δ 172.41, 171.29, 165.84, 68.71, 30.14, 29.68, 28.26, 28.12, 24.85
MS, m/z : 607.2($[\text{M}+\text{K}]^+$), 591.2($[\text{M}+\text{Na}]^+$, base peak), 569.4($[\text{M}+1]^+$, calc. 569), 413.3, 381.4, 353.4, 301.2

6.12 Preparation of 6,6'-(2,2'-oxybis(ethane-2,1-diyl)bis(oxy))bis(3-chloro-1,2,4,5-tetrazine) (79)

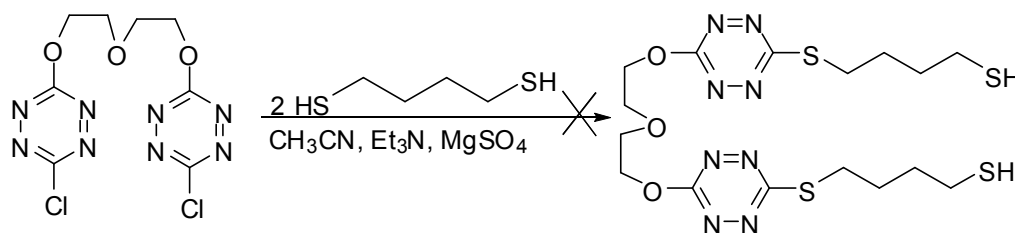


Dichloro-*s*-tetrazine (1.10 g, 7.28 mmol), di-ethyleneglycol (0.28 mL, 2.9 mmol), KHCO_3 (0.58 g, 5.8 mmol), MgSO_4 (0.5 g), 10 mL of anhydrous dichloromethane and a magnetic stirring bar were added into a 20-mL pressure tube. The tube was sealed and heated to 120 °C for 2 hours, then cooled to room temperature. The solids were filtered out and washed with dichloromethane. The filtrates were combined and evaporated. After a short column chromatography (silica, 1:1 ethyl acetate/ petroleum ether) a red fluorescent solid was obtained which was then recrystallized in cyclohexane (40 mg, 4%).

^1H NMR (300MHz, CDCl_3) δ 4.84-4.81(m, 4H), 4.08-4.05(m, 4H)

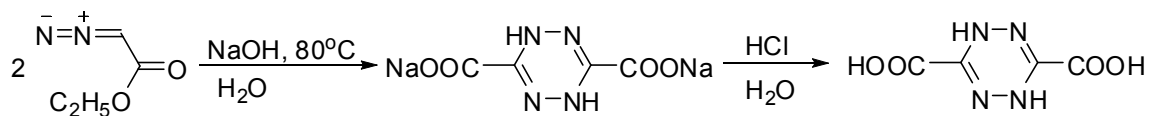
^{13}C NMR (75MHz, CDCl_3) δ 166.53, 164.46, 69.38, 68.76

6.13 Attempt to prepare 4,4'-(6,6'-(2,2'-oxybis(ethane-2,1-diyl)bis(oxy))bis(1,2,4,5-tetrazine-6,3-diyl))bis(sulfanediyl)dibutane-1-thiol



To a solution of 1,4-dithiol (0.33 mL, 6 eq.) and triethylamine (0.14 mL, 2 eq.) in 20mL of anhydrous CH_3CN was added dropwise a solution of 0.17 g 1,4-bis(6-chloro-1,2,4,5-tetrazin-3-yloxy)butane (0.5 mmol) in 50 mL of acetonitrile. The addition was finished in 3 hours, and the solution was stirred overnight, after which time the solution had turned from red to colorless, which indicated most of the tetrazine-containing compounds were decomposed.

6.14 Preparation of 1,4-dihydro-1,2,4,5-tetrazine-3,6-dicarboxylic acid (**103**)



Ethyl diazoacetate (4.04 mL, 35 mmol) was added by syringe to a NaOH solution (6.4 g in 10 mL of H_2O , 160 mmol) at 60~80°C in 15 min. The slurry was stirred for 10 min more and cooled to r. t., then poured into 40 mL of 95% ethanol. The liquid was decanted and solids were washed with 95% ethanol (5 × 30 mL), absolute ethanol (20 mL) and ether (20 mL). After drying in vacuo 3.7g of sodium 1,4-dihydro-1,2,4,5-tetrazine-3,6-dicarboxylate was obtained as a grey solid (99%).

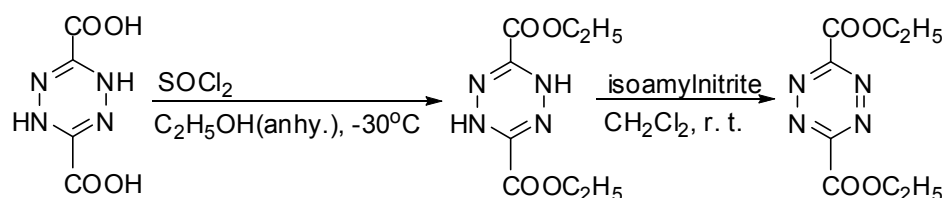
The sodium salt (3.7 g, 17.5 mmol) was dissolved in 10 mL of iced water and the mixture was cooled with an ice bath. 3.5 mL of concentrated HCl (35%, 39.4 mmol, 2 eq.) was added dropwise, and the solution was stirred for another 20 min after addition. The solids

were filtered and washed with ether (5×8 mL). After drying in vacuo 1.86 g of solids were obtained (62.5%).

^1H NMR (300MHz, DMSO- d_6) δ 8.85(s, 2H)

^{13}C NMR (75MHz, DMSO- d_6) δ 159.94, 139.49

6.15 Preparation of diethyl 1,2,4,5-tetrazine-3,6-dicarboxylate (**105**)



SOCl_2 (0.68 mL, 9 mmol) was added slowly by syringe into 20 mL of anhydrous ethanol in a 100-mL 2-necked round bottom flask at $-40^\circ\text{C} \sim -35^\circ\text{C}$ while stirring. Dihydro-tetrazine-dicarboxylic acid (0.194 g, 1.14 mmol) was added portionwise at -35°C , and the temperature was allowed to raise slowly to r. t.. After stirring at r. t. for 1 hour and at 40°C for 2 hours, the mixture was cooled again to -50°C , and the solids were filtered out. The filtrate was evaporated; the residue was put into water and extracted with DM (5×20 mL). The organic layers were combined and dried with MgSO_4 . After evaporation the diethyl 1,4-dihydro-1,2,4,5-tetrazine-3,6-dicarboxylate was obtained as a yellow powder (0.14 g, 55%).

^1H NMR (300MHz, CDCl_3) δ 7.48(s, 2H), 4.37(q, 4H, $J=7.0\text{Hz}$), 1.38(t, 6H, $J=7.0\text{Hz}$)

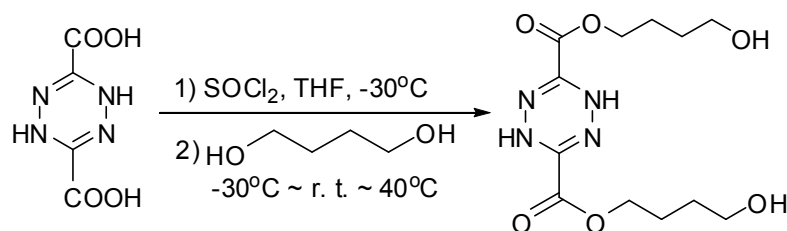
^{13}C NMR (75MHz, CDCl_3) δ 138.94, 123.65, 67.06, 29.80

Isoamyl nitrite (0.24 mL, 1.7 mmol, 3 eq.) was added slowly into the solution of diethyl 1,4-dihydro-1,2,4,5-tetrazine-3,6-dicarboxylate (130 mg, 0.58 mmol) in DM, and the mixture was stirred at r. t. for 2 hours, during which time the solution turned red. After evaporation of the solvent the residue was passed through a short column chromatography (silica, 1:20 methanol/ DM) to give diethyl 1,2,4,5-tetrazine-3,6-dicarboxylate as a red solid which is unstable on TLC plate (78 mg, 60%).

^1H NMR (300MHz, CDCl_3) δ 4.68(q, 4H, 7.4Hz), 1.53(t, 6H, 7.0Hz)

^{13}C NMR (75MHz, CDCl_3) δ 160.16, 159.45, 64.49, 14.22

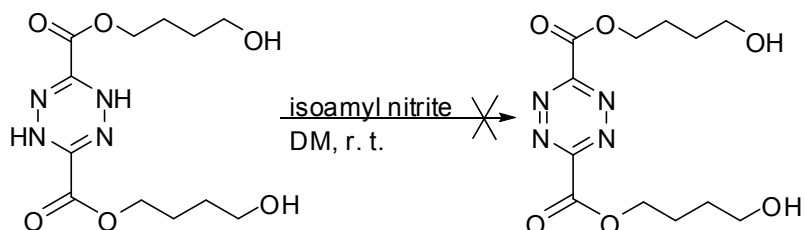
6.16 Preparation of bis(4-hydroxybutyl) 1,4-dihydro-1,2,4,5-tetrazine-3,6-dicarboxylate (**106**)



To a solution of 1,4-butanediol (6 mL, 67 mmol) in 7 mL of anhydrous THF was added SOCl_2 (0.3 mL, 4 mmol) slowly by syringe at -30°C while stirring. The dihydro-tetrazine-dicarboxylic acid (0.34 g, 2 mmol) was added portionwise and the temperature was allowed to rise to r. t., and then kept at r. t. for 1 hour and at 40°C for 2 hours. After evaporation of the solvent the residue was passed through a column chromatography (silica, 1:8 methanol/ DM) to give bis(4-hydroxybutyl) 1,4-dihydro-1,2,4,5-tetrazine-3,6-dicarboxylate as a brown solid (0.27 g, 43%).

^1H NMR (300MHz, CDCl_3) δ 7.62(s, 2H), 4.34(t, 4H, $J=6.6\text{Hz}$), 3.67(t, 4H, $J=6.6\text{Hz}$), 2.14(br., 2H), 1.88-1.79(m, 4H), 1.69-1.62(m, 4H)
 ^{13}C NMR (75MHz, CDCl_3) δ 158.71, 138.50, 67.20, 62.08, 29.00, 25.02

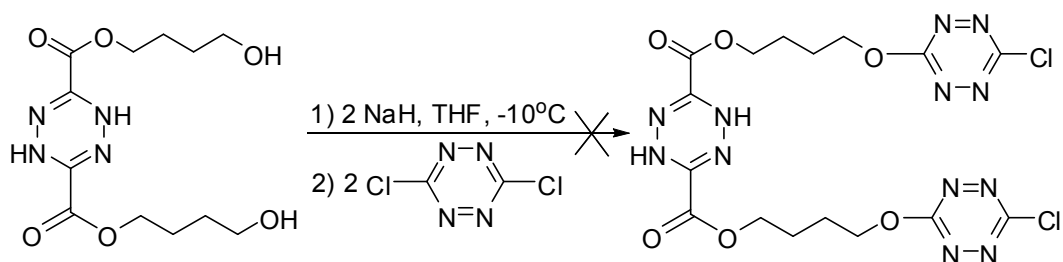
6.17 Attempt to synthesize bis(4-hydroxybutyl) 1,2,4,5-tetrazine-3,6-dicarboxylate (**107**)



Isoamyl nitrite (0.33 mL, 3 eq.) was injected slowly by syringe into a solution of bis(4-hydroxybutyl) 1,4-dihydro-1,2,4,5-tetrazine-3,6-dicarboxylate (0.25 g, 0.8 mmol) in 10 mL of DM. The mixture was stirred for 48 hours and TLC indicated lots of products, which were all decomposed on column when neutral Al_2O_3 was used for a column chromatography (neutral Al_2O_3 , 1:9 methanol/ DM).

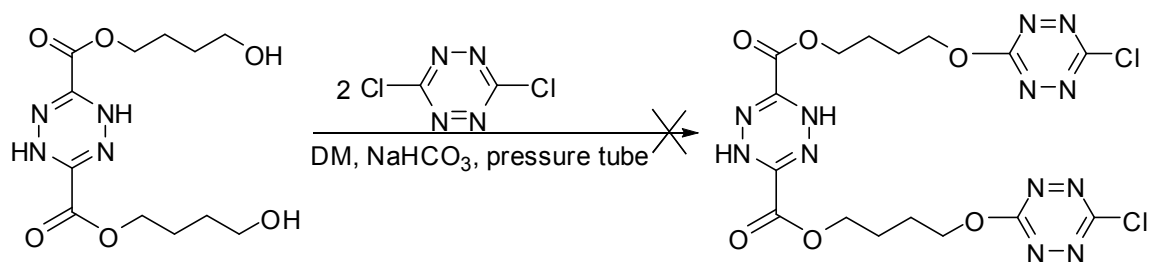
6.18 Attempts to prepare bis(4-(6-chloro-1,2,4,5-tetrazin-3-yloxy)butyl) 1,4-dihydro-1,2,4,5-tetrazine-3,6-dicarboxylate (**108**)

(1)



NaH was added into a solution of bis(4-hydroxybutyl) 1,4-dihydro-1,2,4,5-tetrazine-3,6-dicarboxylate (50 mg, 0.16 mmol) in 20 mL of anhydrous THF at -10°C . After stirring for 0.5 hour, the solution was cooled to -20°C and dichloro-*s*-tetrazine (50 mg, 2 eq.) was added. The temperature was allowed to rise to r. t. and the mixture was stirred for another 1 hour. The solvents were removed by evaporation and the residue was passed through a column chromatography (silica, 1:15 methanol/ DM). 2 red-colored tetrazine-containing products were separated, the ^1H NMR of which were too complex to identify the structure.

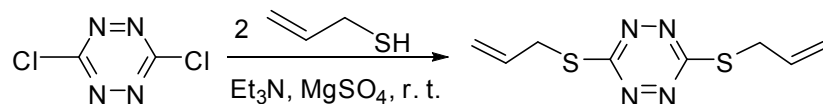
(2)



Dichloro-*s*-tetrazine (0.10 g, 0.6 mmol), bis(4-hydroxybutyl) 1,4-dihydro-1,2,4,5-tetrazine-3,6-dicarboxylate (0.077 g, 0.25 mmol), NaHCO_3 (0.04 g, 2 eq.), 10 mL of anhydrous dichloromethane and a magnetic stirring bar were added into a 20-mL pressure

tube. The tube was sealed and heated at 100 °C overnight, then cooled to room temperature. The solids were filtered out and washed with dichloromethane. The filtrates were combined and evaporated. After a short column chromatography (silica, 1:15 methanol/ DM) a red product was separated, the structure of which couldn't be identified by ¹H NMR.

6.19 Preparation of 3,6-bis(allylthio)-1,2,4,5-tetrazine

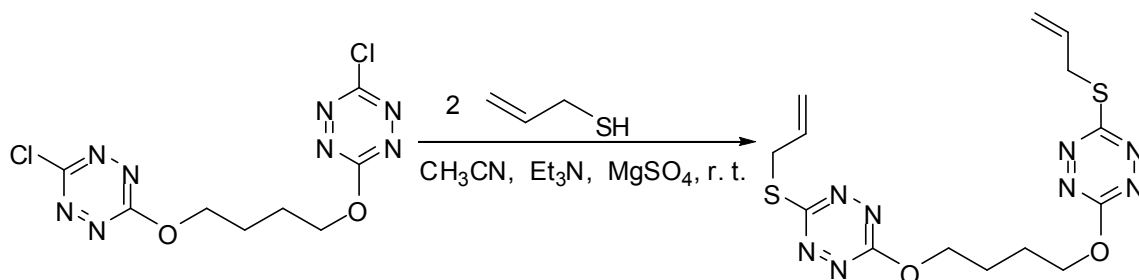


To a solution of prop-2-ene-1-thiol (0.57 mL, 4.1 mmol) and triethylamine (0.58 mL, 4.1 mmol) in 10 mL of acetonitrile was added slowly a solution of dichloro-*s*-tetrazine (0.302 g, 2 mmol) in 100 mL of acetonitrile during 8 hours, after which time the mixture was stirred overnight. The solvents were removed by evaporation and the residue was passed through a column chromatography (silica, 1:10 ethyl acetate/ petroleum ether) to give 3,6-bis(allylthio)-1,2,4,5-tetrazine as a red liquid (0.14g, 31%).

¹H NMR (300MHz, CDCl₃) δ 5.97-5.88(m, 2H), 5.41-5.34(m, 2H), 5.21-5.16(m, 2H), 3.93-3.90(m, 4H)

¹³C NMR (75MHz, CDCl₃) δ 172.20, 131.55, 119.58, 33.14

6.20 Preparation of 1,4-bis(6-(allylthio)-1,2,4,5-tetrazin-3-yloxy)butane (**100**)

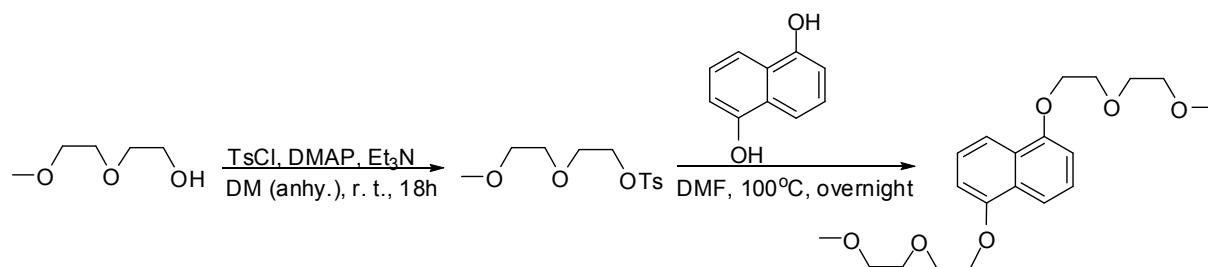


To a solution of prop-2-ene-1-thiol (0.25 mL, 2.2 eq) and triethylamine (0.25 mL, 2.2 eq) in 10 mL of acetonitrile was added slowly a solution of 1,4-bis(6-chloro-1,2,4,5-tetrazin-3-yloxy)butane (0.26 g, 0.85 mmol) in 100 mL of acetonitrile during 10 hours, after which time the mixture was stirred for another 2 hours. The solvents were removed by evaporation and the residue was passed through a column chromatography (silica, DM) to give 1,4-bis(6-(allylthio)-1,2,4,5-tetrazin-3-yloxy)butane as a red solid (0.19 g, 59%).

¹H NMR (300MHz, CDCl₃) δ 6.01-5.90(m, 2H), 5.39(dd, 2H, J=10.7Hz and J=1.5Hz), 5.18(dd, 2H, J=10.1Hz and J=1.1Hz), 4.69-4.65(m, 4H), 3.92(td, 4H, J=7.0Hz and J=1.1Hz), 2.18-2.14(m, 4H)

¹³C NMR (75MHz, CDCl₃) δ 171.13, 166.07, 131.84, 119.47, 69.10, 33.64, 25.33

6.21 Preparation of molecular template (**101**)



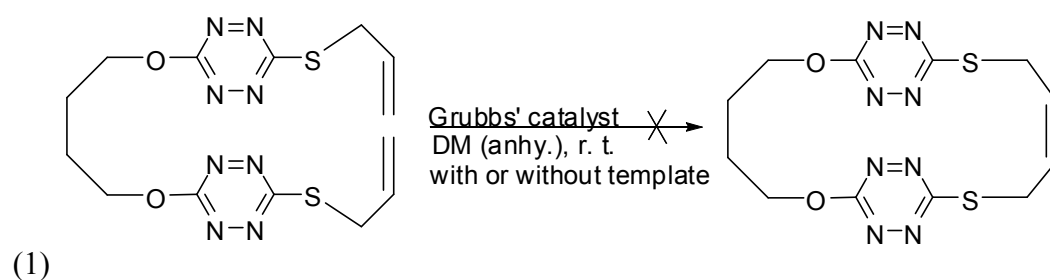
Tosyl chloride (7.86 g, 0.04 mol, 2 eq.) was added slowly into the mixture of monomethyl-diethylene glycol (2.38 mL, 0.02 mol), triethylamine (11.3 mL, 4 eq.), DMAP (0.22 g, 0.09 eq.) and 20 mL of DM at 0°C. The mixture was warmed to r. t. and stirred for 16 hours. The solvent was removed by evaporation and the residue was passed through a column chromatography (silica, 1:50 ethanol/ DM) to give tosyl-diethylene glycol ether as a colorless liquid (4.45g, 61%).

¹H NMR (300MHz, CDCl₃) δ 7.61(d, 2H, J=8.5Hz), 7.21(d, 2H, J=7.7Hz), 4.00(d, 2H, J=3.7Hz), 3.51(d, 2H, J=4.5Hz), 3.39-3.38(m, 2H), 3.30-3.29(m, 2H), 3.16(s, 3H)

Dihydroxynaphthalene (1.32 g, 8 mmol), K₂CO₃ (6.3 g, 3 eq.) and 60 mL of anhydrous DMF were mixed and heated to 80°C, then tosyl-diethylene glycol ether (4.4 g, 0.016 mol) was added by syringe, and the mixture was heated to 100°C. After stirring overnight the mixture was cooled to r. t., poured into water, and extracted with petroleum ether. 0.51 g white plates of 1,5-bis(2-(2-methoxyethoxy)ethoxy)naphthalene was obtained from a column chromatography (silica, ethyl acetate) followed by recrystallization from petroleum ether (17%).

¹H NMR (300MHz, CDCl₃) δ 7.71(d, 2H, J=11.5Hz), 7.14(t, 2H, J=8.1Hz), 6.55(d, 2H, J=7.7Hz), 3.95(t, 4H, J=4.1Hz), 3.66(t, 4H, J=4.5Hz), 3.48(t, 4H, J=6.9Hz), 3.30(t, 4H, J=3.3Hz), 3.14(s, 6H)

6.22 Attempt to synthesize cyclophane **89** through RCM reaction (ring closure metathesis)



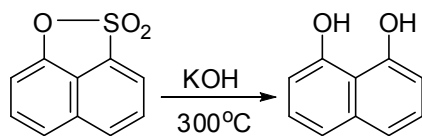
(1)

50 mg (0.13 mmol) 1,4-bis(6-(allylthio)-1,2,4,5-tetrazin-3-yloxy)butane and 0.01 eq. of Grubbs' first generation catalyst were added into 200 mL of anhydrous DM under Ar atmosphere. The mixture was stirred overnight and TLC indicated no reaction.

(2)

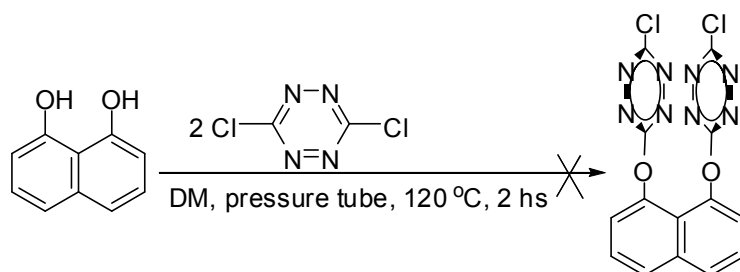
50 mg (0.13 mmol) 1,4-bis(6-(allylthio)-1,2,4,5-tetrazin-3-yloxy)butane, 0.01 eq. of Grubbs' first generation catalyst and 1 eq. of 1,5-bis(2-(2-methoxyethoxy)ethoxy)naphthalene were added into 200 mL of anhydrous DM under Ar atmosphere. The mixture was stirred overnight and TLC indicated no reaction.

6.23 Preparation of naphthalene-1,8-diol



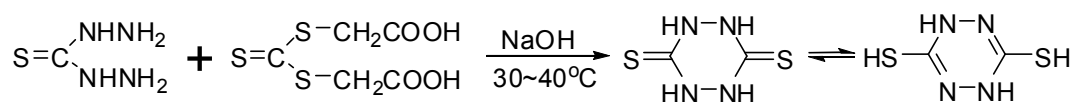
1,8-naphthosulfone (2.0 g, 9.6 mmol) and KOH (9.16 g, 85% pure, 150 mmol) were mixed and heated with stirring in a stainless steel beaker to 300°C until the mixture became a homogeneous black liquid. After 5 min it was cooled to r. t. and neutralized with aq. HCl (conc. HCl/H₂O 1:2). The water layer was extracted with ethyl acetate, and the organic layer was dried with MgSO₄. After a column chromatography (silica, ethyl acetate) 0.7 g of naphthalene-1,8-diol was obtained as a brown solid which turned dark slowly in the air (47%).
¹H NMR (300MHz, CDCl₃) δ 8.23(s, 2H, OH), 7.41(dd, 2H, J=8.3Hz and J=0.9Hz), 7.33(dd, 2H, J=7.5Hz and J=0.9Hz), 6.85(dd, 2H, J=7.4Hz and J=1.1Hz)
¹³C NMR (75MHz, CDCl₃) δ 152.81, 137.13, 126.85, 120.62, 114.66, 109.48

6.24 Attempt to prepare 1,8-bis(6-chloro-1,2,4,5-tetrazin-3-yloxy)naphthalene (**82**)



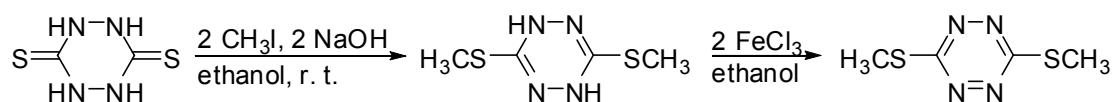
Dichloro-*s*-tetrazine (0.6 g, 4 mmol), naphthalene-1,8-diol (0.16 g, 1 mmol), MgSO₄ (0.3 g), and 8 mL of anhydrous DM were mixed in a 20-mL pressure tube and heated to 120°C for 2 hours. TLC indicated naphthalene-1,8-diol was all consumed while no new tetrazine-containing compounds were formed.

6.25 Preparation of 1,4-dihydro-1,2,4,5-tetrazine-3,6-dithiol



The thiocarbonyl dihydrazide (5.3 g, 0.05 mol) was dissolved in 75 mL of water and heated to 40°C. To this solution was added dropwise a solution of dicarboxymethyl-trithiocarbonate (11.3 g, 0.05 mol) in 100 mL of 1N NaOH. The mixture was stirred at 40°C for another 20 min and at r. t. for 30 min, then cooled to 0°C. The slightly yellow solids were filtered out, washed with water, and dried in vacuo (3.16 g, 43%).

6.26 Preparation of 3,6-bis(methylthio)-1,2,4,5-tetrazine (**29**)



Dithio-*p*-urazine (3.16 g, 0.021 mol) was dissolved in 1N aq. NaOH (1.76 g, 2 eq.) and degassed with Ar. A solution of CH₃I (2.7 mL, 2 eq.) in 20 mL of ethanol was added dropwise through a dropping funnel, during which time a pale yellow solid precipitated. The

mixture was stirred for another 2 hours and the solids were filtered, washed with water and dried in vacuum to give 3,6-bis(methylthio)-1,4-dihydro-1,2,4,5-tetrazine (0.7g, 20%).

$^1\text{H NMR}$ (300MHz, CDCl_3) δ 6.54(br., 2H), 2.41(s, 6H)

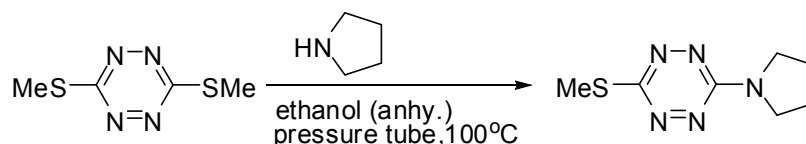
$^{13}\text{C NMR}$ (75MHz, CDCl_3) δ 150.94, 14.14

An aqueous 2N solution of ferric chloride (1.37 g, 8.2 mmol) was added dropwise to the solution of 3,6-bis(methylthio)-1,4-dihydro-1,2,4,5-tetrazine (0.72 g, 4.1 mmol) in ethanol at r. t.. The mixture was stirred for 0.5 hour and extracted with ether. The ether layer was dried with MgSO_4 , and the ether was removed by evaporation. After a short column chromatography (silica, 1:3 ethyl acetate/ petroleum ether) 0.22 g of 3,6-bis(methylthio)-1,2,4,5-tetrazine was obtained as a red solid which is easy to sublime (31%).

$^1\text{H NMR}$ (300MHz, CDCl_3) δ 2.64(s, 6H)

$^{13}\text{C NMR}$ (75MHz, CDCl_3) δ 172.95, 13.53

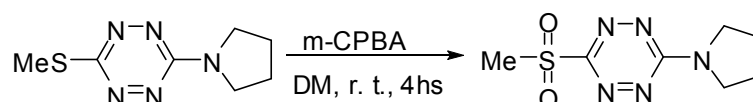
6.27 Preparation of 3-(methylthio)-6-(pyrrolidin-1-yl)-1,2,4,5-tetrazine



Bis(methylthio)-1,2,4,5-tetrazine (63 mg, 0.36 mmol) and pyrrolidine (0.036 mL, 0.43 mmol) were dissolved in absolute ethanol (15 mL) in a pressure tube and heated to 100°C for 15 min with stirring. The mixture was kept stirring at 65°C for another 2 hours, then cooled to r. t.. After evaporation of the solvent the residue was passed through a column chromatography (silica, 1:2 ethyl acetate/ petroleum ether) to give 0.07 g of product (~100%).

$^1\text{H NMR}$ (300MHz, CDCl_3) δ 3.73-3.68(m, 4H), 2.65(s, 3H), 2.11-2.07(m, 4H)

6.28 Preparation of 3-(methylsulfonyl)-6-(pyrrolidin-1-yl)-1,2,4,5-tetrazine

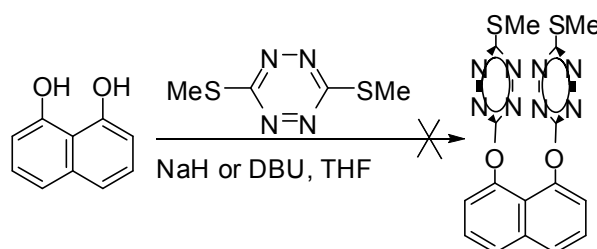


3-(methylthio)-6-(pyrrolidin-1-yl)-1,2,4,5-tetrazine (0.1 g, 0.5 mmol) and m-chloroperoxy benzoic acid (0.31g, 1.3 mmol) were mixed in 25 mL of DM and stirred at r. t. for 4 hours. After evaporation of solvent the residue was passed through a column (silica, ethyl acetate) to give 0.12 g of product (~100%).

$^1\text{H NMR}$ (300MHz, CDCl_3) δ 3.84-3.80(m, 4H), 3.35(s, 3H), 2.16-2.11(m, 4H)

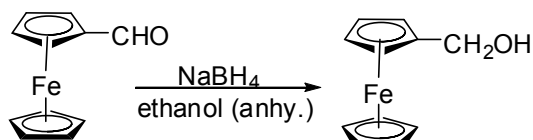
$^{13}\text{C NMR}$ (75MHz, CDCl_3) δ 162.87, 157.51, 47.37, 41.36, 25.13

6.29 Attempt to synthesize 1,8-bis(6-(methylthio)-1,2,4,5-tetrazin-3-yloxy)naphthalene



NaH (0.03 g, 2 eq.) was added into a solution of naphthalene-1,8-diol (0.06 g, 0.37 mmol) in 5 mL of anhydrous THF at r. t., and the solution turned dark quickly. To this solution bis(methylthio)-1,2,4,5-tetrazine (0.13 g, 2 eq.) was added and the mixture was stirred for 24 hours, after which time TLC indicated that most of bis(methylthio)-1,2,4,5-tetrazine and part of naphthalene-1,8-diol remained and no new compound was produced. When DBU was used as base instead of NaH, no reaction took place and both of starting compounds remained mostly.

6.30 Preparation of ferrocenemethanol



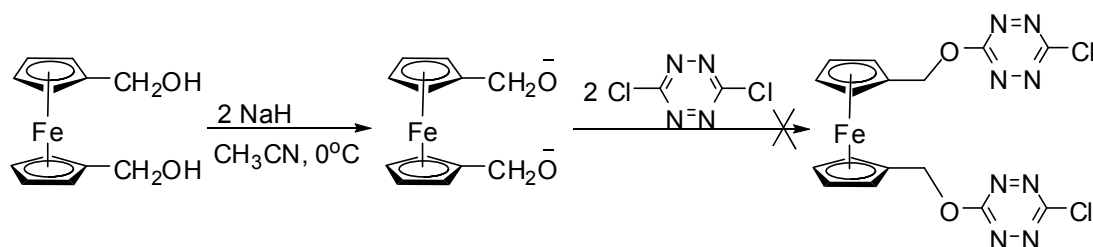
NaBH₄ (0.21 g, 5.5 mmol) was added into a solution of ferrocenealdehyde (1.1 g, 5 mmol) in 20 mL of ethanol and the mixture was stirred at r. t. overnight. The solvent was removed by evaporation and the solids were dissolved in ethyl ether, washed with water and dried over MgSO₄. After evaporation of ether the solids were passed through a short column chromatography (silica, DM) to give 1.0 g of pure product (81%).

¹H NMR (300MHz, CDCl₃) δ 4.27(s, 2H), 4.23(t, 2H, J=1.8Hz), 4.14(t, 2H, 1.8Hz), 4.12(s, 5H), 1.55(s, 1H)

¹³C NMR (75MHz, CDCl₃) δ 69.42, 68.54, 68.42, 68.04

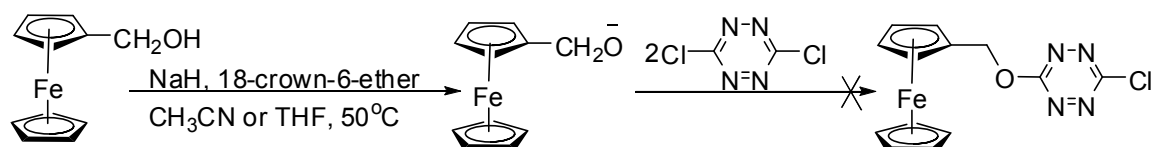
6.31 Attempts to synthesize ferrocenylmethoxy-1,2,4,5-tetrazine (83)

(1)



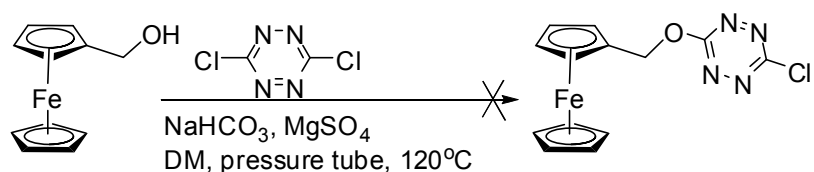
NaH (60% dispersion in oil, 17mg, 0.41mmol) was added into a solution of ferrocenedimethanol (50 mg, 0.2 mmol) in 10 mL of anhydrous acetonitrile at 0°C. The mixture was stirred for 0.5 hour, after which time a solution of dichloro-*s*-tetrazine (62 mg, 0.41 mmol) in 10 mL of acetonitrile was added dropwise and the solution turned black quickly. The mixture was stirred for another 1 hour at r. t. after the addition, and the solvents were removed by evaporation. The residue was passed through a column chromatography (silica, 1:2 ethyl acetate/ petroleum ether) to give a main tetrazine-containing product, of which the ¹H NMR is too complex to deduce the structure.

(2)



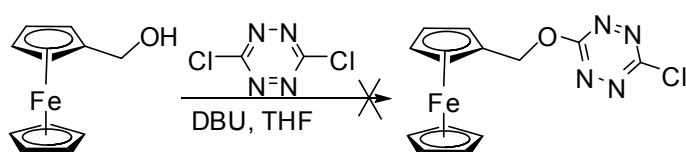
In a similar manner to that described in (1), except that the mixture of ferrocene methanol and NaH was transferred slowly into the dichloro-*s*-tetrazine solution. Dichloro-*s*-tetrazines were all decomposed and most of ferrocenemethanol remained.

(3)



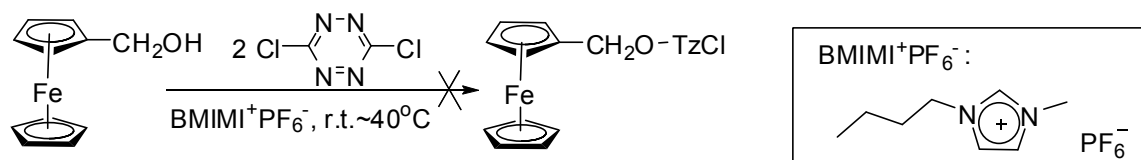
In a same manner to that described in 50.12. Most of ferrocenemethanol and dichloro-*s*-tetrazine remained.

(4)



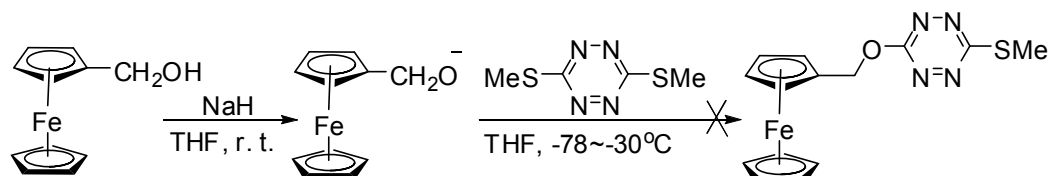
To a solution of ferrocene methanol (50 mg, 0.23 mmol) and dichloro-*s*-tetrazine (60 mg, 0.4 mmol) in anhydrous THF was added DBU (0.035 mL, 0.23 mmol) slowly by syringe at r. t.. TLC indicated that ferrocenemethanol was consumed and a red polymer-like compound was produced which does not move on TLC plate.

(5)



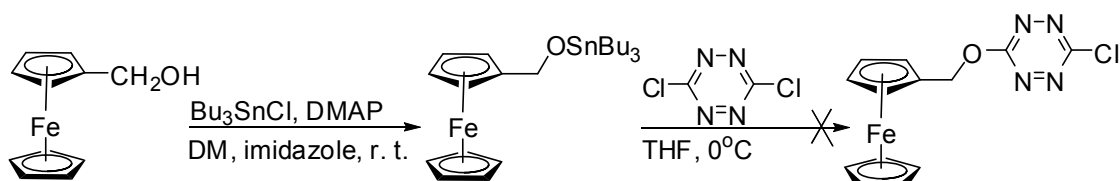
Ferrocenemethanol (0.11 g, 0.5 mmol) and dichloro-*s*-tetrazine (0.15 g, 1 mmol) were mixed in 4 mL of $\text{BMIMI}^+\text{PF}_6^-$ and warmed slowly to 40°C under Ar atmosphere. After 0.5 hour TLC indicated dichloro-*s*-tetrazine was all decomposed, while ferrocenemethanol remained mostly.

(6)



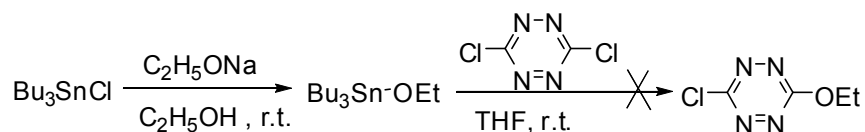
NaH was added into a solution of ferrocenemethanol (68 mg, 0.32 mmol) in THF (5mL) under Ar atmosphere and the mixture was stirred at r. t. for 1 hour, then cooled to -78°C , and transferred through a stainless steel cannula into a solution of bis(methylthio)-1,2,4,5-tetrazine (50 mg, 0.3 mmol) in THF (8 mL) at -78°C . The mixture was stirred at -78°C for 2 hours and -30°C for 1 hour. TLC indicated no reaction. The temperature was allowed to rise slowly to r. t., and bis(methylthio)-tetrazine began to decompose, and ferrocenemethanol remained mostly.

(7)



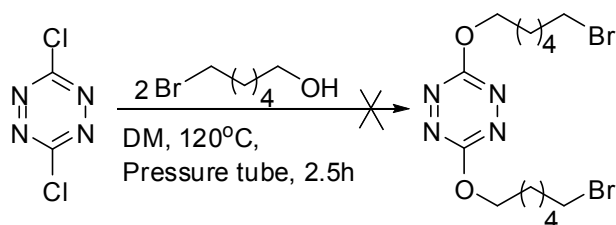
Ferrocenemethanol (0.11 g, 0.5 mmol), tributyl tinchloride (0.14 mL, 0.5 mmol), imidazole (0.05 g, 0.7 mmol) and DMAP (0.006 g, 0.05 mmol) were mixed in 10 mL of anhydrous DM at r. t.. After stirring overnight, dichloro-*s*-tetrazine was added into the solution, and soon decomposed (TLC: 1:3 ethyl acetate/petroleum ether).

(8)



NaH (60% dispersion in oil, 26.5 mg, 2 eq.) was added into 20 mL of anhydrous ethanol. After stirring for 15min, tributyl tinchloride was injected and white solids precipitated, which were filtered. The filtrate was evaporated to give a colorless liquid, which was dissolved in anhydrous THF, followed by addition of a solution of dichloro-*s*-tetrazine (50 mg, 0.033 mmol) in 3 mL of THF. TLC indicated only a polymer-like product formed which did not move on TLC plate even when methanol/DM (1:10) was used as eluent.

6.32 Preparation of 3,6-bis(6-bromohexyloxy)-1,2,4,5-tetrazine



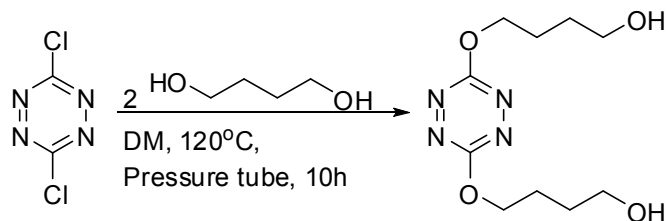
Dichloro-*s*-tetrazine (0.2 g, 12 mmol) and bromohexanol (0.45 g, 2 eq.) were dissolved in 5 mL of DM. The mixture was heated to 128°C in a pressure tube for 2.5 hours, then cooled to r. t.. The solvent was removed by evaporation and the residue was passed through a column chromatography (silica, 1:5 EA/PE) to give a small amount of product which was identified to be the mono-substituted one by ^{13}C NMR analysis.

^1H NMR (300MHz, CDCl_3) δ 4.63(t, 2H, $J=6.3\text{Hz}$), 3.39(t, 2H, $J=6.9\text{Hz}$), 2.00-1.81(m, 4H), 1.55-1.50(m, 4H)

^{13}C NMR (75MHz, CDCl_3) δ 166.70, 164.21, 70.77, 33.64, 32.54, 28.36, 27.73, 24.94

6.33 Synthesis of 4,4'-(1,2,4,5-tetrazine-3,6-diyl)bis(oxy)dibutan-1-ol (112)

(1)



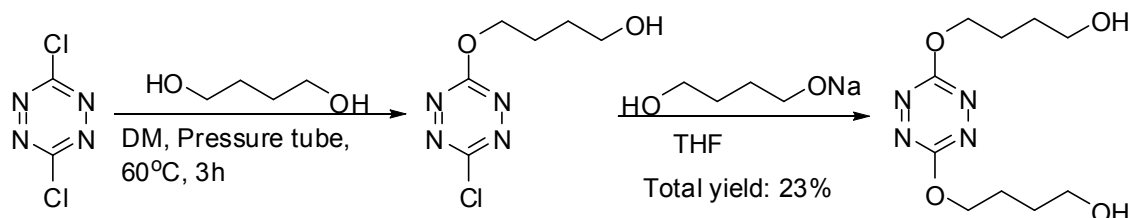
Dichloro-*s*-tetrazine (0.87 g, 5.8 mmol) and 1,4-butanediol (5 mL, ~10 eq.) were mixed in 10 mL of anhydrous DM. The mixture was heated to 120°C in a pressure tube for 10 hours with stirring. After cooling to r. t., the solvent was removed by evaporation and the residue was passed through a column chromatography (silica, 1:8 methanol/DM) to give 0.13 g of product as a red fluorescent solid (9%).

¹H NMR (300MHz, CDCl₃) δ 4.60(t, 2H, J=6.6Hz), 3.75(t, 2H, J=6.3Hz), 2.06-1.97(m, 2H), 1.84-1.75(m, 2H), 1.45 (br., 1H)

¹³C NMR (75MHz, CDCl₃) δ 166.19, 69.83, 62.43, 29.07, 25.35

MS, *m/z*: 281.2([M+Na]⁺, calc. 281.2), 186.3, 142.2

(2)

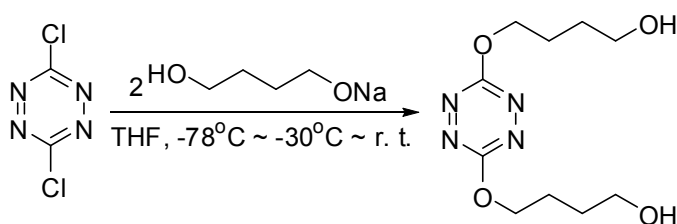


Dichloro-*s*-tetrazine (0.5 g, 3.3 mmol) and 1,4-butanediol (1 mL, ~3 eq.) were mixed in 10 mL of anhydrous DM. The mixture was heated to 60°C in a pressure tube for 3 hours with stirring. After cooling to r. t., the solvent was removed by evaporation and the residue was passed through a column chromatography (silica, 1:8 methanol/DM) to give 0.33 g of the mono-substituted product 4-(6-chloro-1,2,4,5-tetrazin-3-yloxy)butan-1-ol as a red fluorescent solid (50%).

¹H NMR: see 5.9.

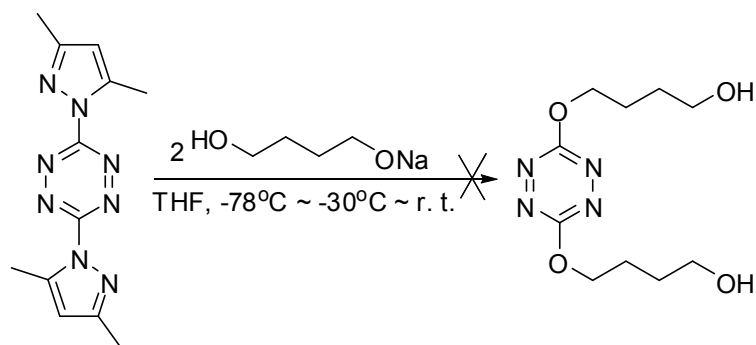
NaH (60% dispersion in oil, 66 mg, 1.7 mmol) was added into a solution of 1,4-diol (0.15 mL, 1.7 mmol) in 5 mL of anhydrous THF. The mixture was stirred at r. t. for 0.5 hour, then cooled to 0°C with an ice bath, and transferred into a solution of 4-(6-chloro-1,2,4,5-tetrazin-3-yloxy)butan-1-ol (0.33g, 1.6 mmol) in 5 mL of THF at -78°C. The mixture was allowed to warm slowly to r. t. and stirred at r. t. for 2 hours. The solids was filtered, washed with DM and the filtrate was concentrated by evaporation and passed through a column chromatography (silica, 1:8 methanol/DM) to give 0.2 g of 4,4'-(1,2,4,5-tetrazine-3,6-diyl)bis(oxy)dibutan-1-ol as a red fluorescent solid (48%).

(3)



NaH (60% dispersion in oil, 265 mg, 6.6 mmol) was added into a solution of 1,4-diol (0.59 mL, 6.6 mmol) in 5 mL of anhydrous THF. The mixture was stirred at r. t. for 0.5 hour, then cooled to -78°C and transferred slowly with a stainless steel cannula into a solution of dichloro-*s*-tetrazine (0.50g, 3.3 mmol) in 5 mL of THF at -78°C . The mixture was allowed to warm slowly to r. t. and stirred at r. t. for 2 hours. The solids were filtered, washed with DM and the filtrate was concentrated by evaporation and passed through a column chromatography (silica, 1:8 methanol/DM) to give 0.21 g 4,4'-(1,2,4,5-tetrazine-3,6-diyl)bis(oxy)dibutan-1-ol as a red fluorescent solid (24%).

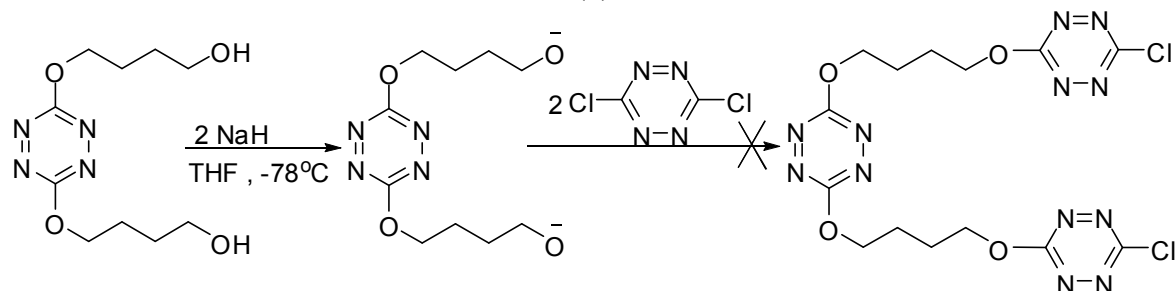
(4)



In a same manner to that described in (3). All tetrazines were decomposed.

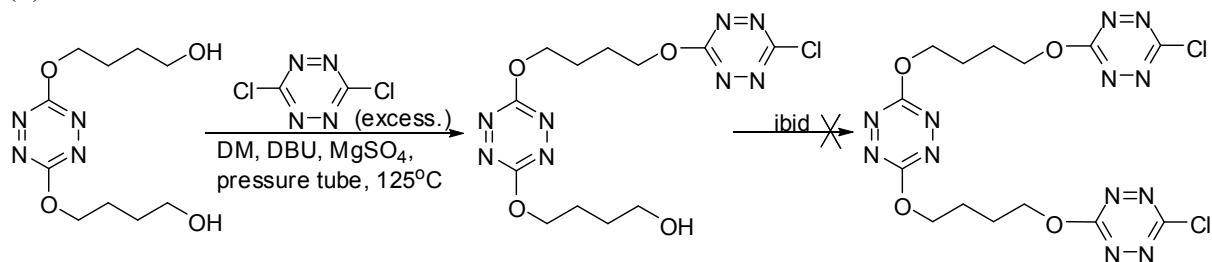
6.34 Attempts to synthesize 3,6-bis(4-(6-chloro-1,2,4,5-tetrazin-3-yloxy)butoxy)-1,2,4,5-tetrazine (**118**)

(1)



In a same manner to that described in 6.33 (3). Only traces amounts of red-colored compound was obtained, the $^1\text{H-NMR}$ of which was not in accordance with the disubstituted or monosubstituted product.

(2)

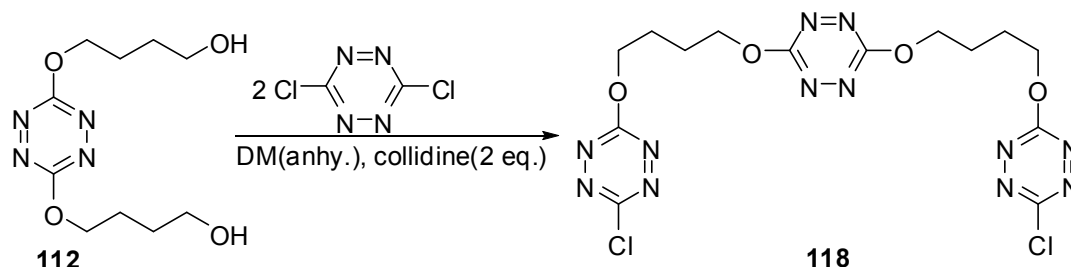


4,4'-(1,2,4,5-tetrazine-3,6-diyl)bis(oxy)dibutan-1-ol (0.20 g, 0.78 mmol), DBU (0.24 mL, 2 eq.), MgSO_4 (0.5 g), and dichloro-*s*-tetrazine (0.47 g, 4 eq.) were mixed in 5 mL of DMF in a pressure tube. The mixture was heated to 125°C for 10 hours, then cooled to r. t.. The

solvent was removed by evaporation and the residue was passed through a column chromatography (silica, 1:5 ethyl acetate/petroleum ether) to give a small amount of the mono-substituted product 4-(6-(4-(6-chloro-1,2,4,5-tetrazin-3-yloxy)butoxy)-1,2,4,5-tetrazin-3-yloxy)butan-1-ol.

The reaction of mono-substituted product with additional tetrazine in the same manner failed.

(3)



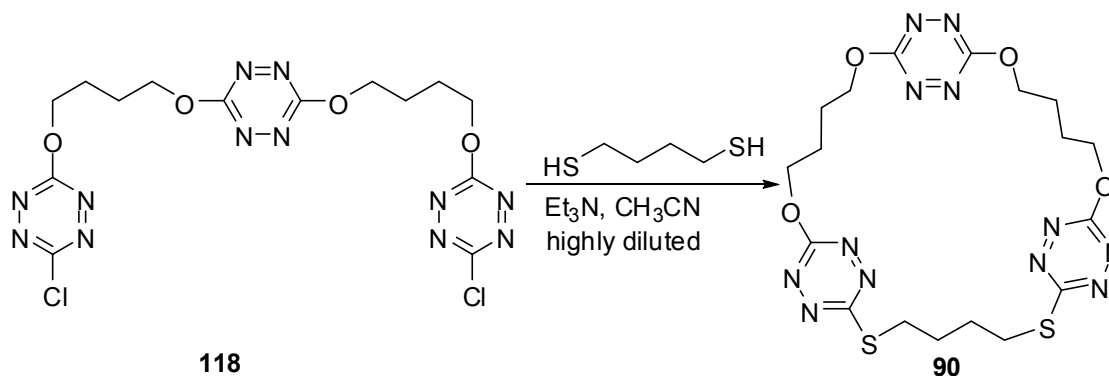
Tetrazine-diol **112** (0.13 g, 0.5 mmol.) and dichloro-*s*-tetrazine (0.151 g, 1 mmol) were dissolved in 15 mL of anhydrous DM. 2,4,6-Collidine (0.13 mL, 1 mmol) was added dropwise into the solution, and the mixture was stirred overnight under Ar atmosphere. The solvent was evaporated and the residue was passed through a column chromatography (silica, DM) to give 3,6-bis(4-(6-chloro-1,2,4,5-tetrazin-3-yloxy)butoxy)-1,2,4,5-tetrazine (**118**) as a red fluorescent solid (0.22 g, 92%).

$^1\text{H NMR}$ (300MHz, CDCl_3) δ 4.77(t, 4H, $J=5.7\text{Hz}$), 4.67(t, 4H, $J=5.7\text{Hz}$), 2.21-2.17(m, 8H)

$^{13}\text{C NMR}$ (75MHz, CDCl_3) δ 166.76, 166.17, 164.56, 70.32, 69.20, 25.32(2C)

MS, m/z : 504($[\text{M}+\text{NH}_4]^+$, calc. 504), 487(base peak), 408, 391, 357, 325, 295, 247, 171

6.35 Synthesis of cyclophane-tetrazine (**90**)



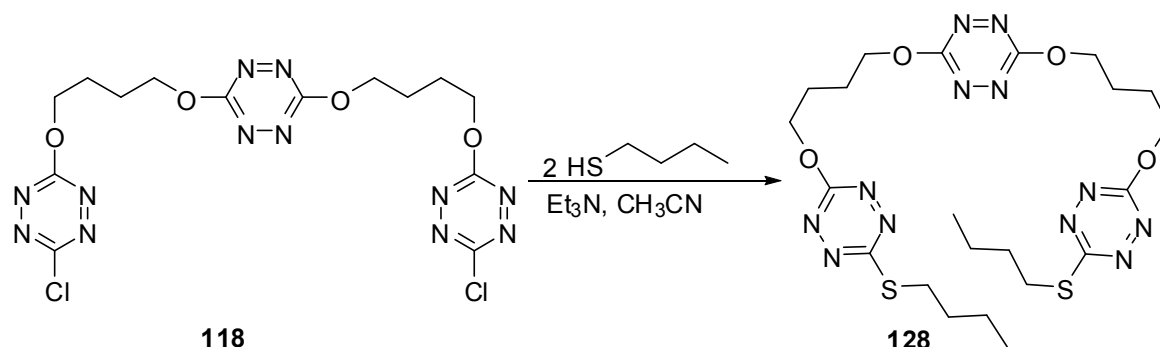
In a 500-mL 3-necked round bottom flask containing 200 mL of anhydrous acetonitrile was added simultaneously in 2 hours a solution of 1,4-dithiol (0.037 mL, 0.31 mmol) and triethylamine (0.087 mL, 0.62 mmol) in 60 mL of acetonitrile in one dropping funnel and a solution of tetrazine **118** (0.15 g, 0.31 mmol) in 60 mL of acetonitrile in another dropping funnel. The mixture was stirred for another 0.5 hour and the solvent was evaporated. After a column chromatography (silica, 1:2 EA/PE) 0.11 g of the cyclophane-tetrazine **90** was obtained as a red solid which is weakly fluorescent on TLC plate (67%).

$^1\text{H NMR}$ (300MHz, CDCl_3) δ 4.77-4.61(m, 8H), 3.32(t, 4H, $J=6.0\text{Hz}$), 2.18-2.11(m, 8H), 1.95-1.91(m, 4H)

$^{13}\text{C NMR}$ (75MHz, CDCl_3) δ 171.30, 166.02, 165.90, 68.93, 68.88, 30.26, 28.08, 24.93, 24.88

MS, m/z: 537([M+1]⁺, calc. 537), 351, 334, 310, 261, 243, 211, 190, 156(base peak), 120

6.36 Synthesis of 3,6-bis(4-(6-(butylthio)-1,2,4,5-tetrazin-3-yloxy)butoxy)-1,2,4,5-tetrazine (128)

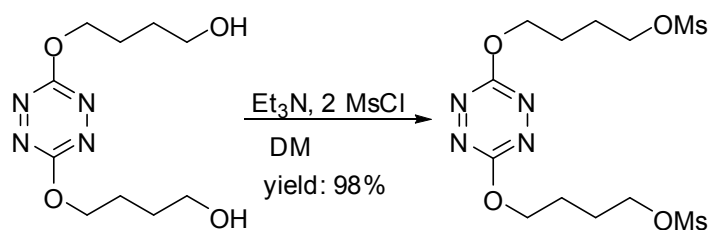


A solution of 1-butanethiol (0.084 mL, 0.78 mmol) and triethylamine (0.11 mL, 0.78 mmol) in 60 mL of acetonitrile was added dropwise through a dropping funnel into a 250-mL round bottom flask containing a solution of tetrazine **118** (0.19 g, 0.39 mmol) in 60 mL of acetonitrile. The mixture was stirred at r. t. for 2 hours and the solvent was evaporated. After a column chromatography (silica, DM→1:34 methanol/DM) 0.11 g product **128** was obtained as a red solid which is weakly fluorescent on TLC plate (47%).

¹H NMR (300MHz, CDCl₃) δ 4.67-4.65(m, 8H), 3.27(t, 4H, J=7.4Hz), 2.19-2.15(m, 8H), 1.81-1.71(m, 4H), 1.55-1.45(m, 4H), 0.95(t, 6H, J=7.4Hz)

¹³C NMR (75MHz, CDCl₃) δ 717.98, 166.13, 165.96, 69.27, 69.08, 30.91, 30.75, 25.36, 25.33, 22.05, 13.67

6.37 Preparation of 4,4'-(1,2,4,5-tetrazine-3,6-diyl)bis(oxy)bis(butane-4,1-diyl) dimethanesulfonate

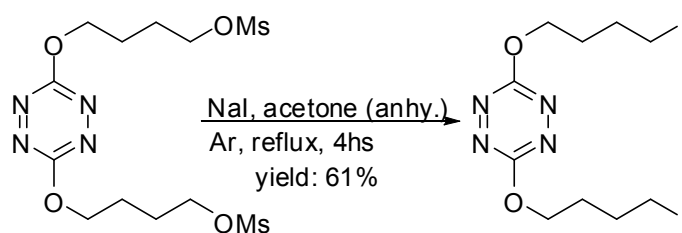


Methanesulfonyl chloride (0.38 mL, 4.8 mmol) was added dropwise into a solution of tetrazine-diol **112** (0.52 g, 2 mmol) and triethylamine (0.85 mL, 6 mmol) in 15 mL of DM at 0°C. The mixture was stirred at 0°C for another 0.5 hours and TLC indicated that the reaction was completed. The solvent was evaporated and the residue was passed through a short column chromatography (silica, 1:6 methanol/DM) to give 0.818 g product as a red fluorescent solid (98%).

¹H NMR (300MHz, CDCl₃) δ 4.61(t, 4H, J=5.9Hz), 4.33(t, 4H, J=5.9Hz), 3.03(t, 6H, J=2.6Hz), 2.07-2.00(m, 8H)

¹³C NMR (75MHz, CDCl₃) δ 166.17, 69.27, 69.10, 37.61, 25.97, 25.07

6.38 Preparation of 3,6-bis(4-iodobutoxy)-1,2,4,5-tetrazine

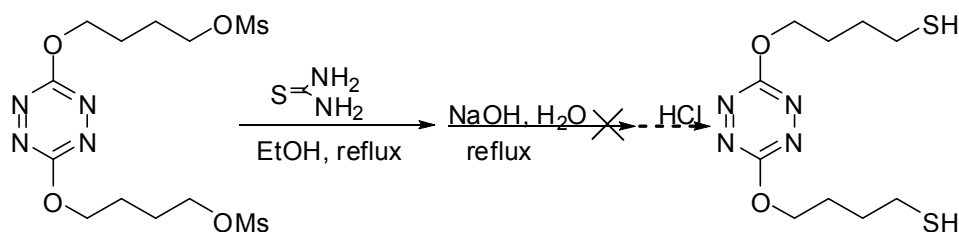


4,4'-(1,2,4,5-tetrazine-3,6-diyl)bis(oxy)bis(butane-4,1-diyl) dimethanesulfonate (0.2 g, 0.48 mmol) and NaI (0.09 g, 1.2 mmol) were added into 20 mL of anhydrous acetone. The mixture was heated to reflux under Ar atmosphere for 4 hours then cooled to r. t.. The solvent was evaporated and the residue was passed through a short column chromatography to give 0.14 g of product as a red fluorescent solid (61%).

$^1\text{H NMR}$ (300MHz, CDCl_3) δ 4.61-4.57(m, 4H), 3.30-3.25(m, 4H), 2.11-2.02(m, 8H)

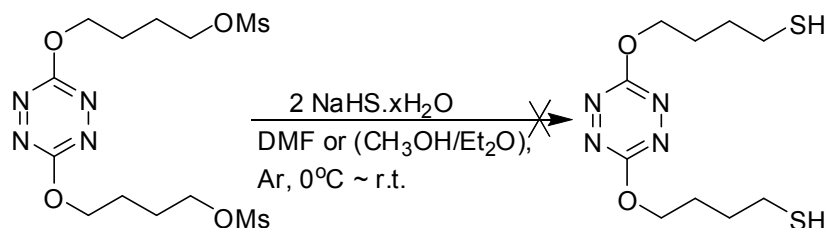
$^{13}\text{C NMR}$ (75MHz, CDCl_3) δ 166.20, 68.80, 29.86, 29.75, 5.64

6.39 Attempts to prepare 4,4'-(1,2,4,5-tetrazine-3,6-diyl)bis(oxy)dibutane-1-thiol (**III**)
(1)



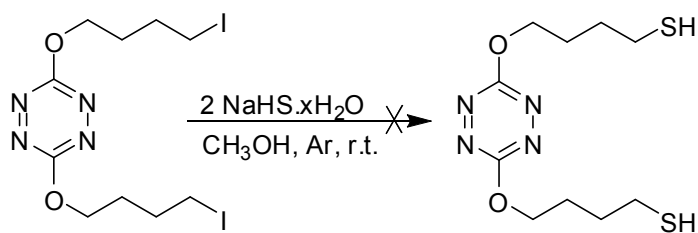
4,4'-(1,2,4,5-tetrazine-3,6-diyl)bis(oxy)bis(butane-4,1-diyl) dimethanesulfonate (0.2 g, 0.48 mmol) and thiourea (0.074 g, 0.97 mmol) were added into a mixture of 20 mL of ethanol and 2mL of DM. the mixture was refluxed for 5 hours and TLC indicated no reaction. NaOH (60 mg) was added and TLC showed that the fluorescence gradually disappeared, indicating the decomposition of tetrazine core.

(2)

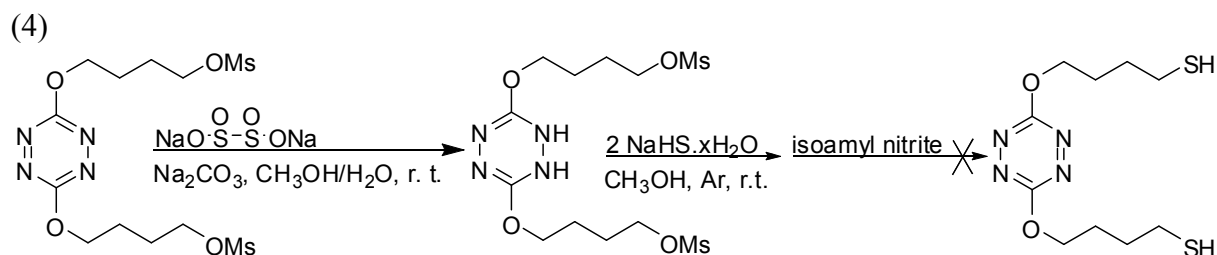


NaHS·H₂O (8mg, 1 eq.) was dissolved in 2 mL of dry methanol and the solution was added slowly into a solution of 4,4'-(1,2,4,5-tetrazine-3,6-diyl)bis(oxy)bis(butane-4,1-diyl) dimethanesulfonate (50 mg, 0.12 mmol) in 10 mL of dry ether at 0°C with stirring. The solution turned from red to colorless. When warmed to room temperature it became red again. Then another 1 eq. of NaHS·H₂O (8mg) was added, and the solution became colorless again. The mixture turned red again after being stirred for 5 min. TLC (EA) indicated some decomposition and some amount of starting compound.

(3)

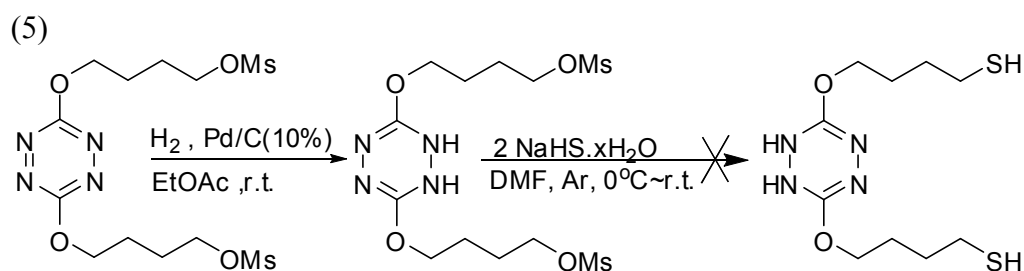


In a same manner to that described in (2), for the same result.



A solution of 4,4'-(1,2,4,5-tetrazine-3,6-diyl)bis(oxy)bis(butane-4,1-diyl) dimethanesulfonate (0.5 g, 1.2 mmol) in 20 mL of methanol and 10 mL of water was heated to 45°C. Na₂CO₃ (0.33 g, 3.1 mmol) and Na₂S₂O₄ (0.55 g, 3.1 mmol) were added, and the mixture was stirred for 8 min, during which time it turned colorless. The mixture was cooled to r. t. and the solids were filtered. The filtrate was extracted with DM, and the organic layer was dried with MgSO₄. The solvents were removed by evaporation to give 0.14 g of a white solid including a small amount of red solid inside.

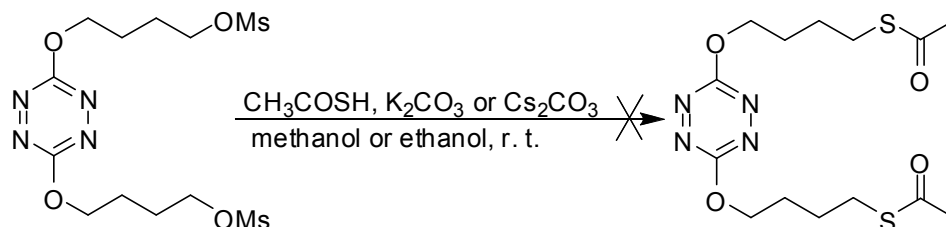
The product obtained above (0.14 g, 0.34 mmol) was dissolved in dry methanol under Ar atmosphere and NaHS·H₂O (50 mg, 2 eq.) was added with stirring. The mixture was stirred for 1 hour, during which time it became more and more red. Isoamyl nitrite (0.05 mL) was added and the mixture was stirred for 0.5 hour. The solvents were evaporated and the residue was passed through a column chromatography (silica, 1:8 EA/PE) to give 20 mg of a red fluorescent solid, which was confirmed to be dimethoxy-tetrazine by ¹H NMR.



Pd/C (10%, 18mg) was added into a solution of 4,4'-(1,2,4,5-tetrazine-3,6-diyl)bis(oxy)bis-(butane-4,1-diyl)dimethanesulfonate (100 mg, 0.24 mmol) in 10 mL of ethyl acetate in a 50- mL flask equipped with a balloon filled with H₂. Air was removed by three vacuum-H₂ charging cycles, and the mixture was stirred at r. t. for 1 hour, during which time the red color faded gradually. The solids were filtered out and the filtrate was quickly transferred into a flask with an Ar balloon protection. A solution of NaHS (30 mg, 0.48 mmol) in 4 mL of DMF was injected slowly by syringe. The red color appeared gradually during the addition of the NaHS solution, and then faded away during the next 2 hours. After another 2 hours' stirring at r. t. the mixture was extracted with ethyl acetate, and the organic layer was washed with water.

The solvents were evaporated and the residue was passed through a column chromatography (silica, EA) to give 90 mg of a red liquid, the ^1H NMR of which was too complex to be resolved.

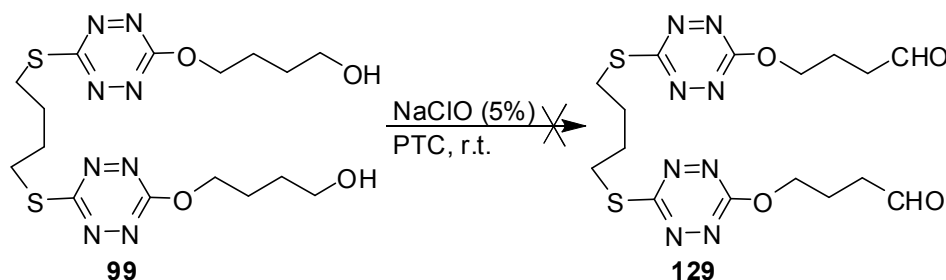
6.40 Attempts to prepare protected tetrazine-dithiol



Potassium carbonate (17 mg, 0.12 mmol) and thiolacetic acid (0.018 mL, 0.24 mmol) were mixed in 2.4 mL of methanol, and 4,4'-(1,2,4,5-tetrazine-3,6-diyl)bis(oxy)bis(butane-4,1-diyl) dimethanesulfonate (50 mg, 0.12 mmol) was added with stirring. The mixture was stirred at r. t. for 3 hours and monitored by TLC (1:30 methanol/DM). The red color faded gradually, which indicated the decomposition of the tetrazine core. The result was the same when Cs_2CO_3 was used instead of K_2CO_3 .

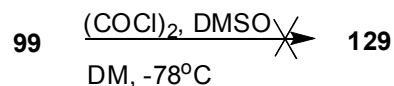
6.41 Attempts to oxidize tetrazine-diol **99**

(1)



Chlorox (9.6% of NaClO , 0.68 mL, 4 eq., diluted to 5%) was added slowly into a solution of **99** (0.1 g, 0.22 mmol) in DM (5 mL) with stirring. Tetrabutyl ammonium bromide (0.012 g, 0.17 eq.) was added as PTC. The mixture was stirred for 1 hour and TLC indicated only traces of conversion. The red color started to fade when more chlorox was added, indicating destruction of the tetrazine core.

(2) Swern oxidation



DMSO (0.04 mL, 0.56 mmol) dissolved in 5 mL of DM was added slowly by syringe into a solution of oxalyl chloride (0.025 mL, 0.28 mmol) in 5 mL of dry DM at -78°C with stirring. The tetrazine-diol **99** (50 mg, 0.11 mmol) dissolved in 3 mL of THF was added, and the mixture was stirred at -78°C for 1 hour, then 0.12 mL of triethylamine was added and the mixture was warmed slowly to r. t.. Water was added and the mixture was extracted with DM, dried with MgSO_4 and concentrated by evaporation. One main product was isolated by column chromatography, the ^1H NMR of which was not in accordance with the expected structure.

(3) Dess-Martin oxidation

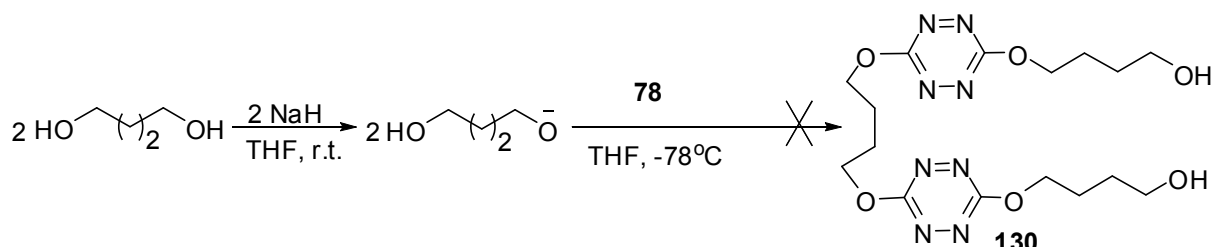


To a solution of Dess-Martin periodinane (0.14 g, 4 eq.) in DM was added by syringe a solution of tetrazine-diol **99** (36 mg, 0.08 mmol) in 5 mL of DM. The mixture was stirred at r. t. for 4 hours. The solids were filtered and the filtrate was concentrated and passed through a short column chromatography (silica, EA) to give 30 mg 4,4'-(6,6'-(butane-1,4-diylbis(sulfaneydiyl))bis(1,2,4,5-tetrazine-6,3-diyl))bis(oxy)dibutanal as a red solid (83%).

$^1\text{H NMR}$ (300MHz, CDCl_3) δ 9.84(s, 2H), 4.61(t, 4H, $J=6.2\text{Hz}$), 3.34-3.29(m, 4H), 2.77-2.72(m, 4H), 2.28-2.19(m, 4H), 2.00-1.95(m, 4H)

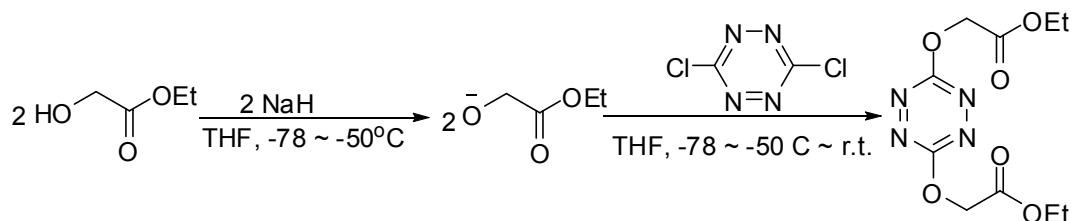
$^{13}\text{C NMR}$ (75MHz, CDCl_3) δ 200.87, 171.56, 165.96, 68.65, 40.15, 30.29, 28.04, 21.30

6.42 Attempt to prepare 4,4'-(6,6'-(butane-1,4-diylbis(oxy))bis(1,2,4,5-tetrazine-6,3-diyl))bis(oxy)dibutan-1-ol (**130**)



The 1,4-butanediol (0.2 mL, 2.3 mmol) and NaH (60% dispersion in oil, 90 mg, 2.3 mmol) were stirred in THF at r. t. for 3 hours, then cooled to -78°C and transferred slowly into a solution of **78** (0.36 g, 1.1 mmol) in 10 mL of THF at -78°C . The mixture was warmed slowly to r. t. and stirred for another 15min. The solids were filtered and the filtrate was concentrated by evaporation. 70 mg of a red solid was obtained from a column chromatography (silica, EA), the $^1\text{H NMR}$ of which was not in accordance with the expected structure.

6.43 Preparation of diethyl 2,2'-(1,2,4,5-tetrazine-3,6-diyl)bis(oxy)diacetate

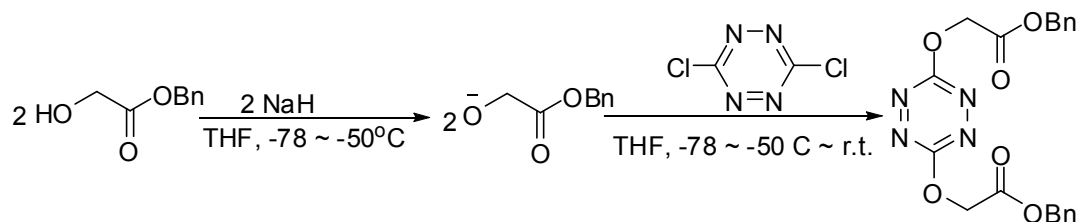


In a same manner to that described in 50.33 (3). EA/PE (1:1) was used as eluent for column chromatography (silica). A red fluorescent solid was obtained (41%).

$^1\text{H NMR}$ (300MHz, CDCl_3) δ 5.12(s, 4H), 4.24(q, 4H, $J=7.0\text{Hz}$), 1.27(t, 6H, 7.2Hz)

$^{13}\text{C NMR}$ (75MHz, CDCl_3) δ 166.94, 165.93, 65.04, 61.96, 14.16

6.44 preparation of benzyl 2,2'-(1,2,4,5-tetrazine-3,6-diyl)bis(oxy)diacetate

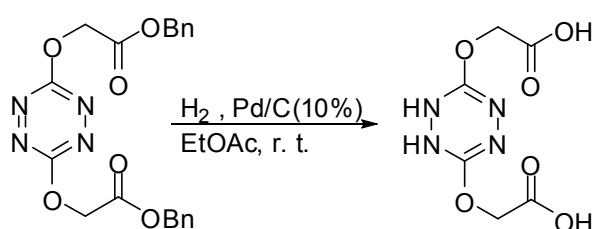


In a same manner to that described in 50.33 (3). DM was used for column chromatography. A red fluorescent solid was obtained (33%).

$^1\text{H NMR}$ (300MHz, CDCl_3) δ 7.38-7.31(m, 10H), 5.22(s, 4H), 5.17(s, 4H)

$^{13}\text{C NMR}$ (75MHz, CDCl_3) δ 166.82, 165.89, 134.85, 128.77, 128.63, 128.54, 67.56, 65.02

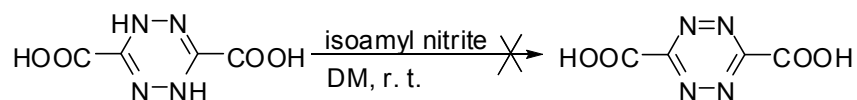
6.45 Deprotection and reduction of benzyl 2,2'-(1,2,4,5-tetrazine-3,6-diyl)bis(oxy)diacetate



Pd/C (10%, 14 mg) was added into a solution of benzyl 2,2'-(1,2,4,5-tetrazine-3,6-diyl)bis(oxy)diacetate (52 mg, 0.12 mmol) in 9 mL of EA in a 50-mL 3-necked round bottom flask equipped with a H_2 balloon. Air was removed by three H_2 charging-vacuum cycles. The mixture was stirred overnight, and solvents were removed by evaporation. The residue was passed through a column chromatography (silica, methanol) to give 25 mg of a white-light red product which is soluble in water but not in chloroform or DMSO (85%).

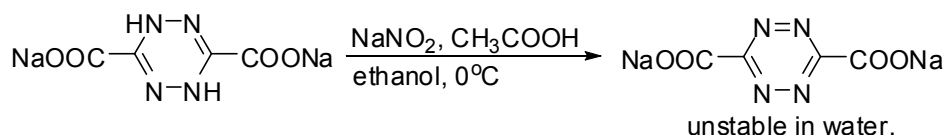
$^1\text{H NMR}$ (300MHz, D_2O) δ 4.51(4H)

6.46 Preparation of 1,2,4,5-tetrazine-3,6-dicarboxylic acid



Isoamyl nitrite (0.3 mL, 2 mmol) and 1,2,4,5-tetrazine-3,6-dicarboxylic acid (0.34 g, 2 mmol) were mixed in 10 mL of DM. The mixture was stirred at r. t. for 2 days and the color remained the same, indicating no reaction.

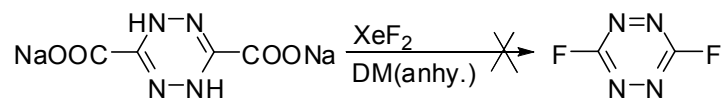
6.47 Preparation of sodium 1,2,4,5-tetrazine-3,6-dicarboxylate



To a solution of sodium 1,2,4,5-tetrazine-3,6-dicarboxylate (0.216 g, 1 mmol) in 10 mL of 95% ethanol was added a solution of NaNO_2 (0.14 g, 2 mmol) in 1 mL of water at 0°C , followed by dropwise addition of acetic acid (0.22 mL, 3.9 mmol). The mixture turned orange-red during 1 hour. The solids were filtered, washed with ethanol and the filtrate was evaporated to give 0.11 g of product (50%).

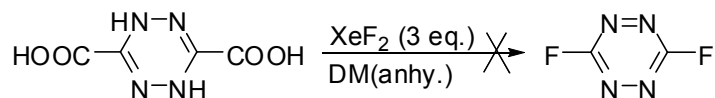
6.48 Attempts to prepare of 3,6-difluoro-1,2,4,5-tetrazine

(1)



Sodium 1,4-dihydro-1,2,4,5-tetrazine-3,6-dicarboxylate (0.1 g, 0.5 mmol) and XeF₂ (3 eq.) were mixed and stirred in 5 mL of anhydrous DM for 1 hour. No reaction took place. 1 drop of H₂SO₄ was added and the mixture was stirred for another 1 hour. After which time one drop of pyrrole was added and the mixture was stirred for 0.5 hour. No expected product was isolated from column chromatography (silica, 1:1 EA/PE).

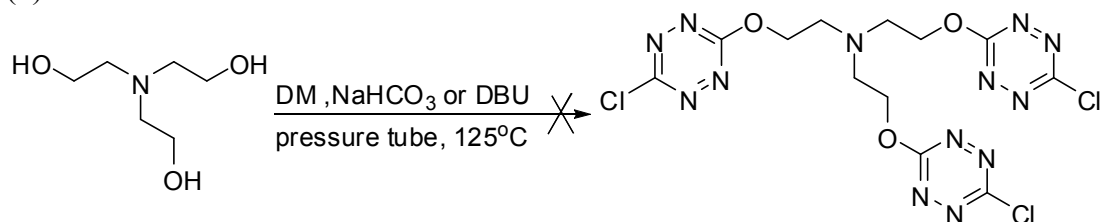
(2)



1,4-dihydro-1,2,4,5-tetrazine-3,6-dicarboxylic acid (100 mg) and XeF₂ (300 mg) were mixed in 3 mL of DM. the mixture was stirred at r. t. for 2 hours, during which time it turned red gradually. The mixture was stirred overnight and TLC indicated that only oxidized tetrazine-carboxylate (highly polar) was formed.

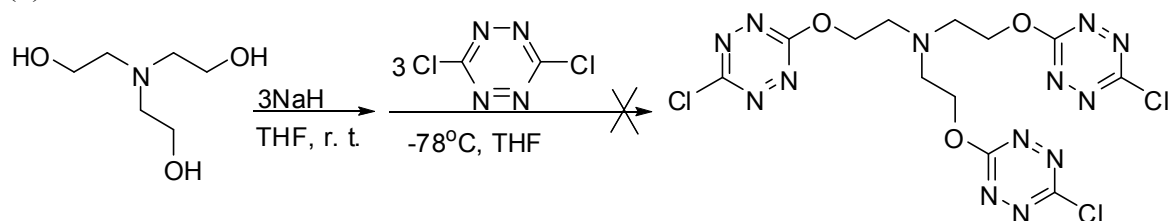
6.49 Attempts to prepare tripod-tetrazine

(1)



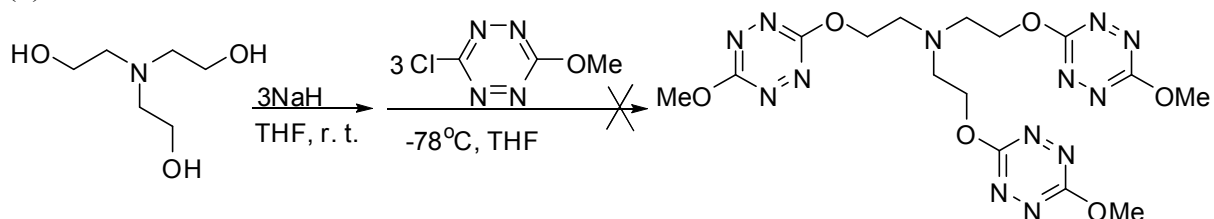
In a same manner to that described in 5.9. No expected products were isolated.

(2)



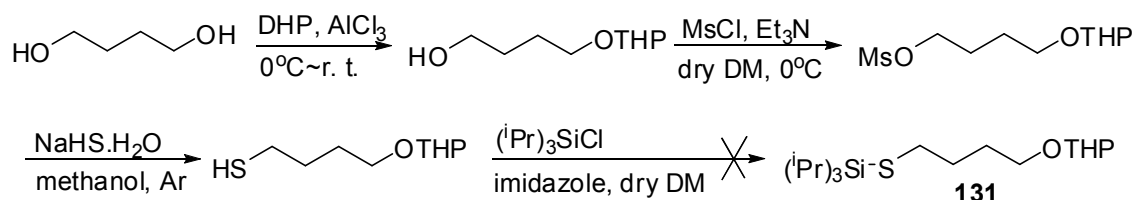
In a same manner to that described in 5.33 (3). All tetrazines were decomposed.

(3)



In a same manner to that described in 5.33 (3). Only traces of dimethoxytetrazine was formed.

6.50 Attempt to synthesize triisopropyl(4-(tetrahydro-2H-pyran-2-yloxy)butylthio)silane (**131**)



1,4-butanediol (1.5 mL, 16.5 mmol) and DHP (1 mL, 11 mmol) were mixed and cooled to 0°C with stirring. Aluminium chloride (18 mg, 0.13 mmol) was added and the mixture was allowed to warm slowly to r. t. and stirred for another 40 min. After a short column (silica, 1:10 EA/PE) 4-(tetrahydro-2H-pyran-2-yloxy)butan-1-ol was obtained as a colorless liquid (1.4 g, 73%).

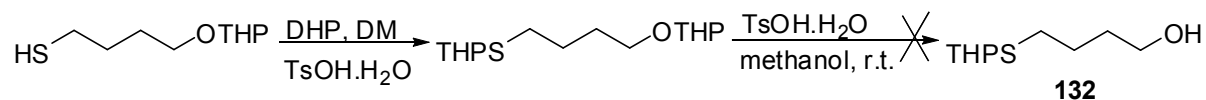
Another method using TsOH·H₂O as catalyst, anhydrous DM as solvent, and freshly distilled DHP was also tested. The yield is lower and the treatment procedure more complex.
¹H NMR (300MHz, CDCl₃) δ 4.61-4.58 (m, 1H), 3.89-3.76 (m, 2H), 3.68-3.64 (m, 2H), 3.52-3.41(m, 2H), 2.14(br., 1H), 1.80-1.53(m, 10H)
¹³C NMR (75MHz, CDCl₃) δ 99.02, 67.65, 62.85, 62.47, 30.75, 30.25, 26.68, 25.51, 19.68

Methanesulfonyl chloride (2.2 mL, 0.028 mol) was added slowly by syringe into a solution of 4-(tetrahydro-2H-pyran-2-yloxy)butan-1-ol (4 g, 0.023 mol) and triethylamine (4.8 mL, 0.035 mol) in 30 mL of anhydrous DM at 0°C. The mixture was warmed slowly to r. t. and stirred for 2 hours. The solids were filtered and the filtrate was washed with water and brine, and the water layer was extracted with EA once. The organic layers were combined and dried with MgSO₄. After evaporation of the solvent 4-(tetrahydro-2H-pyran-2-yloxy)butyl methanesulfonate was obtained which was pure enough for the next step (5.4 g, 93%).
¹H NMR (300MHz, CDCl₃) δ 4.54 (t, 1H, J=3.3Hz), 4.25 (t, 2H, J=6.6Hz), 3.81-3.74(m, 2H), 3.48-3.39(m, 2H), 2.98(s, 3H), 1.85-1.20(m, 10H)
¹³C NMR (75MHz, CDCl₃) δ 99.02, 70.05, 66.65, 62.49, 37.43, 30.77, 26.41, 25.78, 25.49, 19.71

NaHS·H₂O was added into a solution of 4-(tetrahydro-2H-pyran-2-yloxy)butyl methane-sulfonate (5.4 g, 0.021 mol) in 30 mL of methanol under Ar atmosphere at 0°C. The mixture was warmed to r. t. and stirred for 5 hours. The methanol was evaporated and ethyl acetate was added. The solids were filtered and the filtrate was washed with brine and dried with MgSO₄. After a column chromatography (silica, 1:1 EA/PE) the racemic mixture of 4-(tetrahydro-2H-pyran-2-yloxy)butane-1-thiol was obtained as a strongly odorous liquid (1.9 g, 46%).
¹H NMR (300MHz, CDCl₃) δ 4.56(t, 1H, J=2.6Hz), 3.83-3.72(m, 2H), 3.50-3.37(m, 2H), 2.70(t, 1H, J=7.0Hz, -SH), 1.76-1.51(m, 12H)
¹³C NMR (75MHz, CDCl₃) δ 98.92, 67.05, 62.40, 39.01(C-SH), 30.84, 28.70, 26.19, 25.60, 19.71

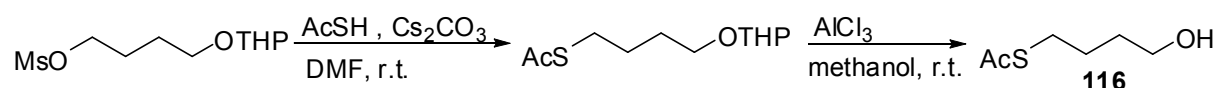
To a solution of 4-(tetrahydro-2H-pyran-2-yloxy)butane-1-thiol (1.9 g, 0.01 mol) and imidazole (0.83 g, 0.012 mol) in 20 mL of anhydrous DM was added by syringe triisopropylsilyl chloride (2.9 mL, 0.013 mol) at 0°C. The mixture was stirred overnight and TLC indicated no reaction.

6.51 Attempt to synthesize 4-(tetrahydro-2H-pyran-2-ylthio)butan-1-ol (132)



4-(tetrahydro-2H-pyran-2-yloxy)butane-1-thiol (1.1 g, 5.8 mmol) and freshly distilled DHP (0.5 g, 1 eq.) were mixed in 20 mL of DM at 0°C. TsOH·H₂O (1.1 g, 1 eq.) was added and the mixture was stirred for 2 hours. The solvent was evaporated and the residue was passed through a column chromatography (silica, 1:1 EA/PE) to give 2-(4-(tetrahydro-2H-pyran-2-yloxy)-butylthio)tetrahydro-2H-pyran as a colorless liquid (0.27 g, 17%). The liquid (0.27 g) and 4-methylbenzenesulfonic acid (1N, 4.1 g) were mixed in 20 mL of methanol and stirred at r. t. for 1 hour. No expected product was obtained.

6.52 Preparation of S-4-hydroxybutyl ethanethioate (116)



4-(tetrahydro-2H-pyran-2-yloxy)butyl methanesulfonate (0.5 g, 0.002 mol) and Cs₂CO₃ (1.96 g, 0.006 mol) were added in 5 mL of anhydrous DMF, and the mixture was stirred at r. t. for 0.5 hour. Thioacetic acid (0.45 mL, 0.006 mol) was added and the mixture was stirred for another 0.5 hour, then poured into water. The water layer was extracted with EA and the organic layer was dried with MgSO₄. After a short column (silica, 1:4 EA/PE) S-4-(tetrahydro-2H-pyran-2-yloxy)butyl ethanethioate was obtained as colorless liquid (0.42 g, 91%).

¹H NMR (300MHz, CDCl₃) δ 4.57-4.55(m, 1H), 3.88-3.69(m, 2H), 3.52-3.36(m, 2H), 2.91-2.88(m, 2H), 2.31(s, 3H, Me-CO), 1.68-1.50(m, 10H)

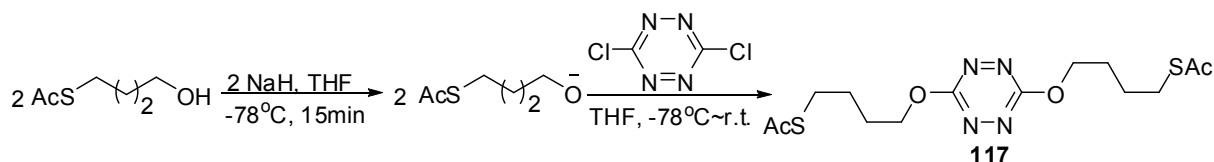
¹³C NMR (75MHz, CDCl₃) δ 195.92, 98.97, 66.98, 62.41, 30.84, 30.72, 29.10, 29.02, 26.61, 25.62, 19.73

S-4-(tetrahydro-2H-pyran-2-yloxy)butyl ethanethioate (0.4 g, 1.7 mmol) was dissolved in 20 mL of anhydrous methanol, and AlCl₃ (2 mg, 0.017 mmol) was added at r. t.. After stirring for 24 hours, the solvent was removed by evaporation and the residue was passed through a column chromatography (silica, 1:5→1:2 EA/PE) to give S-4-hydroxybutyl ethanethioate as a colorless liquid (0.2 g, 80%).

¹H NMR (300MHz, CDCl₃) δ 3.67-3.63(m, 2H), 2.91-2.86(m, 2H), 2.31(s, 3H, Me-CO), 1.76(br., 1H), 1.65-1.61(m, 4H)

¹³C NMR (75MHz, CDCl₃) δ 196.20, 62.26, 31.70, 30.71, 28.90, 26.08

6.53 Preparation of S,S'-4,4'-(1,2,4,5-tetrazine-3,6-diyl)bis(oxy)bis(butane-4,1-diyl) diethanethioate (117)

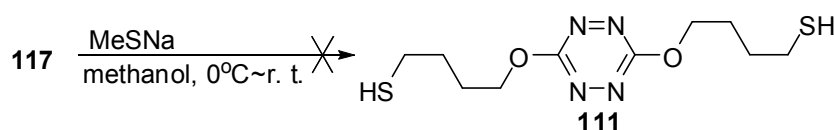


In a same manner to that described in 50.33 (3). 1.44 g S-4-hydroxybutyl ethanethioate (0.01 mol) and 0.76 g dichloro-*s*-tetrazine (0.005 mmol) gave 0.4 g of product (column chrom.: silica, 1:2.5 EA/PE) (21%).

^1H NMR (300MHz, CDCl_3) δ 4.56(t, 4H, $J=6.2\text{Hz}$), 2.95(t, 4H, $J=7.0\text{Hz}$), 2.33(s, 6H), 1.98-1.95(m, 4H), 1.83-1.78(m, 4H)

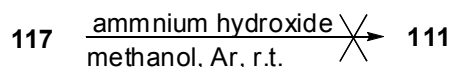
^{13}C NMR (75MHz, CDCl_3) δ 195.75, 166.16, 69.31, 30.74, 28.67, 27.83, 26.15

6.54 Attempts to prepare 4,4'-(1,2,4,5-tetrazine-3,6-diyl)bis(oxy)dibutane-1-thiol (**111**) (1)



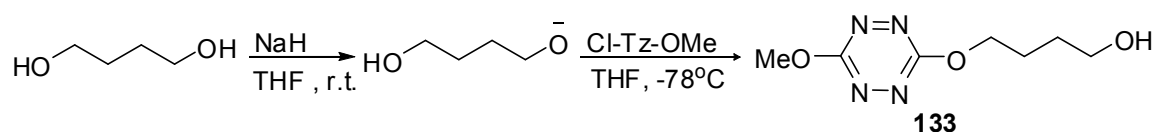
S,S'-4,4'-(1,2,4,5-tetrazine-3,6-diyl)bis(oxy)bis(butane-4,1-diyl) diethanethioate (0.2 g, 0.55 mmol) was dissolved in 2.4 mL of methanol at 0°C under Ar atmosphere. Sodium thiomethoxide (21%, 0.33 mL, 1.1 mmol) was added. TLC indicated that most of the tetrazine was decomposed after 5 min.

(2)



S,S'-4,4'-(1,2,4,5-tetrazine-3,6-diyl)bis(oxy)bis(butane-4,1-diyl) diethanethioate (0.2 g, 0.55 mmol) was dissolved in 2.4 mL of methanol at 0°C under Ar atmosphere. 4 drops of $\text{NH}_3\cdot\text{H}_2\text{O}$ (28%, 2 eq.) was added and the mixture was stirred at r. t. for 1 hour. No reaction took place except some decomposition.

6.55 Preparation of 4-(6-methoxy-1,2,4,5-tetrazin-3-yloxy)butan-1-ol (**133**)



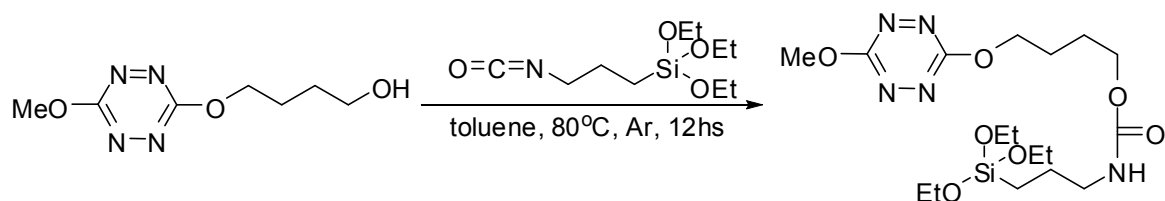
NaH (0.11 g, 2.7 mmol) was added into a solution of 1,4-diol (0.244 mL, 2.7 mmol) in 5 mL of anhydrous THF. The mixture was stirred at r. t. for 0.5 hour, then cooled to -78°C and transferred slowly into a solution of chloromethoxytetrazine (0.40 g, 2.7 mmol) in 5 mL of THF at -78°C . The mixture was allowed to warm slowly to r. t. and stirred at r. t. for 1 hour. The solids were filtered, washed with DM and the filtrate was concentrated by evaporation and passed through a column chromatography (silica, 1:1 EA/PE) to give 0.15 g of 4-(6-methoxy-1,2,4,5-tetrazin-3-yloxy)butan-1-ol as a red fluorescent solid (27%).

^1H NMR (300MHz, CDCl_3) δ 4.61(t, 2H, $J=6.3\text{Hz}$), 4.24(s, 3H), 3.75(t, 2H, $J=6.2\text{Hz}$), 2.05-1.98(m, 2H), 1.84-1.77(m, 2H), 1.56(br., 1H)

^{13}C NMR (75MHz, CDCl_3) δ 166.43, 166.30, 69.86, 62.42, 56.79, 29.06, 25.34

MS, m/z: 223.1([M+Na]⁺, calc. 223.1), 186.3, 142.2

6.56 Preparation of 4-(6-methoxy-1,2,4,5-tetrazin-3-yloxy)butyl 3-(triethoxysilyl)propyl carbamate

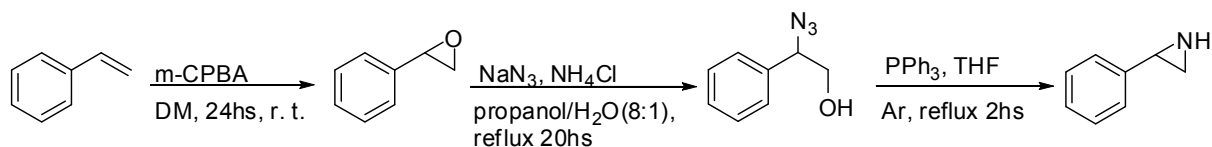


4-(6-methoxy-1,2,4,5-tetrazin-3-yloxy)butan-1-ol (0.1 g, 0.5 mmol) and 3-(triethoxy)silyl isocyanate (0.75 g, 3 mmol) were added into 30 mL of toluene. The mixture was heated to 90°C under Ar atmosphere overnight. The solvent was removed by evaporation and the residue was passed through a column chromatography (silica, EA) to give 0.22 g of 4-(6-methoxy-1,2,4,5-tetrazin-3-yloxy)butyl 3-(triethoxysilyl)propylcarbamate (98%).

¹H NMR (300MHz, CDCl₃) δ 4.56(t, 2H, J=6.2Hz), 4.21(s, 3H), 4.10(t, 2H, 6.0Hz), 3.83-3.76(m, 6H), 3.16-3.13(m, 2H), 2.01-1.52(m, 6H), 1.22-1.17(m, 9H), 0.64(t, 2H, J=8.1Hz)

¹³C NMR (75MHz, CDCl₃) δ 166.39, 166.23, 156.66, 69.48, 58.53, 58.45, 56.70, 45.45, 25.62, 25.45, 23.35, 18.33, 7.70

6.57 Preparation of 2-phenylaziridine



3-chloroperoxybenzoic acid (22.2 g, 0.09 mol) was added into a solution of styrene (5.8 mL, 0.05 mol) in 100 mL of anhydrous DM at 0°C. The mixture was stirred at r. t. for 24 hours, then washed with aq. Na₂S₂O₅ (10%), aq. Na₂CO₃, water and brine. The solvent was removed by evaporation and the residue was passed through a column chromatography (silica, DM) to give 2.3 g of 2-phenyloxirane which is volatile (38%).

¹H NMR (300MHz, CDCl₃) δ 7.43-7.36(m, 5H), 6.10(q, 1H, J=4.0Hz), 4.08-3.92(m, 2H)

¹³C NMR (75MHz, CDCl₃) δ 133.36, 129.85, 128.88, 126.76, 77.95, 66.11

The epoxide (2.3 g, 0.019 mol), sodium azide (4.9 g, 0.076 mol) and ammonium chloride (1.5 g, 0.028 mol) were dissolved in 20 mL of propanol/water (8:1). The mixture was refluxed for 15 hours, then cooled to r. t.. The solids were removed by filtration and the filtrate was concentrated by evaporation. After a column chromatography (silica, 3:7 diethyl ether/PE) 0.8 g of 2-azido-2-phenylethanol was obtained (26%).

¹H NMR (300MHz, CDCl₃) δ 7.39-7.31(m, 5H), 4.68(t, 1H, J=6.4Hz), 3.75(t, 2H, J=6.0Hz), 2.31(br., 1H)

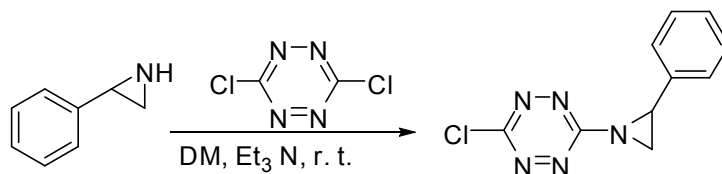
¹³C NMR (75MHz, CDCl₃) δ 136.37, 129.03, 128.81, 127.25, 67.94, 66.56

The azido alcohol (3.6 g, 22 mmol) and triphenylphosphine (7 g, 27 mmol) were added into 100 mL of anhydrous THF and the mixture was heated to reflux under Ar atmosphere for 4 hours. The THF was removed by evaporation and ether was added to

precipitate the phosphine oxide. After a column chromatography (silica, 1:10 methanol/DM) the 2-phenylaziridine was obtained as a high polar colorless liquid (0.3 g, 11%).

$^1\text{H NMR}$ (300MHz, CDCl_3) δ 7.44-7.20(m, 5H), 3.01-2.98(m, 1H), 2.19(d, 1H, $J=6.3\text{Hz}$), 1.78(d, 1H, $J=3.0\text{Hz}$)

6.58 Preparation of 3-chloro-6-(2-phenylaziridin-1-yl)-1,2,4,5-tetrazine

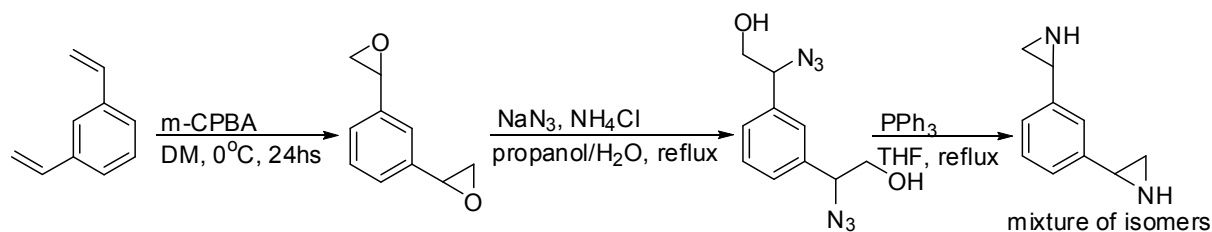


To a solution of dichloro-*s*-tetrazine (0.38 g, 2.52 mmol) and Et_3N (2.52 mmol) in 5 mL of anhydrous DM was added dropwise the aziridine (0.3 g, 2.52 mmol) by syringe. The mixture was stirred for 10 min and TLC indicated the reaction was complete. 30 mg of 3-chloro-6-(2-phenylaziridin-1-yl)-1,2,4,5-tetrazine was obtained by a column chromatography (silica, 3:7 ether/cyclohexane) as a strongly fluorescent solid (5.1%). Another 80 mg of a side product was isolated which is red but not fluorescent.

$^1\text{H NMR}$ (300MHz, CDCl_3) δ 7.44-7.38(m, 5H), 3.90(dd, 1H, $J=6.3\text{Hz}$ and $J=3.7\text{Hz}$), 3.15(d, 1H, 5.9Hz), 2.96(d, 1H, 4.4Hz)

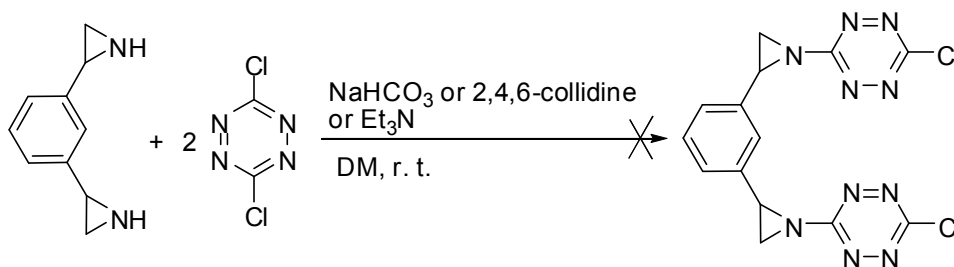
$^{13}\text{C NMR}$ (75MHz, CDCl_3) δ 170.53(tetrazine, C-Cl), 164.65(tetrazine, C-N), 135.84(phenyl), 128.84(phenyl), 128.55(phenyl), 126.57(phenyl), 42.90(aziridine, CH), 37.69(aziridine, CH_2)

6.59 Preparation of diaziridine from divinylbenzene



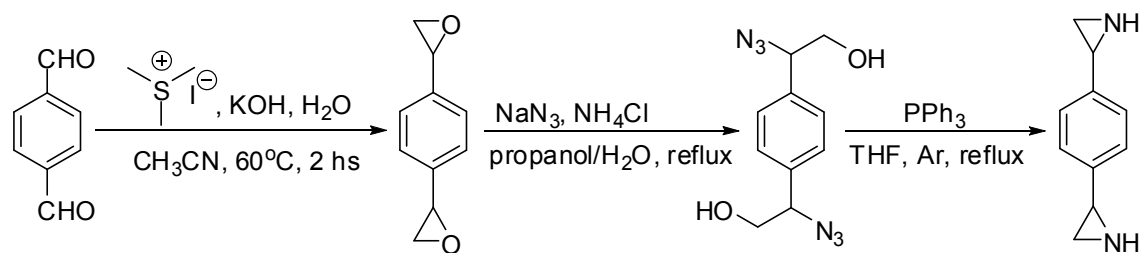
In a same manner to that described in 5.57. A mixture of para- and m- product was obtained.

6.60 Attempt for preparation of 1,3-bis(1-(6-chloro-1,2,4,5-tetrazin-3-yl)aziridin-2-yl)benzene (84)



In a same manner to that described in 5.58. Only two side products were obtained which were not fluorescent.

6.61 Preparation of 1,4-di(aziridin-2-yl)benzene



To a solution of terephthalaldehyde (1.37 g, 10 mmol) and trimethylsulfonium iodide (4.16 g, 20 mmol) in 40 mL of acetonitrile were added grinded KOH (2.5 g, 40 mmol) and 0.1 mL of water with stirring. The mixture was heated to 60°C for 3 hours and cooled to r. t.. The solids were filtered and the filtrate was concentrated by evaporation. After a column chromatography (silica, 1:3 ether/PE) 0.84 g of 1,4-di(oxiran-2-yl)benzene was obtained as a white solid (52%).

$^1\text{H NMR}$ (300MHz, CDCl_3) δ 7.28(s, 4H), 3.87(q, 2H, $J=2.2\text{Hz}$), 3.16(dd, 2H, $J=5.5\text{Hz}$ and $J=1.1\text{Hz}$), 2.80(dd, 2H, $J=5.5\text{Hz}$ and $J=2.5\text{Hz}$)

$^{13}\text{C NMR}$ (75MHz, CDCl_3) δ 137.70, 125.64, 125.63, 52.02, 52.00, 51.08, 51.06

The 1,4-di(aziridin-2-yl)benzene was prepared in a same manner to that described in 5.56 as a viscous liquid which is soluble in DMF but not in DM, EA or acetone.

2,2'-(1,4-phenylene)bis(2-azidoethanol):

$^1\text{H NMR}$ (300MHz, CDCl_3) δ 7.39-7.33(m, 4H), 4.86(dd, 1H, $J=7.4\text{Hz}$ and $J=4.4\text{Hz}$), 4.66(t, 1H, $J=6.6\text{Hz}$), 3.70(d, 2H, 6.6Hz), 3.42(m, 2H)

$^{13}\text{C NMR}$ (75MHz, CDCl_3) δ 140.91, 138.83, 135.78, 128.30, 127.31, 126.33, 74.29, 73.10, 73.07, 67.65, 66.46, 58.33, 58.05

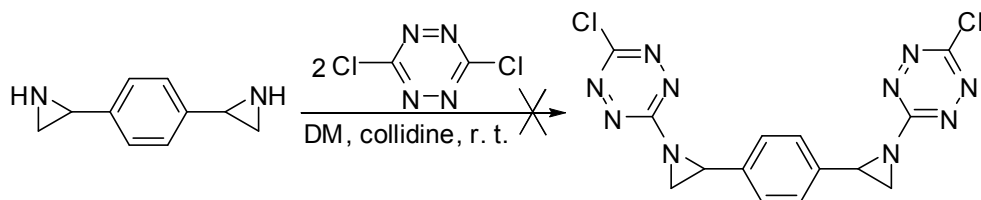
1,4-di(aziridin-2-yl)benzene:

$^1\text{H NMR}$ (300MHz, CDCl_3) δ 7.30-7.16(m, 4H), 3.99-3.95(m, 1H), 3.67-3.63(m, 1H), 3.51-3.40(m, 1H), 3.40-3.35(m, 3H), 3.2-2.4(br., 2H)

$^{13}\text{C NMR}$ (75MHz, CDCl_3) δ 141.49, 139.23, 136.75, 128.03, 126.81, 126.77, 126.00, 125.93, 125.77, 67.82, 57.11,

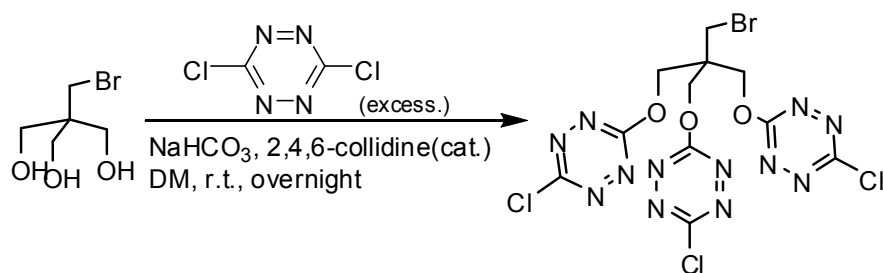
DEPT (75MHz, CDCl_3) δ 126.82, 126.79, 126.00, 125.93, 125.77, 67.80(down), 57.11,

6.62 Attempt to prepare 1,4-bis(1-(6-chloro-1,2,4,5-tetrazin-3-yl)aziridin-2-yl)benzene



The di-aziridine (32 mg, 0.2 mmol) and 2,4,6-trichloro-1,2,4,5-tetrazine (0.053 mL, 2 eq.) were added into 5 mL of anhydrous DMF with stirring. A solution of dichloro-*s*-tetrazine (60 mg, 2 eq.) in 5 mL of THF was added slowly. TLC indicated only decomposition of tetrazines.

6.63 Preparation of 6,6'-(2-(bromomethyl)-2-((6-chloro-1,2,4,5-tetrazin-3-yloxy)methyl)propane-1,3-diyl)bis(oxy)bis(3-chloro-1,2,4,5-tetrazine) (86)



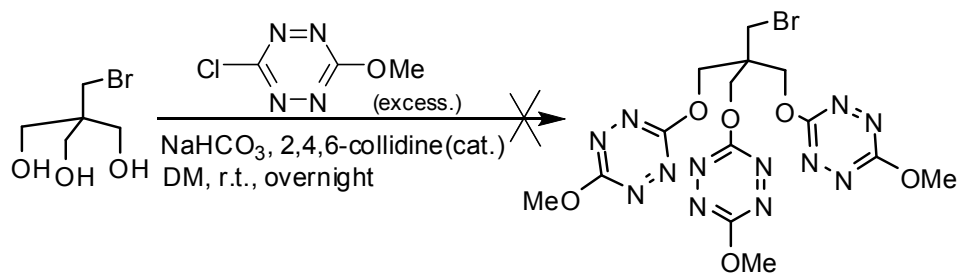
2-(bromomethyl)-2-(hydroxymethyl)propane-1,3-diol (0.2 g, 1 mmol), dichloro-*s*-tetrazine (0.45 g, 3 mmol), sodium bicarbonate (0.34 g, 4 mmol) and 2 drops of 2, 4, 6-collidine were added under Ar atmosphere into 10 mL of anhydrous DM and the mixture was stirred at r. t. overnight. The solids were filtered and washed with DM. the filtrate was concentrated by evaporation and passed through a column chromatography (silica, DM) to give 0.1 g product as a red fluorescent solid (18%).

^1H NMR (300MHz, CDCl_3) δ 5.07(s, 6H), 4.01(s, 2H)

^{13}C NMR (75MHz, CDCl_3) δ 166.42, 165.49, 68.16, 44.23, 30.92

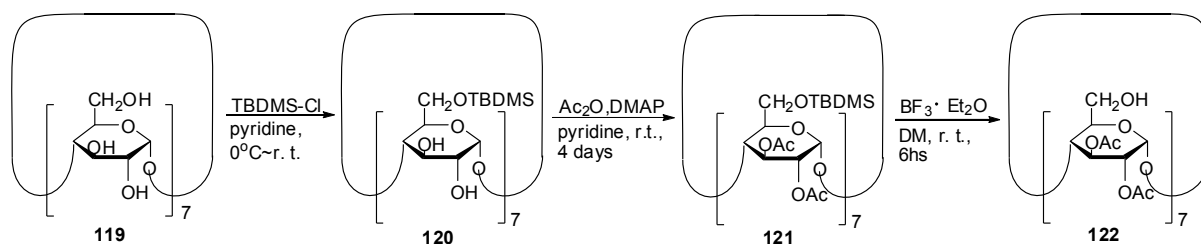
MS, m/z : 560($[\text{M}+\text{NH}_4]^+$, calc. 560, base peak), 533, 508, 479, 463, 411

6.64 Attempted preparation of tripod-methoxytetrazine (**87**)



In a same manner to that described in 5.63. Only trace of dimethoxy-*s*-tetrazine was obtained.

6.65 Modification of β -cyclodextrin



β -cyclodextrin **119** (4.54 g, 4 mmol, dried at 110°C in vacuum over P_2O_5 to constant weight before use) was dissolved in 60 mL of dry pyridine at 0°C . A solution of tert-butyldimethylsilyl chloride (4.7 g, 30 mmol) in 40 mL of dry pyridine was added slowly with stirring. The mixture was kept at 0°C for 3 hours and then at r. t. overnight. Water was added and the precipitate was collected and washed with water. Column chromatography (silica, 84:15:1 DM/methanol/ H_2O) afforded 3.76 g of tert-butyldimethylsilylated product **120** (49%).

^1H NMR (300MHz, CDCl_3) δ 6.69(s, 7H), 5.27(s, 7H), 4.89(d, 7H, $J=3.3\text{Hz}$), 4.00(t, 7H, $J=8.8\text{Hz}$), 3.90(d, 7H, $J=8.8\text{Hz}$), 3.72-3.58(m, 28H), 0.87(s, 63H), 0.03(d, 42H, $J=3.3\text{Hz}$)

^{13}C NMR (75MHz, CDCl_3) δ 102.14, 81.87, 73.73, 73.55, 72.68, 61.76, 26.03, 18.40, -4.95, -5.07

The tert-butyldimethylsilylated β -cyclodextrin **120** (1.11 g, 0.57 mmol) was dissolved in 4 mL of dry pyridine. 3 mL of acetic acid and 20 mg of DMAP were added, and the mixture became transparent after stirring for 5 min. The mixture was stirred at r. t. for 4 days, then 5 mL of methanol was added at 0°C . The mixture was stirred for 5 min and poured into 100 mL of water. The water was extracted with EA (3×100 mL). The organic layers were combined and washed with aq. HCl (1M, 2×50 mL) and water (2×50 mL), then dried with MgSO_4 . Evaporation of the solvent afforded 1.4 g of pure acetylated tert-butyldimethylsilylated product **121** (~100%).

^1H NMR (300MHz, CDCl_3) δ 5.37-5.31(m, 7H), 5.15(d, 7H, $J=3.7\text{Hz}$), 4.70(dd, 7H, $J=9.9\text{Hz}$ and $J=3.7\text{Hz}$), 4.05-3.70(m, 21H), 2.09-2.04(m, 49H), 0.88(s, 63H), 0.04(d, 42H, $J=2.2\text{Hz}$)

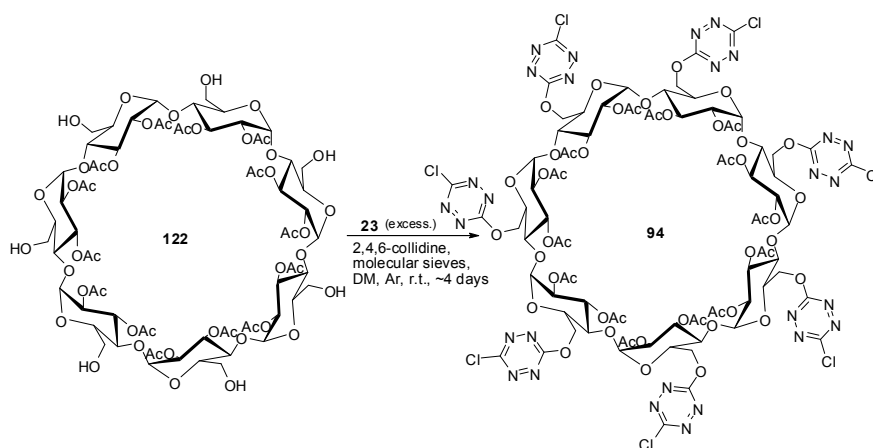
^{13}C NMR (75MHz, CDCl_3) δ 170.90, 169.57, 96.58, 75.36, 71.96, 71.69, 71.35, 61.96, 25.98, 21.02, 20.88, 18.37, -4.88, -5.16

To a solution of Ac-TBDMS- β -cyclodextrin **121** (1.4 g, 0.55 mmol) in 20 mL of dry DM was added boron trifluoride etherate in ether (48%, 2 mL, 23 mmol) at r. t. and the mixture was stirred under Ar atmosphere for 6 hours. The mixture was diluted with 40 mL of DM, then poured into ice water. The organic layer was separated and washed with aq. NaHCO_3 and water, then dried with Na_2SO_4 . A column chromatography (silica, 8:1 \rightarrow 4:1 chloroform/ methanol) afforded 0.64 g of desilylated product **122** (68%).

^1H NMR (300MHz, DMSO-d_6) δ 5.25(t, 7H, $J=9.0\text{Hz}$, H-3), 5.09(d, 7H, 3.0Hz, H-1), 4.80-4.78(m, 7H, H-2), 4.59(dd, 7H, $J=10.3\text{Hz}$ and $J=2.9\text{Hz}$, H-5), 3.86-3.80(m, 21H, H-6+OH), 3.62(d, 7H, $J=7.7\text{Hz}$, H-4)

^{13}C NMR (75MHz, DMSO-d_6) δ 170.20(C=O), 169.35(C=O), 95.97(C-1), 75.24(C-4), 72.00(C-2), 70.69(C-3), 70.41(C-5), 59.61(C-6), 20.62(Me), 20.54(Me)

6.66 Synthesis of β -cyclodextrin-tetrazine (**94**)



Three methods were tried to link tetrazines onto the CD ring: when NaHCO_3 was used as base, only a complicated mixture of tetrazine-containing products was obtained; when 2,4,6-collidine was used as base and without molecular sieves, the target molecule could be obtained but in low yield; with collidine as base and molecular sieves inside, a yield of more than 50% could be achieved.

Method 1.

Ac-protected β -cyclodextrin (20mg, 0.012mmol), dichloro-*s*-tetrazine (14mg, 0.093mol, 8eq.), NaHCO₃ (6.8mg, 0.08mmol, 7eq.), 1g MgSO₄ and 1 drop of 2,4,6-collidine were added into 15mL of anhydrous dichloromethane under argon atmosphere at room temperature. The mixture was stirred in the darkness at room temperature and under argon atmosphere for 6 days. The solids were filtrated and washed twice with dichloromethane. TLC (1:20 methanol/dichloromethane) indicated a lot of red fluorescent tetrazine-containing products which couldn't be separated by column chromatography.

Method 2.

50 mg of Ac-protected β -cyclodextrin and 50 mg of dichloro-*s*-tetrazine were dissolved in 20mL of anhydrous dichloromethane under argon atmosphere at room temperature. 0.04 mL of 2,4,6-collidine (0.3mmol, 10 eq.) was added dropwise by syringe and the mixture was stirred at room temperature and under argon atmosphere for 6 days. TLC (1:15 methane/DM) indicated a lot of tetrazine decompositions and a main product (Rf=0.4). The solids were filtrated and washed twice with dichloromethane. The filtrate was concentrated by evaporation. After a long column chromatography (silica, 1:20 methanol/DM) 10mg of red solid was obtained (yield 13.7%).

Method 3.

To an 100-mL pre-dried 1-necked round bottom flask equipped with an Ar balloon and a magnetic stirring bar was added 50mg of Ac-protected β -cyclodextrin (0.029mmol), 50mg of dichloro-*s*-tetrazine (0.33mmol, 11eq.), 30mL of anhydrous dichloromethane and 5 g of 3 Å molecular sieve (activated at 200 °C for 2 hours before use). 0.04 mL of 2,4,6-collidine (0.3mmol, 10 eq.) was added dropwise by syringe, and the mixture was stirred at room temperature for 4 days. The solids were filtrated and washed twice with dichloromethane. The filtrate was concentrated by evaporation. After a column chromatography (silica, 1:20 methanol/DM) 39 mg of pure red solid was obtained (yield 53%).

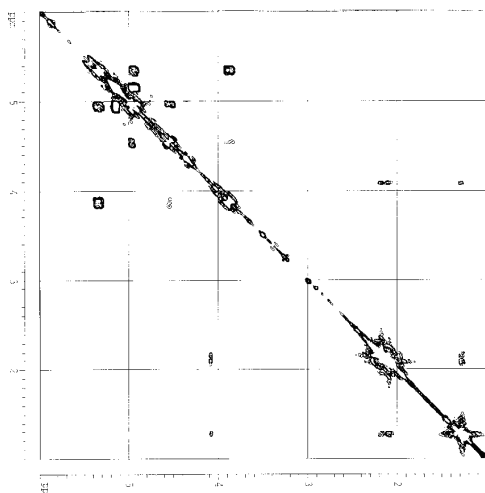
¹H NMR (300MHz, CDCl₃) δ 5.34-5.29 (m, 7H, H-3), 5.12 (d, 7H, J=4.0Hz, H-1), 4.94-4.90 (m, 21H, H-2,6,6'), 4.53-4.50 (m, 7H, H-5), 3.85 (7H, t, J=6.9Hz, H-4), 2.15 (21H, s, Ac), 2.06 (21H, s, Ac)

¹³C NMR (75MHz, CDCl₃) δ 170.47 (Ac), 169.60 (Ac), 166.31 (C-tetrazine), 164.76 (C-tetrazine), 97.73 (C-1), 77.34 (C-4), 70.55 (C-3), 70.23 (C-5), 69.31 (C-2), 68.89(C-6), 20.84 (Ac), 20.78 (Ac)

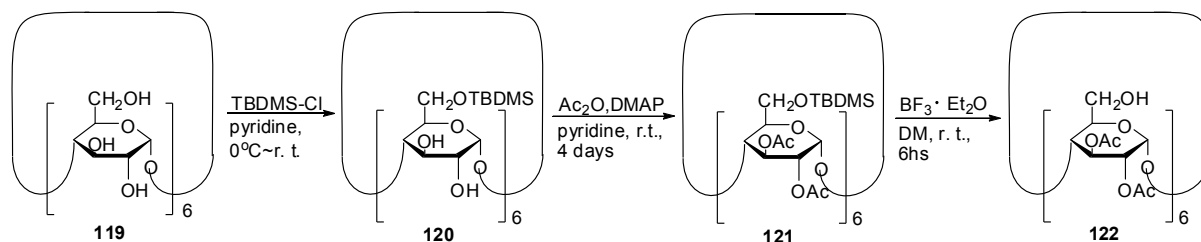
DEPT (75MHz, CDCl₃) δ 97.73, 77.60, 70.55, 70.23, 69.32, 68.89(down), 20.86, 20.81

M.S. (TOF), m/z: 2543.34 ([MNa⁺], calc. 2543.32).

H-H COSY



6.67 Modification of α -cyclodextrin



In a same manner to that described in 5.65:

Tert-butyldimethylsilylated α -cyclodextrin, yield 88%

^1H NMR (300MHz, CDCl_3) δ 6.53(s, 6H), 5.27(s, 6H), 4.88(d, 6H, $J=2.9\text{Hz}$), 4.04-3.54(m, 18H), 0.88(s, 54H), 0.04(d, 36H, $J=2.2\text{Hz}$)

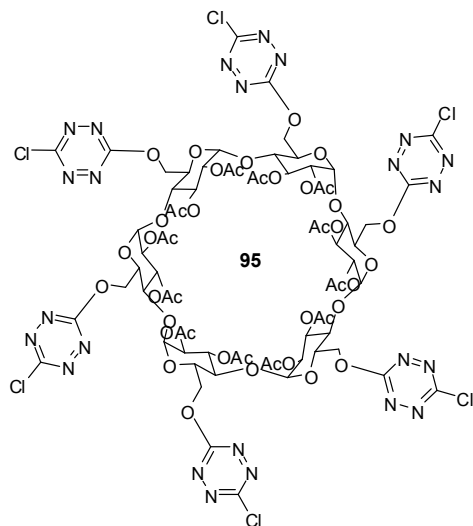
Acetylated tert-butyldimethylsilylated α -cyclodextrin, yield 97%

^1H NMR (300MHz, CDCl_3) δ 5.46(t, 6H, $J=9.0\text{Hz}$), 5.08(d, 6H, $J=3.3\text{Hz}$), 4.69(dd, 6H, $J=10.3\text{Hz}$ and $J=0.6\text{Hz}$), 4.11-3.99(m, 6H), 3.88-3.85(m, 6H), 3.68(d, 6H, $J=11.8\text{Hz}$), 2.05-2.03(m, 42H), 0.88(s, 54H), 0.04(d, 36H, $J=2.6\text{Hz}$)

^{13}C NMR (75MHz, CDCl_3) δ 170.82, 169.57, 96.79, 75.51, 72.20, 72.00, 71.44, 61.98, 21.04, 20.86, 18.37, -4.86, -5.16

Desilylated acetyl α -cyclodextrin, yield 80%.

6.68 preparation of α -cyclodextrin-tetrazine (95)



In a same manner to that described in 6.66 Method 3. $R_f=0.3$ (silica, 1:20 methanol/DM).

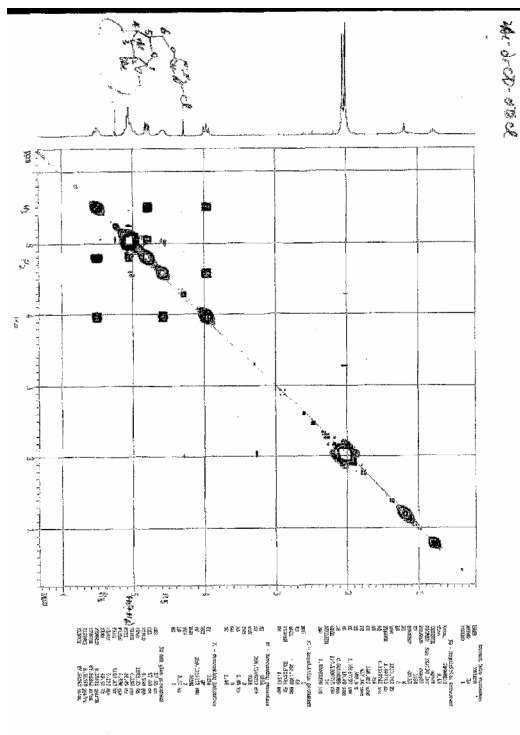
α -cyclodextrin-tetrazine, yield 50%.

^1H NMR (300MHz, CDCl_3) δ 5.56(t, 6H, $J=8.8\text{Hz}$), 5.12-5.01(m, 18H), 4.85(dd, 6H, $J=9.9\text{Hz}$ and $J=3.7\text{Hz}$), 4.63-4.61(m, 6H), 4.01(t, 6H, $J=8.6\text{Hz}$), 2.10(s, 18H), 2.06(s, 18H)

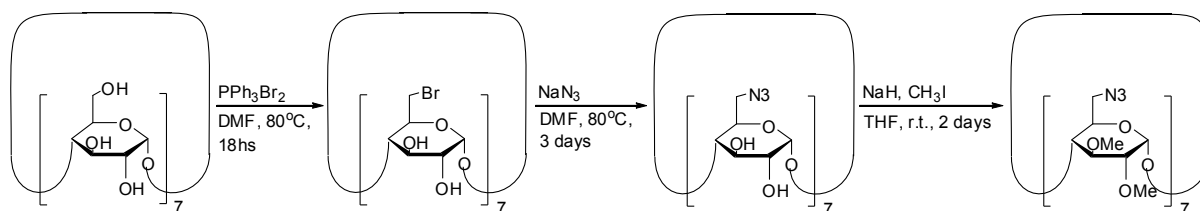
^{13}C NMR (75MHz, CDCl_3) δ 170.39, 169.47, 166.26, 164.65, 97.20, 77.10, 70.57, 70.56, 70.00, 68.71, 20.85, 20.82

DEPT (75MHz, CDCl_3) δ 97.20, 77.10, 70.54, 70.01, 68.71(down), 20.88, 20.85

H-H COSY



6.69 Preparation of 6-azido-2,3-O-methyl-6-deoxy- β -cyclodextrin



Br₂ (3.64 mL, 70.7 mmol) was added slowly by syringe into a solution of PPh₃ (18.7 g, 70.7 mmol) in 70 mL of anhydrous DMF at 0°C. The mixture was warmed to r. t. and stirred for 20 min, then β -cyclodextrin (4.5 g, 3.95 mmol, dried over P₂O₅ in vacuum at 110°C for 3 hours) was added in one portion. The mixture was heated to 80°C for 18 hours, after which time it was concentrated to half of the volume, and neutralized with 25 mL of 3 N NaOMe in methanol. The mixture was stirred for 0.5 hour and then poured into 500 mL of cold water. A white solid was precipitated, which was collected by filtration and washed with water. The solids were dispersed in 200 mL of dichloromethane, stirred for 15 min, and then filtered and washed with dichloromethane. The solids were dissolved in 50 mL of DMF and precipitated again by addition of 200 mL of ice water. After filtration and dryness 3 g of bromo- β -cyclodextrin was obtained as a white solid (48%).

¹H NMR (300MHz, DMSO-d₆) δ 6.04(d, 7H, J=7.0Hz), 5.91(d, 7H, J=0.5Hz), 4.98(d, 7H, J=3.3Hz), 4.01(d, 7H, J=9.9Hz), 3.83(t, 7H, J=8.0Hz), 3.40(q, 14H, J=7.0Hz), 3.34(s, 14H)

¹³C NMR (75MHz, DMSO-d₆) δ 102.07, 84.58, 72.24, 72.01, 70.94, 64.86

Bromo- β -cyclodextrin (1.9 g, 1.2 mmol) and sodium azide (3.47 g, 53.4 mmol) were added in to 40 mL of anhydrous DMF and the mixture was heated to 80°C for 3 days. The solvent was evaporated and the residue was dispersed in water, then filtered and washed with

water. After drying in vacuo the solids were washed with ether and dichloromethane and dried again to afford 1.3 g β -cyclodextrin-azide (83%).

^1H NMR (300MHz, DMSO- d_6) δ 5.93-5.75(m, 21H), 4.91(s, 7H), 3.80-3.36(m, 35H)

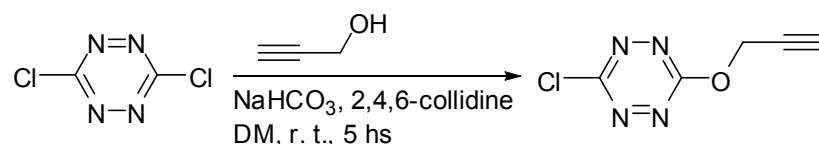
^{13}C NMR (75MHz, DMSO- d_6) δ 102.02, 83.33, 72.55, 71.98, 70.39, 51.32

NaH (60% dispersion in oil, 1.44 g, 36 mmol) was washed with cyclohexane 4 times in an 100-mL flask and then 20 mL of anhydrous THF was added. The mixture was cooled to -5°C with an ethanol-ice bath, and then β -cyclodextrin-azide (1.3 g, 1 mmol) was added in several portions. The mixture was stirred at r. t. for 45 min, then methyl iodide (2.24 mL, 36 mmol) was added and the mixture was stirred for 2 days, then poured into water. The aqueous phase was extracted with dichloromethane 4 times, and the organic layers were combined and dried with MgSO_4 . After a column chromatography (silica, DM \rightarrow EA) the methoxy- β -cyclodextrin-azide was obtained as a white solid (1.17 g, 78%).

^1H NMR (300MHz, CDCl_3) δ 5.03(d, 7H, $J=3.7\text{Hz}$), 3.73-3.68(m, 7H), 3.67-3.57(m, 7H), 3.56-3.51(m, 28H), 3.47-3.36(m, 35H), 3.12(dd, 7H, $J=9.2\text{Hz}$ and $J=3.7\text{Hz}$)

^{13}C NMR (75MHz, CDCl_3) δ 98.59(C-1), 81.52(2C), 80.88, 70.88, 61.36(OMe), 58.75(OMe), 51.74(CH_2N_3)

6.70 Preparation of 3-chloro-6-(prop-2-ynoxy)-1,2,4,5-tetrazine

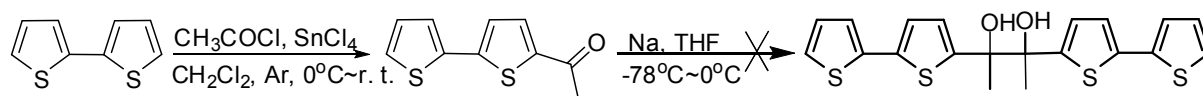


Dichloro-*s*-tetrazine (0.1 g, 0.66 mmol), propargyl alcohol (0.04 mL, 0.66 mmol), 2,4,6-collidine (3 drops) and NaHCO_3 (0.055 g, 0.66 mmol) were added into 20 mL of DM and the mixture was stirred for 3 hours at r. t.. The solvent was evaporated and the residue was passed through a short column chromatography (silica, DM) to give 3-chloro-6-(prop-2-ynoxy)-1,2,4,5-tetrazine as an orange solid (0.27 g, 85%).

^1H NMR (300MHz, CDCl_3) δ 5.29(d, 2H, $J=2.2\text{Hz}$), 2.63(t, 1H, $J=2.2\text{Hz}$)

^{13}C NMR (75MHz, CDCl_3) δ 166.07, 165.18, 77.50, 75.75, 57.82

6.71 Preparation of acetyl bithiophene



Acetyl chloride (0.085 mL, 1.17 mmol) and tin(IV) chloride (0.14 mL, 1.17 mmol) were mixed in 10 mL of anhydrous DM in a dropping funnel and added dropwise into a solution of 2,2'-bithiophene (0.2 g, 1.17 mmol) in 20 mL of DM at 0°C . After the addition the mixture was stirred at 0°C for 2 hours, and 20 mL of water was added. The organic layer was separated and the water layer was extracted once with DM. The DM layers were combined and washed with aqueous NaHCO_3 , then dried with MgSO_4 . A short column chromatography (silica, DM) afforded 0.2 g of acetyl bithiophene as a yellow solid (82%).

^1H NMR (300MHz, CDCl_3) δ 7.58(d, 1H, $J=3.7\text{Hz}$), 7.33-7.31(m, 2H), 7.17(d, 1H, 4.1Hz), 7.07-7.04(m, 1H), 2.55(s, 3H)

^{13}C NMR (75MHz, CDCl_3) δ 190.46, 145.88, 142.56, 136.47, 133.39, 128.35, 126.60, 125.75, 124.25, 26.64

The acetyl bithiophene (0.1 g) was dissolved in 5 mL of anhydrous THF. The solution was cooled to -78°C , and 0.012 g of Na was added. The mixture was warmed slowly to r. t., then to 50°C . TLC (DM) indicated no reactions.

Part II

Synthesis and electrochemical study of ferrocene-containing pyridinium salts

Chapter 1 Introduction

1.1 Introduction of ferrocene

Ferrocene (Figure 1) was discovered for the first time unexpectedly by T. J. Kealy and P. L. Pauson in the early 1950's, when they were trying to synthesize fulvene from cyclopentadienyl magnesium bromide and iron (III) chloride. The mechanism is that Fe^{3+} is firstly reduced by Grignard reagent and then reacts with $\text{C}_5\text{H}_5\text{MgBr}$ to give ferrocene. Almost at the same time, Miller and co-workers have also obtained ferrocene through reactions of Fe with cyclopentadiene under high or normal atmosphere¹. In 1952, Wilkinson and Woodward² have elucidated from measurements of IR, magnetic susceptibility and dipole moment the structure of ferrocene, which was confirmed by X-ray crystallography afterward. The special structure, bonding and aromaticity of ferrocene defied conventional bonding descriptions, thus stirred up the imagination of chemists consumedly. The discovery and characterisation of the structure of ferrocene opened up a new area of chemistry, leading to an explosion of interest in d-block metal carbon bonds and bringing about development and the now flourishing study of organometallic chemistry.

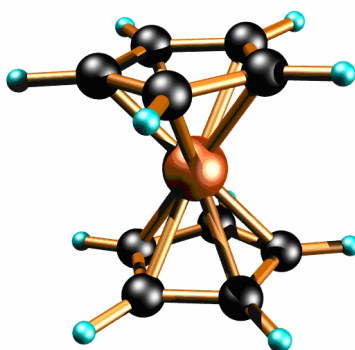


Figure 1. Structure model of ferrocene.

The research for the synthesis, structures and properties of ferrocene derivatives has been continually active during the last several decades. Many ferrocene derivatives have been synthesized and their properties and applications have been thoroughly explored, which has promoted the development of the theory of chemical bond and the structural chemistry. During recent years, based on development in electrochemical technologies, great progress has been made in the research of basic electrochemical behaviors of ferrocene and its derivatives, their applications in intermolecular electron transfer research, electrocatalysis, electroanalysis, molecular recognition, etc..

1.2 Basic electrochemical behaviors

A number of the ferrocene derivatives have been synthesized and used as electronic and optical materials because the cyclopentadienyl (Cp) ligand of ferrocene is readily functionalized by nucleophilic organic reagents and because

electrochemical properties of the Fe(II)Cp₂ fragment can be tuned by selecting the substituents introduced on the Cp ligand. The oxidation between the neutral Fe(II) state and cationic Fe(III) state, involving fast and reversible electron transfer, is the important property of the ferrocene derivatives. Introduction of electrochemically active organic groups on the ligand of ferrocene leads to molecules containing both organometallic and organic redox-active centers, which can be used as electrochemical materials in various applications.

1.3 Development in research of molecules containing multiple ferrocenes

1.3.1 Molecules containing two ferrocene units

There is a growing interest in the study of electron or energy transfer between two redox active and/or photoactive termini across an unsaturated organic bridge³⁻⁷. Molecular wires comprising mixed-valence bimetallic fragments could be used for applications in molecular electronics, optoelectronic devices, and chemical sensor appliances. Systems incorporating ruthenium polypyridyl⁸⁻¹¹ or ferrocene¹²⁻¹⁸ moieties are known with oligoene or oligoyne spacers, and alternations of the bridges with arenes have been explored. In most of the biferrocenes studied, the ferrocene units are linked either directly or using a polyene bridge. If the bridging ligands are phenylene vinylene oligomers, the biferrocenes exhibit a rather diminished solubility, and use of permethylated cyclopentadienyl units is necessary to overcome this drawback. This modification in the cyclopentadienyl moiety also enhances the stability of the oxidized ferrocenium species.

Polyalkene species present high electron transmission efficiency, but their thermal and photochemical instability pose severe drawbacks. On the other hand, the efficiency of the more stable aromatic and acetylene-based systems appears limited by excessive charge confinement. Thiophene-2,5-diylvinylene oligomers are considered a good tradeoff between the efficiency of polyethylenic systems and the stability of the polyaromatic ones¹⁹⁻²¹. Due to this, thiophene-based oligomers and polymers are regarded to have potential for technological applications in electrical and optical devices^{22, 23}. The solubility of the thiophene derivatives can be increased when warranted by incorporating alkyl chains in the 3- and 4-positions of the thiophene nucleus.

Despite these advantages, the reports of ferrocene complexes containing thiophene are very limited. Lin and co-workers²⁴ have designed and synthesized a series of bis-ferrocenes linked by thienyl or furanyl vinyl and thienyl ethynyl spacers (Figure 2).

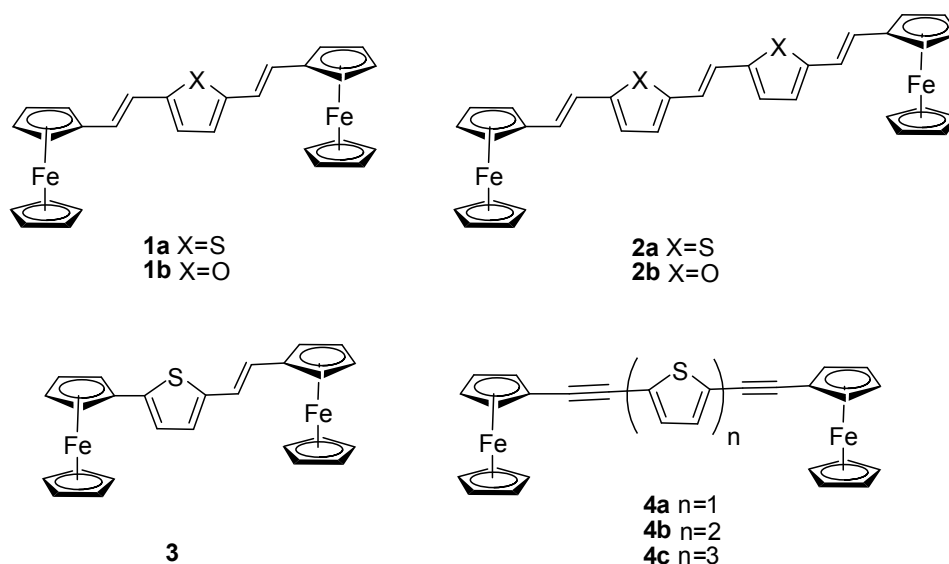


Figure 2. Bis-ferrocenes containing thiophene as spacers.

Cyclic voltammetry (CV) and Osteryoung square wave voltammetry (OSWV) were used to investigate the possibility of “electronic communication” between the two metal centers in these homobimetallic complexes. The results of these electrochemical studies indicated that the proximal disposition of ferrocenyl units in **1a** enhances the through-space electronic communication; in **3**, the two ferrocenyl groups weakly communicate through the less aromatic thiophene conjugation chain. The metal-metal interaction is weak but greater than that in the corresponding phenylene analogues.

Sato and co-workers²⁵ have prepared hexyl-sexithiophene (FHST) and methoxy-terthiophene (FMTT) derivatives with two terminal ferrocenyl groups as model compounds of molecular wires (Figure 3). Electrochemical measurements and absorption spectroscopy were performed to elucidate the oxidation process and the properties of the oxidized states of those model compounds. The first oxidation of the model compounds takes place on one of the terminal ferrocene moieties. In the hexyl-sexithiophene derivative, the resultant oxidized state seeps into the sexithiophene link. In the methoxy-terthiophene derivative, the oxidized species spreads over the entire molecule encompassing the terthiophene link and the other ferrocene moiety, indicating a charge transfer between the terminal complexes via the wire. These conclusions suggest that it is important in the “molecular wire” architecture to coordinate a wire and a terminal, and multi-thiophenes act as good “wire” for electron and charge transfer.

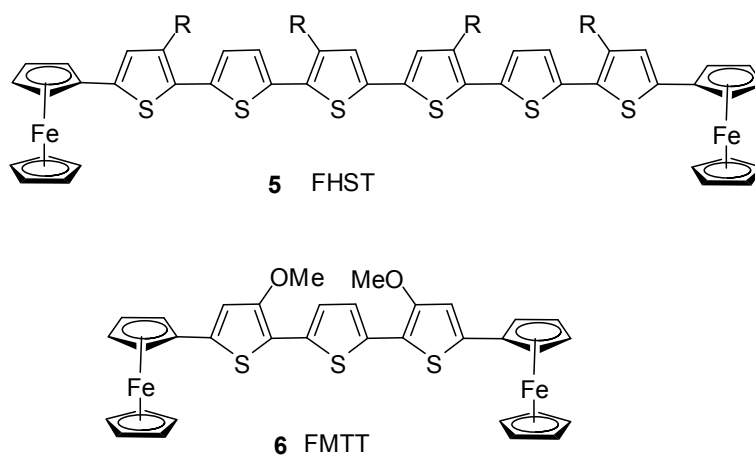


Figure 3. Bis-ferrocenes connected with thiophenes.

Wong and co-workers have synthesized and characterized a new class of biferrocenes bearing some fluorenebased spacers covalently appended to the redox-active ferrocenyl center via an ethynyl bridge (Figure 4). These bis(alkynyl) species are electrochemically active and cyclic voltammetric studies in CH_2Cl_2 solutions reveal that each complex undergoes a concomitant oxidation of the ferrocenyl subunits that are present, the $E_{1/2}$ value of which is influenced by the electronic effect of the substituent at the periphery of the central fluorenyl moiety. However, there is only a very weak electronic communication between the terminal ferrocenyl electrophores.

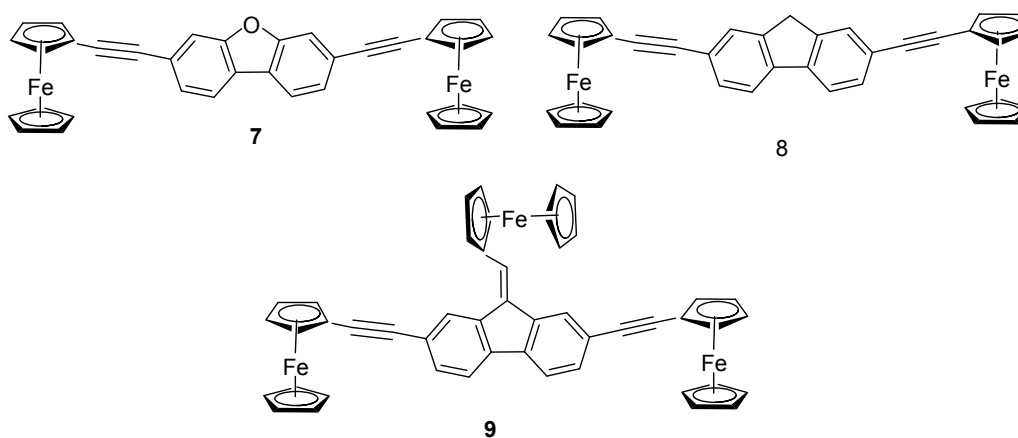


Figure 4. biferrocenes bearing fluorenebased spacers.

Matsuo and colleagues²⁶ have recently reported the synthesis and electrochemistry of a new class of linked diferrocenes that they called double-decker buckyferrocenes **13** and **14** (Figure 5). The linker unit consists of a hoop-shaped, 40 π -electron[10]cyclophenacene and homoconjugatively allows electronic communication between the two ferrocene moieties. They have developed two synthetic approaches to these double-decker buckyferrocenes, which are potentially suitable for synthesis of a variety of bimetallic [60]-fullerene metal complexes possessing symmetric and dissymmetric organic substitution patterns and the same or different metal atoms. The multistep redox behavior accepting and giving up a total of at least four electrons makes these complexes interesting subjects of inorganic and materials studies. They showed that photoexcitation of the buckyferrocene **12** results in the formation of a charge-separated state (ferrocenium and fullerene radical anion),

which agrees with the presence of electronic communication between the two ferrocene moieties in **14**. Given the self-assembling behavior of pentaorganofullerene derivatives, higher-order aggregated structures of the dimetallic complexes will be an intriguing subject of further studies.

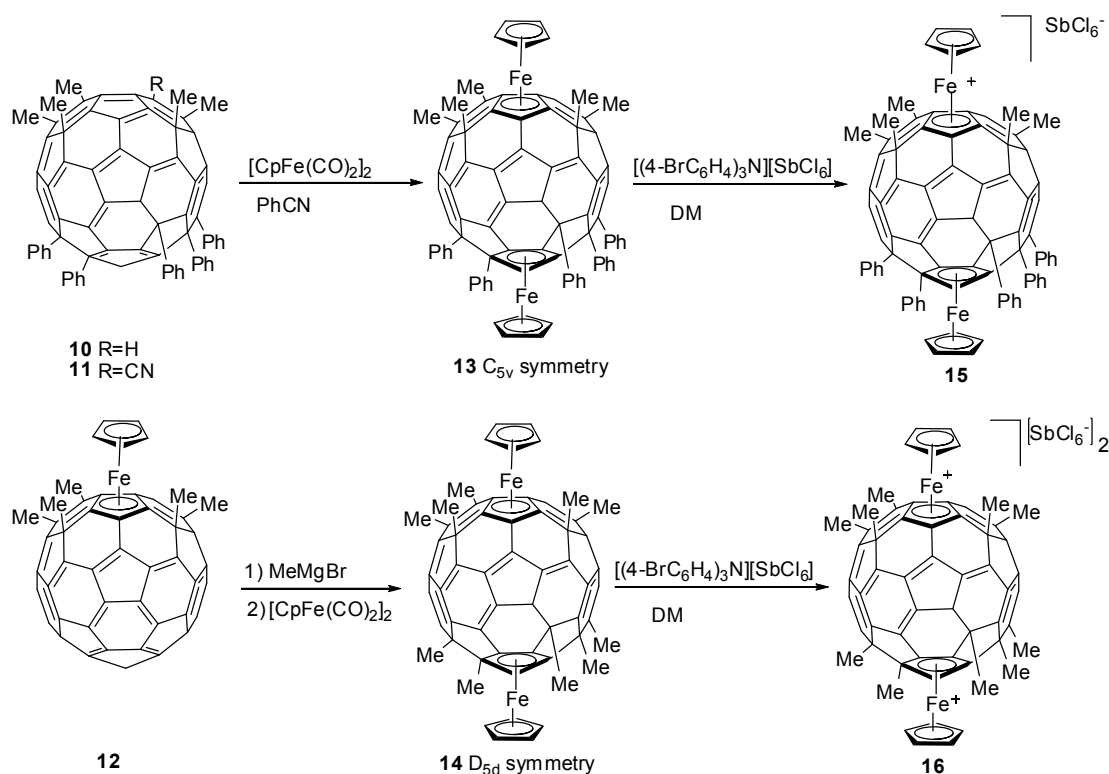
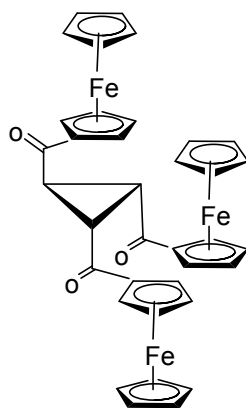


Figure 5. Double-decker buckyferrocenes.

1.3.2 Molecules containing multiple ferrocene units

Electroactive compounds containing multiple but identical redox units are of much current interest because of their potential use as electrode modifiers, multi-electron redox catalysts and electron reservoirs or batteries^{27, 28}. A wide variety of such redox-active compounds have been studied towards these aims²⁹⁻³². Ferrocene, owing to its chemical stability, well-defined electrochemistry such as stable reversible redox properties³³, and ease of functionalization, makes multiple ferrocene-containing compounds the most studied variety in the multiple redox-center containing molecular systems³⁴⁻⁴⁰.

Molina and co-workers⁴¹ have synthesized a molecule containing three ferrocenes on a cyclopropane backbone (Figure 6). The ¹H-NMR spectrum of this tris(ferrocene) compound shows two sets of three well-separated signals in a 2:1 ratio, characteristics of mono-substituted ferrocenes indicating that only two ferrocenyl groups are magnetically equivalents, and the ¹³C-NMR spectrum also reveals the existence in the molecule of two different types of monosubstituted ferrocenes, while cyclic voltammetry responses of the compound with scan rate increasing from 0.02 to 1.00 V s⁻¹ display only a single anodic process with features of chemical reversibility.



17

Figure 6. Tris-ferrocene with a cyclopropane backbone.

Sengupta's group has described the synthesis and electrochemistry of a covalent hexaferrocenyl cluster based on a redox passive hexavalent scaffold cyclotriphosphazene core (Figure 7)⁴². The sixfold substitution reaction of hexachloro-cyclotriphosphazene with 4-ferrocenylphenol gave a covalent hexaferrocenyl cluster, in which all six ferrocene units are electrochemically equivalent. On the other hand, reaction of hexachlorocyclotriphosphazene with ferrocene methanol only produced ferrocene aldehyde.

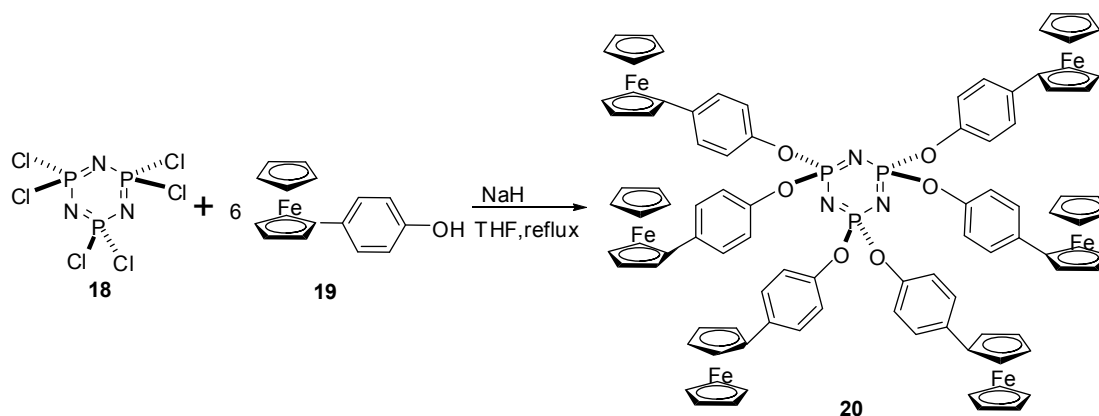


Figure 7. A hexaferrocenyl cluster based on a cyclotriphosphazene core.

Organometallic fragments assembled on substituted benzenes, polyaromatics, and heteroaromatics such as thiophenes and pyridines have received immense interest in recent years due to their potential use as models for organometallic polymers and targets for the study of electron-transfer processes. Also important is the possibility that the mixed-valence materials derived from these multi-metallic systems, after partial oxidation, may exhibit unique magnetic properties. By means of palladium-catalyzed reactions, Peruga and co-workers⁴³ have designed an effective method for the synthesis of several star-shaped ferrocenyl containing compounds. The method shows clear advantages over the traditional Wittig method for the synthesis of olefinated complexes, both in yields and in stereoselectivity of the double bond (all E isomers) (Figure 8). Unfortunately the electrochemical studies do not show any significant interactions between the iron centers of different branches, although there is an important electronic coupling in those complexes in which the ferrocene units are separated by a vinylene unit.

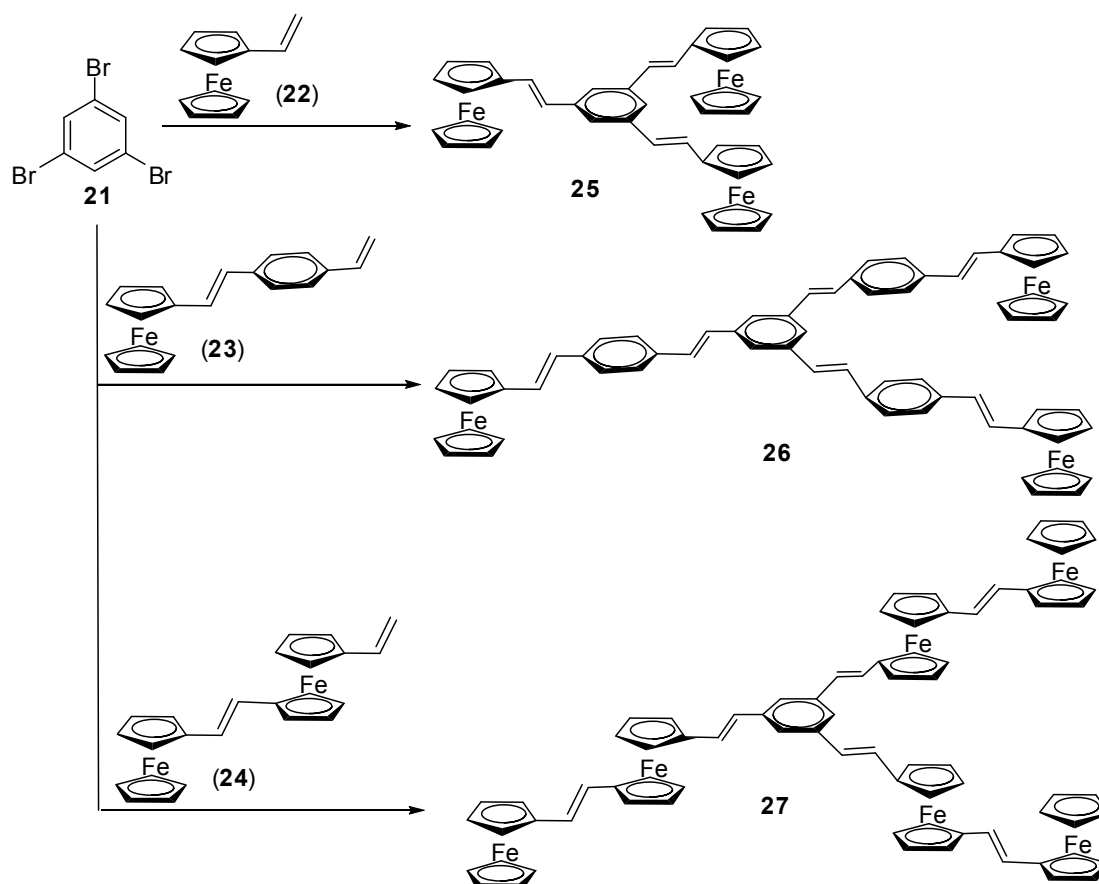


Figure 8. Star-shaped ferrocenyl containing compounds.

The compound **27** is not showing a perfect anti configuration in its neutral form. However, once fully oxidized, it must show a structural rearrangement to a fully expanded form, in which the electrostatic repulsion between all the six iron centers is minimized. This behaviour makes it a good candidate to a size tunable complex, in which the radius of this star-shaped compound can be electrochemically switched (Figure 9).

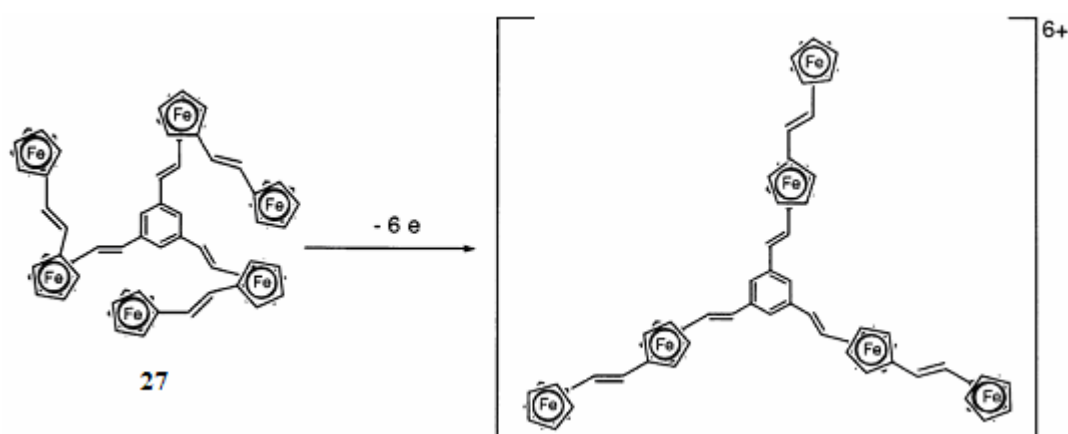


Figure 9. Electrochemical switch of configuration.

Thomas and Lin⁴⁴ have also described a series of tri- or tetra-ferrocenes, covalently attached to either triphenylamine (Figure 10) or thiophene (Figure 11) cores by a triple bond, since triaryl amines and polythiophenes are considered as important classes of compounds in materials science. Triaryl amines, owing to their

low oxidation potentials and easy glass-forming ability, are widely used as holetransporting materials in organic light-emitting diodes. Similarly, thiophenes because of their excellent electronic conducting properties find much use in the construction of opto-electronic devices. In view of these advantages, they have utilized both triphenylamine and thiophene as the core unit for the construction of polyferrocenes. Palladium-catalyzed Sonogashira coupling reactions were used for tailoring the units together by a triple bond.

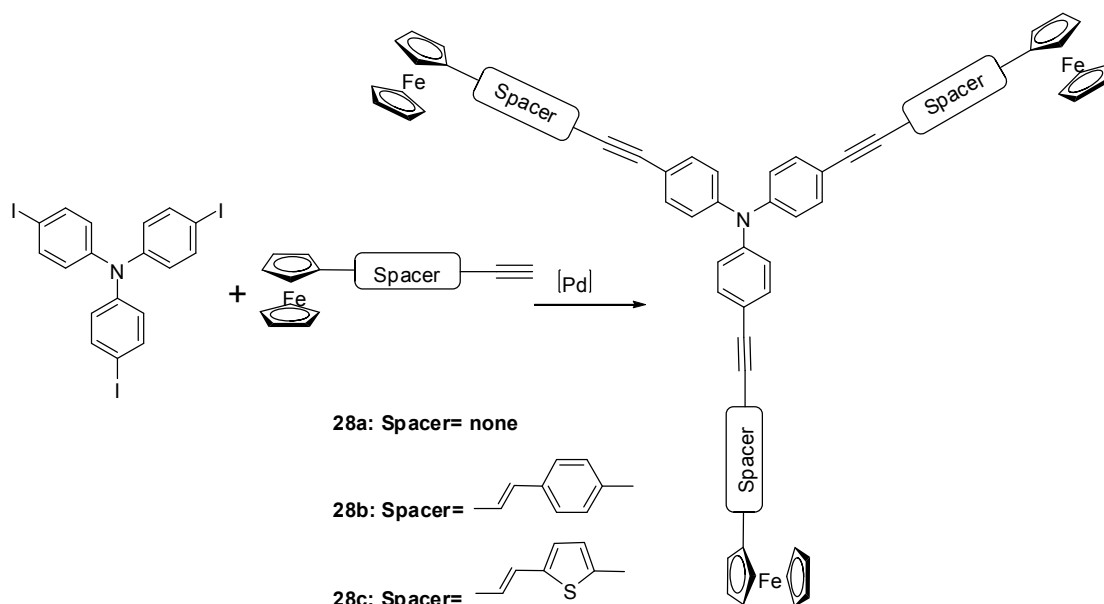


Figure 10. tri-ferrocenes, covalently attached to triphenylamine.

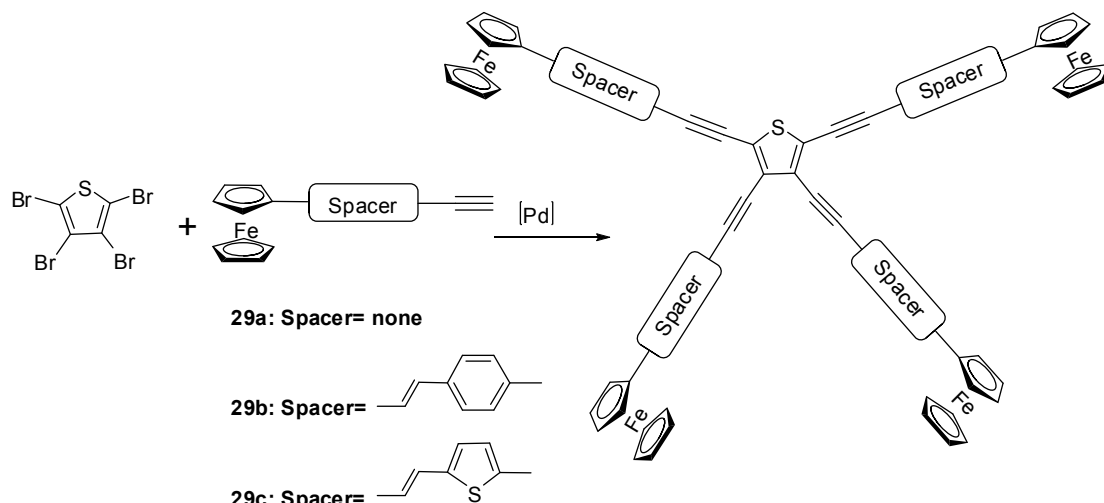


Figure 11. Tetra-ferrocenes covalently attached to thiophene.

Unfortunately, these star-shaped molecules did not exhibit any intramolecular electronic communication between the ferrocene units in these tri- or tetra-metallic systems, which is attributed to the nature and length of the conjugation chain. However, the presence of ferrocene significantly affects the electrochemical behavior of the triphenylamine or thiophene core, and the extended conjugation by triphenylamine or thiophene makes the appended ferrocenes undergo comparatively facile oxidation, indicating a weak electronic interaction between the ferrocene and the central cores (triphenylamine or thiophene).

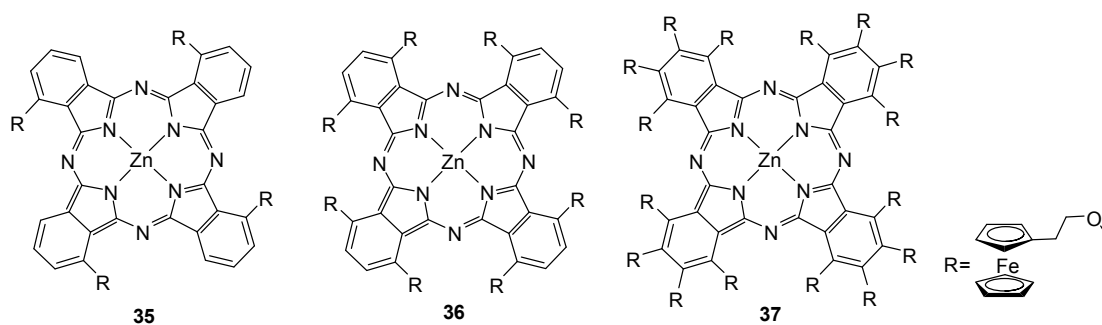


Figure 13. Phthalocyanines containing multiple ferrocenes.

Although much research interests have been focused on the synthesis and electrochemical investigation of multiferrocenyl systems as redox sensors for molecular recognition, as mediators in amperometric biosensors, as building blocks in polymers or as coatings to modify electrode surfaces, only few ferrocenyl and polyferrocenyl systems are water soluble. However, these water soluble ferrocenyl systems are of particular interest as redox mediators, for example in scanning electrochemical microscopy (SECM)⁴⁷ investigations in biological systems. Salmon and colleagues⁴⁸ have prepared and investigated the electrochemical properties of a class of water soluble multiferrocenyl compounds: through quaternization of 2-(N,N-dimethylamino)ethylferrocene or 1,1-bis(2-(N,N-dimethylamino)ethyl)ferrocene with different organic halides, molecules with up to four redox ferrocene units have been obtained (Figure 14):

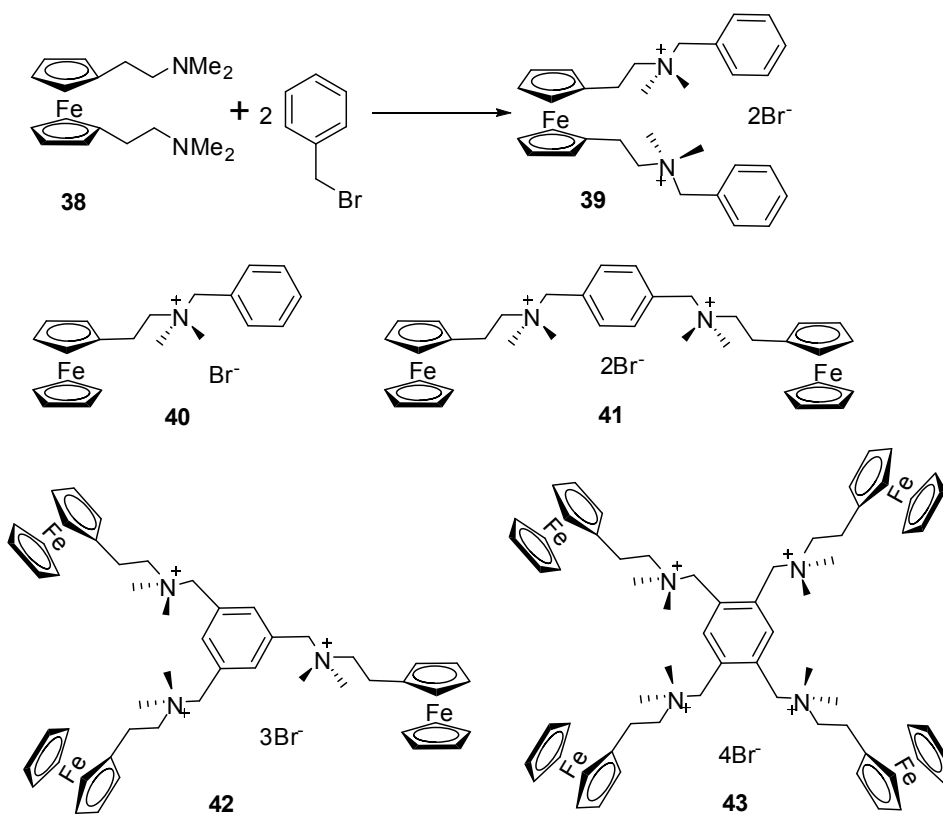


Figure 14. Polyferrocenes derived through quaternization of nitrogen.

Voltammetric investigations of the ferrocenyl systems show that the redox potential depends on the length of the carbon bridge between the redox centre and ammonium group. The diffusion coefficients of the ferrocenyl systems could be

determined by chronocoulometry and chronoamperometry in DMSO solution. The obtained values are a function of the molar weight of the molecules and allow the calculation of the hydrodynamic radii.

1.3.3 Dendrimers containing ferrocenes

The redox activity of dendrimers is of promise in applications as materials devices. The preparation and characterization of ferrocene dendrimers has received considerable attention in recent years since they illustrate the potential access to precise redox active nanoscopic molecules with original properties. Ferrocene dendrimers could serve as supramolecular receptors for molecular recognition. Various redox sensors have been reported on recognition of anions. Other supramolecular aspects of ferrocene dendrimers such as transport and self-assembly have also been exemplified.

Based on the use of well established poly(propylene imine) dendrimers, Salmon and colleagues⁴⁸ have prepared a series of water soluble ferrocene-containing dendrimers: the reductive amination of formyl ferrocene with the NH₂-functions of these macromolecules leads to ferrocenyl dendrimers with 4 to 64 ferrocene units (Figure 15). The multi ammonium salts of these compounds exhibit solubility only in polar solvents. All prepared ferrocene dendrimers have been studied with voltammetric, amperometric and coulometric techniques.

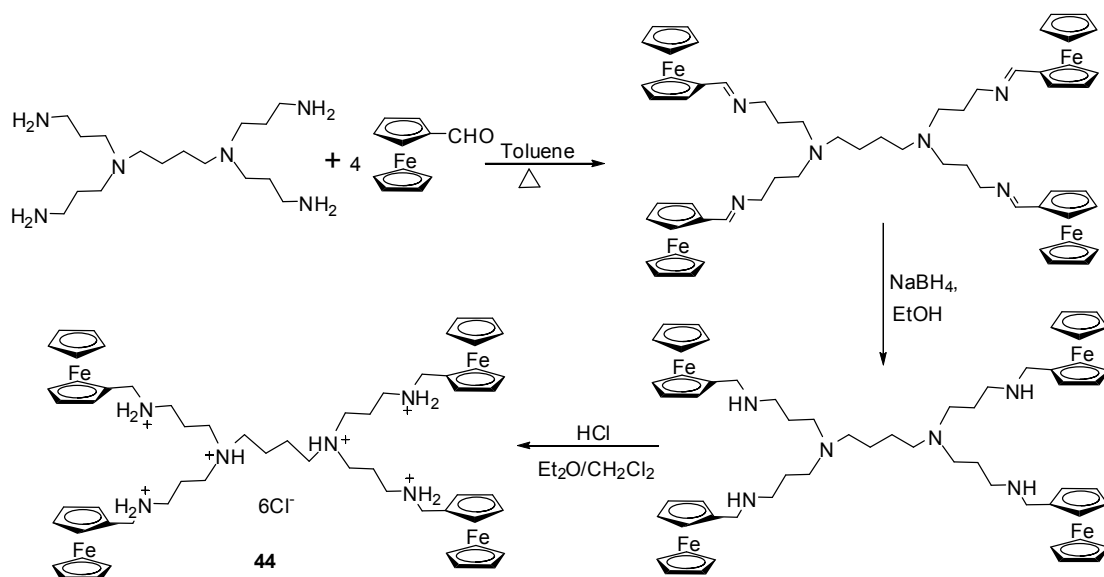


Figure 15. Water soluble poly(propylene imine) dendrimers with 4 ferrocene units.

Astruc's group has synthesized and studied several novel ferrocene-containing dendrimers. For example, based on reactions of amine dendrimers with FcCOCl, they have synthesized several polyamidoferrocene dendrimers containing 3 (compound **45**), 9 (compound **46**) or 18 (compound **47**) ferrocene units (Figure 16)⁴⁹. Titrations of these dendrimers by n-Bu₄N⁺ salts of H₂PO₄⁻, HSO₄⁻, Cl⁻, Br⁻, and NO₃⁻ and monitoring by cyclic voltammetry and ¹H-NMR indicated a remarkable dendritic effect in the recognition of small anions.

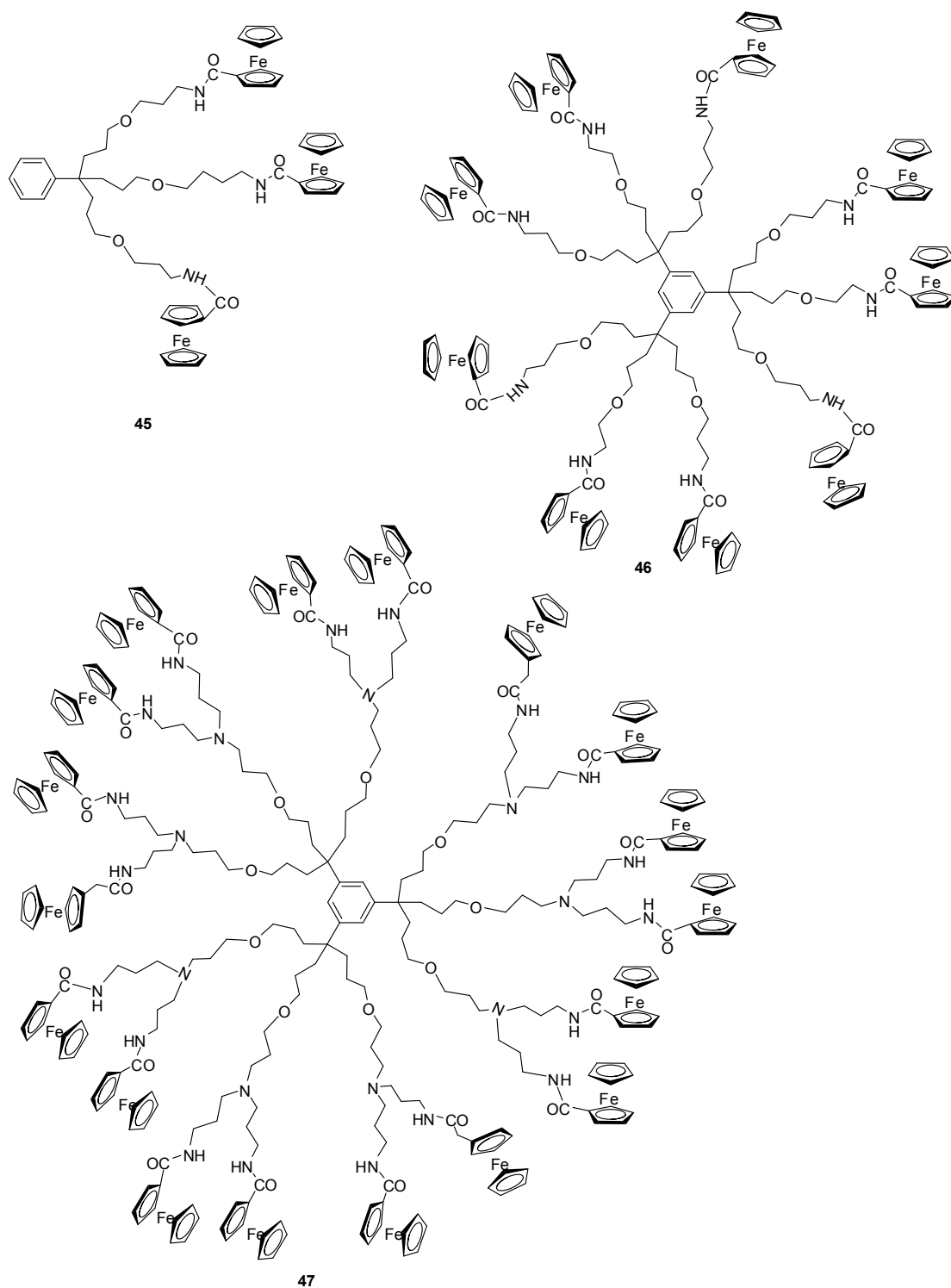


Figure 16. Ferrocene dendrimers synthesized in Astruc's group.

Astruc and colleagues⁵⁰ have also explored the self-assembling of redox-active ferrocene dendrimers (**48**) by multiple H-bonding to possibly benefit from positive dendritic effects for the recognition of anions such as H_2PO_4^- (Figure 17). The titration experiments showed new positive dendritic effects characteristic of amidoferrocenyl dendrimers assembled by H-bonding. They rationalized the completely unusual trends found during electrochemical monitoring of the titration

(half-stoichiometry, sudden wave change, dramatic intensity decrease) in terms of the formation of a dendritic assembly, in which each H_2PO_4^- unit links two amidoferrocenyl groups at the dendrimer periphery.

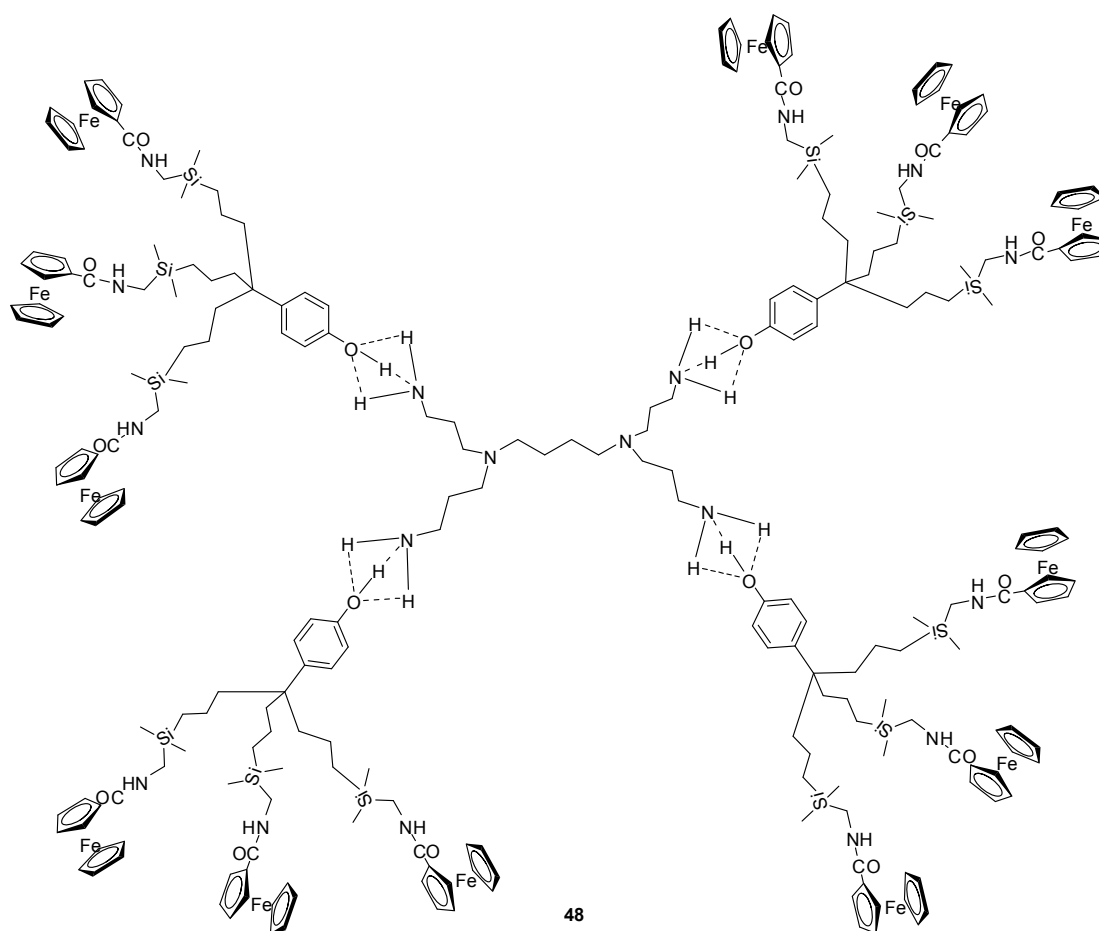


Figure 17. Ferrocene dendrimers assembled by multiple H-bonding.

A 54-ferrocene dendrimer has also been synthesized in their group⁵¹, by a convergent route and can be used to modify a Pt electrode. The dendrimer can be reversibly oxidized in DMF in a single 54-electron wave. The electrochemical reversibility observed for the oxidation of **49** indicates that the structural rearrangement between **49** and $\mathbf{49}^{54+}$ is small. Since the repulsion between the positively charged ferrocenium units in $\mathbf{49}^{54+}$ requires that they be at the periphery of the dendrimer with maximum space expansion, the shape of **49** is relatively closely related to that of $\mathbf{49}^{54+}$. The fact that a single reversible wave is observed is due to fast rotation of the dendrimer compared to the electrochemical timescale, so that all the redox centres come close to the electrode within this timescale. In addition, a kind of *relay*-mechanism from a ferrocene site to the next (hopping electron transfer or *via* π -stacking of the ferrocenes units or *via* the σ bonds between ferrocene units) may eventually occur. Otherwise, the heterogeneous electron transfer between the electrode and the most remote redox sites of the globular dendrimer would be slow, as it is when the redox site is isolated at the center of the dendrimer. This type of stable polyredox dendrimer in which the redox centers are all active and fully chemically and electrochemically reversible at about the same potential could find use in the future as molecular batteries and sensors.

References

- 1 S. A. Miller, *J. Chem. Soc.* **1952**, 632.
- 2 G. Wilkinson, *J. Am. Chem. Soc.* **1952**, 74, 2125.
- 3 J. A. McCleverty, M. D. Ward, *Acc. Chem. Res.* **1998**, 31, 842.
- 4 M. D. Ward, *Chem. Soc. Rev.* **1995**, 121.
- 5 F. Paul, C. Lapinte, *Coord. Chem. Rev.* **1998**, 178-180, 431.
- 6 R. Ziessel, M Hissler, A. El-ghayoury, A. Harriman, *Coord. Chem. Rev.* **1998**, 178-180, 1251.
- 7 Balzani, V.; Juris, A.; Venturi, M.; Campagna, S.; Serroni, S. *Chem. Rev.* **1996**, 96, 759.
- 8 J.-P. Collin, P. Lainé, J.-P. Launay, J.-P. Sauvage, A. Sour, *J. Chem. Soc., Chem. Commun.* **1993**, 434.
- 9 A. Gourdon, J.-P. Launay, *Inorg. Chem.* **1998**, 37, 5336.
- 10 E. Ishow, A. Gourdon, J.-P. Launay, C. Chiorboli, F. Scandola, *Inorg. Chem.* **1999**, 38, 1504.
- 11 C. Patoux, J.-P. Launay, M. Beley, S. Chodorowski-Kimmes, J.-P. Collin, S. James, J.-P. Sauvage, *J. Am. Chem. Soc.* **1998**, 120, 3717.
- 12 D. N. Hendrickson, Q. M. Oh, T.-Y. Dong, T. Kambara, M. Jeohen, M. F. Moore, *Comments Inorg. Chem.* **1985**, 4, 329.
- 13 T.-Y. Dong, C.-H. Huang, C.-K. Chang, Y.-S. Wen, S.-L. Lee, J.-A. Chen, W.-Y. Yeh, A. Yeh, *J. Am. Chem. Soc.* **1993**, 115, 6357.
- 14 T.-Y. Dong, C.-K. Chang, C.-H. Cheng, K.-J. Lin, *Organometallics* **1999**, 18, 1911.
- 15 R. J. Webb, P. M. Hagen, R. J. Wittebort, M. Sorai, D. N. Hendrickson, *Inorg. Chem.* **1992**, 31, 1791.
- 16 A. Hradsky, B. Bildstein, N. Schuler, H. Schottenberger, P. Jaitner, K.-H. Organia, K. Wurst, J.-P. Launay, *Organometallics* **1997**, 16, 392.
- 17 A.-C. Ribou, J.-P. Launay, M. L. Sachtleben, H. Li, C. W. Spangler, *Inorg. Chem.* **1996**, 35, 3735.
- 18 H. Fink, N. J. Long, A. J. Martin, G. Opromolla, A. J. P. White, D. J. Williams, P. Zanello, *Organometallics* **1997**, 16, 2646.

-
- 19 P. R. Varanasi, A. K.-Y. Jen, J. Chandrasekhar, I. N. N. Namboothiri, A. Rathna, *J. Am. Chem. Soc.* **1996**, *118*, 12443.
- 20 S. Thayumanavan, J. Mendex, S. R. Marder, *J. Org. Chem.* **1999**, *64*, 4289.
- 21 I. Jestin, P. Frère, N. Mercier, E. Levillain, D. Stievenard, J. Roncali, *J. Am. Chem. Soc.* **1998**, *120*, 8150.
- 22 R. D. McCullough, *Adv. Mater.* **1998**, *10*, 93.
- 23 M.r. Andersson, O. Thomas, W. Mammo, M. Svensson, M. Theander, O. Inganäs, *J. Mater. Chem.* **1999**, 1933.
- 24 K. R. J. Thomas, J. T. Lin, Y. S. Wen, *Organometallics* **2000**, *19*, 1008-1012
- 25 M. Sato, K. Fukui, M. Sakamoto, S. Kashiwagi, M. Hiroi, *Thin Solid Films* **2001**, *393*, 210-216
- 26 Y. Matsuo, K. Tahara, and E. Nakamura, *J. Am. Chem. Soc.* **2006**, *128*, 7154-7155
- 27 A. J. Bard, *Nature* **1995**, *374*, 13.
- 28 D. Astruc, *Acc. Chem. Res.* **2000**, *33*, 287.
- 29 V. Balzani, S. Campagna, G. Denti, A. Juris, S. Serroni, M. Venturi, *Acc. Chem. Res.* **1998**, *31*, 26.
- 30 M. A. Hearshaw, J. R. Moss, *J. Chem. Soc. Chem. Commun.* **1999**, 1.
- 31 G. R. Newkome, E. He, C. N. Moorefield, *Chem. Rev.* **1999**, *99*, 1689.
- 32 I. Cuadrado, M. Moran, C. M. Casado, B. Alonso, J. Losada, *Coord. Chem. Rev.* **1999**, *395*, 193.
- 33 A. Togni, T. Hayashi (Eds.), *Ferrocenes*, VCH, Weinheim, 1995.
- 34 N. Adrain, D. Astruc, *Bull. Soc. Chim. Fr.* **1995**, *132*, 875.
- 35 C. M. Casado, I. Cuadrado, M. Moran, B. Alonso, B. Garcia, B. Gonzalez, J. Losada, *Coord. Chem. Rev.* **1999**, *186*, 53.
- 36 S. Nlate, J. Ruiz, J. C. Blais, D. Astruc, *J. Chem. Soc., Chem. Commun.* **2000**, 417.
- 37 S. Nlate, J. Ruiz, V. Sartor, R. Navarro, J. C. Blais, D. Astruc, *Chem. Eur. J.* **2000**, *6*, 2544.
- 38 C. Valerio, F. Moulines, J. Ruiz, J.C. Blais, D. Astruc, *J. Org. Chem.* **2000**, *65*, 1996.
- 39 C.-O. Turrin, J. Chiffre, D. de Montauzon, J. -C. Daran, A. M. Camminade, E. Manoury, G. Balavoine, J. -P. Majoral, *Macromolecules* **2000**, *33*, 7328.
- 40 J. Palomero, J. A. Mata, F. Gonzalez, E. Peris, *New J. Chem.* **2002**, *26*, 291.

-
- 41 P. Molina, A. Tárraga, D. Curiel, M. D. Velasco, *J. Organomet. Chem.* **2001**, 637–639, 258.
- 42 S. Sengupta, *Polyhedron* **2003**, 22, 1237.
- 43 A. Peruga, J. A. Mata, D. Sainz, E. Peris, *J. Organomet. Chem.* **2001**, 637–639, 191.
- 44 K. R. J. Thomas, J. T. Lin, *J. Organomet. Chem.* **2001**, 637–639, 139.
- 45 S. S. Kumar, H. W. Roesky, O. Andronesi, M. Baldus, R. F. Winter, *Inorg. Chim. Acta* **2005**, 358, 2349.
- 46 K. -W. Poon, Y. Yan, X. -Y. Li, and D. K. P. Ng, *Organometallics* **1999**, 18, 3528.
- 47 A. J. Bard, G. Denuault, C. Lee, D. Mandler, D. O. Wipf, *Acc. Chem. Res.* **1990**, 23, 357.
- 48 A. Salmon, P. Jutzi, *J. Organomet. Chem.* **2001**, 637–639, 595.
- 49 C. Valério, J. -L. Fillaut, J. Ruiz, J. Guittard, J. -C. Blais, D. Astruc, *J. Am. Chem. Soc.* **1997**, 119, 2588.
- 50 M. -C. Daniel, J. Ruiz, and D. Astruc, *J. Am. Chem. Soc.* **2003**, 125, 1150.
- 51 S. Nlate, J. Ruiz, J.-C. Blais and D. Astruc, *J. Chem. Soc. Chem. Commun.* **2000**, 417.



Chapter 2 Molecular design of ferrocene-containing pyridinium salts

2.1 Previous work in Tang's group

During the previous work in Tang's group, a series of pyridinium salts have been synthesized, primarily for the exploration of their nonlinear optical (NLO) properties (Figure 1). Pyridinium was chosen as a core to construct this kind of molecules because of its stability, and the positive charge that makes it a good candidate as electron acceptor. Besides, the double bonds conjugated to the pyridinium ring can be established efficiently through a classical Knoevenagel condensation between the activated methyl groups on pyridinium ring and aldehydes.

During the continuous research for molecular materials gathering both excellent electrochemical and optical properties, we realized that some of these pyridinium salts, owing to their multiple redox active centers (ferrocene) could also be interesting objects for electrochemical research¹. The ferrocene moiety, with its almost always reversible one electron system, can be switched from a good donor in the reduced state, to a weak attractor in the oxidized one. Therefore it often provides a molecular switch for many physical properties in the case of compounds containing ferrocenes linked to another active moiety²⁻⁵. This is especially true for the linear and nonlinear optical properties, which could thus be triggered through the electrochemical conversion of the compounds, as suggested recently by Audebert *et al.* in the case of ferrocenes-tetrazines⁶.

The different conjugated bridges between the electron deficient pyridinium center and the electron-rich ferrocene ends are expected to allow electron transfer between them, which could be detected by measurement of changes on the redox potentials of the ferrocenes.

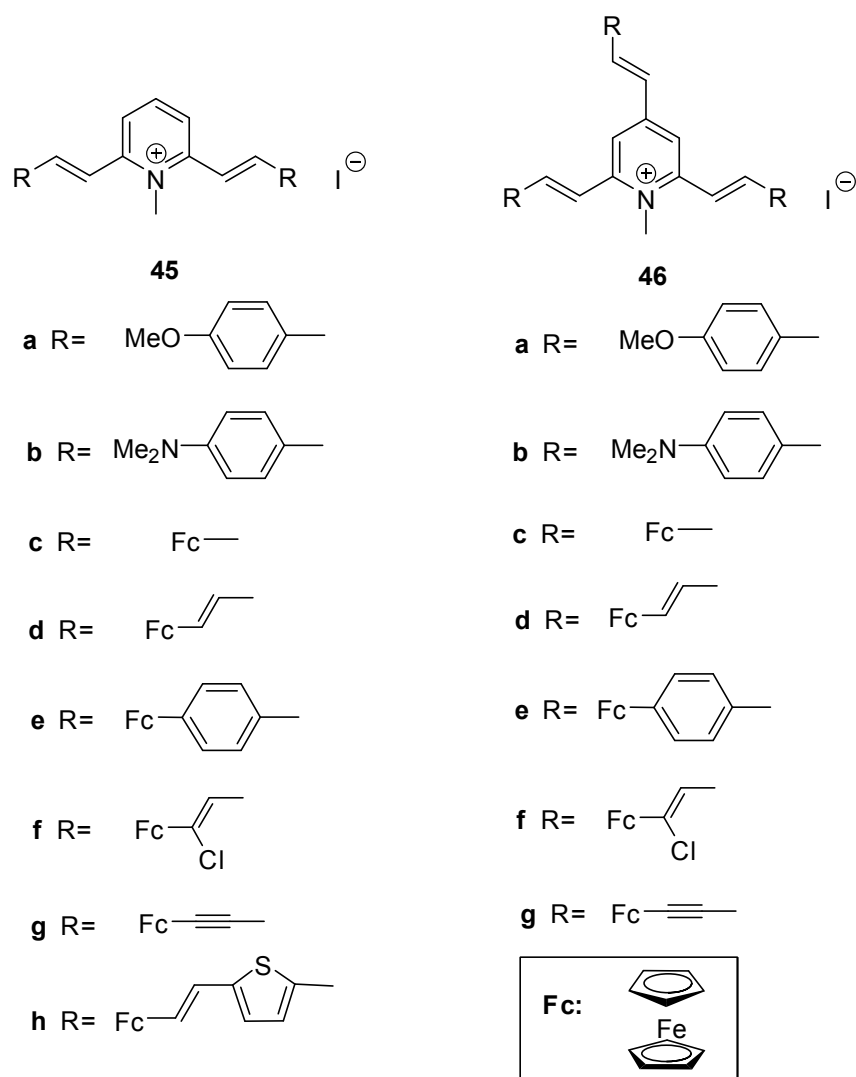


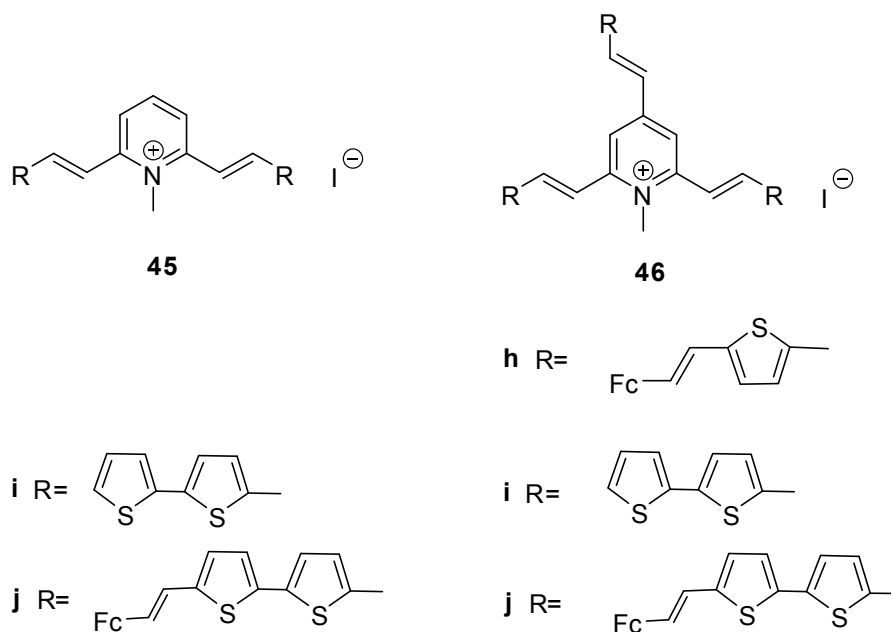
Figure 1. Ferrocene-containing pyridiniums synthesized in Tang's group.

The electrochemical properties of **45e-45h** and **46e-46h** were investigated and the primary results showed that all these multiferrocenyl pyridinium salts are potential electrochemical molecular materials with good oxidation-reduction reversibility.

2.2 Molecular design

As already mentioned before (Chapter 1.3.1), thiophene and bithiophene are often-used building blocks in the construction of molecular candidates with good electrochemical properties, since they present high electron transmission efficiency and high thermal and photochemical stability. As a comparison, polyalkene species present higher electron transmission efficiency, but mediocre thermal and photochemical stability; aromatic and acetylene-based systems are more stable, but their electron transmission efficiency is limited by excessive charge confinement. Thiophene and polythiophene systems are considered a good tradeoff between the efficiency of polyethylenic systems and the stability of the polyaromatic ones⁷⁻⁹. Due to this, thiophene-based oligomers and polymers are regarded to have potential for technological applications in electrical and optical devices^{10,11}.

Therefore, to further investigate the relationship between molecular structures and electrochemical properties of the conjugated pyridinium salts, we planned to prepare the di-branched (**45i**, **45j**) and tri-branched (**46d**, **46i**, **46j**) pyridiniums, and to study their properties by electrochemical methods. The intent to prepare **45i** and **46i** is to investigate the electrochemical behaviour of these pyridinium salts without ferrocenes ends. Concerning the ferrocenes-containing pyridiniums, the bridges between the ferrocene ends and the pyridinium core are varied from trans-ethenyl-thiophenyl-trans-ethenyl to trans-ethenyl-bithiophenyl-trans-ethenyl, offering an opportunity to investigate the influence of bridges for electron transfer.



References

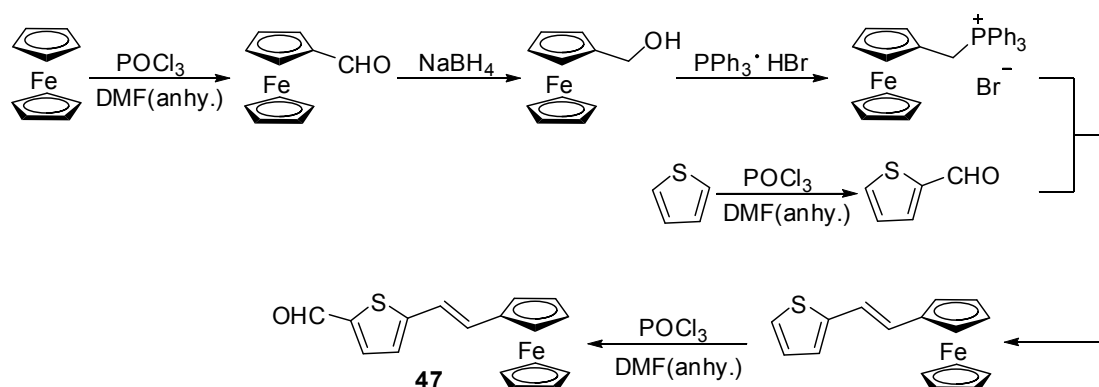
-
- 1 Y. H. Gong, P. Audebert, F. Miomandre, J. Tang, *J. Electroanal. Chem.* **2007**, accepted.
 - 2 R. Deschenaux, M. Schweissguth, M.-T. Vilches, A.-M. Levelut, D. Hautot, G. J. Long and D. Luneau, *Organometallics* **2004**, *18*(26), 5553.
 - 3 M. Suzuki, R. Nakajima, M. Tsuruta, M. Higuchi, Y. Einaga and K. Yamamoto, *Macromolecules* **2006**, *39*(1), 64.
 - 4 C. Engtrakul and L. R. Sita, *Nano Lett.* **2001**, *1*(10), 541.
 - 5 H. Plenio and C. Aberle, *Organometallics* **1997**, *16*(26), 5950.
 - 6 I. Janowska, F. Miomandre, G. Clavier, P. Audebert, J. Zakrzewski, K. H. Thi, and I. Ledoux-Rak, *J. Phys. Chem. A* **2006**, *110*, 12971.
 - 7 P. R. Varanasi, A. K.-Y. Jen, J. Chandrasekhar, I. N. N. Namboothiri, A. Rathna, *J. Am. Chem. Soc.* **1996**, *118*, 12443.
 - 8 S. Thayumanavan, J. Mendex, S. R. Marder, *J. Org. Chem.* **1999**, *64*, 4289.
 - 9 I. Jestin, P. Frère, N. Mercier, E. Levillain, D. Stievenard, J. Roncali, *J. Am. Chem. Soc.* **1998**, *120*, 8150.
 - 10 R. D. McCullough, *Adv. Mater.* **1998**, *10*, 93.
 - 11 M.r. Andersson, O. Thomas, W. Mammo, M. Svensson, M. Theander, O. Inganäs, *J. Mater. Chem.* **1999**, 1933.

Chapter 3 Results and discussion

3.1 Synthesis of dibranched and tribranched pyridiniums

3.1.1 Improvement of synthesis of trans-5-(2-ferrocenyl-vinyl)-2-carbaldehyde-thiophene

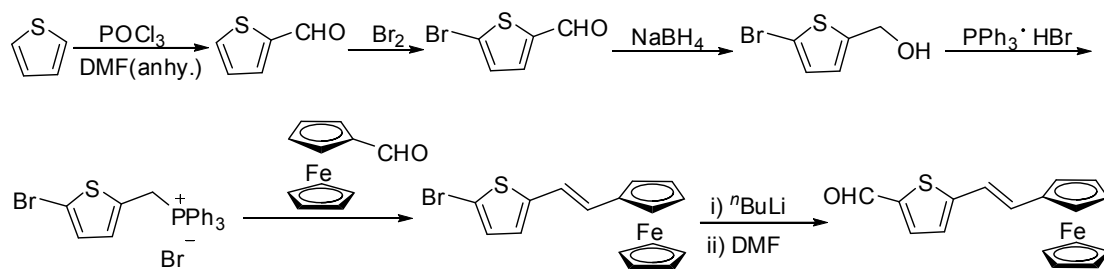
The synthetic route of trans-5-(2-ferrocenyl-vinyl)-2-carbaldehyde-thiophene was firstly established by Lin's group (Scheme 1)¹. Vilsmeier formylation of ferrocene and thiophene gave both ferrocenylaldehyde and thiophenylaldehyde in good yield. The ferrocenylaldehyde was chosen to prepare the phosphonium salt because thiophenylaldehyde is less stable and oxidize readily in air at room temperature. Therefore, ferrocenylaldehyde was reduced by NaBH₄ to give ferrocenemethanol quantitatively. Ferrocenemethyl phosphonium bromide was generated from the reaction of ferrocenemethanol with PPh₃·HBr, and reacted with thiophenyl-carboxyaldehyde under the Wittig olefination condition to give a mixture of cis- and trans- ferrocenylethenylthiophene. The trans- isomer can be obtained by recrystallization of the mixture, or isomerized in toluene in the presence of I₂.



Scheme 1. Lin's synthetic route for trans-5-(2-ferrocenyl-vinyl)-2-carbaldehyde-thiophene.

However, in our laboratory we found that the yield of the last step, selective formylation of trans-ferrocenylvinylthiophene, was very low even when the reaction conditions were carefully controlled, e.g. water-free, air-free, etc. Too high temperature (beyond r. t.), too long reaction time (> 4hs) or excess formylation reagents (POCl₃ with DMF) all led to decomposition of all starting compound (the color of the solution turned dark and TLC indicated no separable products), while under low temperature (below 0°C) and given appropriate reaction time (3~4 hs), a yield of less than 10% could be achieved. We presumed that it is because the conjugated ferrocene ring has similar reactivity with thiophene to formylation that a complex mixture of various formylation products (including multi-formylated products) was produced under the reaction conditions. Therefore, we considered setting up an orienting group onto the thiophene ring to better control the selective formylation on the expected position, and thus a new synthetic route for the

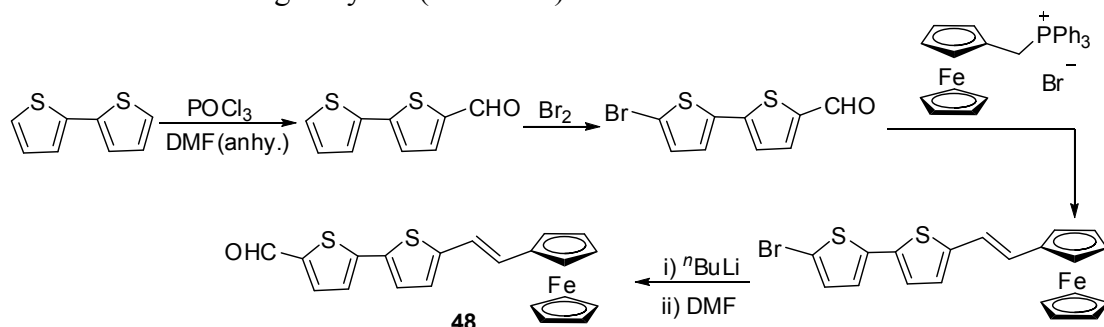
preparation of trans-5-(2-ferrocenyl-vinyl)-2-carbaldehyde-thiophene was established (Scheme 2).



Scheme 2. New synthetic route for trans-5-(2-ferrocenyl-vinyl)-2-carbaldehyde-thiophene.

Thiophenylaldehyde, obtained from Vilsmeier formylation, was firstly brominated in the 5 position to give 5-bromothiophene-2-carbaldehyde, which was reduced and reacted subsequently with $\text{PPh}_3 \cdot \text{HBr}$ to give ((5-bromothiophen-2-yl)methyl)triphenyl phosphonium bromide. Wittig reaction with ferrocenylaldehyde gave cis- and trans- 2-bromo-5-ferrocenylethenylthiophene, which was recrystallized in hot hexane to give pure trans- isomer. The (E)-5-ferrocenylethenylthiophene-2-carbaldehyde was obtained by reaction of n-butyl lithium with (E)-2-bromo-5-ferrocenylethenyl-thiophene followed by subsequent addition of anhydrous DMF at low temperature.

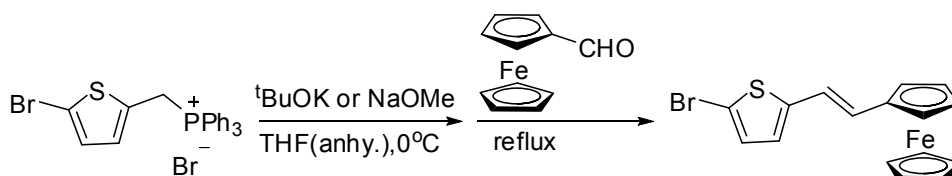
Following almost the same method, ferrocenylethenyl-bithiophenealdehyde was also obtained in good yield (Scheme 3):



Scheme 3. New synthetic route for trans-ferrocenylethenyl-bithiophenealdehyde.

3.1.2 Influence of base for Wittig olefination

Two bases were tried for the Wittig olefination of bromothiophenylmethyl triphenyl phosphonium bromide with ferrocenylaldehyde. When NaOMe was used, only a 30% yield of a mixture of isomers could be obtained, while using a stronger base t-BuOK, the yield of isomers could reach up to 86% (Scheme 4). We assumed that since NaOMe is usually freshly prepared with sodium and anhydrous methanol before its addition, it might be the water getting into the reaction system during the transfer of reagent or the reaction time which destroyed part of the Wittig reagent. Moreover, slower deprotonation speed when using the weaker base NaOMe might also be responsible for the lower yield.

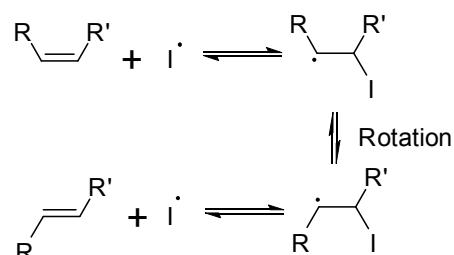


Scheme 4. Wittig olefination of bromothiophenylmethyl triphenyl phosphonium bromide with ferrocenylaldehyde.

3.1.3 Isomerization of *Z*-isomers to *E*-isomers with I_2

The generation of carbon–carbon double bonds in geometrically pure form is one of the most important reactions in organic chemistry² and many elegant methods are known in the literature³. However, mixtures of *Z*- and *E*-alkenes are also often formed together in some reactions such as Wittig reaction in our case. Several methods including applying radical⁴ or photochemical⁵ reactions have been used to transform the *Z*-isomers to the corresponding *E*-ones. For example, isomerization of (*Z*)-stilbene to the *E*-isomer and dimethyl maleate to dimethyl fumarate are usually catalyzed by bromine via the reversible addition of a bromine radical to the double bond⁶. Spencer et al.⁷ have demonstrated a facile palladium(II)-catalyzed isomerization of *Z*-arylalkenes to *E*-arylalkenes. Thereafter Argade and co-workers⁸ have also reported a new method providing an easy access to several types of geometrically pure *E*-olefins using *N*-bromosuccinimidedibenzoyl peroxide/azobisisobutyronitrile (NBS-DBP/AIBN) reagent.

I_2 has been recognized as one of the extremely effective catalysts for the *cis*-*trans* isomerization of olefins for a long time⁹. The iodine radical, usually generated by heating, adds to the double bond to give a carbon radical, which can be converted into the other conformation through internal rotation about the single bond and subsequent release of the iodine radical (Scheme 5).

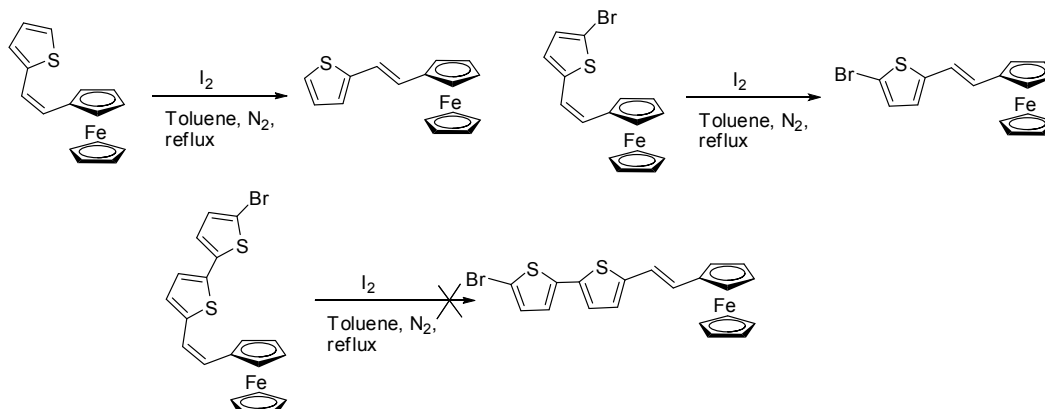


Scheme 5. Isomerization of olefins in presence of I_2 .

Considering the availability of iodide and the simple and convenient operation for isomerization, we have chosen this method to transform the *cis*- products we obtained to their corresponding *trans*- isomers. *Cis*-ferrocenylethenylthiophene and *cis*-2-bromo-5-ferrocenylethenyl-thiophene all gave the corresponding *trans*-isomers after refluxing in toluene under N_2 in less than 0.5 hour, while *cis*-5'-bromo-5-(2-ferrocenylvinyl)-2,2'-bithiophene failed to give the *trans*- isomer after more than 1 hour's reflux (

Scheme 6). In the latter case, ¹H-NMR indicated that the *cis*- isomer mostly remained after the reaction. The reason is still unclear, but the expanded conjugation system which decreases the activity of the double bond to the radical addition, or the more bulky bromobithiophenyl group which increases the activation energy of single bond rotation might be responsible. However, since more than 60% of the *trans*-

isomer could be obtained from recrystallization of the mixture of cis- and trans-isomers, we didn't pursue search for an isomerization method.

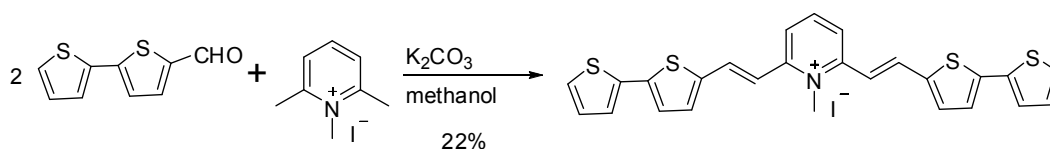


Scheme 6. Isomerization of ferrocenyl compounds in presence of I_2 .

3.1.4 Condensation of aromatic aldehyde with multimethyl-pyridiniums

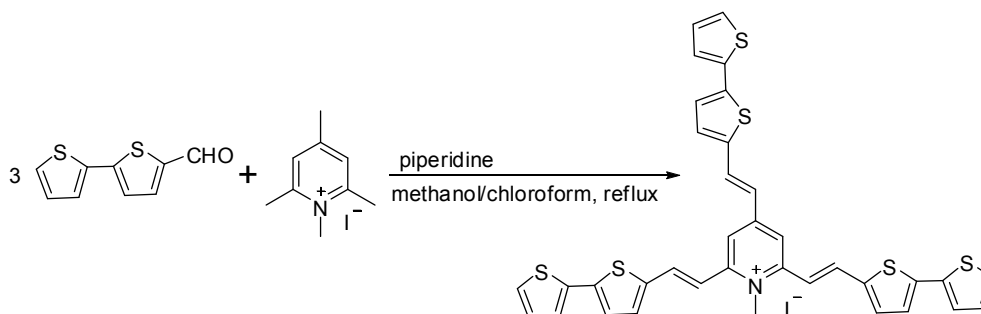
3.1.4.1 Influence of base

Three bases were used for trial in the condensation of bithiophenyl aldehyde with 1,2,6-trimethyl pyridinium or 1,2,4,6-tetramethyl pyridinium: K_2CO_3 , piperidine, and 2,4,6-collidine. When K_2CO_3 was used for the condensation of bithiophenealdehyde with 1,2,6-pyridinium (Scheme 7), the reaction went smoothly in methanol at room temperature, but only 22% of the expected all trans- product was isolated after 4 hours. TLC indicated the all trans- alkene as a major product, 2 minor products, possibly the (cis-, trans-) and the all-cis-, and many degraded products which did not move on TLC plate.



Scheme 7. Condensation of bithiophenyl aldehyde with pyridinium in presence of K_2CO_3 .

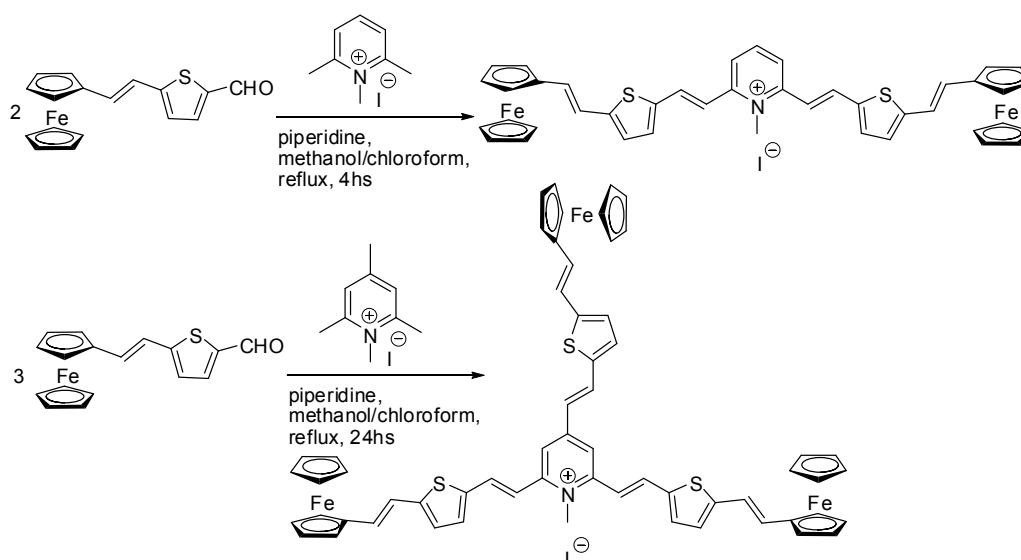
Micro-scale experiment on the same reactants was carried out in the presence of piperidine and subsequent TLC analyses indicated that the yield might be better. Therefore the piperidine was used for the triple condensation of bithiophenylaldehyde with 1,2,4,6-tetramethyl pyridinium salt (Scheme 8).



Scheme 8. Condensation of bithiophenyl aldehyde with pyridinium in presence of piperidine.

After optimization of the reaction conditions (reflux in N₂ atmosphere for 12 hours), a yield of 89% for the all-trans- product was obtained. Traces of minor products could also be detected by TLC but were successfully removed after a column chromatography.

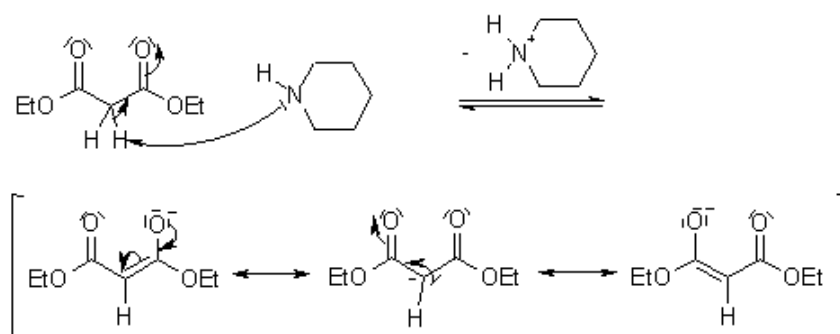
Use of piperidine for the condensation of ferrocenylethenyl-thiophenylaldehyde with 1,2,6-trimethyl pyridinium or 1,2,4,6-tetramethyl pyridinium also gave satisfactory yields, 79% and 33%, respectively (Scheme 9).



Scheme 9. Condensation of ferrocenylethenyl-thiophenylaldehyde with pyridiniums.

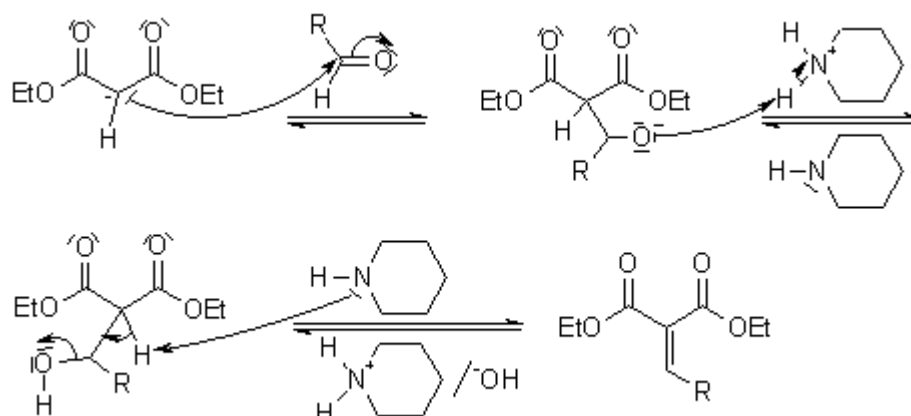
Reactions of (E)-5'-ferrocenylvinyl-2,2'-bithiophene-5-carbaldehyde with 1,2,6-trimethyl pyridinium or 1,2,4,6-tetramethyl pyridinium also gave moderate yields for all-trans- products (49% and 34%, respectively). However, we also tried the 2,4,6-collidine as base. The results showed that in the presence of collidine, the reaction of the aldehyde with 1,2,4,6-tetramethyl pyridinium was cleaner (no degradation), much faster than when using K₂CO₃ or piperidine, but only gave di-branched products. Indeed, ¹H-NMR indicated clearly two signals for methyl groups on the pyridinium ring, one of which is the N-methyl.

We assumed that this is because the mechanisms of condensation between aldehyde and methyl pyridinium depends on the base employed. Usually, when piperidine is used in such condensations, for example, Knoevenagel condensation, an enol intermediate is formed initially (Scheme 10):



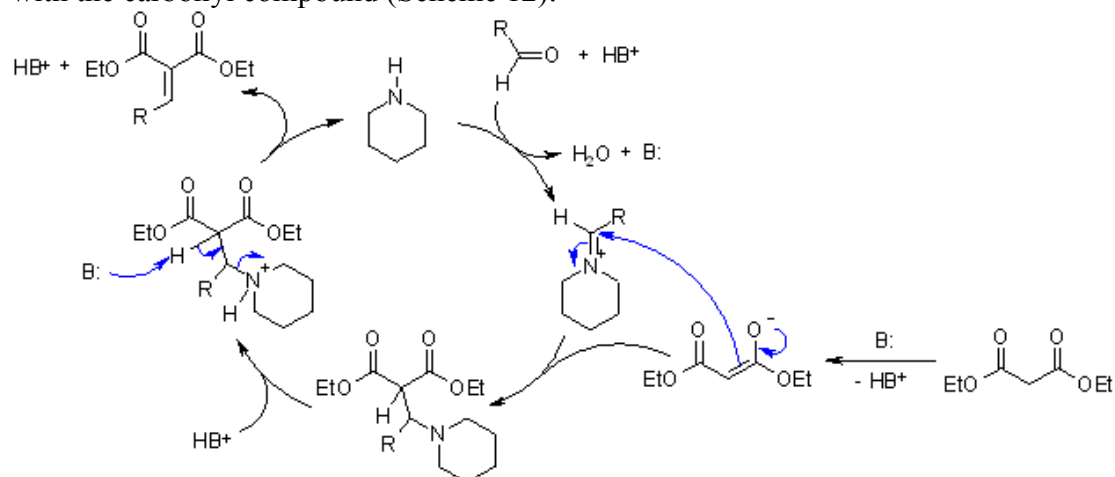
Scheme 10. Formation of an enol intermediate in Knoevenagel Condensation.

Then this enol reacts with the aldehyde, and the resulting aldol undergoes subsequent base-induced elimination (Scheme 11):



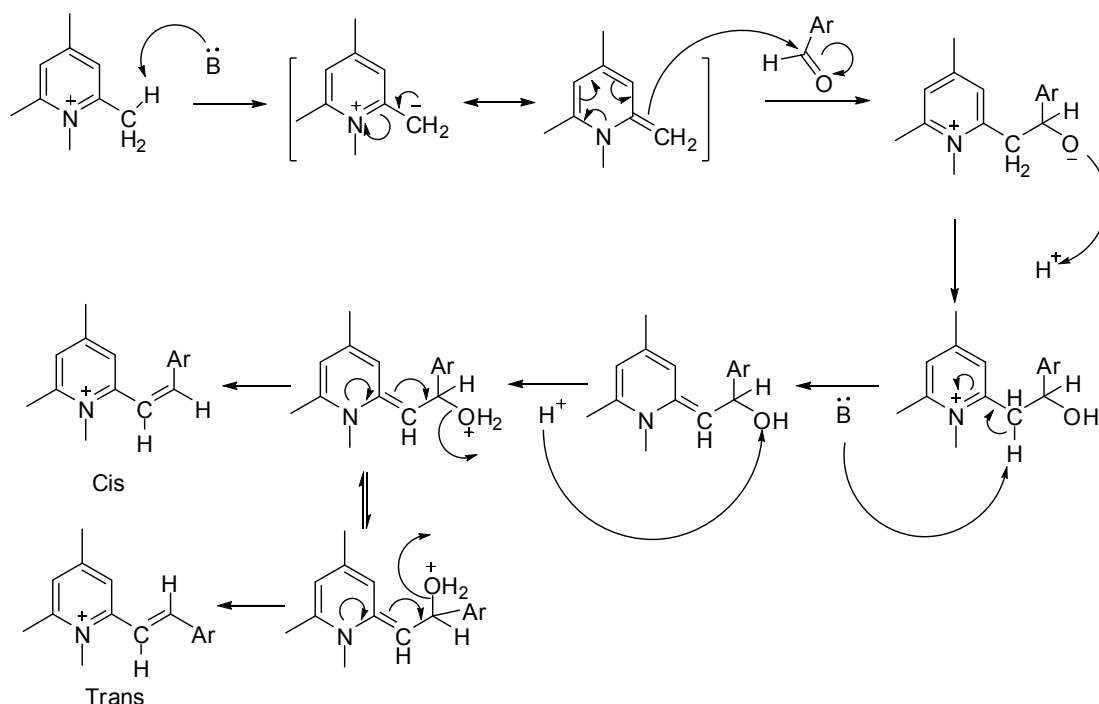
Scheme 11. The subsequent base-induced elimination in Knoevenagel Condensation.

However, as the concept “organocatalysis” was brought forward and was getting more and more attention, the mechanism of this type of condensation was reconsidered and a reasonable variation of the mechanism was suggested. Organocatalysis uses small organic molecules, predominantly composed of C, H, O, N, S and P, to accelerate chemical reactions. The advantages of organocatalysts include their lack of sensitivity to moisture and oxygen, their ready availability, low cost, and low toxicity, which confers a huge direct benefit in the organic synthesis when compared with (transition) metal catalysts. In the example of the Knoevenagel condensation, it is believed that piperidine forms a reactive iminium ion intermediate with the carbonyl compound (Scheme 12):



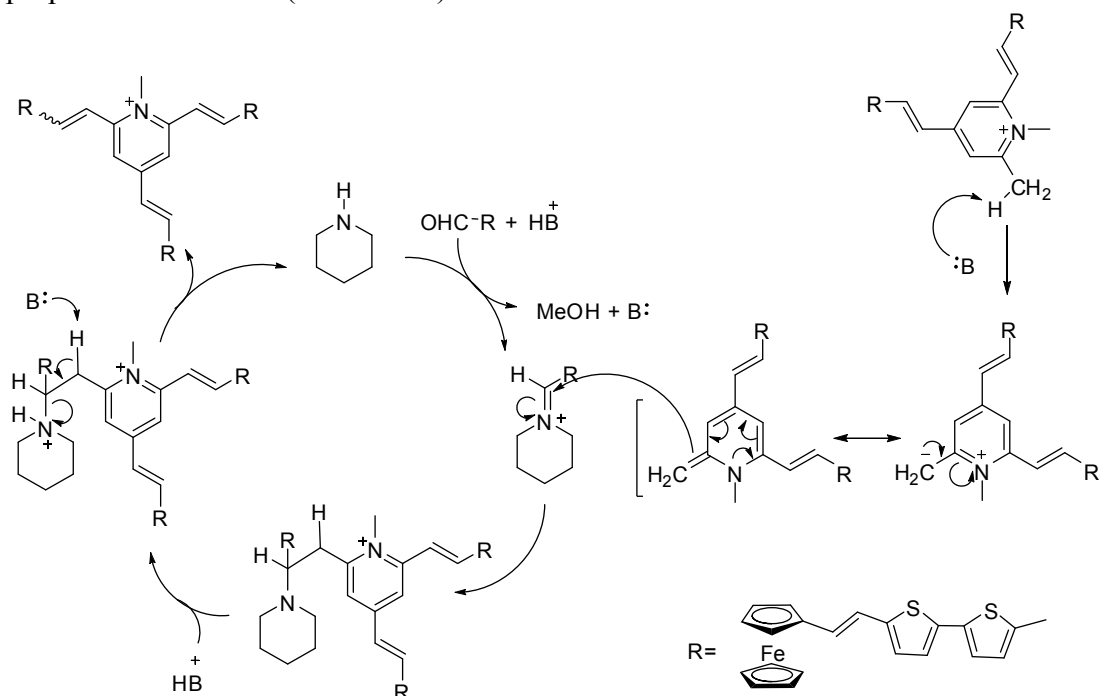
Scheme 12. Condensation mechanism through a reactive iminium ion intermediate with the carbonyl compound.

Therefore, we assumed that for the condensation of the first and second methyl of 1,2,4,6-tetramethyl pyridinium with aromatic aldehyde (E)-5'-ferrocenylvinyl-2,2'-bithiophene-5-carbaldehyde, both collidine and piperidine can catalyze the reaction through the first mechanism (Scheme 13):



Scheme 13. Assumed mechanism for condensation of the first and second methyl groups of pyridinium.

However, after the second condensation, the molecule has a largely expanded conjugated system, which diffuses the positive charge of the pyridinium and thus lowers greatly the reactivity of the third methyl group. In this case collidine, which can't form the more reactive iminium ion with aldehyde, is not able to catalyze the third condensation anymore, while piperidine, due to its ability to form the active iminium ion, continues to catalyze the third condensation through alternative proposed mechanism (Scheme 14).



Scheme 14. Condensation mechanism through reactive iminium ion intermediate.

3.1.4.2 Influence of substituents

When ferrocenealdehyde reacted with 1,2,4,6-tetramethyl pyridinium, TLC indicated clearly one major product (all-trans) with 5 side products, most possibly all-cis, (cis, cis, trans), (cis, trans, cis), (cis, trans, trans), (trans, cis, trans); reaction of bithiophenyl with 1,2,4,6-tetramethyl pyridinium also gave several side products but in less quantity. However, reaction of ferrocenyl-ethenyl-thiophenylaldehyde with 1,2,4,6-tetramethyl pyridinium gave one major product (all trans) and one minor product, and reaction of ferrocenylethenyl-bithiophenylaldehyde gave exclusively the all-trans- product. These results indicate that the size of the aromatic aldehyde influences greatly the cis/trans selectivity of condensation with multimethyl pyridinium: the bulkier the aldehyde, the higher the selectivity to trans- configuration of the newly formed double bond. Moreover, the earlier condensation also influences the subsequent one. Monitoring of reactions of ferrocenylethenyl-bithiophenyl-aldehyde with 1,2,4,6-tetramethyl pyridinium by TLC tracking indicated that after the first condensation with aldehyde, the second became more difficult, and the third was even slower, while at the same time, the latter condensations were more selective (to trans- isomers) than the former ones because of the increased steric hinderance.

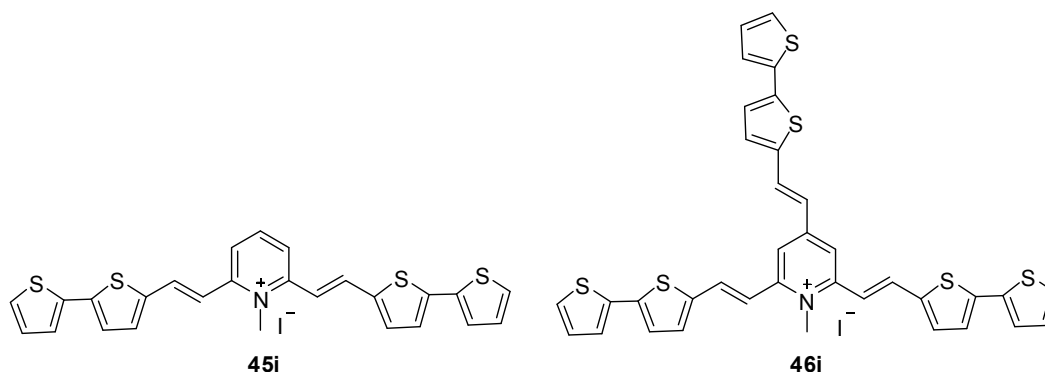
3.1.4.3 Influence of solvents

Solvents influence greatly the reaction of the aldehydes with multimethyl pyridiniums. Reaction of bithiophenyl aldehyde with 1,2,6-trimethyl or 1,2,4,6-tetramethyl pyridinium all give satisfactory yields in methanol. However, when methanol was used as solvent for the condensation of ferrocenylethenyl-thiophenylaldehyde or ferrocenylethenyl-bithiophenyl aldehyde with 1,2,6-trimethyl or 1,2,4,6-tetramethyl pyridinium, no reaction took place after refluxing for 24 hours; when chloroform was used instead, the reaction took place but at a low rate: a lot of aldehyde remained after refluxing for 24 hours.

We assumed that as the conjugated systems of aldehydes expand, their solubility decreases in methanol while increases in chloroform, which makes the reactions faster in chloroform than in methanol. However since highly polar reagents, 1,2,6-trimethyl or 1,2,4,6-tetramethyl pyridinium, are much more soluble in methanol than in chloroform, the addition of methanol increases largely the reaction speed by enhancing the solubility of the mutimethyl-pyridinium. After optimization, the combination of chloroform/methanol in a 3:1 ratio gave the best result.

3.2 Electrochemical results and discussion

3.2.1 Preliminary electrochemical study of 45i and 46i



The cyclic voltammograms of **45i** and **46i** show that the oxidation processes are both irreversible. The current decreased slowly from the second scanning cycle, and the oxidation peak diminished in the 5th one (Figure 1). A black thin film was produced on the surface of the working electrode, indicating the polymerization of the bithiophene units. However, the electrodeposited polymer does not appear to be conducting enough to ensure efficient deposition of multilayer films.

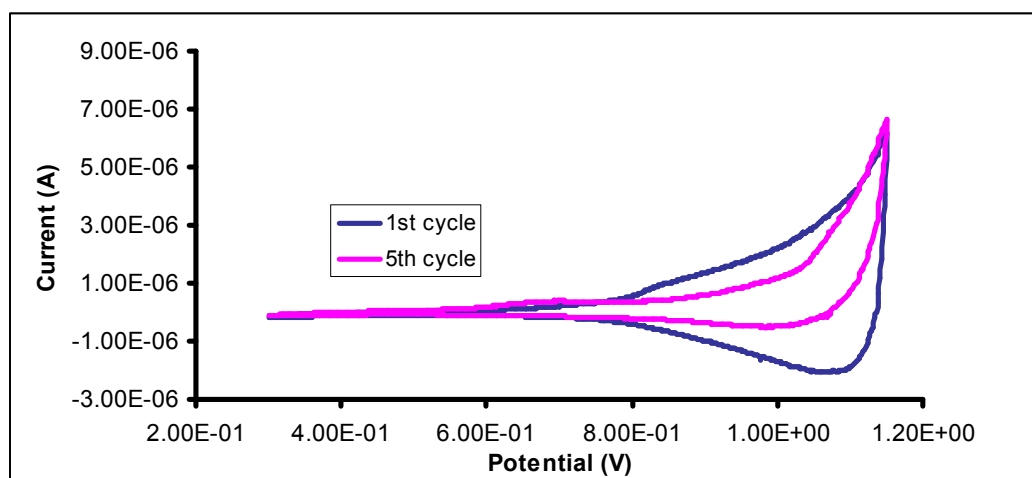


Figure 1. CV of **46i** in acetonitrile (conc. 1.0 mM) on platinum at 100 mV/s.

3.2.2 Preliminary electrochemical study of 45h

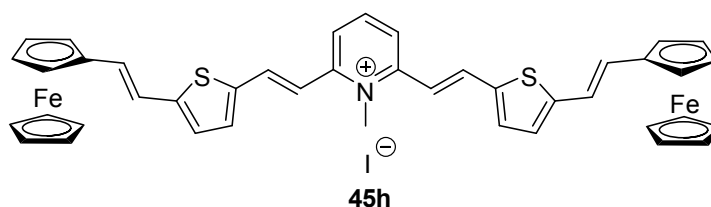


Figure 2 shows the electrochemical response of the dibranched compound **45h**, which features a typical cyclic voltammogram shape of ferrocenic compound. The CV displays a single oxidation peak, which is in accordance with all the dibranched and tribranched ferrocene compounds tested in our laboratory before¹⁰. The fact that

all electrons seem to be transferred at the same potential tends to show that only the molecule center is electronically connected to the branches, and that on the other hand the branches have little influence on each other, and especially the redox state of a given ferrocene end-group has little influence on the redox potential of the others. This result was not at all obvious, since most molecules containing coupled redox centers show differentiated waves. The peak potential difference ($\Delta E_p = E_{p,a} - E_{p,c} = 86 \text{ mV}$) is larger than the expected 35 mV value for ideal non interacting redox centers. This is probably indicative of a small difference for the redox potentials corresponding to successive electron transfers from ferrocenes of one molecule, due to slightly mutual repulsive interactions.

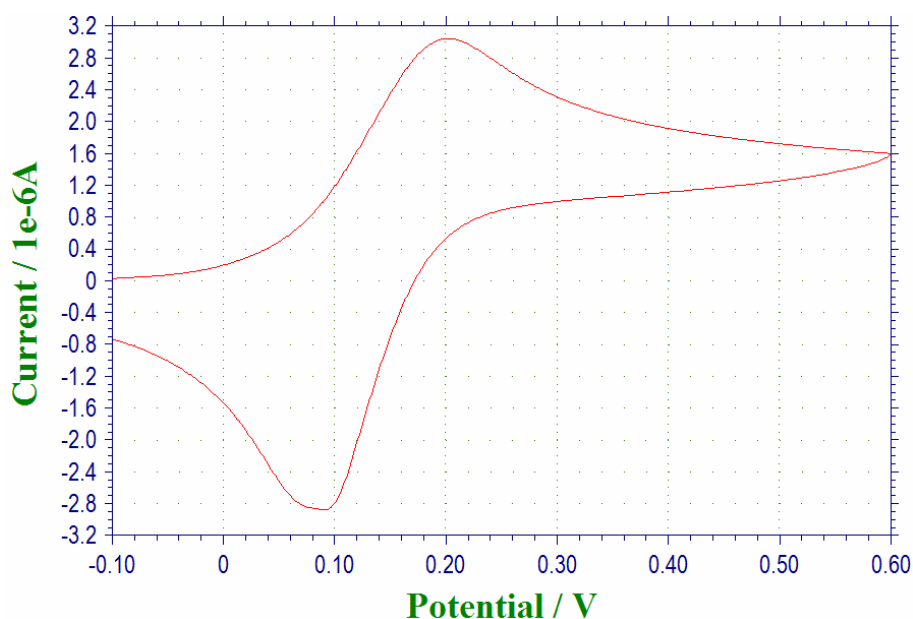


Figure 2. CV of **45h** in dichloromethane (conc. 1.0 mM) on platinum at 100 mV/s. $E_{p,a}$: 0.190V; $E_{p,c}$: 0.094 V.

3.2.3 Preliminary electrochemical study of **46h**

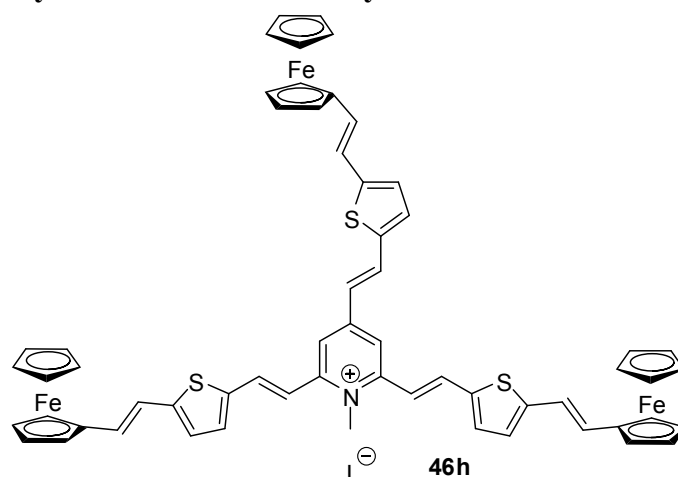


Figure 3 shows the cyclic voltammogram for the tribranched pyridinium compound **46h**. The CV is still reversible, but the shape does no longer look like a typical reversible cyclic voltammogram of ferrocenes. The peak corresponding to the

reduction process is more intense than the oxidative one. Moreover, the peak features an adsorption-like shape, probably because of the generation and precipitation of oligomers on the electrode, due to an uphill electron transfer between ferrocenium cations and the thiophene branches. Therefore the voltammogram is no longer readily analyzable. The broad oxidation peak indicates a larger spreading of the oxidation potentials corresponding to the successive 3 electron transfers in the tribranched **46h** as compared to the 2 electron transfers in the dibranched **45h** in the previous case, due to stronger repulsive interactions.

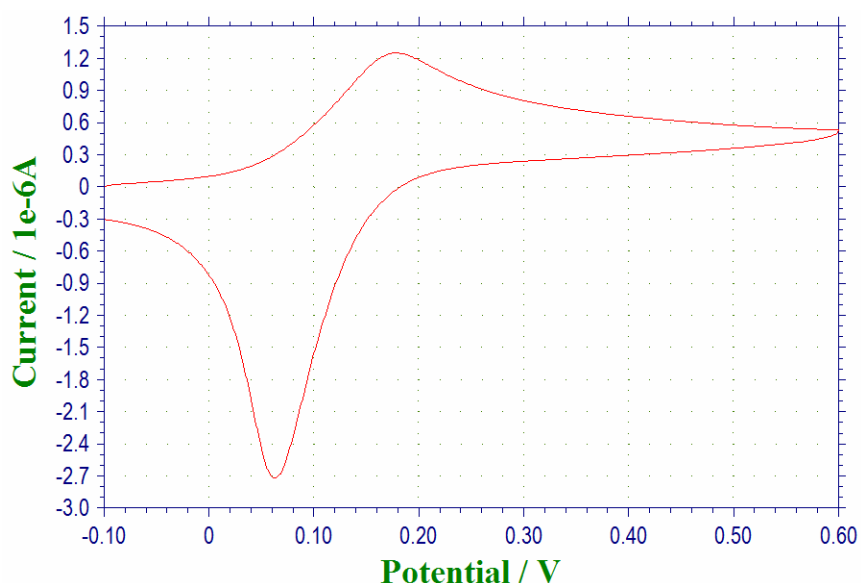


Figure 3. CV of **46h** in dichloromethane (conc. ~ 1.0 mM, roughly) on platinum at 100 mV/s. $E_{p,a}$: 0.178V; $E_{p,c}$: 0.063 V.

The redox potentials of pyridinium ferrocenes are both more positive than the ferrocene's one, but the redox potential of the tribranched **46h** is less shifted than the dibranched one. This is in accordance with the fact that: 1) the pyridinium core plays an attracting role that destabilizes the ferrocenium cation, and 2) this attracting effect is more important in the dibranched compound than in the tribranched one, as a result of sharing of the attractive power of the core between two ferrocenyl branches in the former case instead of three in the latter. However, this effect is not strictly additive, since in this case a larger difference between the two compounds would have been expected.

3.2.4 Preliminary electrochemical study of **45j**

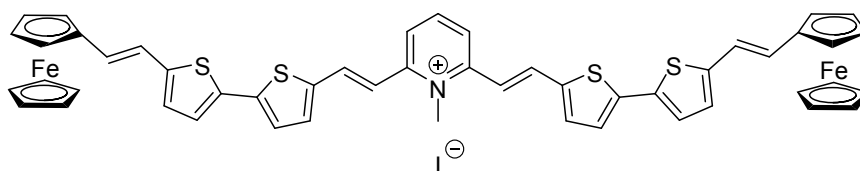


Figure 4 shows the cyclic voltammogram of compound **45j**, the most remarkable character of which is the two oxidative peaks in the range of 0 to 1 V. The first one is reversible, although the shape is unlike the CVs of typical ferrocene compounds. The second one shows up at a much more positive potential (0.840 V) and is completely irreversible. Continuous cyclic voltammetry were tried in the range

-0.1 V to 1.0 V, and the results indicated that the current decreased dramatically from the second cycle, and the peak signals were no more detectable after several cycles. The Pt working electrode was found to be covered with a thin brown film after being taken out from the solution. The electrode was grinded and put back to use, and the same signals were obtained again. We assume that the first peak corresponds to the reversible redox of one of the ferrocene units, and the second one to the signal of polymerization of the bithiophene bridge. The bithiophene unit is oxidized instead of the second ferrocene, because the oxidative potential of the second ferrocene is largely increased due to the first oxidation and the conjugation in the whole molecule. This means that the two ferrocene units in the molecule, both connected to the pyridinium center with trans-ethenyl-bithiophenyl-trans-ethenyl bridge, are not independent one to each other any more. The oxidation of one ferrocene influences greatly the electrochemical behavior of the other, by raising up largely its redox potential, which becomes higher than the potential of the bithiophene unit, and hence the oxidation and subsequent polymerization of bithiophene takes place, instead of oxidation of the other ferrocene. This result also indicates that bithiophene is a good conjugative bridge for electron transfer in molecules.

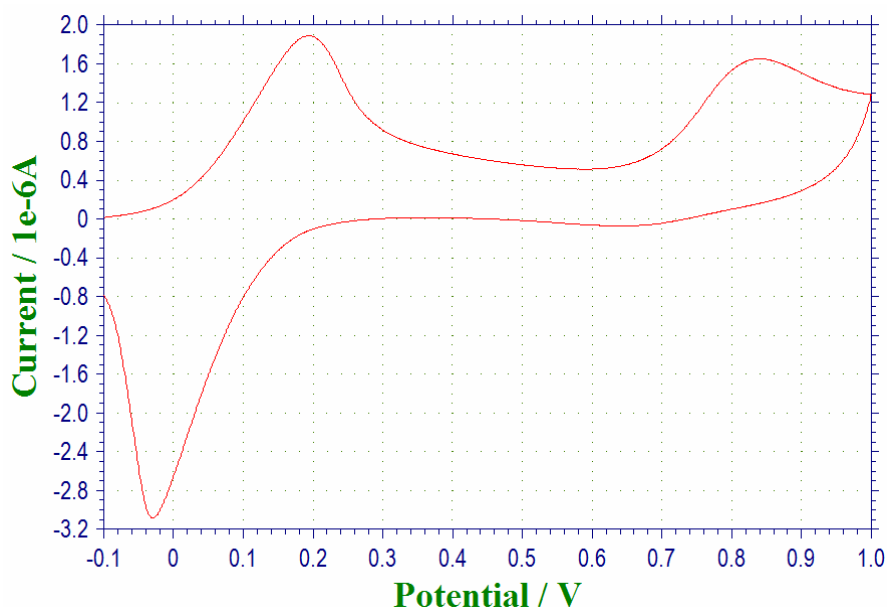


Figure 4. CV of **45j** in dichloromethane (conc. 1.5 mM) on platinum at 50 mV/s. $E_{p,a,1}$: 0.194 V; $E_{p,a,2}$: 0.840 V; $E_{p,c,1}$: -0.03 V.

However, the first peak is quite reversible if the scan potential is kept in a range -0.2 V to 0.5 V, with $E_{p,a}$ of ~ 0.19 V and $E_{p,c}$ of 0.09 V, which is similar to the behaviour of the other dibranched pyridinium **45h** using thiophene instead of bithiophene in the bridge (Figure 5).

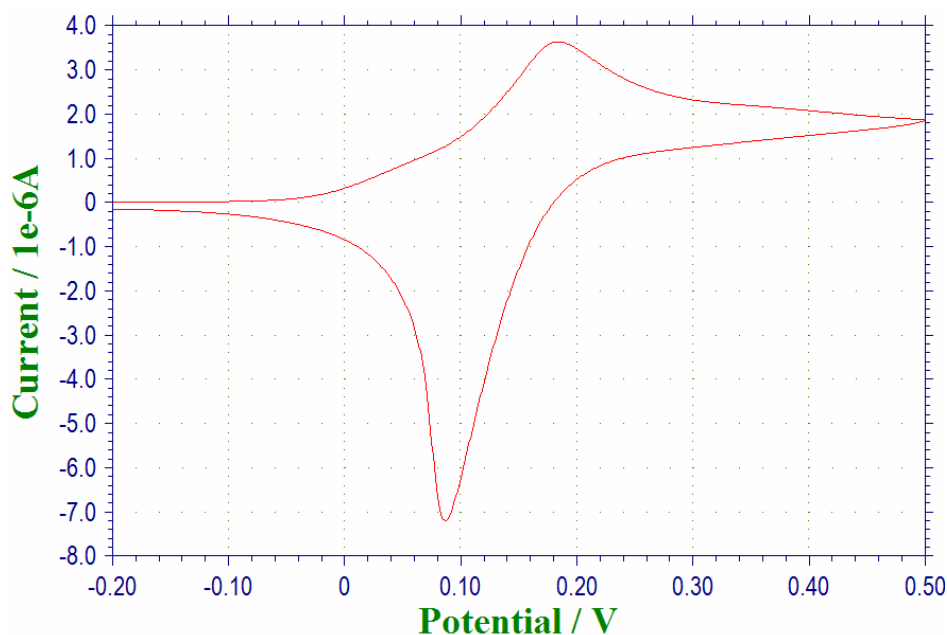
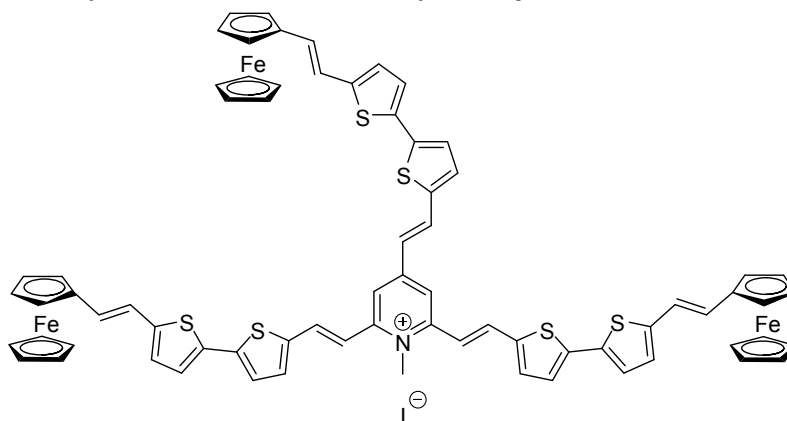


Figure 5. CV of **45j** from -0.2 V to 0.5 V in dichloromethane (conc. 1.5 mM) on platinum at 50 mV/s. $E_{p,a,1}$: 0.185 V; $E_{p,c,1}$: 0.086 V.

3.2.5 Preliminary electrochemical study of **46j**



The cyclic voltammogram of the tribranched pyridinium ferrocene **46j** is completely different from the one of typical ferrocenes, and also different from the dibranched analogue (Figure 6). The CV shows three irreversible oxidation peaks in the range -0.2 V to 1.0 V. The second cycle can still give one signal corresponding to the first peak, while in the third cycle, no peak signals were detectable. A black thin film was produced on the surface of the working electrode, which blocked the reaction pathway and should be responsible for the loss of signals. After polishing the electrode the same signals could be recorded again. The first peak corresponds to the oxidation of ferrocenes, and the second probably corresponds to the first oxidation of the thiophene ethylene units, while the origin the third peak is speculative (maybe the degradation of deposited oligomers).

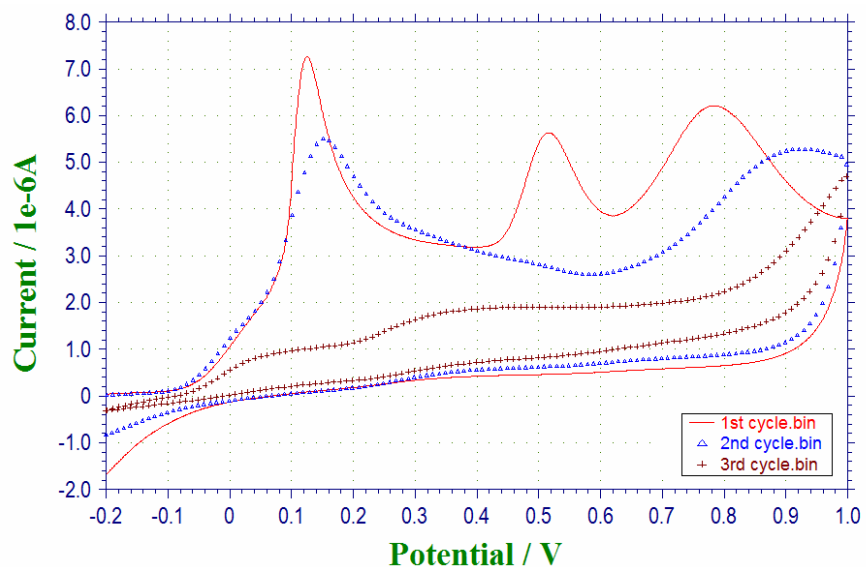


Figure 6. 3 CV cycles of **46j** in dichloromethane (conc. 1.68 mM) on platinum at 50 mV/s. $E_{p,a,1}$: 0.125 V; $E_{p,a,2}$: 0.516 V; $E_{p,a,3}$: 0.784 V.

Given the potential recorded, it is clear that the ferrocenes account for the first system observed. However, the return peak is not reversible, and displays a shape characterized of an electroactive thin layer. This occurs whatever the potential limit of the scan, as can be seen in Figure 4 and Figure 5, and is likely to come from bithiophene oligomers deposition. The fact that bithiophene branches oxidation is observed even when the scan limit is +0.5 V (Figure 5) is indicative of an uphill electron transfer process between the ferrocenes and the bithiophene branches.

References

-
- 1 K. R. J. Thomas, J. T. Lin, Y. S. Wen, *J. Organomet. Chem.* **1999**, 575, 301.
 - 2 D. A. Evans, B. W. Trotter, B. Cote, P. J. Coleman, L. C. Dias, A. N. Tyler, *Angew. Chem., Int. Ed. Engl.* **1997**, 36, 2744.
 - 3 D. A. Evans, D. M. Fitch, T. E. Smith, V. Cee, *J. Am. Chem. Soc.* **2000**, 122, 10033.
 - 4 T. Bosanac, J. Yang, C. S. Wilcox, *Angew. Chem., Int. Ed. Engl.* **2001**, 40, 1875.
 - 5 E. N. Jacobsen, L. Deng, Y. Furukawa, L. E. Martinez, *Tetrahedron* **1994**, 50, 4332.
 - 6 M. Kodomari, T. Sakamoto, S. Yoshitomi, *Bull. Chem. Soc. Jpn.* **1989**, 62, 4053.
 - 7 J. Yu, M. J. Gaunt, J. B. Spencer, *J. Org. Chem.* **2002**, 67, 4627.
 - 8 M. M. Baag, A. Kar and N. P. Argade, *Tetrahedron* **2003**, 59, 6489.
 - 9 S. W. Benson, K. W. Egger, and D. M. Golden, *J. Am. Chem. Soc.* **1965**, 87, 468.
 - 10 Y. H. Gong, P. Audebert, F. Miomandre, J. Tang, *J. Electroanal. Chem.* **2007**, accepted, Ms. No.: JELECHEM-D-06-00643R1.

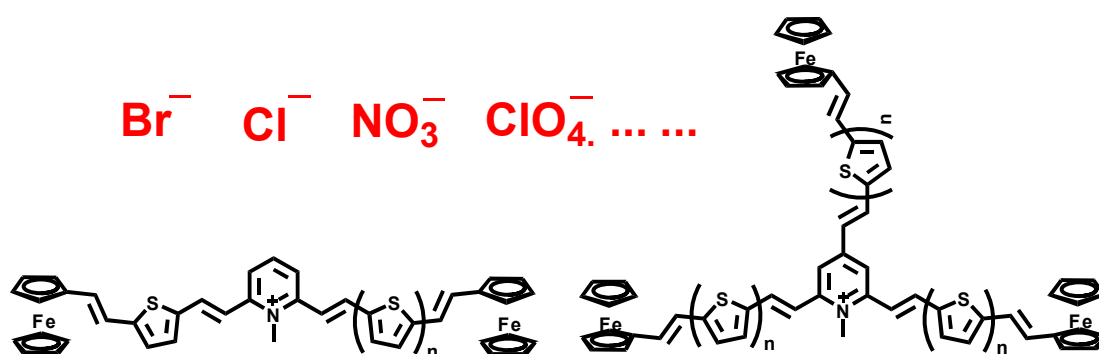


General conclusion and perspectives:

A new dibranched ferrocene-containing pyridinium salt (**45j**) and two tri-branched ones (**46h**, **46j**) have been synthesized through the condensations of 1,2,6-trimethyl pyridinium or 1,2,4,6-tetramethyl pyridinium with corresponding aromatic aldehydes. A new synthetic route has been developed for the two important intermediates, trans-5-(2-ferrocenyl-vinyl)-2-carbaldehyde-thiophene (**47**), and ferrocenylethenyl-bithiophenyl aldehyde (**48**): thiophenylaldehyde, obtained from Vilsmeier formylation, was firstly brominated in the 5 position to give 5-bromothiophene-2-carbaldehyde, which was reduced and reacted subsequently with $\text{PPh}_3 \cdot \text{HBr}$ to give the corresponding phosphonium bromide. Wittig reaction with ferrocenylaldehyde and subsequent recrystallization gave trans-2-bromo-5-ferrocenylethenylthiophene, which produced the intermediate aldehyde **47** through lithiation and subsequent reaction with DMF in good yield. Aldehyde **48** was also obtained using the same protocol. Piperidine was found to catalyze the condensations of 1,2,6-trimethyl pyridinium or 1,2,4,6-tetramethyl pyridinium with aldehydes more efficiently than other bases such as potassium carbonate or 2,4,6-collidine.

Preliminary electrochemical studies show that the conjugated bithiophene bridges influence greatly the redox behaviors of the molecules. Only the reversible oxidations of ferrocene units take place in the case of ferrocenyl pyridiniums containing thiophene bridges (**45h**, **46h**), although the shape of the cyclic voltammogram of **46h** is not like the classical ones of ferrocenes, probably indicating a larger spreading of the redox potentials corresponding to the successive 3 electron transfers in it as compared to the 2 electron transfers in the dibranched one (**45h**). However, the cyclic voltammograms of the ferrocenyl pyridiniums containing bithiophene bridges (**45j**, **46j**) show distinctively different characters from those for ferrocenes. In both cases, a subsequent polymerization take place after the oxidation of ferrocene units, indicating an uphill electron transfer process between the ferrocenes and the bithiophene branches.

At present, an investigation of the nonlinear optical properties of these ferrocene-containing pyridinium salts is anticipated, given their ability to allow electron transfer in molecules. Considering the fact that anions usually play an important role in adjusting non linear optical properties of the molecules, the preparation of these pyridiniums with different anions through anion exchange is ongoing.

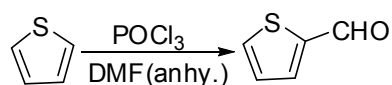


Chapter 4 Experimental section

General procedures

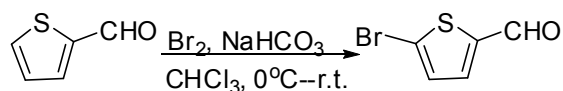
Most of the procedures were performed in a same manner to that described in Part I, Chapter 6, except that NMR spectra were acquired on a Bruker Advance 500 spectrometer, and mass spectrometry was performed on an Agilent 5973N mass spectrometer.

4.1 Preparation of 2-thiophenealdehyde



To a 100-mL three-necked round bottom flask was added 16 mL (0.19 mol) of thiophene, 16.3 mL (0.21 mol) of anhydrous DMF and 40 mL of anhydrous chloroform. The solution was cooled to ~0°C in an ice bath and 19.6 mL of POCl₃ (0.21mol) was added dropwise with stirring. The solution was then warmed to room temperature followed by refluxing for 4 hs, then cooled to room temperature and poured into iced water. The water layer was extracted with dichloromethane (3×50 mL), and the organic layers were combined and washed with water (2×50mL) and saturated aqueous sodium bicarbonate (2×50 mL), and dried over MgSO₄. After evaporation of the solvent 25 g of 2-thiophenealdehyde was obtained from fractional distillation in vacuo (108-112 °C, 53mmHg) as a colorless liquid (70%).

4.2 Preparation of 5-bromo-2-thiophenealdehyde



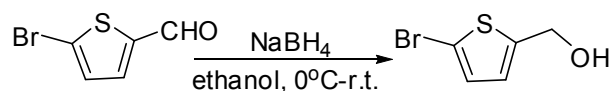
To an ice-cooled solution of 2-thiophenealdehyde(16.2 g, 0.14 mol) and NaHCO₃ (12.6 g, 0.15 mol) in dry chloroform, 7.4 mL of bromine (0.14mol) was added dropwise with stirring, and the mixture was left at room temperature for 2 hours, then poured into water. After separation, the water layer was extracted with dichloromethane (3×20mL), and the organic layer were combined and washed with saturated aqueous sodium bicarbonate, then with water, and dried with MgSO₄. After a short column (silica, 1:20 ethyl acetate/petroleum ether) 21.4 g of product was obtained as a colorless liquid (80%).

¹H NMR (500 MHz, CDCl₃) δ 9.78 (s, 1H), 7.52 (d, 1H, J=4.0 Hz), 7.19 (d, 1H, J=4.0Hz).

Reference: Buu-Hoï, N. P.; Lavit, D. J. *J. Chem. Soc.* **1958**, 1721.

b.p. 148-150 °C (40 mmHg.), No NMR data mentioned.

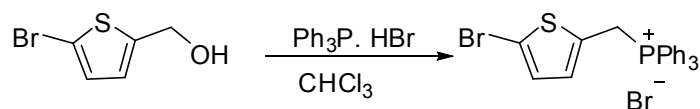
4.3 Preparation 5-bromo-2-thiophenemethanol



To an ice-cooled solution of 5-bromo-2-thiophenealdehyde (15 g, 0.079 mol) in 50 mL of methanol, NaBH₄ (6 g, 0.16 mol, 2eq.) was added portionwise, and the mixture was stirred at room temperature for ~ 4 hours. After evaporation of the solvent, dichloromethane was added to dissolve the residue and the insoluble salts were filtered. After a short column chromatography (silica, 1:10 ethyl acetate/petroleum ether) 11 g of 5-bromo-2-thiophenemethanol was obtained as a colorless liquid (73%).

¹H NMR (500 MHz, CDCl₃) δ 6.92 (d, 1H, J=3.7 Hz), 6.76 (d, 1H, J=3.7 Hz), 4.75 (s, 2H), 1.73 (s, br, 1H).

4.4 Preparation of 5-bromo-2-thiophenemethanol triphenylphosphonium bromide

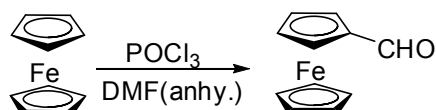


5 g of 5-bromo-2-thiophenemethanol (0.026 mol), 8.9 g of (0.026 mol) triphenylphosphine hydrobromide and 40 mL of anhydrous chloroform were added into a 100-mL flask equipped with a condenser. After refluxing for 1 h, the condenser was replaced by a distillation equipment. The solvent was distilled off slowly until dryness during 1 hour. The crude product was then dissolved in chloroform, and the pure phosphonium bromide was recovered by precipitation with addition of diethyl ether, washed 2 times with ether, and isolated by filtration (12.8 g, 96%).

Reference: Zhang, J.-X.; Dubois, P.; Jerome, R. *Synth. Commun.* **1996**, 26, 3091.

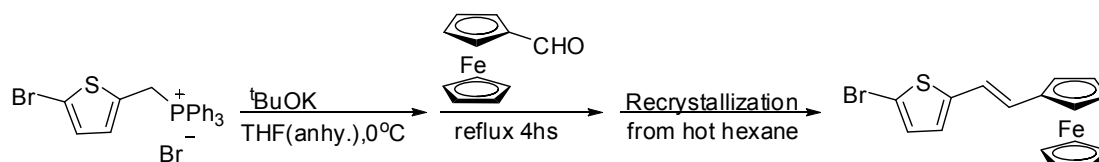
No m.p. data or NMR data reported.

4.5 Preparation of ferrocenealdehyde



To a 500-mL three-necked round bottom flask was added 20 g (0.11 mol) of ferrocene, 17 mL (0.25 mol) of anhydrous DMF and 80 mL of anhydrous chloroform. The solution was cooled to ~0°C in an ice bath and 20.3 mL of POCl₃ (0.08 mol) was added dropwise with stirring. The solution was then warmed to room temperature followed by refluxing for 24 h, then cooled to room temperature and poured into iced water. The mixture was neutralized with saturated aqueous sodium bicarbonate, extracted with dichloromethane (3×150 mL), and the organic layers were combined, washed with water (2×150 mL) and saturated aqueous sodium bicarbonate (2×100 mL), and dried over MgSO₄. After a column chromatography (silica, 1:6 EA/PE) 15 g of ferrocenecarboxaldehyde were obtained as a deep red solid (65%).

4.6 Preparation of *trans*-5-(2-ferrocenyl-vinyl)-2-bromo-thiophene



5.18 g (0.01 mol) of 5-bromo-2-thenyl triphenylphosphonium bromide was dissolved in 30 mL of dry THF in a 3-necked round bottom flask under N_2 atmosphere and cooled to $\sim 0^\circ C$. Potassium *t*-butoxide (1.39 g, 0.012 mol) was added slowly through a side arm while stirring the solution vigorously. The generated deep red solution was stirred at $0^\circ C$ for another 30 mins, then brought to room temperature. Ferrocene carboxaldehyde (2.14 g, 0.01 mol) was added portionwise and the mixture was heated to reflux for 4 hs. The solution was poured into iced water and extracted with diethyl ether. The ether layer was washed with brine and dried with $MgSO_4$. A mixture of *cis*- and *trans*-5-bromo-2-(2-ferrocenyl-vinyl) thiophene was obtained from a short column chromatography (silica, 1:6 DM/PE) as a red solid (3.2 g, 86%).

Recrystallization of 4.4 g of the mixture from hot hexane gave 1.7 g of pure *trans*-5-bromo-2-(2-ferrocenyl-vinyl) thiophene.

The solid obtained after evaporation of the filtrate (2.8 g of *cis/trans* 4:1) was treated with 0.01 eq. of I_2 in refluxing toluene under N_2 atmosphere for 1 hour to give 2.7 g of pure *trans*- product (96%).

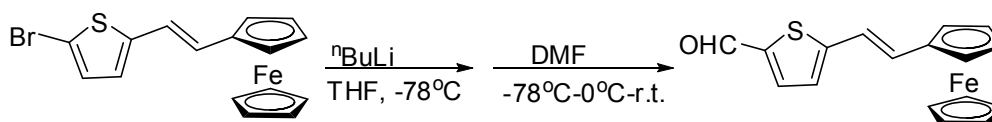
1H NMR (500 MHz, $CDCl_3$) δ 6.90 (d, 1H, $J=4.0Hz$), 6.64 (m, 2H), 6.56 (d, 1H, $J=16.0Hz$), 4.47 (s, 2H), 4.34 (s, 2H), 4.18 (s, 5H).

Reference: Thomas, K. R. J.; Lin, J. T.; Lin, K.-J. *Organometallics*, **1999**, *18*, 5285

NMR data reported:

1H NMR ($CDCl_3$, TMS): δ 6.88 (d, 1H, $J=3.72Hz$), 6.65 (m, 2H), 6.55 (d, 1H, $J=15.9Hz$), 4.39 (m, 2H), 4.27 (m, 2H), 4.12 (s, 5H).

4.7 Preparation of *trans*-5-(2-ferrocenyl-vinyl)-2-carbaldehyde-thiophene

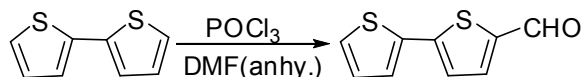


To a cooled ($-78^\circ C$) solution of *trans*-5-(2-ferrocenyl-vinyl)-2-bromo-thiophene (1.64 g, 4.4 mmol) in 30 mL of THF was added dropwise 3.3 mL of *n*-butyllithium (1.6M in hexane, 5.3 mmol, 1.2 eq.). The mixture was stirred for 15mins, allowing the temperature to rise to $-50^\circ C$, then cooled again to $-78^\circ C$. After dropwise addition of anhydrous DMF (0.41 mL, 5.3 mmol, 1.2 eq.), the reaction temperature was allowed to rise to $0^\circ C$ in 2 hours. The reaction mixture was then stirred for 4 hours at $0^\circ C$ and 2 hours at room temperature, then poured into iced water and extracted with dichloromethane, which was then washed with water (2×30 mL) and dried over $MgSO_4$. After a short column chromatography (silica, 1:6 \rightarrow 1:2 dichloromethane/ petroleum ether) 0.85 g of pure product of aldehyde was obtained as a violet solid (60%).

1H NMR (500 MHz, $CDCl_3$) δ 9.83 (s, 1H), 7.61 (d, 1H, $J=4.0Hz$), 7.01 (d, 1H, $J=4.0Hz$), 6.96 (d, 1H, $J=16.0Hz$), 6.79 (d, 1H, $J=16.0Hz$), 4.47 (m, 2H), 4.26 (m, 2H), 4.16 (s, 5H).

NMR data reported (Thomas, K. R. J.; Lin, J. T.; Wen, Y. S. *Journal of Organometallic Chemistry* **1999**, 575, 301.): ^1H NMR (No solvents or frequency mentioned) δ 9.87 (s, 1H), 7.81 (d, 1H, $J=4.2\text{Hz}$), 7.20 (d, 1H, $J=3.8\text{Hz}$), 7.10 (d, 1H, $J=15.9\text{Hz}$), 7.00 (d, 1H, $J=15.9\text{Hz}$), 4.60 (m, 2H), 4.38 (m, 2H), 4.17(s, 5H).

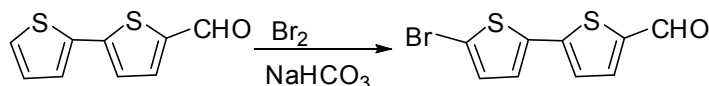
4.8 Preparation of 2,2'-bithiophene-5-carbaldehyde



POCl₃ (2.05 mL, 22 mmol) was added dropwise to a solution of 2,2'-bithiophene (3.43 g, 20 mmol) and anhydrous DMF (1.7 mL, 22 mmol) in anhydrous 1,2-dichloroethane (60 mL) at 0°C under Ar Atmosphere. The solution was warmed to room temperature and then refluxed for 2 hs. After cooling to room temperature, the mixture was poured into an aqueous solution of sodium acetate (1 M, 200 mL) and stirred for 2 hs to complete the hydrolysis. After the separation of the organic phase, the aqueous phase was extracted with CH₂Cl₂ (2×50 mL). The organic phases were combined and dried over MgSO₄, and then evaporated in vacuo. After purification by a column chromatography (silica, 1: 1 DM/PE) 3.77 g of product was obtained as a yellow solid (94%).

^1H NMR (500 MHz, CDCl₃) δ 9.87 (s, 1H), 7.67 (d, 1H, $J=4.0\text{Hz}$), 7.37 (m, 2H), 7.26 (d, 1H, $J=3.0\text{Hz}$), 7.09 (t, 1H, $J=5\text{Hz}$)

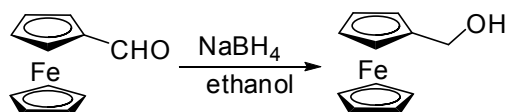
4.9 Preparation of 5'-bromo-2,2'-bithiophene-5-carbaldehyde



A solution of Br₂ (0.97 mL, 18.6 mmol) in 10 mL of CHCl₃ was added dropwise to the refluxing mixture of 2,2'-bithiophene-5-carbaldehyde (3.00 g, 15.5 mmol) and sodium bicarbonate (1.6 g, 18.6 mmol) in 45 mL of CHCl₃. After refluxing for 4 hs, the mixture was cooled to room temperature and poured into iced water. The organic layer was washed with water and saturated aqueous NaHCO₃, and dried over MgSO₄. After evaporation of the solvent, the solid was purified by a column chromatography to afford 3.8 g of pure 5'-bromo-2,2'-bithiophene-5-carbaldehyde (90%).

^1H NMR (500 MHz, CDCl₃) δ 9.90 (s, 1H), 7.68 (d, 1H, $J=4\text{Hz}$), 7.20 (d, 1H, $J=4\text{Hz}$), 7.13 (d, 1H, $J=4\text{Hz}$), 7.06 (d, 1H, $J=4\text{Hz}$)

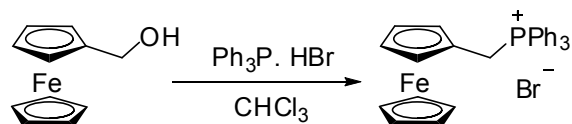
4.10 Preparation of ferrocenemethanol



NaBH₄ (1.5 g, 39.5 mmol) was added portionwise into a solution of ferrocenealdehyde (4.0 g, 18.7 mmol) in 40 mL of ethanol. The mixture was stirred at room temperature for 4 hours, then concentrated by evaporation. The solids were

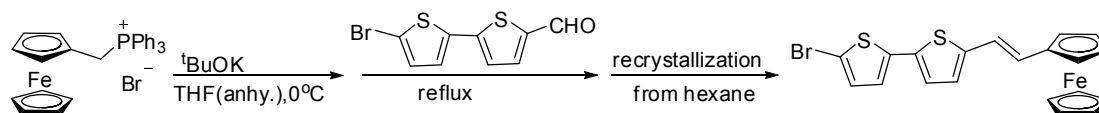
filtered and washed several times with DM. The filtrate was concentrated and passed through a short column chromatography (silica, DM) to give 3.6 g of product as a yellow solid (89%).

4.11 Preparation of ferrocenemethyl triphenylphosphonium bromide



3.6 g of ferrocenemethanol (16.7 mmol), 5.7 g (16.7 mmol) triphenylphosphine hydrobromide and 40 mL of anhydrous chloroform were added into a 100-mL flask equipped with a condenser. After refluxing for 1 h, the condenser was replaced by a distillation equipment. The solvent was distilled off slowly until dryness during 1 hour. The crude product was then dissolved in chloroform, and the phosphonium bromide was recovered by precipitation with addition of diethyl ether, washed 2 times with ether, and isolated by filtration (9.0 g, 97%).

4.12 Preparation of 5'-bromo-5-(2-ferrocenylvinyl)-2,2'-bithiophene



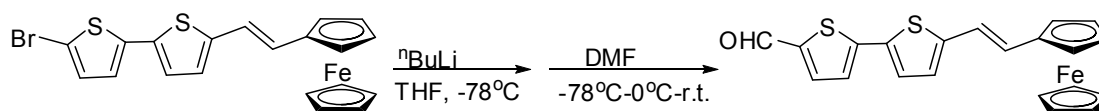
5.31 g (9.8 mmol) ferrocenemethyl triphenylphosphonium bromide was dissolved in 50 mL of dry THF in a 3-necked round bottom flask under N₂ atmosphere and cooled to ~0°C. Potassium *t*-butoxide (1.3 g, 11 mmol) was added slowly through a side arm while stirring the solution vigorously. The generated deep red solution was stirred at 0°C for another 30 mins, then brought to room temperature. 5'-bromo-2,2'-bithiophene-5-carbaldehyde (2.68 g, 9.8 mmol) was added portionwise and the mixture was heated to reflux for 6 hs. The solution was poured into iced water and the water layer was extracted with dichloromethane. The organic layer was washed with brine and dried with MgSO₄. A mixture of *cis*- and *trans*-5'-bromo-5-(2-ferrocenylvinyl)-2,2'-bithiophene was obtained from a short column chromatography (silica, 1:5 DM/PE) as a red solid (3.1 g, 69%).

Recrystallization of 3.1 g of the mixture from hot hexane gave 1.9 g of pure *trans*-5'-bromo-5-(2-ferrocenylvinyl)-2,2'-bithiophene.

¹H NMR (500 MHz, CDCl₃) δ 6.96 (d, 2H, J=3Hz), 6.89 (d, 1H, J=3Hz), 6.80 (m, 1H), 6.67 (m, 2H), 4.46 (s, 2H), 4.33 (s, 2H), 4.17 (s, 5H)

The rest of the mixture (1.2 g, mostly *cis*- isomer) recovered from the filtrate was treated with 0.01 eq. of I₂ in refluxing toluene under N₂ atmosphere for 1 hour but failed to give pure *trans*- product.

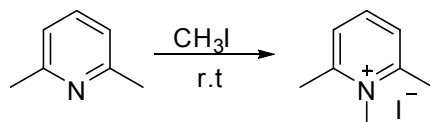
4.13 Preparation of (*E*)-5'-ferrocenylvinyl-2,2'-bithiophene-5-carbaldehyde



To a cooled (-78 °C) solution of trans-5'-bromo-5-(2-ferrocenylvinyl)-2,2'-bithiophene (1.9 g, 4.2 mmol) in 30 mL of THF was added dropwise 2.6 mL of n-butyllithium (1.6M in hexane, 4.2 mmol). The mixture was stirred for 15mins, allowing the temperature to rise to -50 °C, then cooled again to -78 °C. After dropwise addition of anhydrous DMF (0.33 mL, 4.2 mmol), the reaction temperature was allowed to rise slowly to 0 °C in 3 hours and TLC indicated the reaction was finished. The mixture was poured into iced water and extracted with dichloromethane, which was then washed with water (2×30 mL) and dried over MgSO₄. After a short column chromatography (silica, 1:6→1:2 dichloromethane/ petroleum ether) 1.5 g of pure aldehyde was obtained as a violet solid (88%).

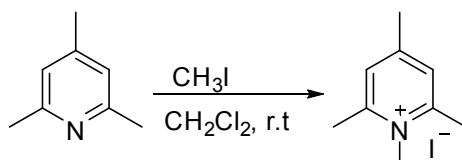
¹H NMR (500 MHz, CDCl₃) δ 9.85 (s, 1H), 7.67 (d, 1H, J=3Hz), 7.24 (d, 1H, J=4Hz), 7.16 (d, 1H, J=4Hz), 6.95 (d, 1H, J=16Hz), 6.71-6.68 (m, 2H), 4.48 (s, 2H), 4.36 (s, 2H), 4.19 (s, 2H)

4.14 Preparation of 1,2,6-trimethylpyridinium iodide



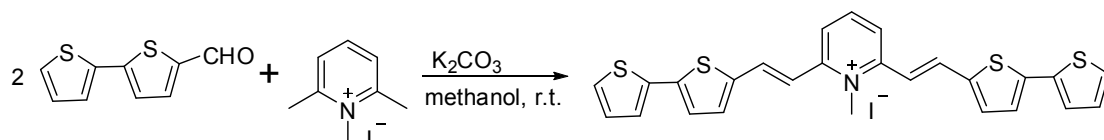
Methyl iodide (10 mL, 0.16 mol) was added dropwise to a solution of 2,6-lutidine (10.7 g, 0.1 mol) in dichloromethane at 0 °C. After stirring at room temperature overnight, the solvent was evaporated to give a white solid which was recrystallized in methanol to give 16 g of product as white needles (64%).

4.15 Preparation of 1,2,4,6-tetramethylpyridinium iodide



Methyl iodide (14.2 mL, 0.23 mol) was added dropwise to 2,4,6-collidine (10.6 mL, 0.08 mol) at 0 °C. After stirring at room temperature overnight, solids precipitated from the solution were filtered, washed several times with dichloromethane and recrystallized in methanol to give 15 g of product as white needles (71%).

4.16 Preparation of 2,6-bis((E)-2-(2,2'-bithiophen-5-yl)vinyl)-1-methylpyridinium



Bithiophenealdehyde (0.582 g, 3 mmol), 1,2,6-trimethylpyridinium iodide (0.249 g, 1 mmol) and potassium carbonate (0.276 g, 2 mmol) were added into 30 mL of anhydrous methanol. The mixture was stirred at room temperature for 4 hours and

TLC indicated that the reaction was finished. After a column chromatography (silica, 1:10 methanol/DM) 0.13 g of product was obtained as a red solid (22%).

^1H NMR (500 MHz, DMSO- d_6) δ 8.36 (t, 1H, $J=8\text{Hz}$, H-4 of pyridinium), 8.20 (d, 2H, $J=8\text{Hz}$, H-3 and H-5 of pyridinium), 7.93 (d, 2H, $J=16\text{Hz}$, trans -HC=), 7.61 (d, 2H, $J=5\text{Hz}$, bithiophene), 7.58 (d, 2H, $J=5\text{Hz}$, bithiophene), 7.45 (d, 2H, $J=3\text{Hz}$, bithiophene), 7.41 (d, 2H, $J=4\text{Hz}$, bithiophene), 7.29 (d, 2H, $J=16\text{Hz}$, trans -HC=), 7.15 (t, 2H, $J=5\text{Hz}$, bithiophene), 4.24 (s, 3H, $\text{N}^+\text{-Me}$)

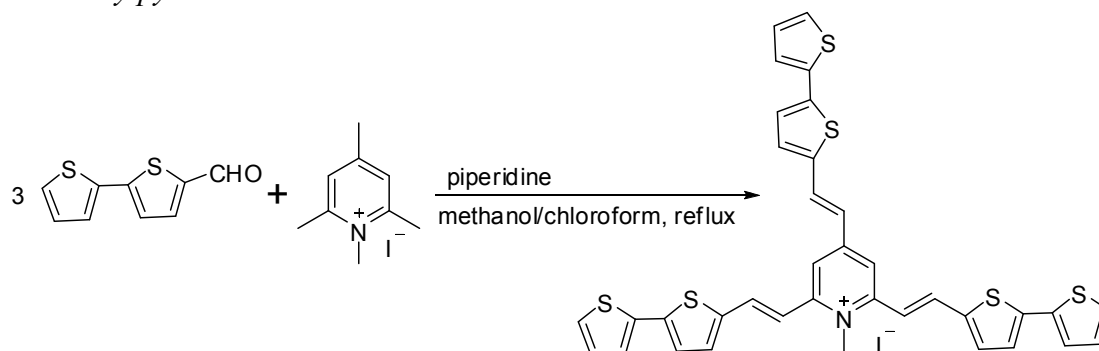
^{13}C NMR (125 MHz, DMSO- d_6) δ 152.78, 142.50, 140.35, 138.61, 135.80, 134.77, 133.02, 128.61, 126.89, 125.34, 125.11, 123.33, 117.21, 41.45 ($\text{N}^+\text{-Me}$)

MS, m/z : 475 ($[\text{M-I}+1]^+$, calc. 475), 426, 280, 249 (base peak)

Anal. Calcd for $\text{C}_{26}\text{H}_{20}\text{NS}_4\text{I}$: C 51.91, H 3.35, N 2.33. Found: C 51.74, H 3.840, N 2.277.

UV (DMF) λ_{max} : 464.00 nm

4.17 Preparation of 2,4,6-tris((*E*)-2-(2,2'-bithiophen-5-yl)vinyl)-1-methylpyridinium iodide



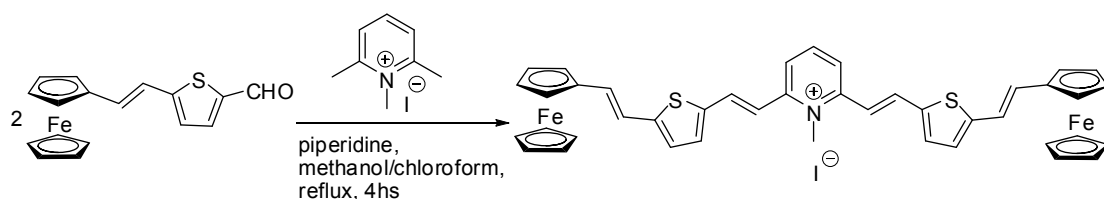
Bithiophenealdehyde (0.194 g, 1 mmol, 4 eq.), 1,2,4,6-tetramethylpyridinium iodide (0.066 g, 0.25 mmol) and 5 drops of piperidine were added into a mixture of 30 mL of anhydrous methanol and 10 mL of chloroform. The mixture was refluxed for 12 hours and TLC indicated that the reaction was finished. After a column chromatography (silica, 1:10 methanol/chloroform) 0.176 g of product was obtained as a deep red solid (89%).

^1H NMR (500 MHz, DMSO- d_6) δ 8.29 (m, 3H, H-3 and H-5, p-HC=), 7.98 (d, 2H, $J=16\text{Hz}$, o-HC=), 7.63 (t, 3H, $J=5\text{Hz}$, bithiophene), 7.58 (d, 2H, $J=4\text{Hz}$, bithiophene), 7.46-7.42 (m, 5H, bithiophene), 7.39 (d, 1H, $J=4\text{Hz}$, bithiophene), 7.24 (m, 3H, 2H of o-HC= and 1H of bithiophene), 7.19-7.14 (m, 3H, bithiophene), 7.05 (d, 1H, $J=16\text{Hz}$, p-HC=), 4.13 (s, 3H, $\text{N}^+\text{-Me}$)

^{13}C NMR (125 MHz, DMSO- d_6) δ 151.92, 140.03, 139.40, 139.38, 139.00, 138.61, 135.75, 135.72, 134.10, 132.80, 128.63, 126.87, 125.31, 125.25, 125.02, 119.10, 117.33, 40.54 ($\text{N}^+\text{-Me}$)

MS, m/z : 663 ($[\text{M-I}]^+$, calc. 663), 473 (base peak), 127

4.18 Preparation of 1-methyl-2,6-bis((*E*)-2-(5-(*E*)-ferrocenylvinyl)thiophen-2-yl)vinylpyridinium iodide

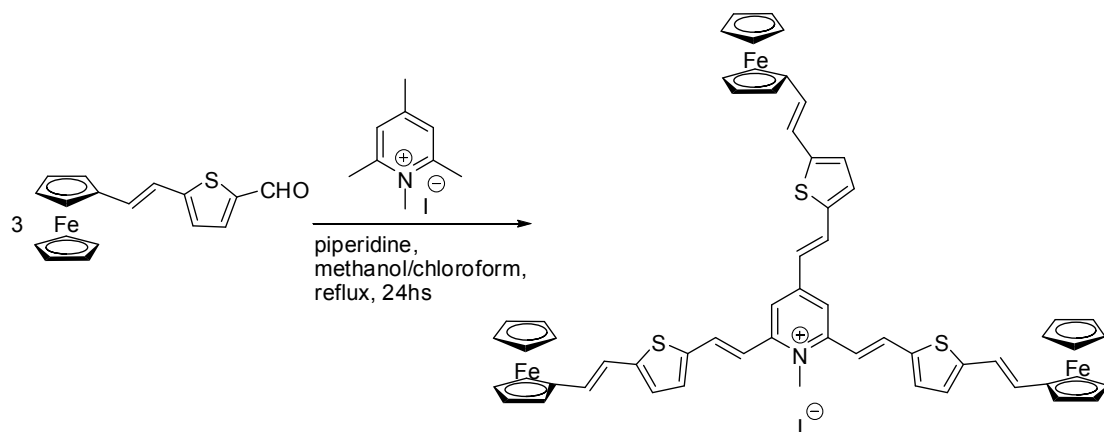


To a 100-mL flask equipped with a condenser, 31 mg (0.12mmol) of 1,2,6-trimethyl pyridinium iodide, 150 mg (0.37mmol, 3 eq.) of trans-5-(2-ferrocenylvinyl)-2-carbaldehyde-thiophene, 30 mL of anhydrous chloroform, 10 mL of anhydrous methanol and 2 drops of piperidine were added. After refluxing for 4 hours under N_2 atmosphere, the solution was cooled to room temperature. The solvent was evaporated and the residue was passed through a column chromatography (silica, 1:15 methanol/dichloromethane) to give 84 mg of all trans- product as a dark violet solid (79%).

1H NMR (500 MHz, $DMSO-d_6$) δ 8.34 (t, 1H, $J=8.1Hz$, H-4 of pyridinium), 8.20 (d, 2H, $J=8Hz$, H-3 and H-5 of pyridinium), 7.97 (d, 2H, $J=15.5Hz$, trans HC=), 7.51 (d, 2H, $J=3.7Hz$, thiophene), 7.21 (d, 2H, $J=15.5Hz$, trans HC=), 7.16 (d, 2H, $J=3.7Hz$, thiophene), 7.03 (d, 2H, $J=15.8Hz$), 6.88 (d, 2H, $J=15.8Hz$, trans HC=), 4.63 (s, 4H), 4.40 (s, 4H), 4.21 (s, 3H, N^+-Me), 4.17 (s, 10H).

^{13}C NMR (125MHz, $DMSO-d_6$) δ 152.67, 147.32, 137.42, 135.04, 133.47, 130.32, 126.27, 122.68, 118.62, 116.29, 81.87, 69.63, 69.12, 67.16, 41.25

4.19 Preparation of 1-methyl-2,4,6-tris((E)-2-(5-(E)-ferrocenylvinyl)-thiophen-2-yl)vinylpyridinium iodide

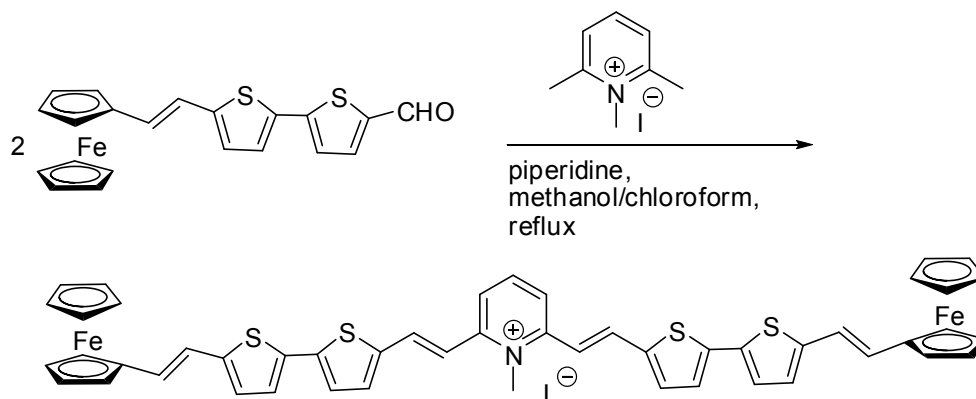


To a 100-mL flask equipped with a condenser, 49 mg (0.19mmol) of 1,2,4,6-trimethyl pyridinium iodide, 180 mg (0.56mmol, 3 eq.) of trans-5-(2-ferrocenylvinyl)-2-carbaldehyde-thiophene, 25 mL of anhydrous chloroform, 10 mL of anhydrous methanol and 4 drops of piperidine were added. After refluxing for 24 hours under N_2 atmosphere, the solution was cooled to room temperature. The solvent was evaporated and the residue was passed through a column chromatography (silica, 1:20 methanol/dichloromethane) to give 80 mg of all trans- product as a dark violet solid (33%).

1H NMR (300 MHz, $DMSO-d_6$) δ 8.29 (s, 2H, H-3 and H-5 of pyridinium), 7.95 (d, 2H, $J=15.5Hz$, trans HC=), 7.49 (d, 2H, $J=3.7Hz$, thiophene), 7.37 (d, 1H, $J=4.1Hz$, thiophene), 7.21-7.16 (m, 5H), 7.03(d, 4H, $J=15.8Hz$, trans HC=), 6.90-6.83 (m, 4H),

4.63 (s, 6H, CH₂ of Cp), 4.40 (s, 6H, CH₂ of Cp), 4.17 (s, 15H, CH₂ of Cp), 4.11 (s, 3H, N⁺-Me)

4.20 Preparation of 1-methyl-2,6-bis((E)-2-(5'-(E)-ferrocenylvinyl-2,2'-bithiophen-5-yl)vinyl)pyridinium iodide

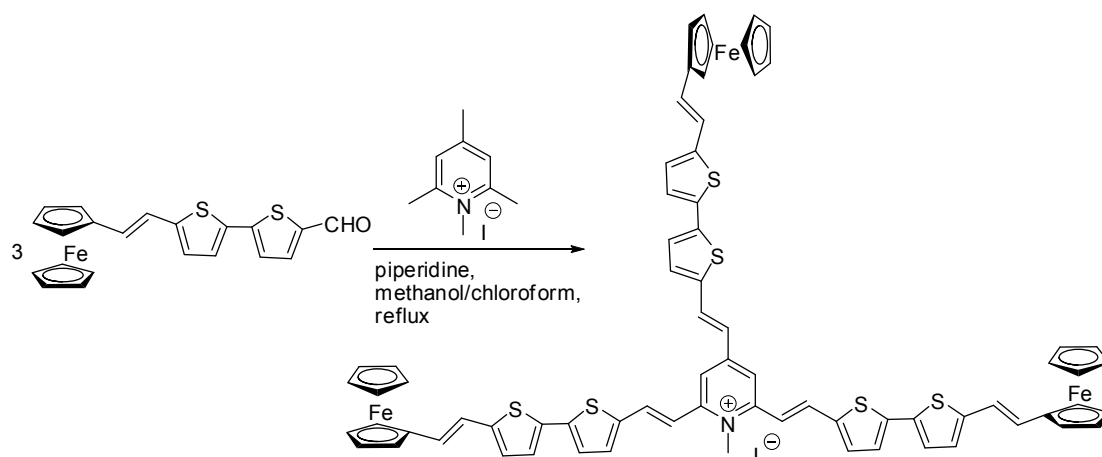


To a 50-mL flask equipped with a condenser, 60 mg (0.24 mmol) 1,2,6-trimethyl pyridinium iodide, 200 mg (0.50 mmol) (E)-5'-ferrocenylvinyl-2,2'-bithiophene-5-carbaldehyde, 30 mL of anhydrous chloroform, 10 mL of anhydrous methanol and 2 drops of piperidine were added. After refluxing overnight under N₂ atmosphere, the solution was cooled to room temperature. The solvent was evaporated and the residue was passed through a column chromatography (silica, 1:20→1:10 methanol/dichloromethane) to give 120 mg of all trans- product as a deep violet solid (49%).

¹H NMR (500 MHz, DMSO-d₆) δ 8.34 (t, 1H, J=8Hz, H-4 of pyridinium), 8.19 (d, 2H, J=9Hz, H-3 and H-5 of pyridinium), 7.96 (d, 2H, J=15Hz, HC=), 7.58 (d, 2H, J=4Hz), 7.40 (d, 2H, J=4Hz), 7.35 (d, 2H, J=4Hz), 7.26 (d, 2H, J=16Hz, HC=), 7.07 (d, 2H, J=3Hz), 6.94 (d, 2H, J=16Hz, HC=), 6.74 (d, 2H, J=16Hz, HC=), 4.60 (s, 4H, Fc), 4.37 (s, 4H, Fc), 4.24 (s, 3H, N⁺-Me), 4.17 (s, 10H, Fc)

¹³C NMR (125MHz, DMSO-d₆) δ 153.13, 147.56, 144.30, 141.01, 138.90, 135.18, 133.93, 133.40, 129.03, 126.77, 126.73, 125.36, 123.55, 119.07, 117.47, 84.53, 69.84, 69.58, 67.43, 41.91

4.21 Preparation of 1-methyl-2,4,6-tris((E)-2-(5'-(E)-ferrocenylvinyl-2,2'-bithiophen-5-yl)vinyl)pyridinium iodide



To a 50-mL flask equipped with a condenser, 60 mg (0.24 mmol) of 1,2,6-trimethyl pyridinium iodide, 277 mg (0.69 mmol) of (E)-5'-ferrocenylvinyl-2,2'-bithiophene-5-carbaldehyde, 30 mL of anhydrous chloroform, 10 mL of anhydrous methanol and 7 drops of piperidine were added. After refluxing for 48 hours under N₂ atmosphere, the solution was cooled to room temperature. The solvent was evaporated and the residue was passed through a column chromatography (silica, 1:20 methanol/dichloromethane) to give 110 mg of all trans- product as a black-violet solid (34%).

¹H NMR (300 MHz, DMSO-d₆) δ 8.30 (s, 2H, H-3 and H-5 of pyridinium), 7.98 (d, 2H, J=15.8Hz, trans HC=), 7.60 (d, 2H, J=3.7Hz), 7.46-7.36 (m, 6H), 7.26 (d, 2H, J=15.1Hz, trans HC=), 7.10 (d, 3H, J=4.1Hz), 6.98 (t, 3H, J=15.8Hz), 6.77 (t, 3H, J=15.8Hz), 4.60 (s, 6H), 4.37 (s, 6H), 4.16 (s, 15H), 4.14 (s, 3H, N⁺-Me)

¹³C NMR (75MHz, DMSO-d₆) δ 143.72, 140.27, 139.78, 139.12, 138.48, 134.00, 132.93, 132.92, 129.57, 128.47, 126.25, 126.24, 124.83, 118.57, 82.20 (CH of Cp), 69.33 (CH₂ of Fc), 69.07 (Cp of Fc), 66.92 (CH₂ of Cp), 45.70 (N⁺-Me)

Liste of publications

1. New tetrazines substituted by heteroatoms including the first tetrazine based cyclophane: Synthesis and electrochemical properties. Yong-Hua Gong, Pierre Audebert, Jie Tang, Fabien Miomandre, Gilles Clavier, Sophie Badré, Rachel Méallet-Renault and Jérôme Marrot, *Journal of Electroanalytical Chemistry*, 592, 147-152 (2006).
2. New pyridinium conjugated ferrocenes: Synthesis and electrochemical properties. Yong-Hua Gong, Pierre Audebert, Fabien Miomandre and Jie Tang, *Journal of Electroanalytical Chemistry*, in press (doi: 10.1016/j.jelechem.2007.04.006).
3. Synthesis and nonlinear optical absorption of two new conjugated ferrocene-bridge- pyridinium Compounds. Fan Yang, Xiu-Ling Xu, Yong-Hua Gong, Wen-Wei Qiu, Zhen-Rong Sun, Jin-wei Zhou, Pierre Audebert, Jie Tang, *Tetrahedron*, accepted.

Acknowledgement

Le temps passe vite. Now it is time to acknowledge all those people that have supported me to complete this thesis, although it is impossible, given so many people that have offered help during these years. I am going to try anyway, and if your name is not listed, rest assured that my gratitude is not less than for those listed below.

First of all I would like to give my special thanks to Professor Damien Prim and Professor Jean-Claude Moutet for being my rapporteurs, and Professor Gérard Jaouen for coming into the jury and being my examinateur.

My deepest gratitude goes first and foremost to my two supervisors, Professor Pierre Audebert and Professor Jie Tang. Thank you Pierre, for having given me the opportunity to be your student, for the encouragement and guidance all along the work of this thesis, for all the invitations to restaurants as well as to your home, for all the wonderful discussions with drinks, and for so many other beautiful things that I have no space to mention here. I also feel a deep sense of gratitude for my supervisor Professor Jie Tang, who led me into the world of research, who has been always supported me and encouraged me in academe and in life during more than 7 years. It is a treasure for all my life.

I would like to express my deep and sincere gratitude to Dr. Gilles Clavier, Chargé de recherche, without whom I definitely could not achieve my work. Thank you for your algate patient instructions for the experiments and for the thesis composition and correction. You are the one who has walked me through all the stages of the work of this thesis, helping me work out all my problems during the difficult course.

I wish to express my warm and sincere thanks to Professor Fabien Miomandre, for the patient instructions in the electrochemical studies, and the tremendous help in the paper writing.

I owe my sincere gratitude to Professor Joanne Xie, for her wonderful insight and suggestions in the synthesis, and her warm receptions which made me feel like at home.

I am deeply grateful to Dr. Robert Pansu (Directeur de Recherche), Professor Rachel Méallet-Renault, Sophie Badré, and Elliot Naidus for the help in fluorescence studies.

I warmly thank Professor Fan yang for the help in study and in life.

I am deeply indebted to all the people in PPSM including those who have ever worked me together but already left, from whom I have got so much help and warmth. Special thanks to the director Professor Jacques Delaire, Professor Keitaro Nakatani, Andrée Husson (Tu m'a aidé à faire tant que de démarche administrative; et le gâteau que tu a fait était tellement délicieux.), Dr. Isabelle Leray, Marie-Claude (Tu sais toujours ou se trouvent les choses.), Laurent, Cécile Dumas, Valérie Alain, Elena

Ishow, Jean-Jacques Vachon, Jean-Baptiste Mulon (toujours très plaisant), Jean-Alexis Spitz (so much fun talking with you), Jacky Fromont (Merci pour avoir résolu tous mes problèmes de l'ordinateur.), Vincent Souchon (star de football!), Minh-huong HA-THI (très agréable de parler avec toi), Khaled (On a joué ensemble tellement de fois !), Arnaud Spangenberg (C'étaient très sympa les matchs de foot et de basket), Arnaud Brosseau (Je me souviens la nuit de billard), Michaël Four, Aurélien, Izabella, Jean-Pierre Bonnet, Béatrice Lama. Vive le PPSM!

I would also like to thank all the people in the Organic Laboratory of ECNU, especially the director Professor Jiaying Lu, Professor Jianbo Zhang, Professor Qingjiang Wang, Dr. Wenwei Qiu and Dr. Meiran Xie for their kind help. I also wish to thank my friends and colleagues in my laboratory in ECNU, Qiaomin Hong, Linmei He, Qing Zhou, Chun Li, Danping Shen.

I would like to gratefully acknowledge the support of the French Ministry of Foreign Affairs who has provided the scholarship to make all these possible, and CROUS (Centre Régionale des Oeuvres Universitaires et Scolaires) de Créteil who has taken care of my affairs in France. Special thanks to Monsieur Jean-Michel Namur for his zealous reception.

I would also like to give my thanks to French Embassy in Beijing and French Consulate in Shanghai for the convenience they have provided.

I would also like to express my special gratitude to the SRI (Service des Relations Internationales) de ENS-Cachan (Un grand merci pour Madame Bogdana Neuville et Madame Elisabeth Lacroix), and the Office of International Affairs of ECNU (Un grand merci pour Madame Yunhua Qian).

Many thanks to the Graduate School of ECNU. Special thanks to Director Benchang Li, Professor Wenhui You and Dr. Haisheng Li.

Un grand merci pour Lucile Martin et Huier Chen.

I would like to thank my family and all my great friends: Jing Long, E Wu, Aifang Wang, Shenghua Hu, Huizhong Xiao, Bin Deng, Hua Yi, Jianfeng Jiang, Yanbing Jiang, Peng Wu, Lu Liu, Juan Nie.